Exploring Plant Stilbenes For Healthy Skin

A thesis submitted to the University of East Anglia

for the degree of Doctor of Philosophy

By

Erica Hawkins

John Innes Centre

Norwich

September 2018

Abstract

Accumulating evidence supports pharmacological roles for the plant stilbene, resveratrol in aging and disease contexts. Pterostilbene, a derivative of resveratrol, has been shown to have higher bioavailability and bio-efficacy than resveratrol, but is not abundant in natural sources.

Previous work demonstrated that expression of the stilbene synthase gene, isolated from grapevine *Vitis vinifera*, under the control of a plant-wide promoter, led to a variety of growth and fertility problems in the transformed plants.

To circumvent this problem two transgenic tomato lines were developed in this thesis to produce resveratrol and pterostilbene specifically in the fruit of tomato.

An *ex vivo* full thickness human skin explant model was used to investigate the biological effects of aqueous tomato juices on normal human skin, and in an inflammatory disease-like context by treatment with inflammatory cytokines.

Microarray analysis and qRT-PCR validation identified the differential regulation of several genes in human skin with tomato juice treatment, including a significant downregulation in expression of the aging-associated matrix metalloproteinase, MMP-12, observed with both wild type and resveratrol-enriched tomato extracts. MMP-12 protein could be detected in human skin explant media but regulation at this level proved elusive. Analysis of elastin fibres, a crucial structural component of skin, revealed subtle effects of tomato extracts.

The effect of tomato extracts on reepithelialisation aspects of wound-healing was assessed using a full thickness skin explant model, in addition to scratch-wounds of keratinocyte and fibroblast skin cell lines. Initial studies of resveratrol- and pterostilbene-enriched tomato extracts indicated a greater biological activity associated with pterostilbene, and a potential inhibitory effect on migration of cells.

Overall novel tomato lines have been generated and their fruit showed effects which could be relevant in the prevention of skin aging and in overcoming the consequences of inflammation.

Acknowledgements

There are many people that I would like to thank for their support over the last four years. Firstly, I would like to thank my supervisors Prof. Cathie Martin, and Dr Jelena Gavrilovic for giving me the opportunity to join their labs and providing me with scientific and emotional support throughout my PhD.

I am extremely grateful to all of those in both the Martin and Gavrilovic labs, past and present, who helped to show me numerous techniques, and who shared their knowledge with me. I am fortunate to have had a lab filled with so many friends, and with whom I can share countless memories.

A special thanks to Dr Eugenio Butelli and Dr Damon Bevan who taught me so much throughout my project, and kept the project going as I moved between the JIC and UEA! Dr Daniel Knevitt, thank you for being my office pal for two years, and keeping me entertained, and Dr Lionel Hill, thank you for helping me solve all the conundrums I came to you with, and for your friendship.

None of this would have been possible without the support of my family. Mum, Dad and Kirsten, you put up with me through all my highs and lows, and I do not know what I would have done without you.

To all my friends here in Norwich, thank you for making the last four years so memorable, I am lucky to have shared them with you. Finally, Athina and Fabi, all my love and gratitude go to you both, for your unending friendship and ability to always brighten my day.

List of Abbreviations

3T3	"3-day transfer, inoculum 3×10^5 cells." Mouse fibroblast cell line
4CL	4-courmarate coenzyme A
A. tumefaciens	*Agrobacterium tumefaciens*
ACN	Acetonitrile
AKT	Protein kinase B
ANS	Anthocyanin Synthase
BCA	Bicinchoninic Acid
C4H	Cinnamate-4 hydroxylase
CaMV	Cauliflower mosaic virus
cDNA	Complementary DNA
CHI	Chalcone isomerase
CHS	Chalcone synthase
COL17A1	Collagen, type 17, alpha 1
COL7A1	Collagen, type 7, alpha 1
COX	Cyclooxygenase
C_T	Cycle threshold
DAB	3,3' Diaminobenzidine
DFR	Dihydroflavonol-4-Reductase
dH_2O	Distilled water
DMEM	Dulbecco's Modified Eagle Medium
DMSO	Dimethyl sulfoxide
dNTPs	Deoxyribonucleotide Triphosphate
DW	Dry Weight
E. *coli*	*Escherichia coli*
EB	Epidermolysis bullosa
ECM	Extracellular matrix
EDN1	Endothelin 1
EDTA	Ethylenediaminetetraacetic acid
EGF	Epidermal Growth Factor
EGFR	Epidermal Growth Factor Receptor
EGTA	Egtazic acid
F3H	flavanone-3-hydroxylase
FCS	Foetal Calf Serum
FLS	Flavonol Synthase
FW	Fresh weight

GW	Gateway
HaCaT	Human Keratinocyte cell line
HPLC	High Performance Liquid Chromatography
HRP	Horseradish Peroxidase
IFS	Isoflavone Hydroxylase
IHC	Immuno Histochemistry
IL	Interleukin
IL-1A	Interleukin 1 alpha
iNOS	Induced Nitric Oxide Synthase
JIC	John Innes Centre
kb	Kilobase pair
kDa	Kilo Dalton
KO	Knock Out
LCMS IT-TOF	Ion Trap and time of flight liquid chromatography/ mass spectrometer
MAPK	Mitogen-activated protein kinase
MBW	MYB-bHLH-WD40 complex
MeOH	Methanol
MM	Money Maker (WT tomato)
MMP	Matrix metalloproteinase
mRNA	Messenger RNA
NF-$_{\kappa}$B	Nuclear factor kappa-light-chain-enhancer of activated B cells)
NHEK	Normal Human Epidermal Keratinocytes
OSM	Oncostatin M
PAL	Phenylalanine
PBS	Phosphate Buffered Saline
PCR	Polymerase Chain Reaction
PDA	Photo Diode Detector
PI3	Phosphoinositide 3-kinase
PVDF	Polyvinylidene difluoride
qRT-PCR	Quantitative Reverse Transcriptase Polymerase Chain Reaction
RIPA	Radioimmunoprecipitation assay buffer
RNA	Ribonucleic acid
ROMT	Resveratrol-o-methyltransferase
SDS-PAGE	sodium dodecyl sulphate polyacrylamide gel electrophoresis
StSy	Stilbene Synthase
TCA	Trichloroacteic acid

UEA	University of East Anglia
UV	Ultraviolet
v/v	Volume/volume
w/v	Weight/volume
WB	Western Blot
WT	Wild type

Table of Contents

Table of Figures

Table of Tables

Chapter 1: Introduction

1.1 Plant secondary metabolites

Plants are constantly exposed to a wide range of both abiotic and biotic stresses from their natural environments (Jeandet et al., 2010). The production of secondary (or specialised) metabolites confers a selective advantage to plants against these environmental stresses, because they form part of the defensive mechanisms such as the production of nitric oxide, and antimicrobial compounds that aid survival of the plant (Taddese et al., 2008).

Of the many secondary metabolites produced by plants the family of compounds known as stilbenes, synthesised via the phenylpropanoid pathway, have become the focus of considerable research in recent years. The stilbene resveratrol, and its methylated derivative pterostilbene, have gained much interest in recent years due to their wide range of biological actions including anti-inflammatory and anti-carcinogenic roles.

1.2 Stilbenes

Stilbenes are phenylpropanoids that are synthesised by several plant families including grape (*Vitaceae*), pine (*Pinacaea*), and peanut (*Fabaceae*) in response to biotic and abiotic stresses. The major role attributed to stilbenes, particularly those found in grape and pine, is to act as a phytoalexin, to prevent and protect against fungal and bacterial infections (Jeandet et al., 2002, Jeandet et al., 2010).

Plant stilbenes are synthesised from the phenylpropanoid pathway, (Figure 1.1*).* All species of land plants possess the first three steps of the phenylpropanoid pathway (highlighted in Figure 1.1) which synthesise Co-enzyme-A esters from phenylalanine. These three steps comprise the general phenylpropanoid pathway, which is ubiquitous across seed plant species. The general phenylpropanoid pathway is common to the synthesis of several secondary plant metabolites including flavonoids, anthocyanins, monolignols and stilbenes, reviewed in (Chong et al., 2009). After the synthesis of -coumaroyl CoA the synthesis pathways diverge and for stilbene synthesis the enzyme stilbene synthase is required (Chong et al., 2009, Weihermann et al., 2017).

Although many plants can synthesise malonyl-CoA and CoA-esters (such as p-coumaroyl CoA), for condensation by the polyketide synthase enzyme chalcone synthase to produce chalcone naringenin for the synthesis of flavonoids, only a few plant species are able to synthesise stilbenes from these two compounds. This is because many plants lack the enzyme stilbene synthase, crucial for stilbene synthesis. Stilbene synthase has probably evolved from chalcone synthase (to which it is structurally related) on several occasions during the evolution of land plants. Resveratrol stilbene synthase (StSy) catalyses the biosynthesis of resveratrol from three molecules of malonyl-CoA and one of a CoA-ester (*p*-coumaroyl CoA) Figure 1.1. There are several StSy enzymes, which synthesise different stilbenes, such as resveratrol synthase and pinosylvin synthase. Although some stilbene

synthases are very specific producing only one stilbene from one substrate, some StSy enzymes are able to synthesise several different stilbenes depending on the starting substrates (Makrantonaki and Zouboulis, 2007).

Members of the stilbene family are characterised by a 1, 2-diphenylethylene backbone, varying in the functional groups positioned on the backbone (Figure 1.2), which provide members of the stilbene family with a large chemical diversity, *cis* isoforms can also be formed but these are not associated with human-related biological activities. A large number of stilbenes are derived from trans-resveratrol, especially within the peanut and grapevine families (Bernstein et al., 1994). Trans-resveratrol and its derivative trans-pterostilbene have been the centre of much research over recent years, due to their potential pharmacological functions, and will be discussed in more detail next.

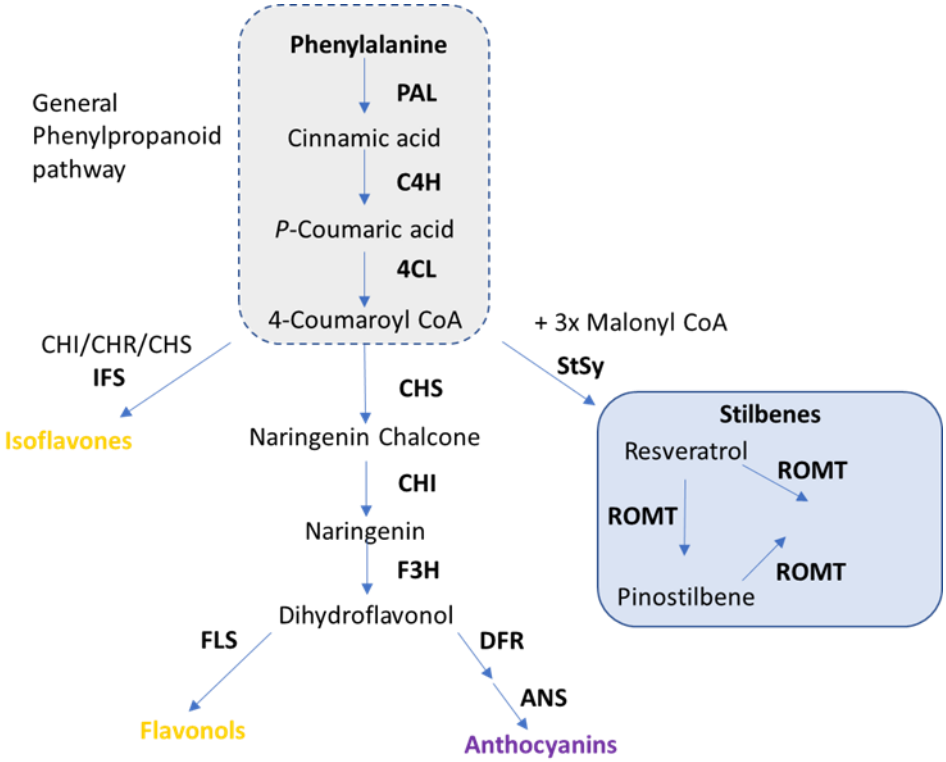

Figure 1.1 Basic phenylpropanoid biosynthesis pathway, highlighting the general phenylpropanoid pathway, and stilbene biosynthesis.

Schematic representation of the phenylpropanoid pathway leading to stilbene synthesis. PAL, phenylalanine ammonia lyase; C4H, cinnamate 4-hydroxylase; 4CL, 4-coumarate coenzyme A ligase;, IFS, Isoflavone hydroxylase; CHS, chalcone synthase, CHI, chalcone isomerase, F3H, flavanone-3-hydroxylase; FLS, Flavonol synthase; DFR, dihydroflavonol reductase; ANS, anthocyanidin synthase; StSy, Stilbene synthase, ROMT, resveratrol-o-methyltransferase

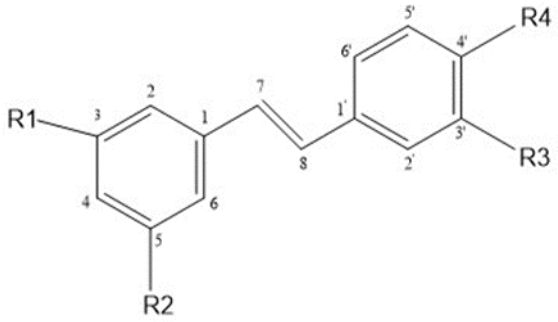

Stilbene	
Trans-Piceid	R1=OH, R2=GlcO, R3=H, R4=OH
Trans-resveratrol	R1=OH, R2=OH, R3=H, R4=OH
Pinostilbene	R1=OH, R2=OCH_3, R3=OH
Pterostilbene	R1=OCH_3, R2=OCH_3, R3=OH

Figure 1.2 Basic structure of stilbene.

Schematic diagram of the basic stilbene structure, and the different functional groups found positions R1-R4 to form the most common stilbenes *trans*-piceid, *trans*-resveratrol, pinostilbene and pterostilbene

1.2.1 Resveratrol

Resveratrol (3, 4', 5-trihydroxystilbene) (Figure 1.3) is synthesised from p-coumaroyl CoA and 3 malonyl-CoA units by resveratrol synthase, as illustrated in Figure 1.2. Resveratrol was first isolated from the roots of the oriental plant *Polygonum cupsidatum* (Pervaiz, 2003), and was later identified to be the active ingredient in many oriental folk remedies. In 1976, *trans*-resveratrol was also identified to be produced by leaf tissue in *Vitis vinfera* (grapevine), to counteract fungal infections (Langcake and Pryce, 1976). Resveratrol has since been documented to be present in several plants with highest expression in *Polygonum cupsidatum, Vitis vinifera* species of grapevine, peanuts and spruce pine.

1.2.2 Pterostilbene

Pterostilbene (3, 5-dimethoxy-4'-hydroxy-trans-stilbene) is a methylated derivative of resveratrol (Figure 1.3). Like resveratrol, pterostilbene functions as a bactericide and fungicide, although reports have suggested that it may have a higher functional activity compared to resveratrol, resulting from the presence of methyl groups on its aromatic rings (Jeandet et al., 2010).

Until very recently the mechanism of pterostilbene biosynthesis was largely unknown. However, a study published in 2008 by Schmidlin *et al.* shed some light onto the biosynthesis of pterostilbene. Schmidlin *et al*. (2008) used a candidate gene approach to identify, and subsequently characterise a resveratrol O-methyltransferase (ROMT) from the grapevine *Vitis vinifera*. Transient co-expression of ROMT and grapevine stilbene synthase (StSy) in tobacco (*Nicotiana benthamiana*) led to the accumulation of pterostilbene as the major stilbene. As well as catalysing the methylation of resveratrol to produce pterostilbene, ROMT was also shown to methylate pinostilbene (Figure 1.4). These results indicated that co-expression of StSy and ROMT could be used to synthesise

pterostilbene from resveratrol as the major stilbene and provided insight into how pterostilbene could be metabolically engineered.

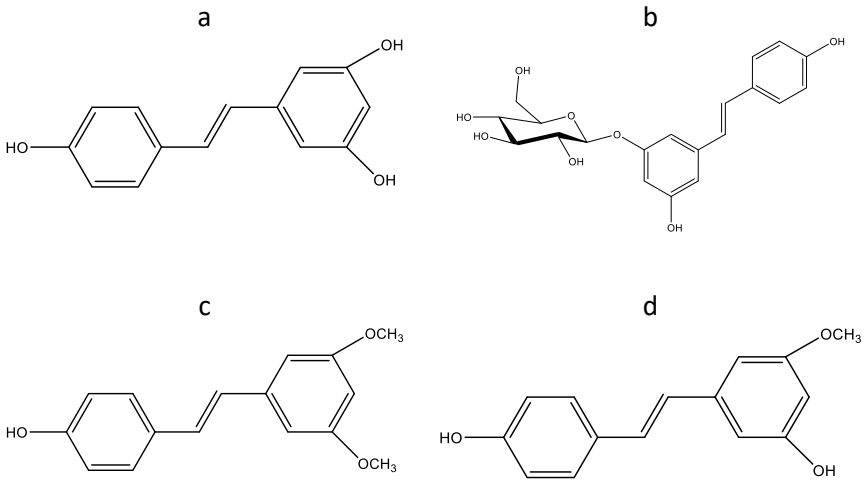

Figure 1.3 Structure of Stilbenes: (a) Resveratrol, (b) Polydatin, (c) Pterostilbene and (d) Pinostilbene

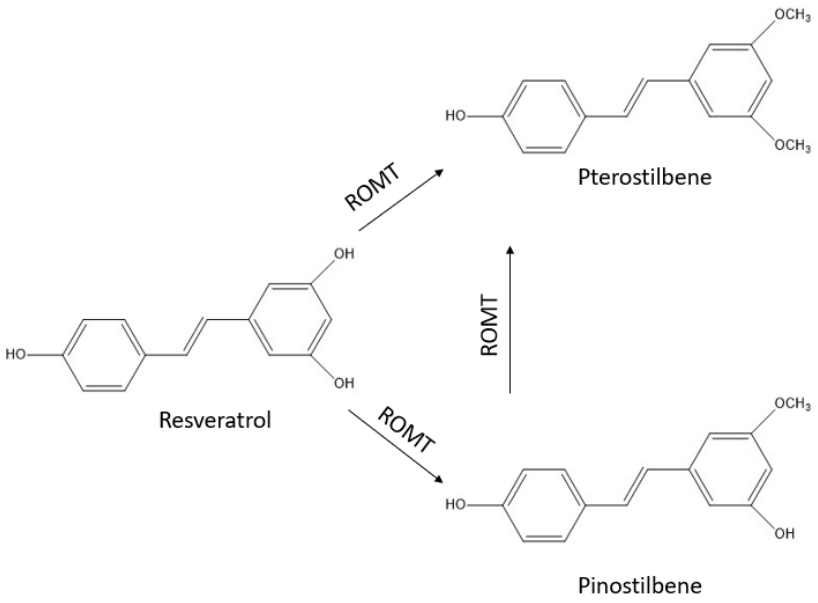

Figure 1.4 The basic mechanism of pterostilbene synthesis from resveratrol and pinostilbene

1.3 Industrially synthesising stilbenes

Plants such as grapevine and *Polygonum cupsidatum* only produce resveratrol and its derivatives under stress, and even then, only at lower levels. For example, red grapes, one of the prime dietary sources of resveratrol, contain only between 50 to 100 µg/g fresh weight of resveratrol (Jeandet et al., 1991). *Polygonum cupsidatum* roots are known to contain significantly higher levels of resveratrol than grape, however, extraction of resveratrol from roots remains inefficient and costly despite efforts to improve extraction processes(Mantegna et al., 2012). With the current high market demand for resveratrol and its derivatives, metabolic engineering has offered a possible alternative to large scale production of plant stilbenes.

Metabolic engineering of both bacterial (Jeong et al., 2014, Katsuyama et al., 2007, Lim et al., 2011) and yeast (Kowalczyk et al., 2010) systems for production of stilbenes has also been looked at widely over the last few years. Neither of these two organisms contain genes encoding enzymes of the general phenylpropanoid pathway required for the synthesis of stilbenes. This means that two routes could be used for stilbene synthesis- either all the enzymes of the general phenylpropanoid pathway need to be engineered into the organism, or a single enzyme could be engineered into the organism and the required substrate added to culture. However, both approaches have major drawbacks- being both time consuming and costly due to the complexity of the phenylpropanoid pathway (Figure 1.4) and the cost of derivatives needed to supplement cultures.

Jeong et al. (2014) metabolically engineered *Escherichia coli* to produce methylated resveratrol derivatives by introducing resveratrol-o-methyltransferase genes from *Sorghum bicolour* and *Vitis riparia*. Although, the E. *coli* synthesised was able to convert resveratrol into its two methylated derivatives pterostilbene and pinostilbene, only a maximal amount of 34mg/L of pterostilbene was made. In addition, these cultured bacteria required resveratrol to be added to the culture to synthesise pterostilbene, and because they contained only the resveratrol methyltransferase gene they could not make other stilbenes by themselves.

More recently, Heo et al. (2017) metabolically engineered E. *coli* capable of synthesising up to 33.6 mg/L pterostilbene by integration of a multifunctional caffeic acid methyltransferase from *Arabidopsis* into a L-tyrosine over producing strain of *E.coli*. However, to produce pterostilbene, addition of L-methionine to media was required. Additionally, the ROMT currently used leads to high levels of pinostilbene production, which hampers pterostilbene synthesis. To resolve this bottle neck in pterostilbene production, further optimisation of the system is required. Finally, additional processes would need to be used and optimised to purify pterostilbene products from the culture media.

These studies show that although microbes can be used for engineering of stilbenes, a lot of optimisation, and different engineering steps are required to produce purified stilbenes at high levels.

Yeast bio-fermentation has shown more promise for production of high levels of polyphenols, with a group recently engineering yeast to produce high levels of stilbenes (800mg L^{-1}) from glucose (Li et al., 2016b). Although this is a great improvement from other yeast-based platforms, a lot of work is still required to scale this production up from a lab-based to industrial scale. In addition, further optimisation would be required in order to make bio-fermentation economically viable (Chen et al., 2002).

Finally, a downside of using these metabolically engineered fermentation techniques is that they lead only to the production of the one core compound, this approach potentially misses other biologically important stilbene derivatives produced by the plant-based pathway. For example, in planta production of polyphenols leads to the generation of hundreds of compounds with different and distinct side chain modifications. This lack of chemical diversification is a major drawback of microbial production of plant-compound synthesis.

1.3.1 Plant Cell cultures

An alternative method for resveratrol production is the use of plant cell cultures. Grapevine cell suspensions for the synthesis of resveratrol and its methylated derivatives have been investigated. A benefit of this method is that medium used for cell cultures is inexpensive, and by applying stresses cell cultures can be induced to increase production of resveratrol (Blake et al., 1990). Cell cultures have been able to produce up to 2 g/L of resveratrol once treated with methyl jasmonate and/or methylated-cyclodextrin (Guo et al., 2008). The cells secrete resveratrol, but polydatin remains in the cells themselves, and so two types of extraction and purification protocols are required to gain maximal yield of stilbene. Overall this system could offer a good alternative production line for stilbenes, although it still requires optimisation for high level production of stilbenes, and there remain some questions about how to effectively scale this operation up.

1.4 Engineering plants for increased stilbene production

Considering the drawbacks of using microbial systems for production of stilbenes, metabolic engineering of plants for production of stilbenes *in planta* represents a good alternative method for high stilbene production.

Fleshy fruits provide an inexpensive and natural bio factory to produce a wide range of metabolites, which can subsequently be used directly, through ingestion of the fruits, or whose juice can be extracted (Guo et al., 2008). Tomato is an excellent bio-factory for the synthesis of health-promoting compounds, as the whole genome sequence is available for fruit specific production of

secondary metabolites in fruit does not affect growth of the plant or yield, and multiple techniques are available for use in tomatoes.

In addition, commercial tomato plants produce a variety of flavonoids naturally, and already have the general phenylpropanoid pathway active in fruit. This therefore means that only the two enzymes; stilbene synthase and resveratrol-O-methyltransferase, need to be introduced into tomato.

1.4.1 Metabolically engineering a high-stilbene tomato

Two aspects must be considered in the engineering of stilbenes in tomatoes. Firstly, in terms of stilbene biosynthesis in tomatoes, the introduction of additional genes via metabolic engineering is required. Although the general phenylpropanoid pathway is present within tomatoes, tomatoes lack the required enzymes for stilbene biosynthesis. Therefore, for resveratrol production, resveratrol stilbene synthase needs to be introduced, and for pterostilbene synthesis, resveratrol O-methyltransferase is also required.

Secondly, the rate limiting step associated with synthesis of the phenylpropanoids needs to be identified and engineered, to ensure high levels of synthesis, essential for a successful bio factory. Tomatoes already contain most of the general phenylpropanoid pathway, enabling them to produce flavonoids and anthocyanins at low levels naturally.

One of the major limitations associated with production of phenylpropanoids in tomato is the low concentrations at which they were synthesised. This is due to the action of the transcriptional regulators of the phenylpropanoid pathway.

The main transcriptional regulators of the flavonoid and anthocyanin biosynthesis pathways are MYB, WD repeat proteins (WD40), and basic helix loop helix (bHLH) proteins (Jimenez et al., 2006). These factors interact with each other to form the MYB-bHLH-WD40 (MBW) ternary transcriptional complex (Sinha et al., 2014). The MBW complex is involved in both developmental and environmental regulation at the transcriptional level. In flavonoid biosynthesis the MBW complex is mainly involved with activation of biosynthetic genes involved in anthocyanin biosynthesis (Jimenez et al., 2006), whilst for flavonol biosynthesis a single MYB transcription factor, MYB12, can activate all steps of the pathway (Zhang et al., 2015).

MYB transcription factors are characterised by an N-terminal MYB domain consisting of up to four imperfect sequence repeats (R) of 52 amino acids, involved in DNA binding (Tewari et al., 2014), and a highly conserved C-terminal domain that regulates target gene expression (Vaalamo et al., 1999). There are four classes of MYB transcription factors, based upon the number and placement of repeats: 1R (R1/2,R2-MYB), 2R (R2R3-MYB), 3R (R1R2R3-MYB) and 4R (4 R1/R2 like repeats)(Liu

et al.). The R2R3-MYB class are the largest class of MYB factors in plants, and are involved in the regulation of flavonoids and anthocyanins (Zhang et al., 2014, Hichri et al., 2011, Li, 2014)

Plant bHLH transcription factors can be classified into 12 sub-groups characterised by their conserved N-terminal domain (Hichri et al., 2011). Those belonging to the 111f subgroup, which interact with various R2R3-MYBs, are the best described in plant biosynthesis regulation. The N-terminal domain of the bHLH interacts with the MYB factor within the MBW complexes which regulate both anthocyanin and proanthocyanin biosynthesis (Xu et al., 2015).

WD40 proteins (WDR) are characterised by a peptide motif of 44-60 amino acids. Several WD40 proteins have been identified to be involved in flavonoid biosynthesis, most prominently *Arabidopsis thaliana* TTG1 (Transparent Testa Glabra 1). WD40 proteins appear to be highly conserved between plant species, and function within the MBW complex as a docking platform (Hichri et al., 2011).

Both MYB and bHLH proteins of the MBW complex can induce all steps within the flavonoid and anthocyanin biosynthesis pathways. However, it is the activity of the R2R3MYB proteins that is the main determining factor in regulation of synthesis, by determining the target gene that the MBW complex binds to and activates (Zhang et al., 2014).

Within tomato, engineering low synthesis levels of phenylpropanoid compounds was due to rate limitation exhibited by the MYB transcription factors (Butelli et al., 2008). Therefore, to increase synthesis of phenylpropanoid compounds a transcription factor needed to be identified which could be used for engineering the general phenylpropanoid pathway.

In 2008, a tomato line able to produce high levels of flavonols in fruit using the upregulated expression of a single gene from *Arabidopsis thaliana,* encoding the MYB transcription factor AtMYB12 (Luo et al., 2008, Zhang et al., 2014).

The transcription factor *At*MYB12 had been identified as a flavonol-specific transcription factor in *Arabidopsis thaliana* (Mehrtens et al., 2005*)*. Luo et al. (2008) determined that when *At*MYB12 was expressed in a fruit tissue-specific manner in tomato, it was able to mirror the activity of the orthologous MYB12-like protein found in tomato, upregulating both the caffeoyl quinic acid biosynthetic pathway and flavonol pathway. These data indicated that AtMYB12 had a substantial capacity for transcriptional activation of phenylpropanoid metabolism in tomato, and therefore could be used to amplify synthesis of multiple polyphenolic compounds.

It has subsequently been determined that AtMYB12 can induce all steps in the phenylpropanoid pathway. This therefore, makes AtMYB12 an excellent general tool to engineer the phenylpropanoid pathway in tomato, and produce fruits containing high concentrations of phenylpropanoid compounds (Zhang et al., 2014).

The promoter to be used to control and initiate transcription of the genes needs to be considered. A common promoter used in plant metabolic biology is the cauliflower mosaic virus (CaMV) 35S promoter (Benfey and Chua, 1990, Bhullar et al., 2007). Previous work (Zhang et al., 2015) had used this promoter to engineer a resveratrol synthesising tomato, but production of resveratrol throughout the plant led to several deleterious effects on plant growth and development of tomato plants.

Due to the poor health associated with plant-wide expression of resveratrol, a fruit specific promoter represents a good alternative promoter for stilbene biosynthesis. The tomato E8 gene is an ethylene regulated promoter, expressed only in flowers and fruits during ripening (Kneissl and Deikman, 1996). Use of this fruit-specific promoter would therefore, ensure that stilbene synthesis is initiated only within the fruits of tomato, and during the ripening of the tomatoes.

1.5 Health benefits of polyphenols

The physiological role of plant compounds such as anthocyanins, flavonoids and stilbenes has been a growing area of research since the late 1990s. Resveratrol and its derivative pterostilbene have received considerable research interest due to their promise as therapeutics for humans. However, there is still much debate concerning the effects of these compounds on human diseases, and their modes of action.

Jang et al. (1997) published a seminal paper that indicated a chemo-preventive role for resveratrol. Resveratrol had previously been identified to be a cyclooxygenase (COX) inhibitor. Since COX, an enzyme which catalyses the conversion of arachidonic acid to pro-inflammatory substrates, had been linked to carcinogenesis, Jang et al. (1997) investigated the potential anti-inflammatory and cancer-preventive activities of resveratrol. It was determined that resveratrol was able to inhibit multiple stages of tumorigenesis including initiation, promotion, and progression. Resveratrol inhibited each of these stages of tumour development in a dose-dependent manner. Additionally, topical application of 25µM resveratrol to mice over an 18-week period reduced the number of skin tumours per mouse by 98%, strongly suggesting that resveratrol functions as a chemo-preventive agent.

The study by Jang et al. (1997) put resveratrol on the map, and kick-started research into resveratrol as a pharmacological agent. Since 1997, *in vitro* experiments have implicated resveratrol in cardiovascular protection (Sato et al., 2002, Hung et al., 2000), neuroprotection (Bastianetto et al., 2014) and resveratrol has been shown to have anti-inflammatory and controversial anti-aging roles (de la Lastra and Villegas, 2005).

Despite the multitude of biological activities attributed to resveratrol *in vitro,* it has been difficult to replicate these results *in vivo*. A major reason for the discrepancy between *in vitro* and *in vivo*

studies may be due to the low bioavailability of resveratrol. A lot of animal studies have based research on oral consumption of resveratrol, which leads to a particularly low overall bioavailability of resveratrol of just 1%, due to extensive metabolism of resveratrol by the intestines and liver (Walle, 2011). In addition, resveratrol is known to have a short half-life, which presents several problems when considering the use of resveratrol in oral supplements or topical treatments (Boocock et al., 2007). Therefore, resveratrol analogues, such as the methylated derivative pterostilbene, may overcome these limitations to pharmacokinetic efficiency

1.5.1 Pterostilbene and health

Pterostilbene is structurally similar to resveratrol, however due to the presence of two methoxy groups, it exhibits increased bioavailability and half-life. The presence of the two methoxy groups greatly increases lipophilic and oral absorption. In animal studies, pterostilbene has been shown to have a bioavailability of 80% compared to just 20% for resveratrol, highlighting the potential therapeutic advantage of pterostilbene compared to resveratrol (Kapetanovic et al., 2011).

Pterostilbene has also been shown in several studies to have very similar biological activities to resveratrol. Rimando et al. (2002) investigated the potential chemo preventive activity of pterostilbene, by considering its activity against cyclooxygenase (COX), and compared its activity to that of resveratrol. It was determined that pterostilbene has a similar antioxidant activity *in vitro* to resveratrol. Additionally, using a mouse mammary gland culture model of carcinogenesis, pterostilbene was confirmed to function as a chemo preventive agent. However, although shown to be a cancer chemo preventive agent, the exact molecular mechanism underlying pterostilbene activity, as for resveratrol, remains undetermined.

Subsequently, many studies have investigated the possible mechanisms of pterostilbene action as a chemo preventive agent. Pan et al. (2008) showed that the anti-inflammatory action of pterostilbene could be a major underlying contributor to its chemo preventive properties. It was determined that pterostilbene could inhibit gene expression of inflammatory COX-2, and inducible Nitric Oxide Synthase (iNOS) which have both been associated with the development of malignant tumours (Lechner et al., 2005). Pterostilbene inhibited COX-2 and iNOS by reducing lipopolysaccharide-induced nuclear translocation of the nuclear factor NFκB, thereby decreasing expression of the PI3/AKT and MAPK transcriptional pathways which normally activate COX-2 and iNOS.

Additionally, pterostilbene has been observed to have high anti-oxidant activity (Remsberg et al., 2008), which has been linked to its functionality as a chemo preventive agent (Remsberg et al., 2008). High oxidation levels have been shown to increase inflammation and have been implicated in the development of cancers. Therefore, it is highly likely that the anti-inflammatory, anti-oxidant and chemo-preventive actions of pterostilbene are all linked.

Research into the mechanisms of action of pterostilbene is still in its infancy, and pterostilbene has been studied much less than resveratrol. However, as discussed above, pterostilbene, like resveratrol, has several means of exerting its chemo preventive activity and has multiple cellular targets. Although the exact mechanisms of action of pterostilbene are still unclear, the multitude of positive biological effects exerted by pterostilbene shows that further research on its bioactivity is warranted.

Due to the high biological activity of pterostilbene in addition to increased bioavailability and half-life compared to resveratrol, pterostilbene may represent a better therapeutic agent. Many studies have been based upon oral ingestion of resveratrol or pterostilbene, however this is an inefficient mechanism for delivery of these compounds. Topical application represents an alternative means of therapeutic delivery. Studies have shown that resveratrol is able to effectively permeate the skin, with both oral and topical routes of administration giving comparable tissue distribution profiles of resveratrol, confirming that delivery of resveratrol via skin may offer a potent way to achieve therapeutic effects of resveratrol (Hung et al., 2008, Murakami et al., 2014).

1.6 Plant polyphenols and skin

Both resveratrol and pterostilbene, as discussed above, have shown great promise as chemo-preventive agents for cancers. Much of the preventive and protective effects of resveratrol and pterostilbene are thought to derive from their anti-oxidant activity. As oxidative stress is believed to be a key factor in the development of photo-aged skin and cancers, many studies have begun to look at the *in vitro* effects of resveratrol, in the hope that this plant-derived metabolite can be used within skin care products. As such, several cosmetic companies such as L'Oréal now have several cosmetic compositions containing resveratrol in combinations with other bioactives, with several patents defining its use.

The effects of plant-derived metabolites on skin have been widely studied in regards to sunscreen effects (ability to prevent penetration of UV light), anti-inflammatory effects, anti-oxidant effects, and ability to repair induced damage (Nichols and Katiyar, 2010).

Due to the anti-oxidant and cancer chemo preventive properties associated with resveratrol and pterostilbene, these molecules have been researched as potential photo-protective, and chemo-preventive agents.

Evidence of the photoprotective effect of resveratrol has come from several studies which have pre-treated cells with resveratrol before exposing to UVB. Adhami et al. (2003) demonstrated resveratrol pre-treatment can block UVB-mediated activation of the nuclear transcription factor kappa B (NF-κB) in both a time-dependent and dose-dependent manner in normal human epidermal keratinocytes (NHEK). This photo-protective function of resveratrol was also shown in a

study by Park and Lee (2008) where pre-treatment of human keratinocyte cell lines (HaCaT cells) with resveratrol before UVB-radiation increased cell survival and decreased production of reactive oxygen species. In addition, activity of caspases 8, 9 and 3 were decreased in pre-treated HaCaT cells, indicating resveratrol exerted photo-protective effects by modulating caspase activation pathways.

The photo-protective capability of resveratrol has also been observed *in vivo*, with short-term protection to UVB-radiation being gained in SKH1-hairless mice with topical resveratrol pre-treatment (Afaq et al., 2003). Topical application of resveratrol (25µmol/0.2 ml acetone) to SKH1-hairless mice prior to UVB radiation was found to inhibit UVB-mediated induction of both COX and ornithine decarboxylase (ODC) enzymes.

A comparison of the effect of topical resveratrol and pterostilbene pre-treatment to UVB-radiation in SKH1-hairless mice confirmed inhibition of UVB-induced oxidative damage. Both resveratrol and pterostilbene have UV absorption properties, which may account for some of the photo-protective effects displayed by these two compounds (Walle et al., 2004), and may be significant in their use in topical applications. Additionally, it was found that pterostilbene-treated mice showed a much-decreased incidence of UVB-induced carcinogenesis, which was not observed in resveratrol treated mice. Furthermore, pterostilbene pre-treatment prevented skin fold thickness, redness, and photo-aging associated wrinkling to a greater extent than resveratrol treatment, suggesting a higher biological activity associated with pterostilbene (Sirerol et al., 2015). These properties of resveratrol and pterostilbene are suggestive of chemo preventive effects.

Many aging and inflammatory skin conditions stem from ultraviolet damage and oxidative stress, and so the potential of resveratrol and pterostilbene to inhibit UVB- induced responses has much promise in the use of these two plant polyphenols for skin diseases.

Lephart et al. (2014) quantified differential gene expression in human skin equivalent cultures which had been exposed to 1.0% resveratrol for 24 hours. This study showed that resveratrol treatment significantly modified expression of genes linked to aging and development of skin-disease: extracellular matrix proteins, the anti-aging factor sirtuin 1 anti-oxidant markers, inflammatory markers, and skin-aging molecules. This study however, considered only the effect of resveratrol on human EpiDerm full thickness skin cultures which had not been previously exposed to any stress stimulus. Additionally, resveratrol treatment was only performed at a concentration of 1% within a DMSO solution, over 24 hours.

Nevertheless, the results from this study demonstrated that resveratrol positively stimulated several genes associated with anti-aging (Scharffetter-Kochanek et al., 2000) such as the collagen and elastin biomarkers. In addition, resveratrol was shown to down regulate expression of genes

commonly associated with the development of skin aging and cancers, such as MMPs and interleukins (Scharffetter-Kochanek et al., 2000). The results from this study demonstrated the potential that topical application of resveratrol has for skin, in terms of anti-aging and chemo-prevention. However, the results from this study need to be expanded considerably to allow full understanding of the functionality of resveratrol and its potential as a topical treatment.

The data from the *in vitro* and *in vivo* studies discussed above suggest that resveratrol and its derivatives such as pterostilbene, have the potential to be developed as a photo- and chemo preventive agents, to treat and prevent skin disorders such as photo-aging, and associated changes in skin morphology such as wrinkling.

However, both the *in vitro* and *in vivo* studies discussed above have limitations in their application to human skin disorders and treatments. *In vitro* cell culture models are effective tools for research, but as these are usually monolayer skin cell cultures they do not exhibit the complex cellular layers and interactions observed in human skin. The *in vivo* mouse-based studies on the other hand, do account for the wide-ranging interactions within skin, but resveratrol action and bioavailability may be significantly different between mice and humans due to the structural differences in murine and human skin.

Additionally, whilst the above studies show that resveratrol shows considerable promise as a photo protective and chemo protective agent, they also highlight the lack of understanding of the mechanisms by which resveratrol exhibits its biological activities. Therefore, more research is required into the biological action of resveratrol, as well its bioavailability via topical skin applications. In addition, more research needs to be undertaken concerning pterostilbene, which has shown promise as a more potent agent than resveratrol, but which has not been investigated in as much detail in skin despite its potentially greater bio-efficacy.

1.7 Introduction to Skin

1.7.1 Skin structure and function

The skin is the body's largest organ and is composed of two primary layers: The epidermis and dermis (Figure 1.5). The epidermis is the outermost layer of mammalian skin, which acts as the first barrier to environmental stresses. The epidermis is predominantly composed of keratinocytes which account for 95% of cells, with melanocytes, Langerhans and Merkel cells contributing the remaining 5%. The very outermost layer of the epidermis, the stratum corneum, is composed of corneocytes, which are terminally differentiated keratinocytes (Menon, 2002). The dermis, which forms the majority of the skin, is composed of elastin, collagens and glycosaminoglycans and glycoproteins, which together are known as the extracellular matrix (ECM). The dermis is highly vascular and contains a complex collection of cell types including mast cells, adipose cells, fibroblasts and leukocytes.

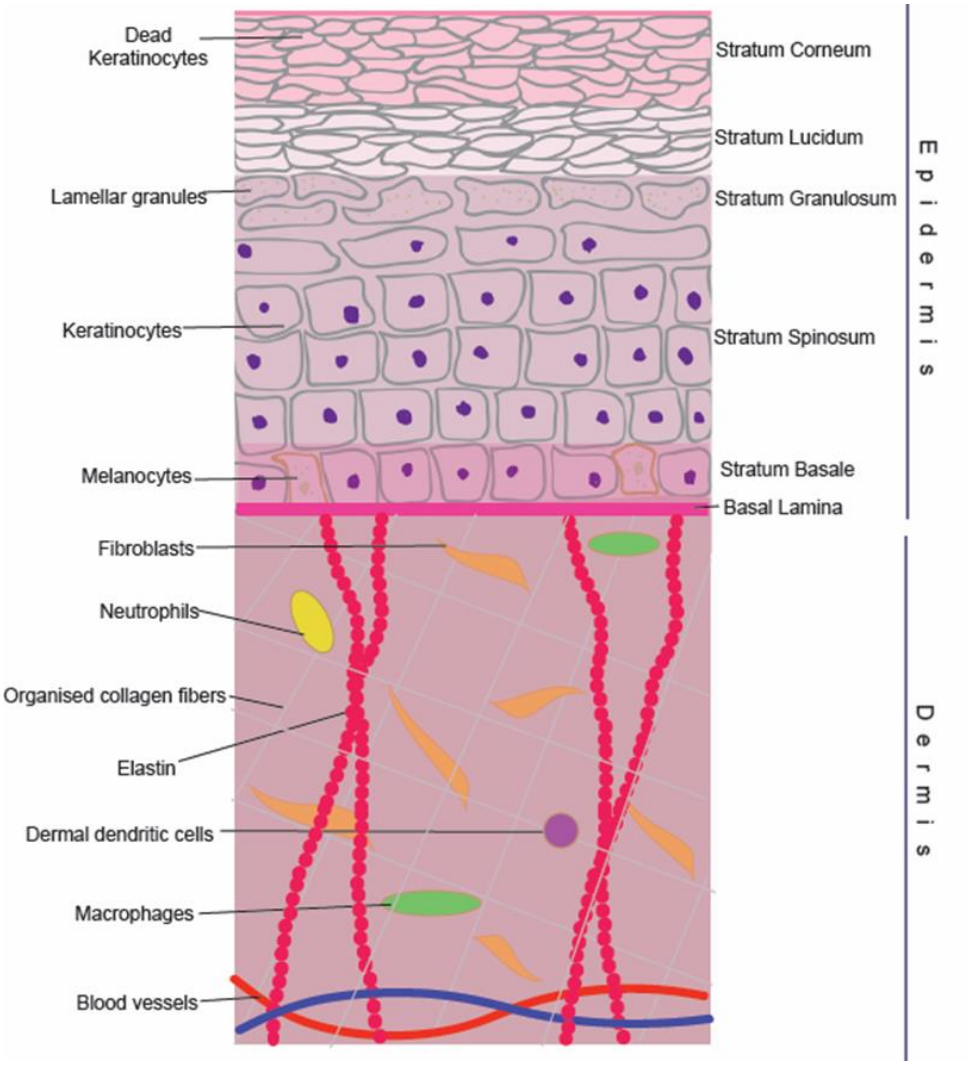

Figure 1.5 The mammalian skin structure.

The skin is composed of three two primary layers: the epidermis and the dermis. The dermis is mainly composed of layers of keratinocytes, as they migrate to the stratum corneum they become terminally differentiated. Between the epidermal and dermal layers is the basement membrane. The dermis is composed of extracellular matrix components of collagen, elastin and glycosaminoglycans and can be subdivided into the papillary dermis and reticular dermis. Figure comprised using information from (Menon, 2002).

1.8 Skin aging

Skin aging is a process in which intrinsic and extrinsic factors lead to gradual loss of structural integrity and physiological function of skin (Makrantonaki and Zouboulis, 2007). Intrinsic aging is the natural aging process and is related to genetically pre-determined rates such as ethnicity, hormones and underlying anatomy. Extrinsic aging is caused by external damaging factors, such as exposure to pollution, chemicals, and UV light. Exposure to UV light (photo-aging) is the predominant factor leading to pre-mature skin aging and is thought to contribute to 90% of visible skin aging. Excess UV light is extremely damaging to the skin and can lead to inflammation, pre-mature aging, and development of cancer.

UV damage imitates a complex series of biochemical reactions in the skin, which ultimately leads to the physical changes associated with aging such as wrinkling, and hyperpigmentation. Underlying these physical changes are significant structural changes within the skin including thinning of epidermis, degradation of elastin and formation of abnormal fibre bundles, changes in collagen organisation and a reduction in melanocyte number (Fisher et al., 2002).

1.9 Inflammation in skin

Inflammation is a multicomponent response to tissue stress, damage, wounding and infection. The process of inflammation is complex, requiring co-ordinated responses from several different cell types, which is conducted through activation and expression of different pro-inflammatory mediators such as cytokines and growth factors (Medzhitov and Horng, 2009). These mediators act to both induce signal transduction pathways and promote infiltration and activation of immune cells.

The inflammatory response is normally beneficial to human skin, helping the wound healing response after injury and to fight infection. However, when the inflammatory response is not regulated correctly it can lead to the development of skin disorders such as psoriasis and eczema as well as pre-mature aging (Kähäri and Saarialho-Kere, 1997). Dysregulation of matrix metalloproteinases, (MMPs) which play an important role in the degradation and maintenance of the extracellular matrix, have been linked to several skin diseases including bullous diseases, also known as skin blistering diseases, which are characterised by a breakdown of structural proteins that maintain cell-cell and cell-matrix adhesion in the skin (Mihai and Sitaru, 2007). Examples are granulomas, which are masses of granulation tissue typically produced in response to immune response due to altered ECM deposition, and dermal fibrosis such as that found in systemic scleroderma in which formation of excess fibrous connective tissue leads to scarring and thickening of skin (Kähäri and Saarialho-Kere, 1997).

1.10 Matrix metalloproteinases

Matrix metalloproteinases (MMPs) are a family of zinc endopeptidases which function in the maintenance of the extracellular matrix (ECM). These enzymes are synthesised by several different cells including fibroblasts and keratinocytes in response to exogenous signals such as cytokines and growth factors (Kähäri and Saarialho-Kere, 1997). There are 23 human MMPs which can be classified into 5 main groups based on their ECM substrate specificity: Collagenases, Gelatinases, Stromelysins, Matrilysins and membrane-type MMPs Table 1:1). The main role of MMPs is the remodelling, healing and repair of tissue, although in recent years it has become apparent that MMPs have a broad range of physiological effects including cell migration, modulation of the cell environment, progression of disease and immune responses (Nagase et al., 2006, Murphy and Nagase, 2008).

In normal, sun protected skin, MMP expression levels are very low, but under inflammatory conditions their expression is greatly increased. UV irradiation induces inflammatory cytokines such as interleukin-1 and tumour necrosis factor-α which co-ordinately induce MMPs (Newby, 2006). The induction of MMPs such as MMP1, MMP9 and MMP12 lead to degradation of collagen and elastin within the dermis (Quan et al., 2009, Tewari et al., 2014). It is the increased expression of these MMPs following UV irradiation which is thought to play a major role in the development of skin morphology associated with aged skin (Makrantonaki and Zouboulis, 2007).

Despite these negative effects associated with overexpression of MMPs, there are circumstances where high expression of MMPs are required. For example, within wounded skin, where MMPs are crucial for the remodelling and repair of the extracellular matrix. Within wounds, certain MMPs promote re-epithelialisation and the migration of epithelial cells across the wound bed, and by degrading/modifying the ECM at the wound site promote healing whilst reducing fibrosis (Rohani and Parks, 2015)

Due to the activity of MMPs on ECM, regulation of expression and activation is tightly controlled. MMPs are secreted as proenzymes and require cleavage to their active forms. Additionally, there are four groups of endogenous tissue inhibitors of metalloproteinases (TIMPs), which are capable of inhibiting all the active forms of MMPs (Nagase et al., 2006).

Table 1:1 Summary of 23 identified human matrix metalloproteases, common names and ECM substrates.

Information for this table adapted from (Newby, 2006, McCawley and Matrisian, 2001, Itoh, 2015).

Protease	ECM substrates
Collagenases	
MMP-1 (Collagenase 1)	Collagen types I, II, III, VII, VIII, X, and gelatin, aggrecan, casein, nidogen, serpins, versican, perlecan, proteoglycan link protein, and tenascin-
MMP-8 (Collagenase 2)	Collagen types I, II, III, V, VII, VIII, X, and gelatin, aggrecan, laminin, and nidogen
MMP- 13 (Collagenase 3)	Collagen types I, II, III, IV, V, IX, X, XI, and gelatin, aggrecan, fibronectin, laminin, perlecan, and tenascin
Gelatinase	
MMP-2 (Gelatinase A)	Collagen types I, IV, V, VII, X, XI, XIV, and gelatin, aggrecan, elastin, fibronectin, laminin, nidogen, proteoglycan link protein, and versican
MMP-9 (Gelatinase B)	Collagen types IV, V, VII, X, and XIV, fibronectin, laminin, nidogen, proteoglycan link protein, and versican
Stromelysins	
MMP-3 (stromelysin 1)	Collagen types II, IV, IX, X, and gelatin, aggrecan, casein, decorin, elastin, fibronectin, laminin, nidogen, perlecan, proteoglycan, proteoglycan link protein, and versican
MMP-10 (stromelysin 2)	Collagen types III, IV, V, and gelatin, fibronectin, laminin, and nidogen
Matrilysin	
MMP-7 (Matrilysin 1)	Collagen types I, II, III, V, IV, and X, aggrecan, casein, elastin, enactin, laminin, and proteoglycan link protein
MMP-11 (Stromelysin 3)	Laminin
MMP-26 (Matrilysin 2)	Gelatin, collagen IV, fibronectin, fibrinogen
Membrane Type MMPs	
MMP-14 (MT1-MMP)	Collagen types I, II, III, and gelatin, aggrecan, dermatan sulphate proteoglycan, fibrin, fibronectin, laminin, nidogen, perlecan, tenascin, and vitronectin
MMP-15 (MT2-MMP)	Collagen types I, II, III, and gelatin, aggrecan, fibronectin, laminin, nidogen, perlecan, tenascin, and vitronectin
MMP-16 (MT3-MMP)	Collagen types I, III, and gelatin, aggrecan, casein, fibronectin, laminin, perlecan, and vitronectin
MMP-17 (MT4-MMP)	Gelatin, fibrin, fibronectin
MMP-17 (MT4-MMP)	Gelatin, fibrin, fibronectin
MMP-24 (MT5-MMP)	Fibronectin, proteoglycan, gelatin
Other MMPs	
MMP-12 (Macrophage metalloelastase)	Elastin
MMP-20 (Enamelysin)	Amelogenin, aggrecan
MMP-23 (CA-MMP)	Gelatin
MMP-27	No substrates defined
MMP-28 (Epilysin)	Casein

1.11 The inflammatory response and wound healing

Wounding healing is a process by which skin tissue is remodelled and repaired after injury which induces a pro-inflammatory response. Wound healing is made up of three basic phases: Inflammation, proliferation and maturation, and requires the co-ordination of many different cell types including immune cells, keratinocytes and fibroblasts (Li et al., 2007).

Upon injury of the epidermis, keratinocytes secrete several cytokines and chemokines including interleukin 1 (Barrientos et al., 2008) a pro-inflammatory cytokine which acts to stimulate and recruit inflammatory cells such as macrophages and monocytes to the site of injury. With the recruitment of inflammatory cells, additional inflammatory mediators are expressed including growth factors such as fibroblast growth factor and endothelial growth factor. These growth factors help to promote migration of epithelial cells surrounding the wound site. In order to aid the migration of epithelial cells across the open wound site, epithelial cells secrete more cytokines and chemokines leading to the secretion of matrix metalloproteinases which function to remodel the matrix to aid wound healing and re-epithelialisation (Barrientos et al., 2008).

1.12 Modelling inflammation

To model inflammation in *in vitro* studies, cytokines are commonly added to cell cultures to induce inflammatory effects.

IL-1A is associated with both acute and chronic inflammation, and as such is one of the primary cytokines that propagates inflammation. Secretion of IL-1A by cells in response to inflammation leads to the activation of several signal cascades and the expression of secondary mediators including pro-inflammatory factors, growth factors and adhesion molecules (Magcwebeba et al., 2012). Addition of IL1 has been well established in vitro cell cultures to effectively induce inflammatory effects leading to a multitude of biological responses normally seen in inflammation (Dinarello, 2011, Dinarello, 1988). As such, use of IL1 in *in vitro* and in vivo models, has become a well-used approach to study chemo-prevention to reduce or prevent cancer, inflammation and toxicity.

Another key cytokine in mediation of inflammation, particularly within skin is Oncostatin M. Oncostatin M belongs to the interleukin-6 family of cytokines, and is synthesised by monocytes, dendritic cells and T-cells (Hermanns, 2015). Oncostatin M is an important cytokine in cutaneous inflammation and has been shown to have a potent effect on the migration of keratinocytes in vitro. Additionally, Oncostatin M expression has been found to be significantly increased in the inflammatory skin diseases psoriasis and atopic dermatitis, highlighting its important role in skin inflammation (Boniface et al., 2007).

Together the addition of these two cytokines to *in vitro* skin models facilitate effective modelling of inflammation of the skin.

1.13 Current models for skin studies

In the past, animal models such as mice were commonly used to study potential dermatological treatments and new pharmaceuticals. Now, *in vitro* skin models such as normal human keratinocytes (NKEK), and human skin keratinocyte cell lines (HaCaT) are commonly used alongside or in place of animal models. In addition, recent developments in human "skin equivalents" and other models have enabled more physiological *in vitro* analysis. The current skin models used for researching skin diseases, and topical drug treatments *in vitro, in vivo* and *ex vivo*, are considered below.

1.13.1 Normal human keratinocytes and HaCaT cells:

Normal human keratinocytes (NHEKs) are isolated from normal human epidermis. NHEKs make an ideal *in vitro* model as they generally display the endogenous biochemical processes performed by keratinocytes in the skin. However, NHEKs are difficult to culture, and are only able to be passaged a limited number of times, which has led to alternative cell types being developed for *in vitro* culture (Liu et al., 2012). One of the most widely used alternative cell type is the immortalised human skin keratinocyte (HaCaT).

HaCaT cells have many attractive features for an *in vitro* keratinocyte differentiation model; they can be grown and cultured in traditional media for long periods of time, they maintain their epidermal differentiation capacity, and remain non-tumorigenic (Liu et al., 2012, Deyrieux and Wilson, 2007). These features have led to HaCaT cells becoming the most widely used cell culture for research on skin diseases.

These *in vitro* cell model cultures form a single monolayer, and therefore do not mimic the *in vivo* multicellular structure of skin. Co-cultures have therefore been developed to try and mimic *in vivo* skin more effectively. Co-cultures were first demonstrated to be possible in 1975, where keratinocyte growth was stimulated by co-cultured fibroblasts (Schoop et al., 1999). Since this pioneering work, more complex *in vitro* models have been subsequently developed, such as organotypic cultures, and living skin equivalents.

1.14 Organotypic skin cultures

In recent years the use of organotypic skin cultures for studying skin diseases, and drug interactions has greatly increased compared to other systems such as living dermal equivalents. Organotypic skin cultures offer a way to grow complex biological tissues in 3D, and therefore study *in vivo*- like behaviour within an *in vitro* environment. A basic skin model consists of a collagen-rich stroma

dominated by fibroblasts and topped with stratified epidermis. In addition, other cells can be incorporated into the basic keratinocyte and fibroblast model if required, such as melanocytes and immune cells (Oh et al., 2013).

Although organotypic skin cultures provide an effective model for *in vitro* study of skin diseases, and pharmacological drug screening, complex systemic responses are not able to be studied within this model, and it only shows part of normal skin organisation and function (Oh et al., 2013). In addition, the micro-anatomy of OCSs is much simpler than that of skin, and it lacks signalling feedback. These features therefore limit the use of OCSs for studying more complex processes such as wound healing.

1.14.1 *In vivo* animal models

Although cell models such as those described above offer a good way to analyse effects of pharmaceutical applications, as well as under environmental stresses, they have several disadvantages. The main disadvantage is that they are not able to model the complexity of human skin in particular since the epidermis in mice comprises far fewer layers of cells than in man (Zomer and Trentin, 2018) and other parameters are different, for example mechanisms of wound healing (Nunan et al., 2014, Dunn et al., 2013).

Despite these differences, animal models such as mice, rabbits, rats and pigs (Avci et al., 2013) have been used commonly to analyse potential new pharmaceuticals. Over the years in addition to 'normal' control animal models, many transgenic models have been developed for different skin diseases, including the flaky tail mouse for atopic dermatitis, SKH-1 hairless mice for studying photo-aging and photo-carcinogenesis, and EB mouse models for the study of Epidermolysis bullosa (Avci et al., 2013). These models have enabled specific aspects of skin diseases to be well studied and have led to many breakthroughs concerning the underlying mechanisms of these diseases.

Testing human skin directly *in vivo* is the only way to determine effects on humans reliably, but, this would not be ethical nor possible to perform on sufficient numbers of volunteers with an untested drug and is used only in the final stages of drug development. However, *ex vivo* human skin explants offer a means to test biological effects of compounds on cultured human skin and may offer a more efficient and accurate model for research.

1.14.2 Skin explant organ culture

Skin explant organ culture provides a very efficient and accurate means to study skin biology. The considerations that need to be made when using skin explants are the morphology of the explants, and the ethics surrounding skin explants.

Early studies demonstrated that skin could be kept in organ culture in a defined medium for up to 8 days with preserved morphology, cell migration and DNA synthesis (Tammi et al., 1979, Gaylarde Pm Fau - Sarkany and Sarkany). This early work demonstrated that it was possible to effectively use skin explants *in vitro* for research purposes.

After these early studies, skin explants became more regularly used to examine different aspects of skin biology, in addition to drug development for skin treatments and topical applications. Backvall et al. (2002) described the use of a skin explant model to examine responses to UV-irradiation. Crucially, it was determined that the epidermal UV-responses and repair responses in skin organ cultures were very similar to those typically observed *in vivo*. Therefore, skin organ cultures offer a valuable tool for studies of the effects of UV-irradiation and subsequently, photo-aging and skin cancer.

More recently, skin organ culture has also been shown to provide a good model for the study of oxidative stress and inflammation in response to UVB-induced photodamage (Portugal-Cohen et al., 2011). Currently no *in vitro* models are available to study human skin barrier repair, although a study published in 2015 demonstrated that *ex vivo* human skin offers a suitable model for this type of research (Danso et al., 2015). This demonstrates the importance of human skin explants as a model for the study of skin biology.

Finally, the skin culture organ model has been shown to more accurately reproduce the biological responses seen *in vivo* compared to other *in vitro* cultures (Liu et al., 2014). Skin organ culture models will help the study of the true biological mechanisms and responses of topical drug application *in vitro*, which cannot be obtained from currently available *in vitro* culture models, or *in vivo* animal models.

1.15 Models for skin wound healing

1.15.1 Scratch wound healing model

Wound closure is a complex process involving numerous factors. Wound healing can be broadly divided into three phases: inflammation (as described above), proliferation and remodelling (Singer and Clark, 1999), see Figure 3.8. Inflammation is the first stage of wound repair and is typified by the migration of immune cells such as neutrophils and monocytes to the wound site. Next, new tissue is formed though proliferation and migration of various skin cells. During this step, re-epithelialisation takes place, whereby the wound is covered via keratinocytes. Finally, remodelling of the wound granulation tissue takes place (Loo et al., 2011).

The scratch-wound model is commonly used to replicate accurately the *in vivo* proliferation and migration of keratinocytes during reepithelialisation. In the scratch wound model, cells such as HaCaT keratinocytes or Fibroblasts, are grown *in vitro,* and mechanically wounded (Loo et al., 2011).

These wounded cells are then monitored, together with application of any required drugs or stress inducers, to determine wound responses. Use of mono-layer cultures are effective in allowing researchers to investigate the effects of compounds/treatments on responses in specific cell types. However, as discussed above, this approach is not able to model wound healing fully, as the physiological complexities of human skin cannot be completely reproduced by simple cell cultures (Xu et al., 2012).

Organotypic cultures as described earlier, have also been utilised for wound healing studies., in which incisional wound healing can be investigated (Oberringer et al., 2007) Although these cultures offer a more complex system than mono-layer cell cultures to investigate wound healing, they are still not able to replicate fully wound healing, mechanistically.

1.15.2 Animal models of skin wound healing.

In vivo animal models have also commonly been used to study the process of skin repair, however, as discussed earlier, animal models show several differences to humans, which can influence the observed results. Additionally, wounded mice and rats, commonly used to study wound healing, heal by contraction of the subcutaneous muscle rather than by re-epithelialisation as seen in humans (Steinstraesser et al., 2010). This difference in the wound healing mechanism means that the use of mouse and rat wound models for the quantitative and qualitative evaluation of wound healing is limited.

To replicate the human mechanism of wound healing in murine models, wound splinting is now widely used to eliminate wound contraction. The addition of a silicone ring around the edge of the wound allows for wound healing to occur via re-epithelialisation (Galiano et al., 2004). However, wound splinting may cause inflammation, and thereby interfere with the wounding response. Additionally, wound splinting does not address some of the underlying differences between murine and human skin wound healing in terms of gene expression. For example, Epidermal growth factor receptor (EGFR), a factor important in the regulation of wound healing in humans, is not expressed to the same high levels in mice, and as such treatments targeting EGFR do not have the same biological effects in mouse models (Zomer and Trentin, 2018).

1.15.3 Human skin ex-vivo explant wound healing models

Recently, effective skin explant-based models have been described for the study of wound healing (Ud-Din and Bayat, 2017). As discussed earlier, skin explants fully represent the *in vivo* complexities of human skin, and therefore offer the best way in which to study a complex process such as wound-healing.

Several methods have been described in relation to *ex vivo* skin culture. Xu et al. (2012) used a partial thickness human skin *ex vivo* model for study of cutaneous wound healing. Within this

model, a thin layer of skin with complete epidermis and partial-thickness dermis was cultured on a thin nylon mesh and fixed with sutures. This culture method allowed for a liquid-air interface thereby replicating *in vivo* skin conditions. Incisional skin wounds were made through the epidermal layer of skin using a scalpel, and wounded skin was studied over 14 days. This study demonstrated that skin explants are still physiologically comparable *to in vivo* skin for at least a week of culturing, with differentiation, proliferation and migration of keratinocytes maintained until day 12. Additionally, wound healing was observed, with wounds showing epithelial differentiation and proliferation in the epidermis, and collagen deposition in the dermis (Xu et al., 2012). This study therefore demonstrated that skin explants offer a unique and physiologically relevant model in which to study wound healing, and the effect of treatments on wound healing.

This model has now been developed further into the so-called donut-shaped wound healing model. The donut-shaped wound healing model differs from the method described by Xu et al. (2012) in that rather than a excisional wound made with a scalpel, the donut-model wounds skin by making taking a small punch biopsy (4mm wound) inside a 8mm full tissue biopsy.(Sebastian et al., 2015). In addition, the donut-model does not require skin explants to be cultured on a mesh, or to be fixed with sutures, and the wound will be a standardised diameter throughout making for more readily quantifiable analysis of wound healing. This model has been shown to be suitable for the study of cutaneous wound healing, and given the use of standardised punch biopsies offers a good standardising method of wounding which can be replicated accurately (Sebastian et al., 2015), in addition to showing wound healing in a model physiologically the same as *in vivo* human skin.

1.16 Summary

Plant polyphenols have huge potential for use in medical treatments of human diseases. The compound resveratrol has been shown to have a wide range of biological activities from anti-inflammation, to anti-carcinogenic properties, although its low bioavailability is currently limiting further development for pharmacological uses. Pterostilbene, the methylated derivative of resveratrol has been shown to have very similar biological functions as resveratrol, in addition to a higher bioavailability, and therefore could be a more suitable compound for development into medicinal treatments.

Considerable research on the activity of plant polyphenols has been focused upon oral intake, although this mechanism is extremely inefficient, and leads to only a very small concentration of active compound in biological systems. An alternative mode of treatment is topical application, which has been shown to offer a biological comparable mode of treatment and may offer a method of more targeted treatment.

As such, treatment of resveratrol and pterostilbene has been shown to have potentially beneficial effects for skin health in multiple *in vitro* studies, and animal models. However, these models are not an accurate representation of the intricate structure of human skin, and therefore results cannot be extrapolated accurately to biological effects from these models to humans. Development of an *ex vivo* skin model therefore offers a unique opportunity to investigate the biological effects of bioactive compounds on full thickness human skin.

1.17 Project aims

Metabolic engineering of plants offers a unique opportunity to improve the production of medicinal compounds within plants. During my research I aimed to:

- Generate two transgenic high-stilbene tomato lines, one to accumulate high levels of resveratrol and its methylated derivative pterostilbene. A metabolic engineering strategy was developed to modify a previously engineered ResTom tomato line to improve its overall performance whilst maintaining its high production of resveratrol. Using this line, a second transgenic plant was engineered to incorporate resveratrol-o-methyltransferase in order to allow the production of pterostilbene, a methylated derivative of resveratrol.
- Using an *ex vivo* skin explant system, the biological activity of wild-type (Money maker) and ResTom extracts were investigated in human skin to establish the biological activity of tomato juice and determine how enhancement of juice with bioactive phytochemicals can improve biological activity. Furthermore, the biological activity of resveratrol containing tomato extracts was briefly compared to pterostilbene containing tomato extracts to investigate if the structural stability of pterostilbene increases bioactivity of tomato juice, and overall function.

Chapter 2: General Materials and Methods

2.1 Plant general methods

2.1.1 Chemicals

All chemicals used for Plant research were of molecular biology grade and obtained from Invitrogen, Promega, Roche, Qiagen, Sigma, BioRad, Melford Laboratories and New England BioLabs. Chemicals for HPLC were purchased from Fischer Scientific.

All skin culture reagents were from Gibco Invitrogen Corporation, and tissue culture plastics from Nunc Thermo Fisher Scientific. Unless otherwise stated, chemical reagents were purchased from Sigma-Aldrich Inc.

2.1.2 Purified Polyphenols

The stilbenes, resveratrol, polydatin, pterostilbene and pinostilbene were purchased from Sigma-Aldrich Inc.

2.1.3 Enzymes

All restriction enzymes used for the generation of constructs for transformation were purchased from New England Biolabs, Invitrogen or Roche. The polymerases for amplification of PCR products were from Qiagen (Taq polymerase) or Thermo Scientific (Phusion® High-fidelity DNA polymerase). BP clonase™ and LR clonase™ for generation of constructs using Gateway® technology were supplied with Gateway® BP clonase II® enzyme mix and Gateway® LR Clonase® II enzyme mix (Thermo Fisher-scientific).

2.1.4 Antibiotics

Antibiotics were used for the selection of bacteria and transgenic plant material as required. Stock and working concentrations are shown in Table 2:1.

Table 2:1 : Working antibiotic concentrations

Antibiotic	Purpose	Working Concentration (µg/ml)	Original stock concentration (mg/ml)
Kanamycin	For selection of E. *coli* For selection of transformed plants	100 100	100 100
Carbenicillin	For selection of Agrobacterium AGL-1	50	50
Chloramphenicol	Gateway cloning	34	34
Gentamycin	Gateway Cloning For selection of Agrobacterium GV 3101	50	50
Rifampicin	For selection of Agrobacterium	50	50
Timentin	For selection of transformed plants	320	-
Zeatin riboside	For selection of transformed plants	2	-
Cefotoxamine	For selection of transformed plants	250	-

2.1.5 Plant Material:

WT tomato (*Solanum lycopersicum* var. Money Maker) was used for plant transformation. Transgenic tomato ResTom (35S: StSy, E8:*At*MYB12) in MoneyMaker, E8:AtMYB12 in MoneyMaker, and Bronze (E8: Myb, E8: Del/Ros, 35S: StSy) tomato lines were obtained from lab stocks. E8: StSy, E8:*At*MYB12, and E8: ROMT, E8:*At*MYB12 lines were crossed by Dr. Eugenio Butelli (Martin Lab, JIC). Bronze MoneyMaker was crossed with E8:*At*MYB12, E8: ROMT lines by Dr. Eugenio Butelli.

2.1.6 Seed isolation and sterilisation

Seeds harvested from mature fruits were incubated with 50% HCL for 15 minutes with shaking at room temperature. Seeds were washed, before being incubated with 10% Na_3PO_4 for 15 minutes with shaking at room temperature. Seeds were washed again and left to dry for 2-3 days before storage.

2.1.7 Bacterial strains:

The bacterial strains used for the expression and maintenance of plasmids were E. *coli* DH5- α and the Agrobacterium strains GV3101 (for transient transformation) and AGL1 for (stable transformation). Strains were grown in medium according to Table 2:2, with appropriate antibiotic selection for plasmids.

Table 2:2 bacterial strains and growth conditions required
LB= Lysogeny Broth, TY= Tryptone, Yeast media

Plasmid/strain	Description	Liquid media	Solid Media	Antibiotic	Growth conditions
DH5- α	E. *coli*	LB	LB	Kanamycin	37°C liquid cultures require shaking
GV3101	A. *tumefaciens*	TY	TY	Rifampicin Gentamycin	28°C liquid cultures require shaking
AGL-1	A. *tumefaciens*	TY	TY	Rifampicin Carbenicillin	28°C liquid cultures require shaking

2.1.8 Plasmids

Vectors used and constructed are listed as in Table 2:3

Table 2:3 Vectors used

Name	Size (bp)	Purpose	Selective Antibiotics	Supplier/Reference
pGEM-T easy	3003	Cloning PCR products	Ampicillin	Promega
pDONR-207	5585	Gateway donor vector	Gentamycin, Chloramphenicol	Invitrogen
pBin19-E8-AtMyb12	15375	Backbone for pJAM 2253	Kanamycin	Dr Eugenio Butelli
pJIT60-E8-VVStSY	6380	Vector containing StSy gene	Kanamycin	Dr Eugenio Butelli
pJAM 2252	17810	Stable transformation (E8:GW/E8:Myb12 in pBin19)	Kanamycin	Dr Eugenio Butelli
pJAM 2253	19039	Stable transformation (E8: StSy/E8:MYB12 in pBin19)	Kanamycin	This Thesis
pJAM 2254	20328	Stable transformation (E8: ROMT/E8:MYB12 in pBin 19)	Kanamycin	This Thesis
pJAM 2255	19766	Gateway cloning (E8:GW/E8:GW/E8:MYB 12 in pBin19)	Kanamycin	Dr Eugenio Butelli
pJAM 22556	23413	Stable transformation (E8: ROMT/E8: StSy/E8:MYB12 in pBin 19)	Kanamycin	This Thesis

2.1.9 Medium recipes

Recipes for media used to grow bacteria, *Agrobacterium tumefaciens* and for tomato transformation are shown in Appendices.

2.1.10 Primer design and supply:

Primers were designed using the online open web software Primer3Plus (www.bioinformatics.nl/primer3plus*)*, and synthesised and supplied by sigma. Primers were designed to have a GC content of between 40-60% and primer pairs to have matching melting temperature (Tm) values. To confirm gene presence, primers were designed to align with coding sequences. For resveratrol-o-methyltransferase primers were designed to with exon-exon junctions to only amplify cDNA rather than genomic DNA. For Gateway cloning *att*B1 and *att*B2 sites were added to the 5'end of the forward and reverse primers. (Details of primer sequences can be found in appendices, Table S 1).

2.1.11 PCR

PCR reactions were performed using Taq DNA polymerase (Qiagen) for colony PCR. Phusion® High-fidelity DNA polymerase was used for the cloning of gene and cDNA sequence. Go Taq green master mix (Promega) was used for genotyping of transformations. PCR conditions varied based upon the annealing temperatures of primers, the length of the expected product and the polymerase used, standard PCR protocol is outlined in Table 2:4. A standard PCR reaction mix contained 20-50 ng of template, 0.1 µM of each mix (containing 100 µM of dNTPs, 1x concentration of DNA polymerase and 1x concentration of buffer in a total volume of 15 µl.

Table 2:4 Standard PCR conditions

	Step	Time	Temperature(°C)
	Initial denaturation	04:00	94
Cycling x 30-40	Denaturation	00:45	94
	Annealing	00:30	60
	Extension	01:00	72
	Final extension	05:00	72

2.1.12 Agarose gel electrophoresis

PCR and restriction digests were run on 1% agarose gels in 1x Tris Borate EDTA buffer (TBE 10x: 0.89 mM Boric Acid and 20 mM EDTA; pH 8), and ethidium bromide used to visualise DNA on the gel. A 2-log DNA ladder (New England Biolabs) was used for size estimations.

2.1.13 Purification of DNA bands from agarose gels

After running PCR products on agarose gels, DNA bands were visualised using a long wavelength UV transilluminator. The required bands were cut out of the gel using a sterile scalpel blade, before purifying according to Qiagen purification protocol.

2.2 Methods of construct design:

2.2.1 Bacterial transformation

Heat shock transformation was used to produce competent DH5- α cells with desired plasmid. Competent DH5- α cells from -80°C were thawed on ice, and 10-50 ng of desired plasmid mix was added before incubating on ice for 30 minutes. The mix was then heat shocked at 42°C for 1 minute before incubating on ice for 3 minutes. 900 µl LB medium was added to the cells, and the mixture incubated at 37°C with shaking for 2 hours. The cells were then pelleted by centrifugation at 8,000rpm, for 2 mins and resuspended in 100 µl of LB. A total of 20 µl of cells was plated onto LB agar containing suitable selective antibiotics and incubated overnight at 37°C.

2.2.2 Plasmid DNA isolation for E. coli

E. coli containing plasmid was grown up in 10 ml LB overnight. The culture was centrifuged at 2000 x g for 5 minutes, and the resulting pellet used in the Qiagen mini-prep protocol. Briefly, the pelleted bacterial cells were resuspended in 250 µl buffer P1 and transferred to a micro-centrifuge before adding 250 µl buffer P2. The tube was inverted several times to mix gently. Once the solution became viscous and slightly clear, 350 µl buffer N3 were added, and the tubes inverted to mix. The mix was centrifuge for 10 mins at 13,000rpm, and the supernatant transferred to a QIAprep 2.0 spin column. The column was centrifuged for 30 seconds and the flow through discarded. The column was then washed with buffer PB followed by buffer PE, and the flow through discarded. Finally, the column was transferred to a new Eppendorf, and DNA eluted in 50 µl buffer EB.

2.2.3 Plasmid and PCR digests

Restriction digests of PCR products and vectors were performed using 0.5-1 µg plasmid or PCR DNA, 10-20 units of respective restriction enzyme (Table 2:5), and 1x final concentration of buffer and dH_2O to make up to the required reaction volume. Reactions were incubated for 1 hr at 37°C or the temperature specified for the enzyme. To check for successful digestion a small aliquot of digestion mixture was loaded on a 1% agarose gel, if only partial digestion was observed reactions were re-incubated for up to 4 hours. Digestive reaction was stopped by heat inactivation at 65° for 15 mins.

Table 2:5 Restriction enzymes

Restriction enzyme	Digestion of
Sst1	PBin19-E8-AtMyb12
Bgl II	PBin19-E8-AtMyb12
BamHF	PBin19-E8-AtMyb12-vvstsy
Sac 1 HF	PBin19-E8-AtMyb12-vvstsy
EcoR1	pGEM-T easy vector

2.2.4 Ligation

Ligation reactions were set up with a concentration of 3:1 of insert to vector DNA. Ligation reactions were made to a final volume of 10 µl, containing 2x rapid ligation buffer, 5-10 units of T4 DNA ligase and dH_2O. The reaction was performed overnight at 4°C.

2.2.5 Quantification of DNA

Purified DNA samples were quantified using a NanoDrop UV-Vis spectrophotometer (Thermo Scientific).

2.2.6 Gateway® cloning

The Gateway® recombination cloning technology (Invitrogen) allows the transfer of DNA sequences between plasmids using a set of recombinant Gateway® sites and BP and LR clonase enzymes. The gene of interest firstly requires amplification with gateway® primers to add attB gateway® sites (see

appendix for primer details). The gene of interest with attB sites is then moved pDONR-207 vector using BP clonase™ (Invitrogen) following the manufacturer's instructions, creating an entry vector. Recombination reactions were incubated at 16°C overnight. The reaction was stopped by adding 1 µl of proteinase K and incubation at 37° for 10 minutes. A total of 5 µl BP reaction mix was used for DH5-α transformation.

Next the gene of interest is shuttled to a destination vector using LR clonase™ (Invitrogen) following the manufacturer's instructions. The reaction was stopped by adding 1 µl of proteinase K and incubation at 37° for 10 minutes. A total of 5 µl LR reaction mix was used for DH5-α transformation. All LR and BP reactions were performed in a 3:1 ratio. Plasmid integration was checked via growth on plates with selective antibiotics and colony PCR.

2.3 Preparing constructs for transformation

2.3.1 Extraction of DNA from plant material

DNA was isolated from plant leaves using the Qiagen DNeasy kit following the manufacturer's protocol.

Plant tissue was disrupted using a mortar and pestle. To grind plant material, 400 µl Buffer AP1 (10 mM Tris-HCL pH 8, 1 mM EDTA pH 8, 0.1% SDS, 0.1 M NaCl, 1X polyvinylpyrrolidone, 10mM DTT) and 4µl RNase A were added before incubating for 10 minutes at 65°C. After incubation 130 µl of Buffer P3 (3 M potassium acetate pH 5.5) were added, before incubating on ice for 5 minutes. The lysate was then centrifuged at 20,000 x g for 5 minutes and transferred into a QIAshredder spin column before centrifuging again for 2 minutes at 20,000 x g. The flow through was transferred to a new tube, without disturbing the pellet and 1.5 volumes of Buffer AW1 (Wash buffer) were added. The mixture was transferred to a DNeasy mini column and centrifuged for 1 min at 6000 x g. The flow through was discarded and 500 µl Buffer AW2 (wash buffer) added before centrifuging at 6000 x g for 1 minute. This step was repeated a second time with the centrifugation time increased to 2 minutes. The spin column was transferred to a new microcentrifuge tube, and 100 µl Buffer AE (10 mM Tris-HCl, 0.5 mM EDTA, pH 9) were added to elute the RNA. Buffer AE was incubated on the spin column for 5 minutes at room temperature, before centrifuging at 6000 x g for 1 minutes. This last step was repeated, and the combined eluate was frozen at -20°C until required.

2.3.2 RNA extraction from leaves

Total RNA was isolated for plant leaves using the Qiagen RNeasy mini kit. Briefly, plant material was ground in liquid nitrogen and buffer RLT (lysis buffer) added before vortexing. The lysate was transferred to a QIAshredder column and centrifuged for 2 mins at full speed. The supernatant was added to 0.5 volume of 100% ethanol and mixed well, before transferring to a RNeasy spin column and centrifuging for 15s at 8000 x g. The flow through was discarded, and buffer RW1 added to the spin column before centrifuging at 8000 x g for 15 seconds. The flow through was discarded and

buffer RPE (Washing buffer) added to the spin column before centrifuging at 8000 x g for 15 seconds. This step was repeated, but for a longer centrifugation time of 2 minutes. To prevent any carry over of Buffer RPE, the spin column was transferred to a new 1.5 ml collection tube before centrifuging at maximum speed for 1 minute. The RNeasy spin column was transferred to a new collection tube, and RNA was eluted in 30 µl RNase free water. Quantity and quality of RNA was measured on a NanoDrop (Thermo Scientific) and stored at -20°C until required.

2.3.3 RNA extraction from tomato fruits

Tomato fruit were harvested at required developmental stages, sliced and seeds removed before being frozen in liquid nitrogen, and storage in -80°C until further use.

RNA was isolated using TRI Reagent. Tomato fruit tissue (200 mg) was ground in liquid nitrogen before adding 1.5 ml TRI Reagent. The homogenised sample and TRI Reagent were vortexed vigorously before incubating for 5 minutes at room temperature with shaking (in dark). After incubation, 150 µl 1-bromo-3-chloropropane (BCP) were added. The sample was mixed thoroughly for a minimum of 15 seconds before incubating for 10 minutes at room temperature with shaking (in dark). The sample was then centrifuged for 10 minutes at 12,000 x g at 4°C. The aqueous upper phase, containing RNA, was transferred to a new Eppendorf tube, taking care to not disturb the interface. To the aqueous phase, 750µl isopropanol were added before vortexing and incubating for 5 minutes at room temperature, allowing the RNA to precipitate. The sample was centrifuged for 8 minutes at 12000 x g at 4°C before discarding the supernatant and washing with 500 µl isopropanol. Without disturbing the pellet, the supernatant was removed, and the RNA pellet washed 1.0 ml of 75% ethanol. The supernatant was discarded and the ethanol washing step repeated before air-drying the pellet at room temperature for 5 minutes. The pellet was resuspended in 40 µl RNase-free water and incubated at 4°C for 60 minutes to dissolve the RNA. The sample was spun down at 12000 x g for 5minutes at 4°C and the supernatant transferred to a new tube. To the supernatant 4 µl 10 x DNase1 buffer and 4 µl 10 x DNase1 was added before incubating at room temperature for 45 minutes. The reaction was stopped by the addition of 4 µl 25 mM EDTA and incubation at 65°C for 10 minutes.

2.3.4 cDNA synthesis

DNase treated RNA (3 µg) was mixed with 1 µl of 10 mM primer mix (10µM oligo dT: 10µM random primers), 1 µl of 10 mM dNTPs, and RNase free water to a total volume of 20 µl. The mix was heated to 65°C for 5 minutes, before cooling on ice. Reverse transcription was performed using SuperScript™ III (Invitrogen) reverse transcriptase kit. To 20µl of primer annealed RNA, 6µl of 5x first strand buffer (250 mM Tris-HCl (pH 8.3), 375 mM KCl, 15 mM $MgCl_2$), 2µl of 0.1M DTT, 1 µl of RNA- guard (RNase inhibitor, Amersham) and 1 µl of superscript 3 (10,000 units total, at 200 U/µL)

were added, and mixed gently. The mix was then heated for 60 minutes at 50°C and 15 minutes at 70°C, before storing samples at -20°C.

2.4 Preparing competent *Agrobacterium tumefacien* cells

Competent *Agrobacterium tumefaciens* (GV3101) cells from a single colony were inoculated in 10ml LB supplemented with 50mg/L rifampicin at 28°C overnight. 2ml of overnight culture was inoculated into 100ml LB at 28° and incubated until a OD600 of 0.5-0.8 was reached. The culture was cooled down on ice, before transferring to pre-cooled 50 ml tubes. The tubes were centrifuged at 4000rpm for 15 mins at 4°C. The supernatant was removed, and pellet resuspended into 50 ml of cold 10% glycerol. The mix was centrifuged again at 4000 rpm for 15 mins at 4°, before resuspending the pellet into 25 ml cold 10% glycerol. Finally, the mix was centrifuge at 4000rpm for 15mins at 4° before resuspending the pellet into 2 ml cold 10% glycerol. The final culture was divided into 100 µl aliquots which were stored at -80°

2.5 Agrobacterium Transformation

Competent *Agrobacterium tumefacien* cells were thawed on ice, before adding 200 ng of Plasmid DNA. The mixture was incubated on ice for 30 minutes before electroporating at 2.5 kV, 400Ω for 10 seconds (BioRad Pulser). Growth medium was added straight to electroporated mix, before incubating with shaking at 28°C for 3 hours. The mix was then plated on plates containing suitable selective antibiotics and incubated for 2 days at 28°C.

2.5.1 Transient transformation

Plasmids maintained in *Agrobacterium tumefaciens*, strain GV3101 were used for agroinfiltration. Cultures were grown at 28°C with shaking to stable phase in LB medium supplemented with appropriate antibiotics. Cultures were centrifuged at 2000 x g for 5 minutes to pellet. The pellet was resuspended in MMA (10 mM MES pH 5.6, 10 mM $MgCl_2$, 100 µM Acetosyringone) to an OD_{600} of 0.3 before incubating at room temperature for 2-4 hours with shaking. For co-infiltration equal volumes of resuspension cultures were mixed together before incubating for 2-4 hours. Suspensions were pressure infiltrated into *Nicotiana benthamiana* leaves. After 5 days leaves were harvested and freeze dried for HPLC analysis, or frozen in liquid nitrogen for RNA extraction.

(a)

(b)

Figure 2.1 : Map of the pEAQ-Destination vectors used for transient transformation. (a) showing map of pEAQ-Dest1 with Stilbene synthase gene, and (b) with the resveratrol-o-methyltransferase gene

2.6 Stable transformation

2.6.1 Growth media and supplements

Media for the propagation of transformants were prepared freshy on the day for use, recipes can be found in the *Appendices*).

2.6.2 A. *tumefaciens* mediated tomato transformation

Firstly, tomato seeds (Money maker variety) were prepared for seeding onto germination plates by washing in 70% ethanol to loosen the gelatinous seed coating, and then incubating with 10% bleach for 3 hours with shaking. After washing the seeds, the treated seeds were plated, and stored for at least two weeks at 4°C. Seedlings were grown for 7-10 days with a 16-hour photoperiod.

A 24-hour culture of *Agrobacterium tumefaciens* AGL-1 containing the vector for transformation of tomato was set up at 28°C with shaking. The same day feeder plates were prepared by spreading 1ml of fine tobacco suspension culture onto plates containing MS medium+ vitamins, with 3% sucrose, 0.5 mg/L 2,4-D, and 0.6% agarose (kindly prepared by Matthew Smoker, TSL). Unsealed plates were incubated overnight in the cell culture room in low light levels.

Cotyledons aged between 7-10 days were harvested and placed in sterile water. The cotyledon tips were cut using a sterile scalpel blade to give two explants of 0.5 cm long, before transferring to another petri dish of sterile water to prevent any further damage.

At the same time the agrobacterium cultures were spun down at 4000 rpm for 5 minutes, and the pellet resuspended in MS + vitamins medium containing 3% sucrose, to an OD_{600} of 0.4-0.5. Cotyledon explants were immersed in the bacterial suspension, before blotting on sterile filter paper to remove excess solution. Feeder plates were collected, and sterile filter paper placed over the top of the tobacco cell suspension to prevent direct contact between the tomato explants and the tobacco suspension. Up to 40 cotyledon explants were placed on feeder plates, abaxil surface up. The feeder plates were then transferred to the culture room at 25°C under low light conditions to co-cultivate for 48 hours.

After the co-cultivation period, explants were transferred onto regeneration plates containing timentin at 320 mg/ml and zeatin riboside at 2 mg/L and the appropriate antibiotic to select for the T-DNA transformation marker. Cotyledons were placed adoxial side up, so they curled towards the medium ensuring good contact between the cut edges of the leaf and the medium. Between 12-16 explants were placed per plate. Plates were left unsealed and returned to the cell culture room for 2 weeks. The explants were left to generate calli and leaves, and were transferred to fresh medium every 2-3 weeks, containing in addition to timentin, 250 mg/L cefotoxamine.

Once shoots had developed from the calli, the shoot was excised from the callus structure and transferred to individual jars containing fresh rooting medium containing antibiotics for selection in addition to timentin at 320 mg/L. Multiple shoots could come from a single callus. Once the shoots had developed a well-formed root system they were transferred to soil and moved to the glass house. Positive transformants were identified by PCR specific for the target genes introduced into the plant.

2.6.3 Tomato crosses:

Transgenic parental lines (E8: StSy, E8:MYB12 and E8: ROMT, E8:MYB12) were crossed to create a T1 plant generation with the genes of interest. Tomato crosses were performed by Dr Eugenio Butelli. Briefly, tomato crosses were performed by removing the stamen of the flower of the female parent before the flower opened. One day after the removal of the stamen, the pollen from a flower of the male parent was brushed against the female stigma. Seeds were collected from fully matured fruits, as in Methods 2.1.6.

2.7 Quantifying gene expression

2.7.1 Real time quantitative-PCR (RT-qPCR)

Three independent biological samples of tomato fruit at breaker stage were pooled and RNA extracted as in (Methods 2.3.3). Expression of Stilbene biosynthetic pathway genes (primers in Table S 2) were measured by qRT-PCR using SYBR® Green Jumpstart™ *Taq* ReadyMix™ (Sigma). RNA quantity was normalised to the housekeeping gene GAPDH. For each qRT-PCR reaction 50 ng of cDNA were mixed with 5 µM forward and reverse primers, with 10 µl of SYBR® Green Jumpstart™ *Taq* ReadyMix™. PCR reactions were made to a total of 20 µl with RNase free water. All reactions were performed in triplicate, and real time detection was performed using an Opticon™ DNA Engine 2 thermal cycler (MJ research).

2.8 Human cell general methods

2.8.1 Cell culture

Both the human keratinocyte cell line (HaCaT; isolated by (Boukamp et al., 1988) originally obtained from the Fusenig laboratory by Dr Andrew Chantry) and mouse fibroblast cell line (3T3; from ATCC) were grown in high glucose Dulbecco's modified Eagle medium (DMEM, catalogue number: 11965092), liquid medium containing 100 units/ml penicillin/ streptomycin antibiotic, 5 mM L-Glutamine, supplemented with 10% (v/v) Foetal calf serum unless stated otherwise. Cells were incubated at 37°, 5% CO_2 and passaged at a 1:3 ratio every three days (depending on confluency) with 0.25% Trypsin. For experiments, cells were plated at a cell density of 100,000 in 24 well culture plates (unless stated otherwise). Fibroblasts were cultured by Dr Damon Bevan, (Gavrilovic group, UEA).

2.8.2 *Ex Vivo* explant assay

An *ex vivo* human skin explant model was developed with Dr Damon Bevan (UEA). For *ex vivo* skin cultures, skin explants donated human abdominal skin, (surplus to surgical needs performed by Prof Marc Moncrieff and his team at the Norfolk and Norwich University Hospital) with ethical approval (20142015 – 47 HT) was used. Subcutaneous fat was removed from the donated skin, before pinning skin samples out and taking 6mm diameter punch biopsies.

A

B

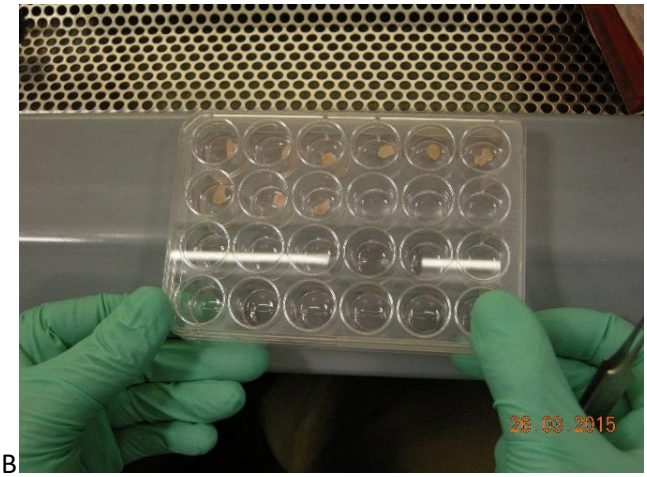

Figure 2.2: Images depicting two steps of the methodology used for collection of skin tissue.

A) Skin from which subcutaneous fat had been removed, was pinned down and 6mm biopsies taken. B) 6mm biopsies were washed in PBS, before transferring to a 24 well culture plate containing EpiLife® medium. Skin explants were submerged.

Cultured biopsies, termed explants, were washed in sterile PBS supplemented with gentamycin (125 µg/ml) and amphotericin B (1.87 µg/ml) before being added to a 24 well plate containing 500µl EpiLife® medium (*catalogue number MEPICF500)* supplemented with EpiLife™ defined growth supplement (*catalogue number: S0125*) in addition to gentamycin (75µg/ml), amphotericin B (1.125 µg/ml), and calcium chloride (1.2 mM). Explants were submerged in culture media. Additional biopsies were snap frozen on the day in liquid nitrogen or stored in RNA later as T-0 samples. In total 6 biopsies were taken for each condition, 3 for RNA extraction, 2 to be snap frozen, and 1 for

wax embedding. Experiments were carried out over a 5-day period (see timeline in figure), briefly, biopsies were cultured overnight. Media was removed and replaced with fresh EpiLife® supplemented as required for the different treatments (D1). For induction of inflammation the two cytokines Interleukin 1 (35 ng/ml) and Oncostatin M (100 ng/ml) were added as required. Tomato juice extracts were added directly to culture in wells as required in a 1 in 10 dilutions. Explants were cultured for another two days, before restimulation (D3), for this media was replaced with new media supplemented with required treatments. The explants were cultured for an additional two days, before collection on Day 5, explants were stored as stated above. Additionally, conditioned media from wells was collected at day 5 and snap frozen at -20°.

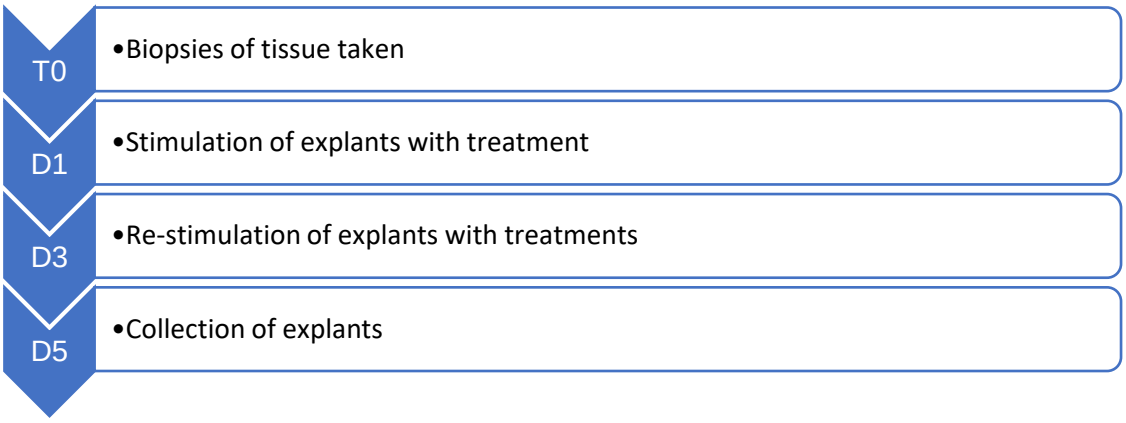

Figure 2.3 Experimental timeline for 5-day ex vivo skin experiments.

2.9 Cell and whole skin treatments

2.9.1 Inflammatory treatments

2.9.1.1 *IL1-alpha*

Stock solutions of Interleukin 1 alpha (IL1-alpha; R&D systems) were prepared by Dr Damon Bevan, UEA, to a dilution of 4 µg/ml. IL1-A was diluted to the final concentration of 35 ng/ml in the culture medium.

2.9.1.2 *OSM*

Stock solution of Oncostatin M (OSM; R&D systems) was prepared by Dr Damon Bevan, UEA, to a concentration of 20 µg/ml. OSM was diluted to a final concentration of 100 ng/ml in the culture medium.

A combination treatment of Il-1A (35ng/ml) and OSM (100ng/ml) was used to model inflammatory response in all experiments. This treatment combination is referred to either IL1/OSM or Cytokines.

2.9.2 Water-Based tomato extracts

Tomato juice extracts were prepared by Dr Eugenio Butelli, JIC, Cathie Martin Group. Tomatoes were cut up and homogenised a blender. The extract was centrifuged at 4°C at maximum speed for 20 minutes. After centrifugation, the top layer of the extract was removed to leave a clear extract which was passed through filter paper. The clear extract was stored at -80°C for a few hours before being moved to 4°C storage overnight, this process allows for the removal of pectin from the extract. The extract was then centrifuged again at maximum speed for 20 minutes at 4°C, and the clear supernatant filtered through a 0.22-µ filter before aliquoting into falcon tubes. Aqueous extracts were filtered again through a 0.22-µ filter under sterile conditions, before aliquoting into 1 ml Eppendorf's and stored at -80°C until required.

All aqueous tomato extracts were added direct to culture media in a 1:10 dilution, tomato extracts will be referred to as outlined in Table 2:6.

Table 2:6 Abbreviations used to describe tomato lines

Abbreviation	Tomato line details
MM (WT)	Wild type tomato, MoneyMaker line
ResTom	Original resveratrol producing tomato 35S: StSy/ E8:MYB12
Hi-Resv	New resveratrol tomato E8: StSy/E8:MYB12
PteroTom	Pterostilbene tomato E8: StSy/E8: ROMT/E8:MYB12

2.9.3 Methanol tomato extract preparation for cell studies.

Methanol extracts of tomatoes were made as outlined in (Methods 2.9.3, prepared by Dr Eugenio Butelli, JIC), a small quantity (100 µl) was taken for use in HPLC analysis, and the remainder concentrated using a rotary evaporator. The solvent was evaporated until the extracts were almost dry and had reached a gel-like composition. The tomato derived extracts were then re-dissolved at a 1:10 dilution in 50% MeOH (v/v). The resolubilised extracts were then stored at -20°C. A final concentration of between 0.1% and 1% of the methanolic tomato extract was used in cell culture. A 1% methanol tomato extract is the equivalent dosage as the 1:10 dilution of aqueous tomato extract used in cell culture media.

2.9.4 Preparation of purified resveratrol and polydatin

Plant polyphenols were purchased from Sigma and dissolved in DMSO to a final concentration of 50 mM

2.9.5 RNA extraction from whole tissue:

Skin explants were stored in RNA later after collection on day 0 and day 5, before storing at 4°C overnight, and then storing in -80°C until further use. RNA was isolated using Trizol (Reno et al., 1997). Skin tissue was cut into small pieces using scissors before adding to 600 µl Trizol. Tissue was then fully homogenised with ball bearings using the TissueLyser II (Qiagen) at 30 Hz. Samples were centrifuged at 14,000 x g for 10 minutes at 4°C and supernatant added to fresh tubes containing 200µl of chloroform. The samples were mixed thoroughly for a minimum of 15 seconds before centrifuging for 15 minutes at 14,000 x g. The aqueous upper phase containing RNA, was transferred to a new Eppendorf tube containing 200 µl of 95% ethanol, taking care to not disturb the interphase. After thorough mixing, the supernatant was transferred to a RNeasy mini spin column, before centrifuging for 20 seconds at 8000 x g and the supernatant disposed. Following this the membrane was treated with DNase to degrade any DNA contaminants. To remove all cell contaminants, and to further bind RNA to the membrane a series of washes were performed using buffer RW1 and RPE as according to the manufacturer. Following the wash steps, the membrane was dried, and purified RNA eluted in RNase-free water for storage at -20°C. Quality of RNA was checked (OD 260/280 ratio) by NanoDrop and concentration recorded. RNA purification of Skin tissue up to SPL011 was performed by Dr Damon Bevan, UEA. RNA from SPL012 and SPL013 was performed by undergraduate student Stuart Keppie.

2.9.6 Total RNA extraction from cell lines:

Total RNA was purified from keratinocyte and fibroblast cell lines using the RNeasy MiniKit (Qiagen) according to the manufacturer's instructions. Briefly, culture medium was removed from adherent cells, and cells were lysed in lysis buffer with β-mercaptoethanol. To cell lysis mix, 70% (v/v) ethanol was added to homogenise cells and promote binding of RNA to RNeasy mini sin column membrane.

The membrane was treated with DNase to degrade any DNA contaminants, before washing the membrane with wash buffer. After washing, the membrane was air dried before eluting purified RNA in RNase-free water for storage at -20°. All RNA purification steps were performed at room temperature, at 14,000 rpm. RNA yield was measured using the NanoDrop at 260 and 280nm.

2.9.7 Two step reverse transcription to cDNA using M-MLV

RNA was extracted as outlined above. RNA quantity and quality was measured using the NanoDrop ND-100 spectrophotometer (Nanodrop technologies). RNA concentration was measure at 260nm, and ratios of 260/280 and 260/230 were used to analyse quality of RNA. Samples with a ratio above 1.8 were deemed as high quality with respect to contaminants.

Purified RNA was diluted to a total of 500 ng/µl in RNase free water before mixing with random primers (0.5 µg/µg RNA) (Invitrogen), and heating to 70°C for 10 minutes to melt the secondary structures within the template. Samples were then immediately cooled on ice to prevent secondary structures reforming. To the annealed primer/template M-MLV transcriptase (200 µ/µg RNA), 0.2 mM dNTPs (Promega), and 5 µl 5x M-MLV reaction buffer (Promega) were added. Samples were made up to a total volume of 25 µl with Ribonuclease Inhibitor (Promega) before heating to 42°C for 50 minutes to allow for first strand cDNA synthesis. Enzyme activity was stopped by heating samples to 70°C for 10 minutes. Samples were stored at -20°C until required.

2.9.8 Quantitative Real-time PCR using dual labelled probes

Quantitative real time PCR (qRT-PCR) reactions were performed using the 7500 RT-PCR systems (applied Biosystems) according to manufacturer's instructions. Five nanograms of cDNA were used for gene expression analysis, with 2x qPCR MasterMix (PCR Biosystems) 100 nM each of forward and reverse primers, and 200nM of probe in a total volume of 15 µl. Standard TaqMan cycling conditions were used (Table 2:7). Gene expression was normalised using the relative standard curve method against expression of the 18S housekeeping gene (Table S 3 and Table S 4.) Cycle threshold values (C_T) cDNA within each sample were determined and normalised to the 18S cDNA for that sample. Data is represented as the level of target mRNA relative to the level of 18S mRNA in that sample or converted to fold change expression relative to 18S.

Table 2:7 Standard TaqMan cycling conditions for qRT-PCR using dual labelled probes. All data was collected under the Tamra channel.

	Step	Time	Temperature (°C)
Enzyme deactivation	Hold[a]	02:00	50
	Hold[b]	10:00	95
Cycling x40	PCR Melt	00.15	95
	Extension/annealing	01:00	60

2.9.9 Generation of custom primer/probe sets using the Universal ProbeLibrary

Custom made primer/probe sets for use with the universal ProbeLibrary (UPL, Roche), for use with qRT-PCR were designed using the UPL assay design centre. Assays were designed to be intron-spanning, to eliminate potential for amplification of any contaminating gDNA in samples. Designed primers were synthesised and ordered from sigma Aldrich and used in combination with the relevant UPL probe (Roche) labelled with 5' fluorescein (FAM) and 3'-end labelled dark quencher dye. In qRT-PCR reactions using UPL probes, primers were used at a concentration of 250 nM, and probes at 125 nM. The same standard taqman cycling conditions were used as with dual-labelled probes (Table 2:7), primer sequences and corresponding probes are in (appendices, Table S 3 and Table S 4).

2.9.10 Tissue embedding and sectioning:

Tissue embedding for SPL003-13 were carried out by Dr Damon Bevan, UEA. For all samples the protocol below was followed.

After the indicated number of days, skin explants were stored in 4% Paraffin wax or snap frozen in liquid nitrogen. Subsequently, tissue explants stored in 4% Paraffin wax were processed as follows using gentle agitation for 45 minutes: PBS x2, 50% EtOH, 70%EtOH, 95% EtOH, 100% EtOH x2, Clearene x 2, paraffin wax, overnight embedding in molten wax.

Snap frozen skin tissues were sectioned by Dr Damon Bevan into 10 µm sections with the Microm HM560 cyrostar cryostat (Thermo Scientific) before mounting on Poly-Lysine coated slides. Frozen sections were fixed in acetone and stored at -20°C prior to H and E staining and immunohistochemistry.

2.9.11 Haemotoxylin and Eosin staining

Paraffin embedded skin tissues were sectioned into 10 µm sections before mounting on PolyLysine slides. Tissues were deparaffinised in 2 changes of clearene for 5 minutes each, before rehydrating through 2 changes of 100% EtOH (v/v) for 5 minutes each, 90% EtOH (v/v) for 30 seconds, and 70% EtOH (v/v) for 30 seconds. Sections were washed in H_2O before staining for 30 seconds with Harris Haemotoxylin (Sigma-Aldrich) to visualise structural morphology of skin sections. After washing in running tap water sections were counter stained with Eosin (Thermo Scientific) for 2 minutes. The sections were then dehydrated through 90% (v/v) EtOH and 2 changes of 100% (v/v) EtOH before clearing in 2 changes of xylene for 5 minutes each. Sections were then mounted with DEPEX mounting medium (Electron Microscopy Sciences).

2.10 Statistical Analysis

Statistical analysis was performed using one-way ANOVA with Tukey post-hoc test, or Bonferroni multiple comparison test unless otherwise stated using GraphPad Prism software. All error bars

represent standard error of mean (SEM). To represent statistical significance, the standard 'star' system was used unless otherwise stated, with annotations as below:

*	p.value < 0.05
**	p.value <0.01
***	p.value < 0.001
****	p.value <0.0001

Chapter 3: Developing tomato lines with increased stilbene content

3.1 Introduction

Plants produce a wide range of metabolites which often confer selective advantages against stresses in their environments. Stilbenes are a family of secondary plant metabolites which are derived from the phenylpropanoid pathway. Stilbenes are involved in responses to biotic and abiotic stresses, including protection against UV light, and signalling of defence responses (Chong et al., 2009). Phenyl propanoids and stilbenoids more specifically have gained interest more recently due to their biological activities and potential pharmacological applications. The stilbene resveratrol, and its bi-methylated derivative pterostilbene have gained much interest in recent years due to their wide range of biological activities including anti-inflammatory, and anti-carcinogenic actions (as discussed in 1.5).

Stilbenes are synthesised by a small number of plant species *Polygonum cupsidatum,* grapevine *(Vitis vinifera)*, peanuts, blue berries and some coniferous species (Chong et al., 2009). Within these plants stilbene biosynthesis is normally induced by stress, for example it has been well documented that stilbene synthesis in grapevine is induced by fungal infections such as botrytis (Jeandet et al., 1995). Plants that can synthesise resveratrol; normally contain low levels and only under stress, such as fungal infection, do they induce synthesis of resveratrol and its derivatives. Even following abiotic and biotic stresses, resveratrol is synthesised in low concentrations. In grapes, resveratrol mainly accumulates in the skin and seeds, with fresh grapes containing between 50 to 100 µg/g fresh weight of resveratrol (Jeandet et al., 1991). As such, it is not possible to obtain significant quantities of dietary resveratrol from plants.

Microbial synthesis and fermentation processes for production of stilbenes have progressed in recent years (as discussed, in Introduction). These, however require much optimisation and substantial engineering steps to produce stilbenes at high yields (Mei et al., 2015). Additionally, use of metabolically engineered microbes and fermentation techniques lead only to the production of one core compound. This therefore represents a missed opportunity to co-produce other biologically important side products that are made in plant-based systems.

Metabolic engineering of plants to enhance production of stilbenes therefore represents a good alternative strategy. Commercial tomato plants produce a variety of flavonoids naturally, although not stilbenes, and already have the general phenylpropanoid pathway (Colliver et al., 2002). This therefore means that only the two enzymes; stilbene synthase and resveratrol-o-methyltransferase need to be introduced into tomato to produce resveratrol and pterostilbene respectively, see Figure 1.1.

In 2008, it was shown that expression of the transcription factor AtMYB12 from *Arabidopsis thaliana* under the control of the fruit specific E8 promoter from tomato, led to the production of

extremely high levels of polyphenols within tomato fruit (Luo et al., 2008), and highlighted the potential use of AtMYB12 for engineering phenylpropanoid metabolism. Overexpression of stilbene synthase, isolated from the grapevine *Vitis vinifera*, in tomato has been shown to result in the accumulation of up to 0.5mg g^{-1} DW resveratrol in tomato fruit (Ingrosso et al., 2011). By crossing a E8:AtMYB12 (MYB12 transcription factor under the E8 fruit specific promoter), Zhang et al. (2015) were able to generate a tomato producing up to 6mg g^{-1} DW. This work showed that activation of an existing plant pathway by AtMYB12 , and introduction of a specific gene encoding stilbene synthase was all that was required for high resveratrol production in tomato (Zhang et al., 2015).

The stilbene synthase gene in this original high resveratrol-producing tomato (known as ResTom) was under control of a 35S promoter (cauliflower mosaic virus, CaMV, 35S promoter). Although this did allow for high levels of resveratrol to be produced in fruit, the 35S promoter is active throughout the plant, which led to a variety of growth and fertility problems in the transformed plants which reduced their viability. With the identification of the fruit specific E8 promoter, and the knowledge of metabolic engineering of tomato, I aimed to engineer an E8: StSy tomato capable of producing high levels of resveratrol specifically in fruits. In addition, the introduction of a resveratrol-o-methyltransferase gene into this metabolic system should allow production of the methylated resveratrol derivative, pterostilbene, in tomato fruit.

Despite a wide range of health-benefits associated with resveratrol, a major factor currently preventing further development of resveratrol for medical treatments is its low bioavailability (Walle, 2011). Pterostilbene, is a methylated derivative of resveratrol. Due to the presence of the two methoxy groups, pterostilbene has greater lipophilic and oral absorption than resveratrol (McCormack and McFadden, 2013). Additionally, pterostilbene has been shown to have a much-increased bioavailability, with an oral bioavailability of up to 80% compared to the low 20% associated with resveratrol (Kapetanovic et al., 2011).

Pterostilbene has been implicated in the prevention and treatment of a range of diseases including cancer, inflammation, diabetes and aging (as discussed in section 1.5.1), and has been shown to have a higher biological activity than resveratrol (Chang et al., 2012, Chiou et al., 2011, Kapetanovic et al., 2011). Therefore, pterostilbene represents a better therapeutic compound than resveratrol.

Pterostilbene is primarily found in blueberries, grapes and the tree *Pterocarpus marsupium* (Manickam et al., 1997, Rimando et al., 2004). Due to the wide availability and consumption of berries, pterostilbene production by these fruits has been of considerable interest. The pterostilbene content of berries varies between varieties, with *Vaccinium ashei* (rabbiteye blueberry) producing 99 ng/g dry sample, and *Vaccinium stamineum* (deerberry) producing up to

520 ng/g dry sample (Rimando et al., 2004). Due to the low abundancy of pterostilbene in natural sources, the full therapeutic potential of pterostilbene has yet to be reached.

Progress has been made in the synthesis of pterostilbene from microbial, fermentation, and grapevine cell culture systems (Ascensión et al., 2016, Heo et al., 2017, Li et al., 2016b), although these systems currently produce pterostilbene in low yields, and as such are unviable for commercial production of pterostilbenes.

Therefore, this project aims to utilise and improve the current tomato production system for resveratrol, by exchanging the 35S promoter from Cauliflower Mosaic Virus (CaMV) for the fruit specific promoter E8- thereby producing resveratrol solely in the fruits. Additionally, a new tomato cell line will be engineered to synthesise high levels of pterostilbene. Juice extracts will be subsequently produced from the fruit of both resveratrol and pterostilbene tomato plants, and biological activity compared and analysed for both compounds, using human skin explant models.

3.2 Aims

In this chapter the metabolic engineering of a high pterostilbene tomato is described. A gene encoding resveratrol-o-methyltransferase was isolated from grapevine, *Vitis vinifera*. Co-expression of stilbene synthase and resveratrol-o-methyltransferase *in planta* allowed for significant production of pterostilbene. This work confirmed that significant levels of the stilbenes resveratrol, polydatin and pterostilbene can be produced in tomato fruits, showcasing the metabolic engineering potential of tomato. Furthermore, the resveratrol and pterostilbene tomato lines can be crossed with other transgenic tomatoes producing high levels of other medically important compounds. The production of these different tomato lines, within the Money Maker genetic background, will allow the fruits to be used as models to investigate the health promoting effects of different stilbenes. In addition, combinations of tomatoes producing several different medically beneficial compounds can be compared to see how combinations of the compounds affect health promoting effects of tomato extracts individually and in combinations.

3.3 Methods:

3.4 Plasmid construction

3.4.1 Constructing the MYB12- StSy plasmid

The plasmids pBin19E8-AtMYB12 (backbone) and pJIT60-E8-*Vv*StSy (insert) were provided by Dr Eugenio Butelli. To make a construct combining E8, *At*MYB12 and *Vv*StSy genes, the insert was firstly prepared by isolating the StSy gene from pJIT60-E8-*Vv*StSy. The pJIT60-E8-VvStSy was digested with *BamHI* High Fidelity (HF) and *SacI-HF,* and the digestion mixture was run on an agarose gel for purification of the DNA encoding StSy.

pBin19E8-AtMYB12 acted as the backbone for the new plasmid. Firstly pBin19E8-*Vv*StSy was digested with *Sst1* and *BglII* before dephosphorylating, to prevent re-circularisation, using the USB Shrimp Alkaline Phosphatase (SAP) (Guy et al.) protocol. Briefly, 1-5µg of plasmid DNA was digested in a total 20µl volume, with 2µl 10x restriction enzyme buffer, 1µl restriction endonuclease and nuclease free water to a total of 20µl. The mix was incubated at for 1 hour at 37°C before adding shrimp alkaline phosphatase (at a concentration of 1µg to 3kb plasmid) and incubating for 30-60 minutes at 37°C. The mix was heated to 65°C to inactivate the SAP.

Next the StSy gene insert was ligated into the SAP-treated backbone, using T4 ligase, resulting in the binary construct pBIn19-E8-*At*MYB12-*Vv*StSy (pJAM 2253). After ligation the plasmid was transformed into competent DH5- α cells.

3.4.2 Constructing the MYB12-ROMT plasmid

Genomic DNA was extracted from Cabernet Sauvignon grape buds. The ROMT (size 2228bp) gene was subsequently amplified from the genomic DNA by PCR (See Table S 1 for information on genes and primers.) The ROMT gene fragment had adenine nucleotides added to each 3' terminus of the PCR product (because the fragments had been amplified using Phusion polymerase), before ligation into a pGEM-T easy vector (Promega) using T4 DNA ligase. The ligation reaction was incubated overnight at 16°C and was used to transform E. *coli* DH5α cells (as described in Methods, 2.2.1).

3.4.3 Ligation of ROMT into destination vector

Transformed E. *coli* cells containing pGEM-T-ROMT were selected for on agar plates containing the selective antibiotic gentamycin. The presence of ROMT in the plasmid was confirmed by colony PCR. Briefly, with a pipette tip an individual colony was transfected into a PCR tube containing the master mix and amplified using a normal PCR reaction. Colonies containing the ROMT gene were selected and grown at 37°C overnight with shaking in 10ml L-medium with gentamycin. Plasmid DNA from pGEM-T-ROMT containing E. *coli* was extracted using the Qiagen spin miniprep kit as described in general methods.

3.4.3.1 *Site directed mutagenesis*

Site directed mutagenesis was used to convert a serine residue within the ROMT genomic DNA amplified to a proline residue Figure 3.1. The proline residue is highly conserved in ROMT genes across several plant species and required for correct functionality of the gene.

ATGGATTTGGCAAACGGTGTGATATCAGCTGAGCTGCTTCATGCTCAAGCTCATGTCTGGAATC
ATATATTCAACTTCATAAAGTCTATGTCACTAAAATGTGCTATTCAACTAGGCATCCCAGACAT
CATCCACAACCATGGCAAGCCCATGACTCTTCCTGAGCTGGTCGCTAAGCTCCCAGTCCACCCT
AAAAGGAGTCAGTGCGTGTACCGTCTCATGCGCATTCTTGTTCATTCTGGCTTCCTTGCTGCGC
AAAGAGTCCAACAAGGTAAGGAAGAAGAGGGGTATGTGCTTACAGATGCCTCTAGGCTCCTTCT
AATGGATGACTCCTTGAGCATAAGGCCCTTGGTGCTTGCCATGCTCGACCCAATTTTAACTAAA
CCATGGCATTATCTGAGTGCTTGGTTTCAAAATGATGATCCCACTCCGTTCCACACTGCTTACG
AGCGGTCATTTTGGGATTATGCCGGCCATGAACCCCAGCTCAACAATTCCTTCAATGAAGCCAT
GGCTAGCGATGCTCGCTTACTCACCAGCGTGCTGCTTAAGGAGGGCCAGGGCGTATTTGCGGGG
TTGAACTCATTAGTTGATGTAGGGGGTGGCACAGGAAAAGTGGCCAAGGCCATTGCTAACGCTT
TCCCACATTTGAACTGCACCGTGTTAGATCTCTCCCACGTGGTTGCTGGCTTGCAAGGGAGCAA
GAACTTGAACTACTTTGCAGGTGATATGTTTGAGGCAATTCCTCCTGCAGATGCAATTTTACTC
AAGTGGATACTGCACGACTGGAGCAATGAAGAATGCGTGAAGATACTAAAGCGATGCAGGGAAG
CAATTCCGAGCAAGGAAAACGGAGGAAAGGTGATTATCATAGACATGATCATGATGAAGAATCA
AGGAGACTACAAGTCCACAGAAACACAGCTGTTCTTTGATATGACGATGATGATTTTCGCCCCG
GGTAGAGAGAGGGACGAGAACGAATGGGAGAAGCTATTCTTGGATGCTGGTTTCAGTCACTACA
AGATAACTCCCATTTTGGGTTTGAGGTCCCTCATTGAGGTTTATCCTTGA

Figure 3.1 ROMT cDNA sequence from colony with incorrect serine codon highlighted.

This serine codon was targeted by site-directed mutagenesis, using primers to target the sequence highlighted in red in to convert to proline codon.

A total of 4 PCRs were performed to produce the product with a mutated base pair. Firstly, two PCRs were performed using the genomic DNA as a template. The first PCR used a forward ROMT primer, and a reverse primer which was designed to amplify across the site of the base-pair needed to be mutated and containing the desired new base pair. The second PCR used a reverse ROMT primer and a forward primer designed for site directed mutagenesis (Table 3:1). The products of these two PCRs were run on agarose gels, and the bands extracted and purified to remove any impurities and primers which could interfere with the next step. The two PCR products were mixed together, in a new PCR tube in addition to dNTPs, *Taq* DNA polymerase and *Taq* Buffer, were annealed using a normal PCR protocol (general methods, 2.1.11) with a temperature reduced to 50°C and just 5-10 cycles.

Finally, the annealed product was amplified using a normal PCR protocol (general methods) using the forward and reverse gene specific ROMT primers to give a PCR product with the desired mutation. The PCR product was run on an agarose gel before the desired band was extracted and purified before ligating into pGEMT-easy vector and transforming into DH5-α cells. This time no adenylation of the PCR fragment was necessary because Taq polymerase was used, which automatically adds a A residue to the 3' end. The product was sequenced to confirm that the site-directed mutation had been successful.

Table 3:1 Primers for site-directed mutagenesis

Primer Name	Sequence (5'-3')
Proline-F	GTGTTAGATCTCCCCCACGTGGGTTGCTGGC
Proline-R	GCCAGCAACCACGTGGGGGAGATCTAACAC
ROMT-Bis F	GATACATGGATTTGGCAAACGGTGTGA
ROMT-BIS R	ATAGAGCATCAAGGATAAACCTCAATGA

3.4.3.2 Addition of Gateway att® sites to ROMT

After transforming DH5-α E. *coli* with the proline-corrected ROMT gene, the cells were grown overnight at 37°C with shaking, before performing a mini-prep. Next, the ROMT gene was reamplified using primers designed to introduce Gateway® *attB1* and *attB2* sites (see appendix Table S 1 for primer details). The *att*-flanked ROMT was inserted into the Gateway® entry clone pDONR 207 by Gateway BP-clonase-mediated recombination (as outlined in general methods 2.2.6), resulting in pDONR207-ROMT.

3.4.4 Generation of E8: ROMT/E8:MYB12 construct

Using Gateway® cloning the region containing ROMT from pDONR-207-ROMT was cloned into pJAM 2251 (E8:GW/E8:MYB12 in pBin19) resulting in the construct E8: ROMT/E8:MYB12 (pJAM 2255) suitable for transformation in tomato.

Transformed E. *coli* cells containing pJAM 2255 were selected on agar plates with the selective antibody kanamycin, and colony PCR was used to confirm gene integration.

3.4.5 Generation of E8: ROMT/E8: StSy/E8:MYB12 construct

To generate a plasmid containing all genes required for pterostilbene synthesis, a triple ligation was performed with pJAM 2254, pJAM 2253 and pJAM 2252 (E8:GW/E8:GW/E8:MYB12 in pBin19), to give the construct E8: ROMT/E8: StSy/E8:MYB12 (pJAM 2256). Transformed E. *coli* cells containing pJAM 2255 were selected on agar plates with the selective antibody kanamycin, and colony PCR was used to confirm gene integration.

3.4.6 Quantifying gene expression.

Expression of StSy and ROMT in E8:StSy/E8:MYB12 and E8:ROMT/E8:MYB12 transformants was detected using quantitative reverse transcriptase PCR (qRT-PCR, as described in the general methods 2.7.1). The plants with best expression of the target genes were then grown up for tomato crosses.

3.5 Metabolite analysis

3.5.1 Stilbene and flavonol extraction

Tomato fruit samples were freeze dried before grinding into a fine powder using liquid nitrogen. The extraction solution, 80% methanol, was added to the powdered sample at 1.25ml per 50mg plant material and incubated overnight at 4°C with shaking. After overnight incubation, samples were centrifuged at maximum speed for 15 minutes at 4°C, and the supernatant collected and stored at -20°C for further analysis. To the pellet an additional 1.25ml 80% methanol were added before incubating for another 3 hours at 4°C with shaking. After incubation the sample was centrifuged at 14,000 x g speed for 15 minutes at 4°C, before collecting the supernatant and storing at -20°C. The supernatant was passed through a filter syringe before use in LCMS-IT-TOF analysis.

3.5.2 LCMS-IT-TOF analysis and quantification

Stilbenes were analysed using an Ion trap (IT) and time of flight (TOF) liquid chromatography (LC)/mass spectrometer (MS)/TOF mass spectrometer to determine which compounds were present. Plant extracts were run on a 100x2.1mm 2.6µm kinetex EVO C18 column. Separation was achieved using a gradient (Table 3:2) of 100% acetonitrile (ACN) versus 0.1% formic acid (FA) in water, run at 0.5ml min^{-1} and 40°C. The elution products were monitored with a photo diode array (PDA) detector over a range of 200-600nm, and by positive mode electrospray MD, collecting spectra from *m/z* 200-2000. Stilbene and flavonol masses and fragmentation were determined using Quant Browser. Standards for resveratrol, polydatin, pinostilbene and pterostilbene, kaempferol-3-rutinoside, rutin, naringenin and naringin were used for quantification of flavonoids and stilbenes. Calibration curves were run before and after running the samples.

Polyphenols and other flavonoids were quantified using standards of resveratrol, polydatin, pterostilbene, pinostilbene, rutin, kaempferol rutinoside, naringenin, naringenin, and genistein.

Table 3:2 Solvent gradient for the separation of polyphenolic compounds with LCMS IT-TOF

Retention time (min)	% Acetonitrile
0.01	2
0.50	2
3.00	10
13.00	30
18.00	90
18.80	90
19.00	2
23.10	2

3.5.3 Quantification of stilbenes by XEVO analysis

Due to the low abundance of stilbenes in tomato samples, to accurately quantify stilbene content, tomato samples were run on the Waters Xevo TQ-S Tandem LC-MS. Samples were prepared as for IT-TOF and run on an Acquity UPLC attached to a Xevo TQS tandem mass spectrometer. Separation was achieved using a 50x2.1mm 2.6u Kinetex EVO C18 column using a gradient of acetonitrile vs 0.1% formic acid in water, at 500µl min^{-1} at room temperature (Table 3:3). The runs were performed by Dr Lionel Hill (JIC).

Table 3:3 Solvent gradient for separation of polyphenolic compound with Xevo

Time (minutes)	% ACN
0	2
6	94
8	94
8.1	2
10.5	2

Standards for resveratrol, pinostilbene, pterostilbene and polydatin were used to detect and quantify stilbenes within the tomato extracts. All compounds were detected in positive mode using the following mass transitions (show in Table 3:4). The quantification of stilbenes was performed by Dr Lionel Hill (JIC).

Table 3:4 Mass transitions

Compound	Precursor mass	Fragment mass	Cone voltage	Collision energy
Resveratrol	229.2	91	20	24
		107.1	20	24
		135.1	20	14
Pinostilbene	243.0404	91.1667	18	28
		121.1069	18	22
		133.1452	18	16
		149.1548	18	16
		165.1657	18	28
Pterostilbene	257.2	105.1	35	22
		133.1	35	16
		181.1	35	35

3.6 Results

3.6.1 Co-expression of stilbene synthase and resveratrol-O- methyl-transferase enables pterostilbene production in *Nicotiana benthamiana*

Stilbene synthase (StSy) and resveratrol O-methyltransferase (ROMT) are two genes from grape vine *Vitis vinifera,* which encode enzymes that enable the conversion of p-coumaroyl CoA into resveratrol and pterostilbene. The production of pterostilbene is reliant upon the expression of both StSy to produce resveratrol from p-coumaroyl coA and malonyl coA, and ROMT to methylate resveratrol to form pterostilbene.

Previous work by Zhang et al. (2015) showed that the introduction of a StSy gene from grapevine (*Vitis vinifera*) under the control of the cauliflower mosaic virus promoter, 35S, in addition to the *Arabidopsis thaliana* transcription factor MYB12 (*At*MYB12) enabled high level production of resveratrol in tomato. These plants (35S: *VvStSy*, E8:*At*MYB12) were referred to as ResTom plants and displayed very high levels of resveratrol production within fruits. Use of the CaMV 35S promoter drives expression of transgenes not only in fruits, but also in the vegetative tissues. Whilst this is often not a problem, in the case of resveratrol synthesis, plant-wide expression led to reduced fertility, and stunted growth of transgenic plants. Taking this knowledge forward, the vector design used for engineering the ResTom was used as a basis for the construction of a pterostilbene production system in tomato. However, the 35S promoter was replaced with the fruit-specific E8 promoter to drive StSy expression specifically in ripe fruit (Hirai et al., 2011).

To continue the metabolic pathway leading to pterostilbene production in tomato, a ROMT gene needed to be co-expressed with the StSy gene. A ROMT gene was isolated from *Vitis vinifera*. To test the functionality of the isolated ROMT gene, and to confirm that co-expression of the ROMT gene with StSy would lead to the synthesis of pterostilbene in planta, transient transformation was used to co-express the two genes in *Nicotiana benthamiana*.

Nicotiana benthamiana does not produce either resveratrol or pterostilbene naturally, and therefore represented a good system in which to test the functionality of both the StSy and ROMT constructs. Using the Hypertrans system developed by Sainsbury et al. (2009) leaves were injected with *Agrobacterium tumefaciens* strain GV3101 containing a single gene vector, both gene vectors, or were left uninjected. Uninjected leaves acted as a control.

LCMS-IT-TOF was used to analyse the metabolites in each of the *Nicotiana benthamiana* leaves. Using standards of resveratrol, polydatin and pterostilbene, the presence of these compounds in plant tissue was confirmed via the distinct retention times of each stilbene (Table 3:5), and molecular weights.

Table 3:5 Retention times and molecular weight of plant stilbenes

	Retention time (mins)	Molecular weight (g)
Resveratrol	8.760	228.2
Polydatin	6.412	390.38
Pterostilbene	15.6	256.3

LC/MS IT-TOF analysis of methanol extracts of *Nicotiana benthamiana* (Figure 3.2 and Figure 3.3) confirmed the presence of polydatin and pterostilbene in leaves injected with both ROMT and StSy genes showing that co-expression of ROMT and StSy enables the production of polydatin and pterostilbene and confirming functionality of the two genes, StSy and ROMT.

Although polydatin was detected in both StSy, and StSy: ROMT samples, resveratrol was not. The predominant form of resveratrol in planta is its glycosylated form polydatin, and as such, low levels of resveratrol are often present within plants. Unfortunately, due to the low solubility of resveratrol, LCMS IT-TOF system was not able to detect resveratrol at low concentrations, however presence of polydatin confirmed the activity of StSy.

Having confirmed the functionality of StSy and ROMT genes, Money Maker tomatoes were stably transformed with StSy and ROMT constructs.

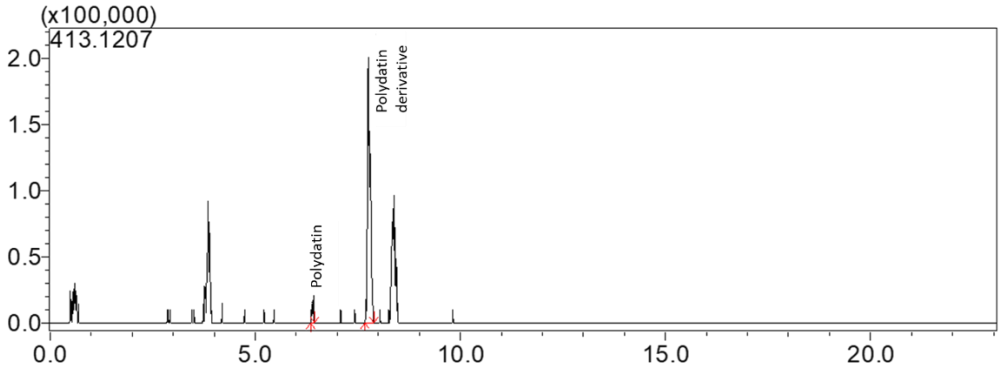

Figure 3.2 LC/MS analysis of stilbenes from the leaf of Nicotiana benthamiana injected with StSy shows the presence of polydatin, but no pterostilbene.

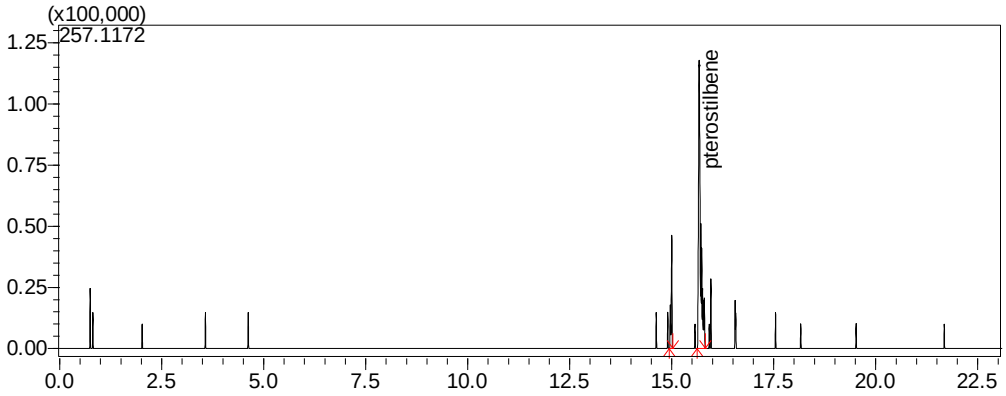

Figure 3.3 LC/MS analysis of stilbenes from the leaf of Nicotiana benthamiana injected with StSy:ROMT shows the presence of pterostilbene.

3.6.2 Engineering pterostilbene tomatoes

To engineer a tomato that produced pterostilbene at high levels, we looked to engineer tomato plants with a E8: StSy/E8: ROMT/E8:MYB12 genotype.

Unfortunately, the triple construct (Figure 3.4) was not stable, therefore instead of using a one-step transformation procedure, two separate tomato transformations needed to be performed to generate tomato plants with E8:StSy/E8:MYB12 and E8:ROMT/E8:MYB12 genotypes (Figure 3.5) which could then be crossed to produce a plant with the E8:StSy,E8:ROMT,E8:MYB12 genotype .

T0 plants were genotyped, and plants expressing the required genes were transferred to soil. The plants developed normally, however both plants produced relatively few fruits compared to wild type, and often had fruits which contained no seeds. This was not an unexpected outcome, as this was also observed with the previous 35S:StSy tomato line, and resveratrol production in tomatoes is known to induce parthenocarpy in fruits (Ingrosso et al., 2011).

We were able to confirm activity of the StSy gene in E8: StSy/E8:MYB12 positive plants via LCMS IT-TOF and the presence of resveratrol and polydatin in *Nicotiana benthamiana* extracts (Figure 3.3). However, as E8: ROMT/E8:MYB12 plants contained no enzymes for resveratrol synthesis and hence for pterostilbene synthesis, we could not confirm activity of the ROMT gene via LCMS IT-TOF. Therefore, activity of the ROMT gene was analysed via qRT-PCR (Figure 3.6).

Plants which showed the highest levels of ROMT gene expression were selected to cross with E8: StSy/E8:MYB12 plants which via LCMS IT-TOF analysis produced high levels of resveratrol. Crosses were performed by Dr Eugenio Butelli. Unfortunately, although SPL51 (2) showed the highest expression levels of ROMT, the plant was not able to be successfully crossed, and instead SPL51 (5) was used as the parental plant.

Seeds from the fruits of successful crosses were grown and genotyped to confirm the presence of all the required genes. Plants with the genotype E8: StSy/E8: ROMT/E8:MYB12 were named PteroTom. Fruit from positive plants were then collected and analysed. This generation of tomatoes had poor development of fruits, producing small fruit but very few fruits. In addition, the fruits produced contained relatively few seeds compared to wild type plants, and when these seeds were in turn planted, exhibited a low growth success rate, which hampered the growth and collection of fruits for analysis with the *ex vivo* skin system. Furthermore, not all seeds collected from these positive parent plants contained all three ROMT, StSy and MYB12 genes, the generation of positive offspring containing all three genes was 1 plant in 20. However, experience in the lab suggested that with future generations of these tomatoes the overall success of offspring growth will increase.

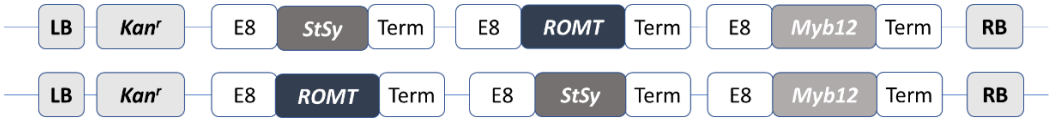

Figure 3.4 Map of T-DNA region of binary vector for single step transformation of tomato plants for stilbene synthesis.

LB, left T-DNA border region, Kanr, nptII gene conferring kanamycin resistance under the control of the nos promoter, E8, ethylene-responsive fruit ripening promoter, StSy V. vinifera stilbene synthase, ROMT V. vinifera Resveratrol o-methyltransferase, Term, CaMV terminator, RB right T-DNA border region.

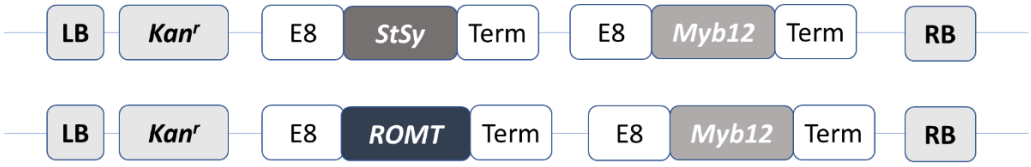

Figure 3.5 Map of T-DNA region of binary vectors used for the transformation of tomato plants for stilbene synthesis.

Positive transformants would be crossed to gain plant of genotype E8:StSy/E8:ROMT/E8:MYB12. LB, left T-DNA border region, Kan^r, nptII gene conferring kanamycin resistance under the control of the nos promoter, E8, ethylene-responsive fruit ripening promoter, StSy V. *vinifera* stilbene synthase, ROMT V.*vinifera* Resveratrol o-methyltransferase, Term, CaMV terminator, RB right T-DNA border region.

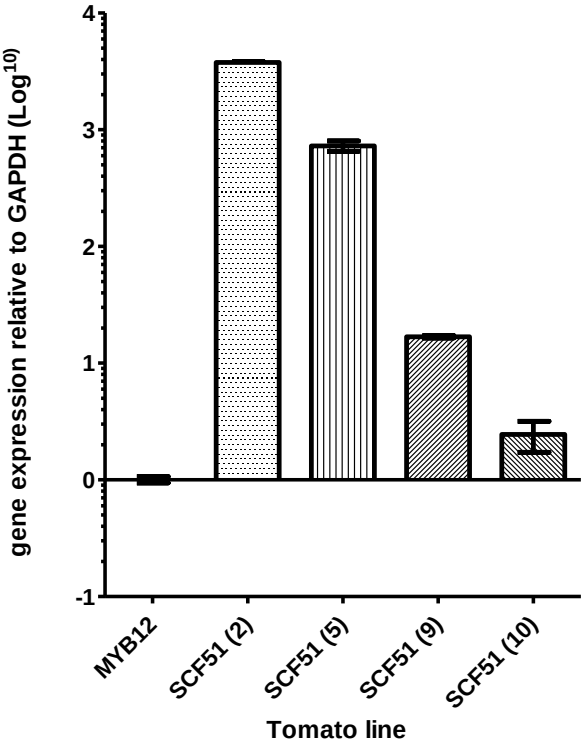

Figure 3.6 Fold expression change of E8:MYB12/E8:ROMT lines

qRT-PCR was performed on cDNA extracted from leaf samples of 5 different tomato plants identified as positive for E8:MYB12/E8:ROMT gene by PCR (SCF51 2,5,9,10). The expression of genes were normalised to GAPDH. Each bar represents the mean of 3 samples +/- SEM. For this fold change analysis, the control (MYB12) was set as 1.

3.6.3 Production of pterostilbene in tomato via co-expression of StSy and ROMT

As with previous tomato lines, both aqueous extracts and methanolic extracts were made from tomatoes and analysed via IT-TOF for stilbene and flavonol content. Upon analysis of aqueous tomato extracts, and methanol extractions, we were unable to see any peaks associated with pterostilbene or resveratrol via IT-TOF, and only very small peaks of polydatin. IT-TOF, although very good for giving an overview of all compounds within a solution, does have a reduced sensitivity of compounds at low levels. Therefore, to confirm the presence of pterostilbene, we ran extra analysis of both the aqueous extract and methanol extract using Xevo analysis. Xevo analysis was performed by Dr Lionel Hill. Unlike IT-TOF, Xevo is extremely sensitive to low levels of compounds, although it is only able to quantify compounds based upon their associated standards. This means that although Xevo analysis was useful for confirmation of the presence of specific compounds in the tomato extracts, we could not accurately quantify peaks of stilbene derivatives present in tomato.

Xevo analysis confirmed the presence of resveratrol, polydatin, pinostilbene and pterostilbene in PteroTom fruits (Figure 3.7, Figure 3.8 and Figure 3.9**Error! Reference source not found.**), with pterostilbene composing nearly half the total stilbene content in the fruits (Figure 3.10).

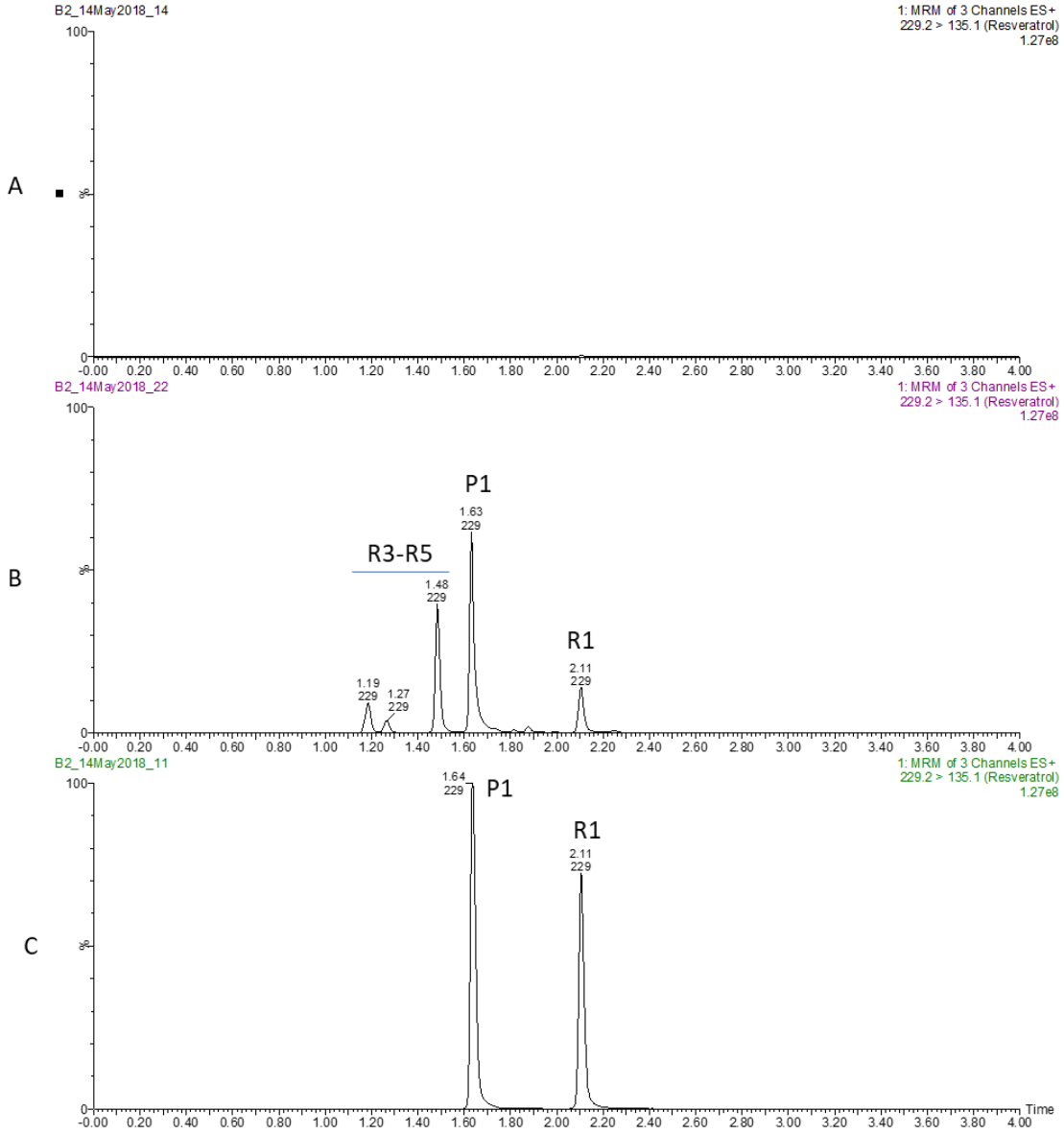

Figure 3.7 Xevo analysis of stilbenes from the fruits of PteroTom.

A) Chromatogram of Money Maker (wild type control) tomato juice for polydatin and resveratrol. B) Chromatogram of PteroTom tomato juice with peaks of polydatin and resveratrol P1= polydatin, and R1= resveratrol. Peaks R3-5 are glycosylated resveratrol derivatives. C) Chromatogram of standards for polydatin and resveratrol

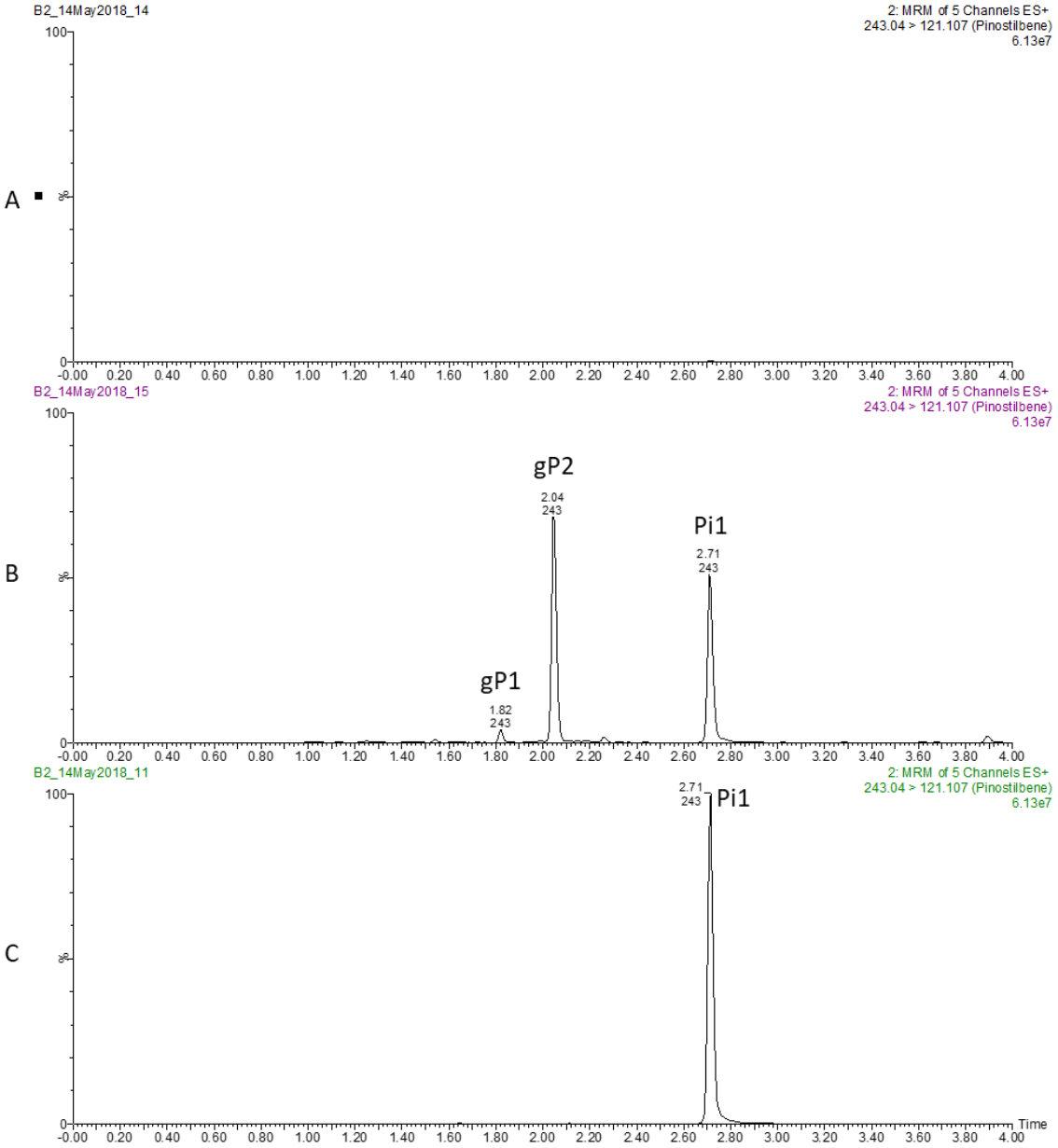

Figure 3.8 Xevo analysis of PteroTom juice for pinostilbene.

A) Chromatogram of Money Maker (wild type control) tomato juice. B) Chromatogram of PteroTom juice showing peaks for pinostilbene (pi1), and pinostilbene derivatives (gp1 and gp2). B) Standard chromatogram of Pinostilbene.

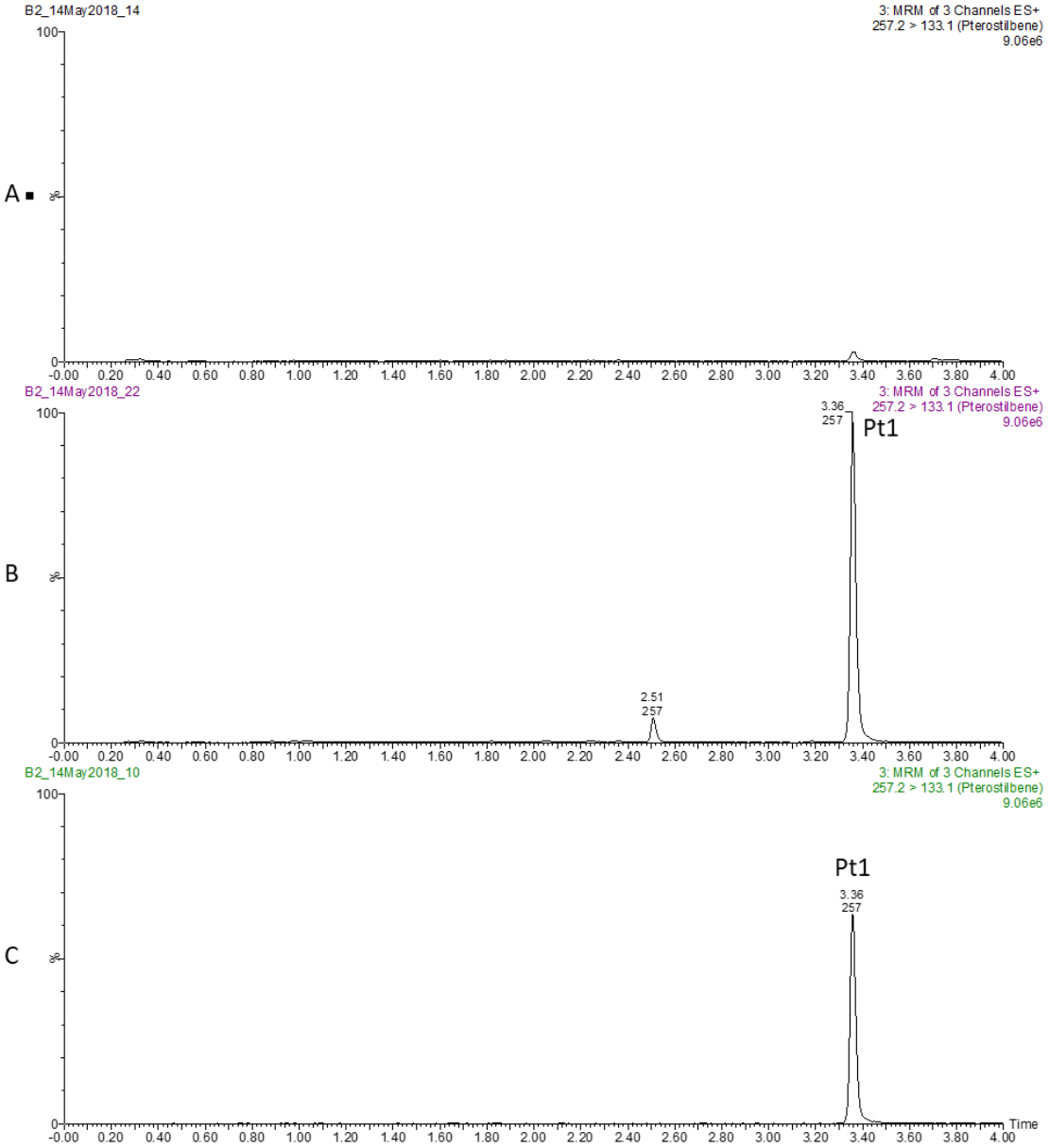

Figure 3.9 Xevo analysis of PteroTom juice for pterostilbene.

A) Chromatogram of Money Maker (wild type control) tomato juice. B) Chromatogram of PteroTom juice showing peaks for pterostilbene (pt1). C) Standard chromatogram for pterostilbene.

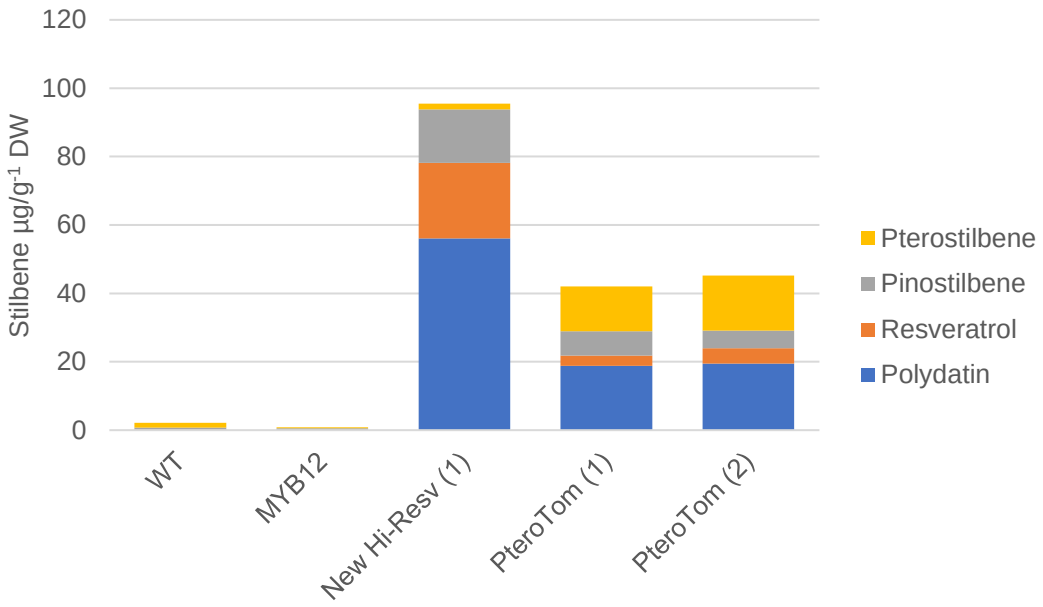

Figure 3.10 Comparative analysis of stilbenes in E8:MYB12 (control) and transgenic lines E8:StSy/E8:MYB12 (New Hi-Resv) and E8:StSy/E8:ROMT/E8:MYB12 (PteroTom).

Quantification based upon Xevo analysis of 80% Methanol (v/v) extracts of ripe tomatoes. Identification of compounds based upon absorbance of standards.

3.6.4 High levels of pterostilbene are produced in fruits of E8: StSy/E8: ROMT/E8:MYB12 tomato fruits

Quantification of pterostilbene levels from xevo analysis showed that PteroTom fruits contained up to 16 µg/g DW pterostilbene (Figure 3.10) and accounted for over 30% of total stilbene content in fruits. As a comparison, pterostilbene has been found to be present in levels of up to 110 ng/g dry weight in blueberries (Rodríguez-Bonilla et al., 2011), and 520 ng/g DW in *Vaccinium stamineum* (deerberry) (Rimando et al., 2004). This means that the level of pterostilbene measured in fruits of E8: StSy/E8: ROMT/E8:MYB12 tomatoes was 30 times more than that of *Vaccinium* berries, and 145 times more than blueberries.

In addition to producing significant levels of pterostilbene, PteroTom tomatoes also produced high levels of polydatin, resveratrol and pinostilbene (Figure 3.10). PteroTom tomatoes did show a significant decrease in both resveratrol and pinostilbene compared to Hi-Resv tomatoes, which corresponds to the production of pterostilbene for which they are both substrates. Overall there was a reduction in the total stilbene content of the PteroTom compared to the New Hi-Resv, this could indicate instability in the new compounds, or inefficient conversion from starting substrate. However, this may also have been due to conversion of resveratrol to other methylated derivatives, which were not identified this analysis.

Although the Xevo analysis presents an excellent method to quantify compounds, it is only able to quantify known compounds. This means that any derivatives of pterostilbene, or resveratrol within the PteroTom fruits would not be able to be identified using this method, for examples peaks 3-5 in **Error! Reference source not found.** could be identified as glycosylated-resveratrol derivatives, however without a standard for these we were not able to quantify levels of these compounds. The IT-TOF would represent a good alternate method to further identify other stilbenes within PteroTom fruit, although this would require optimisation as currently the IT-TOF is not sensitive enough to accurately identify compounds from the low concentrations of stilbenes within the tomato extracts.

3.6.5 Pterostilbene is not present in aqueous tomato extracts

Xevo analysis confirmed the production of pterostilbene, in addition to polydatin, and resveratrol in E8: StSy, E8: ROMT, E8:MYB12 methanol extracts. Interestingly, no peak for pterostilbene was detectable in aqueous extracts, despite its confirmed presence in methanol-based extracts of the same fruits. Pterostilbene is known to have a poor water solubility, although this is also true for resveratrol which was detectable in aqueous extracts. This suggested that in preparing Pterostilbene containing tomato extracts, methanol is required for pterostilbene extraction from tomato fruits. This has implications for the development and use of tomato extracts in skin-care treatments.

3.6.6 Comparison of polyphenolic content of PteroTom (E8: StSy/E8: ROMT/E8:MYB12) fruits to other tomato lines

Using LCMS IT-TOF analysis we were able to look at the composition of other polyphenolic compounds within PteroTom, and compare to the new Hi-Resv (E8:StSy/E8:MYB12), WT and MYB12 (E8:MYB12) fruits (Figure 3.11). Both the PteroTom and Hi-Resv tomato lines showed similar flavonoid compositions to each other, with the E8: StSy/E8:MYB12 fruits having a slightly increased level of naringenin chalcone compared to PteroTom. Overall there was not a significant change in total levels of flavonoids in either PteroTom or ResTom fruits compared to wild type, however there was a 7-fold increase in kaempferol-rutinoside, and an 8.5-fold increase in kaempferol rutinoside glucoside compared to wild type fruits.

Both ResTom and PteroTom fruits also contain the MYB12 transcription factor to promote activity of the general phenylpropanoid pathway, although both showed a decreased total flavonoid content compared to MYB12 tomato fruits.

The flavonol biosynthesis and stilbene synthesis pathways both require the production of malonyl CoA and p-coumaroyl CoA. In the production of flavonols the enzyme chalcone synthase uses Malonyl CoA and p-coumaroyl CoA for the synthesis of chalcone thereby starting the flavonol pathway. Whereas, in stilbene synthesis the enzyme resveratrol synthase/stilbene synthase uses malonyl CoA and p-coumaroyl CoA for the synthesis of resveratrol. This therefore means that both the flavonol and stilbene pathways are competing for the same initial substrates- malonyl CoA and p-coumaroyl CoA. The reduced content of flavonols in the PteroTom does coincide with the diversion of malonyl CoA and p-coumaroyl CoA to the stilbenoid pathway rather than the flavonoid pathway (Figure 1.1).

MYB12 tomatoes have a total flavonoid content 2x higher than that observed in PteroTom tomatoes, despite the production of stilbenes in this tomato line. Considering the inclusion of the MYB12 transcription factor, a higher level of flavonols in the PteroTom as well, or a similar total level across the flavonols and stilbenes, would be expected. As this was not the case, this suggested that in this new tomato line the MYB12 transcription factor was working sub optimally. By crossing this tomato line with the original MYB12 line we may be able to increase total stilbene content even higher, and therefore gain an even higher production of pterostilbenes in tomato fruit.

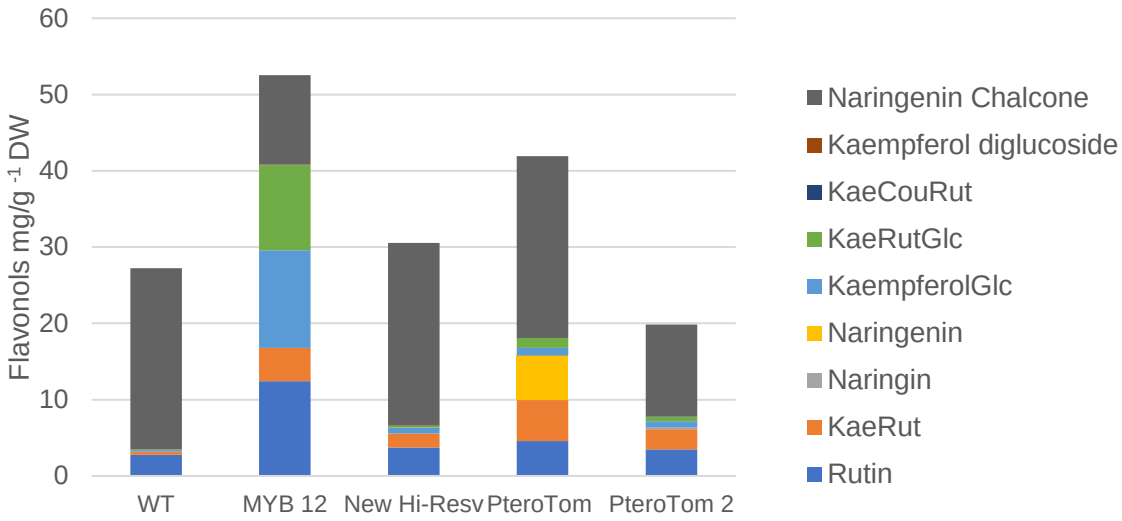

Figure 3.11 Comparative analysis of flavonoid content and composition of wild type, MYB12 (high flavonol) and transgenic StSy/ROMT lines.

IT-TOF analysis recorded at 340-360nm of 50% methanol (v/v) extracts of ripe tomato fruits. Classification and identification of compounds was performed on the basis of PDA absorbance and mass spectrometry.

3.6.7 Use of an E8 fruit specific promoter for resveratrol synthesis

By putting the StSy gene under the control of the E8: promoter, in addition to the AtMYB12 transcription factor it was hypothesised that we would be able to increase the amount of resveratrol and polydatin produced in planta. However, currently the levels of resveratrol and polydatin produced in these plants are less than that in the 35S:StSy genotype plants (Zhang et al., 2015). The new Hi-Resveratrol (E8:StSy, E8:MYB12) plants produce up to 46 µg/g DW resveratrol, and 56 µg/g DW polydatin (not including derivatives), whereas the 35S:StSy tomato fruits produce up to 6 mg/g DW resveratrol (Zhang et al., 2015). This could be a result of the transgenes only being expressed after fruit ripening in E8 lines, leading to reduced accumulation of stilbenes. By growing the tomatoes for more generations, and back crossing with the strongest plants to make the transgenes homozygous, we should be able to improve the overall production of stilbenes.

3.6.8 Further improving the medicinal output of tomatoes

The Bronze tomato line (E8:MYB12, E8:Del/Ros, 35S:StSy) was developed by crossing two lines generated by Zhang et al. (2014) using Indigo (E8:MYB12, E8:Del/Ros) and ResTom (E8:MYB12, 35StSy) parental plants, enabling the production of flavanols, anthocyanins and stilbenoids within fruit. A recent study comparing the activity of different tomato-enriched diets on mice with induced chronic colitis, showed significant reduction in gut inflammation in mice fed a diet containing 1% Bronze (Scarano et al., 2018). Additionally, mice fed 1% Bronze-enriched diets showed a greater reduction in pro-inflammatory cytokine production than mice fed with 1% of Indigo, ResTom or MM suggesting an increased biological activity associated with Bronze tomato. These data also suggest synergistic effects occurring between the multiple plant bioactives within Bronze tomatoes. As such, Bronze tomato represents an interesting tomato in terms of therapeutic potential and would benefit from expression of StSy under the E8 promoter rather than 35S, which would help improve health of the plant, in addition to overall yield of resveratrol in fruit. Furthermore, the introduction of ROMT into the bronze tomato background could potentially boost biological activity of this tomato further due to the increased biological activity associated with pterostilbene.

Using the double construct E8:MYB12, E8: StSy alongside a E8: Del/Ros parental plant Dr Eugenio Butelli was able to produce a new version of the Bronze tomato line ‘New-Bronze’, now with the StSy gene under control of the fruit specific E8 promoter rather than the 35S promoter.

In addition, Dr Eugenio Butelli was able to cross this new Bronze tomato plant with a E8: ROMT/E8:MYB12 double construct parental plant, to produce a new tomato line named the PteroBronze tomato. This new tomato allows for the additional production of pterostilbene in fruit alongside anthocyanins, flavonols and resveratrol. Xevo analysis of the fruits from both the ‘New bronze’ tomato (E8:MYB12, E8:Del/Ros1, E8:StSy) and PteroBronze tomato compared to the PteroTom tomato showed an increase in stilbene content in these new tomato lines (Figure 3.12).

The PteroBronze tomato showed an increased pterostilbene production, with production increased on average by 1.5-fold compared to PteroTom, with as much as 31 µg/g pterostilbene produced in fruits.

In addition, these data suggest that production of pterostilbene could be improved further, by crossing with another E8:MYB12 plant. It may be that in the current PteroTom plants, the MYB12 genes are not working as efficiently as they might. This possibly is also supported by data from comparative LCMS IT-TOF data based upon flavonol content in the tomato lines.

Quantitative analysis shows very small levels of pterostilbene in the four lines which do not contain the ROMT gene (New Bronze 1 and 2, New-Hi-Resv and MYB12). These peaks accounted for between 0.04µM and 0.4µM pterostilbene and could be discounted as artefacts or perhaps, could be the result of non-specific methylation by other OMTs in tomato fruit.

The three lines (New bronze 1,2 and New Hi-Resv) which do not contain resveratrol-o-methyltransferase produced higher levels of pinostilbene than ROMT- containing lines. This may be the result of the use of pinostilbene as a substrate for pterostilbene synthesising ROMT. Resveratrol and pinostilbene appear to be the preferred substrate for ROMT, with a reduction of 20-30% in lines without and with ROMT (Figure 3.12), whereas, only a 10% reduction in overall polydatin content is observed.

The new Bronze, and PteroBronze lines have significantly higher levels of flavonols than the PteroTom tomato (Figure 3.13), which suggests that at the moment the PteroTom plant may be performing sub-optimally. This demonstrates that we may be able to increase the capacity for pterostilbene production further in planta.

As well as substantial production of stilbenes and flavonols, the PteroBronze tomato also produced anthocyanins, data not shown. This tomato which produces high levels of several medicinally important compounds represents an interesting future material for trialling for bioactivity.

Although I initially set out to make an individual line containing E8:MYB12/ E8: StSy/ E8: ROMT, the route we took, which required the production of two separate plants E8: StSy/E8:MYB12, and E8: ROMT/E8:MYB12, has opened up greater possibilities of further crosses in the future, and the development of tomatoes producing a variety of different products. This is an exciting prospect, as using the different ‘base’ plant constructs now available, we could effectively tailor tomatoes to produce specific sets of compounds.

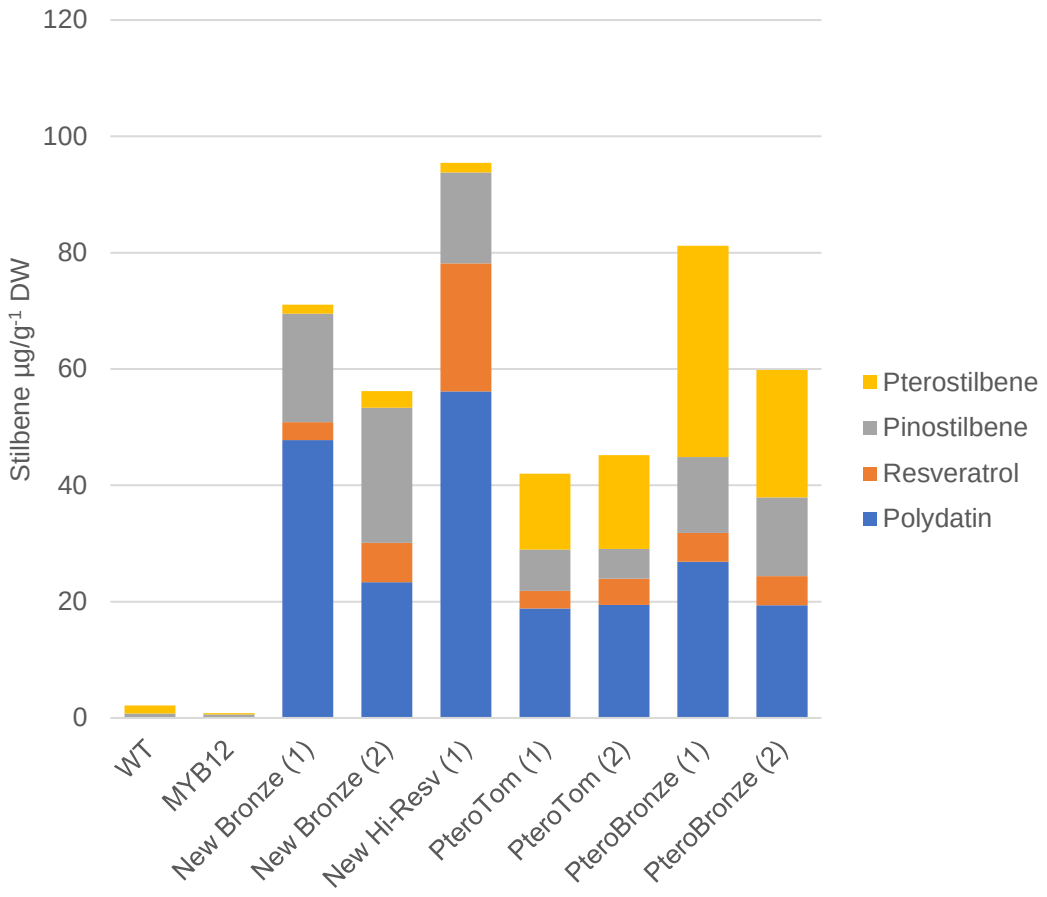

Figure 3.12 Comparative analysis of Stilbene content of tomato lines.

Xevo analysis was used for identification and quantification of compounds in WT, MYB12, New Bronze (E8:MYB12,E8:StSy,E8:Del,E8:ROS1), New Hi-Resv (E8:MYB12, E8:StSy), PteroTom (E8:MYB12,E8:StSy,E8:ROMT), PteroBronze (E8:MYB12,E8:StSt,E8:ROMT,E8:Del,E8:Ros1) and MYB12 (E8:MYB12) transgenic lines. µg/g DW calculated from µM quantification.

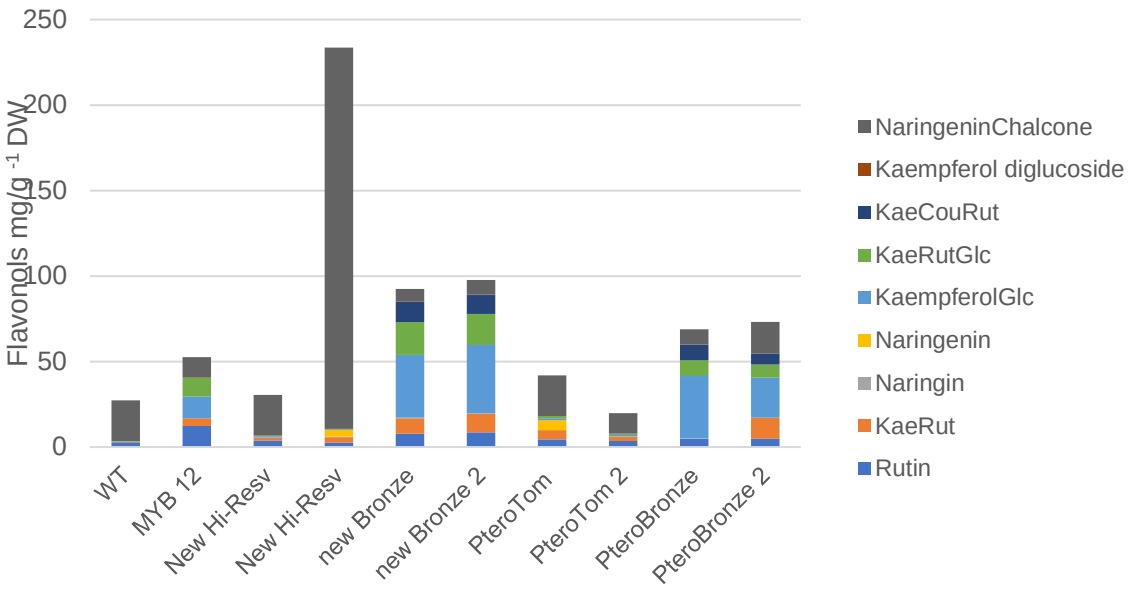

Figure 3.13 Comparative analysis of flavonols in different transgenic tomato lines.

IT-TOF analysis of 80% methanol (v/v) extracts of ripe tomato fruits: New Bronze (E8:MYB12,E8:StSy,E8:Del,E8:ROS1), New Hi-Resv (E8:MYB12, E8:StSy), PteroTom (E8:MYB12,E8:StSy,E8:ROMT), Pterobronze (E8:MYB12,E8:StSt,E8:ROMT,E8:Del,E8:Ros1) and MYB12 (E8:MYB12).

3.7 Discussion

Plant metabolic engineering is an important tool in molecular biology, and represents a powerful alternative to microbial engineering, and plant cell cultures, to synthesise high levels of multiple medically relevant compounds (Li et al., 2018).

Several plant compounds including stilbenes, flavonols and carotenoids have been identified as having health benefits. With the advance in metabolic engineering of plants, this has led to increased research into the development of food crops as bio factories for medicinal compounds.

The identification of transcription factors, such as MYB transcription factors has allowed upregulation of specific pathways in planta, such as the flavonoid pathway by AtMYB12. Increasing understanding of secondary plant metabolism pathways has also allowed the identification of key biosynthetic enzymes. This means that we are able to engineer and modify plants, via the introduction of key metabolic enzymes, and modification of transcriptional regulatory mechanisms, to enable high level production of important plant compounds such as flavonoids Zhang et al. (2015), anthocyanins (Zhang et al., 2014), betalains (Guy et al., 2016) and terpenes (Wang et al., 2016) *in planta*. This represents a unique way in which we can produce high yields of medicinally important compounds *in planta*, and a potentially more economically viable method of producing bioactive plant metabolites compared to microbial engineering and cell cultures currently used.

By combining metabolic approaches we are able to effectively modify biosynthetic pathways *in planta*. Zhang et al. (2014) identified the transcription factor AtMYB12 as an effective activator of the phenylpropanoid pathway, which when engineered into tomatoes produced high levels of phenylpropanoids. By exploiting this enhanced pathway functionality, other speciality phenylpropanoids have been engineered in tomato. By introducing stilbene synthase, resveratrol, a natural phytoalexin shown to have a wide range of biological activities, was synthesised in high levels in tomato (Zhang et al., 2015), in addition to flavonoids. By modifying biosynthetic pathways, we were able to generate different varieties of tomatoes producing different combinations of health-promoting compounds, all in the same genetic background; Money Maker tomato. This offered a novel way in which to study health benefits of these compounds, as well as to establish how combinations of these compounds may work.

The successful development of a resveratrol producing tomato, with a high level of resveratrol, showcased the ability of tomato to act as a good bio factory for the production of stilbenes, and with the potential for upscaling production to a larger scale (Li et al., 2018, Zhang et al., 2015). Due to the medicinal importance of stilbenes, in recent years several strategies have been investigated for the enhanced production of resveratrol and its derivatives. In particular, focus has been on plant cell cultures and metabolic engineering of bacterial and yeast cultures. However, current reports of

resveratrol production in microbial cultures have shown relatively low production levels of 32.32 mg/L resveratrol in a S*. cerevisiae* system (Li et al., 2016b), and just 2.0 mg/L resveratrol in E.*coli.* In comparison, the High-Res, resveratrol tomato (35S: StSy) produces the equivalent of 7mg/L of resveratrol, with a total concentration of all resveratrol derivatives (i.e. glycosylated and methylated derivatives) of 229.9 mg/L, which is significantly higher than the total resveratrol content from either yeast or bacterial systems. This shows that using tomato as a bio factory for production of stilbenes is effective (Li et al., 2018). In addition, this level of resveratrol is found in the juice of the tomato, without processing, purification or extraction methods, which is a significant advantage for adding to products such as cosmetics.

Resveratrol is known to have several beneficial biological affects including anti-inflammatory properties, and anti-oxidant properties. However, despite this, little is known about the functionality of resveratrol and its derivatives. Pterostilbene the di-methylated derivative of resveratrol is known to have higher bioavailability, and biological activity compared to resveratrol in addition to being more stable. This makes pterostilbene a very promising alternative to resveratrol. However, in planta such as grapevine, natural levels of pterostilbenes are extremely low, making extraction of and efficient production unfeasible. Metabolic engineering of E. *coli* and grapevine cell cultures have resulted in only negligible levels of pterostilbene (Jeong et al., 2015, Ascensión et al., 2016). Moreover, resveratrol and its derivatives are not readily soluble in either aqueous solutions, or cell suspension cultures. In order to improve solubility of stilbenes in cell suspensions additional treatments with cyclodextrin, a carrier molecule used to facilitate dissolution, is required (Jeandet et al., 2016). As such, no good production method has been available for high-level production of resveratrol derivatives.

We hypothesised, that, given the high efficiency of the ResTom in producing resveratrol, metabolic engineering of a tomato to contain resveratrol-O-methyltransferase in conjunction with stilbene synthase, and MYB12 transcription factor would allow for high level production of pterostilbene.

To generate high pterostilbene producing tomatoes I followed a metabolic engineering strategy that utilised the transcription factor MYB12, and the E8 fruit specific promoter in addition to stilbene synthase and resveratrol-O-methyltransferase. It was hypothesised that using a E8 fruit specific promoter rather than the previously used 35S promoter would allow for the specific production of stilbenes within the fruits of the tomato. The previously engineered resveratrol producing tomato utilised the 35S promoter, which although this allowed for high production of resveratrol, led to the plant having ill health due to the constitutive expression of StSy in all tissues. It was hypothesised that using a E8 fruit specific promoter, which allows for the specific expression of StSy in tomato fruit, would help to reduce any negative effects high stilbene production has on plant health.

At first, I set out to make one tomato line containing E8:MYB12/E8: StSy/E8: ROMT, however this triple construct was unstable with this gene set, and so two separate tomato lines E8:MYB12/E8: StSy and E8:MYB12/E8: ROMT were generated. The instability of this proposed construct was most likely due to the presence of 3 E8 promoters. Despite the use of the E8 promoter, these plant lines still displayed reduced fertility affecting the development of both anther and pollen in plants, which impacted on the timeline of generation of the PteroTom tomato.

However, the creation of these two separate tomato lines has opened up several new opportunities of incorporating these genes into other current tomato lines, including the bronze tomato.

The resulting E8:MYB12/E8: StSy/E8: ROMT plant was able to produce up to 16 µg/g DW of pterostilbene, 30x more than *vaccinium* berries which is one of the highest producers of pterostilbene, confirming the efficiency of tomato as a bio factory for pterostilbene production.

Interestingly, with the E8 promoter accumulation of total stilbenes was lower than the previous ResTom tomato line which utilised 35S promoter. There are several possible reasons for this apparent reduction in activity with the E8 promoter. Firstly, in this new tomato line the 2 genes may be hemizygous rather than homozygous. As the tomato lines are maintained through more generations, this may well improve as the transgenes are brought to homozygosity.

In addition, the E8 promoter is transcriptionally activated at the onset of ripening. This means that unlike the 35S lines, in E8 transgenic lines the tomatoes will only begin synthesis and accumulation of stilbenes after the onset of ripening, whereas in the 35S lines accumulation can begin as soon as fruits begin developing. This may in turn lead to a reduction in the overall levels of stilbene accumulation in E8 fruits.

Comparison of different promoters, including E8 and CaMV 35S have shown that there are sometimes differences in the level of expression depending on promoter, with 35S CaMV often showing a higher promoter activity. This difference in strength of promoter may also account for the reduction in overall stilbene levels seen in E8 promoter vs 35S promoter tomato stilbene lines (Hueso et al., 2009).

Our current observations suggest that we should be able to increase the accumulation of stilbenes in this line further. Dr Butelli was able to use the PteroTom and new Hi-Resv lines with the bronze tomato line (E8:MYB12, E8: Del/Ros, 35S: StSy) to generate a new PteroBronze tomato, which can produce high levels of flavonols, stilbenes and anthocyanins. In this line pterostilbene production was substantially increased to 31 µg/g DW. This suggests that in the current PteroTom tomato pterostilbene production is currently at sub-optimal levels, however crossing with E8:MYB12 plants, and 35S: StSy should allow us to develop lines with higher pterostilbene production.

Interestingly, during analysis of tomato juice extracts we found that pterostilbene is not present in quantifiable levels in aqueous tomato extracts, despite its presence in methanol-based extracts. This is most likely a result of pterostilbene's low water solubility. Although we can efficiently extract pterostilbene via methanol extraction methods, this does pose a problem for taking pterostilbene tomatoes on to development for skin-treatments. Further studies investigating how to make extracts from pterostilbene tomatoes suitable for topical skin treatments are required.

Chapter 4: Implementing an *ex-vivo* human skin model for analysis of tomato juice activity, and identification of novel gene regulation

4.1 Introduction

Polyphenols have been widely studied in relation to their effects on human health and disease. A high proportion of this research has focused on dietary consumption of polyphenols, which has shown that compounds such as resveratrol have chemoprotective activities (Harper et al., 2007), anti-oxidant activities (Robb et al., 2008) and anti-inflammatory roles (Sánchez-Fidalgo et al., 2010) in model systems. However, although resveratrol has high absorption rates via oral consumption, it has low bioavailability in humans (Walle et al., 2004).

Due to the low bioavailability of these compounds, their usefulness and the molecular basis of their functionality remains unclear. A transdermal system of polyphenol treatments could offer a viable alternative delivery mechanism to oral intake. There have been several studies based upon flavonols such as the green tea flavonol epigallocatechin gallate (EGCg) (Batchelder et al., 2004, Huang et al., 1992) , and quercetin (Casagrande et al., 2006) which show high transdermal delivery of plant extracts at biologically effective dosages.

Topical application of polyphenols would offer several benefits, including the direct targeting of polyphenols to exposed skin, and increased bioavailability. In addition, direct application of polyphenols to skin will help to circumnavigate the barriers of dietary intake such as high metabolism of polyphenols, and low uptake via tissues (Pinnell, 2003).

4.1.1 Stilbenes and skin models

The role of resveratrol in skin health has shown promise in several studies. For example, work with normal human epidermal keratinocytes (NHEK) cells has shown that topical application of resveratrol helps to protect cells from adverse effects of UV radiation, such as DNA damage, via modulation of the NF-kB pathway (Adhami et al., 2003). In addition, resveratrol has been shown to be able to modulate inflammatory chemokines in primary keratinocytes (Pastore et al., 2012b), as well as endogenous antioxidant pathways (Soeur et al., 2015) and aging pathways (Lephart et al., 2014). A study by Lephart et., al (2014) investigated the effects of resveratrol on gene expression using an *ex vivo* skin model, and found significant changes in several inflammatory and dermal-aging genes (Lephart et al., 2014). These data suggested that resveratrol may have several beneficial roles within the skin. However, although some pathways have been studied in cell cultures, mouse models, and skin, the overall effect resveratrol has on intact human skin is largely unknown.

Most of our current understanding of the health effects of resveratrol have come through skin cell cultures of normal keratinocytes, or fibroblasts. These *in vitro* experiments help to provide information regarding the regulation in individual skin cell types by compounds such as resveratrol. In *vivo* skin studies have been performed in mouse models, and although these represent a more

complex structure than single cell cultures, due to the many differences in mouse and human skin, including a much thinner epidermis, high follicle density, and lack of elastic fibres (Rittié, 2016), these structural differences mean that extrapolating data from murine models to humans is problematic.

In addition, in these experiments the resveratrol tested has been synthetic, and the effects of synthetic resveratrol may be different to those of resveratrol within a complex matrix such as tomato juice.

4.2 Aims

1. To develop a working assay for testing biological activity of plant-based compounds on human skin,
2. To determine effects on gene expression levels in non-inflammatory and inflammatory environments.
3. To identify genes differentially regulated by MM and ResTom juice to determine the biological effect of these treatments on human skin.

4.3 Methods:

4.3.1 *Ex vivo* skin explant assay:

An *ex vivo* human skin explant model was developed with Dr Damon Bevan (Gavrilovic group, Norwich Skin Platform, UEA). For *ex vivo* skin explants donated human abdominal skin, (surplus to surgical needs performed by Prof Marc Moncrieff and his team at the Norfolk and Norwich University Hospital) with ethical approval (20142015 – 47 HT) was used (Table 4:1) Unfortunately, we have not been able to confirm the age of SPL007 or SPL012, but, from the other donor responses and age-spread of donors, we did not observe a correlation in response to treatment in a specific age group. As such, analysis of data from SPL007 and SPL012 has still been included despite the unknown age of the donors.

Table 4:1 Skin platform donors.

Each skin donor was assigned a tissue bank number, and a skin platform code. The skin platform code is used throughout to refer to each donor. Information concerning the age of the patient taken. (-) indicate data which is not available. *Ex vivo* skin explants donated human abdominal skin, (surplus to surgical needs performed by Prof Marc Moncrieff and his team at the Norfolk and Norwich University Hospital) with ethical approval 20142015 – 47 HT.

Skin Platform code	Age at time of recruitment
SPL003	69
SPL005	54
SPL006	47
SPL007	-
SPL008	66
SPL009	69
SPL010	48
SPL012	-
SPL013	58
SPL014	49
SPL015	44
SPL026	67
SPL029	39
SPL031	69
SPL032	59

Subcutaneous fat was removed from the donated skin, before pinning skin samples out and taking 6mm diameter punch biopsies (as described in general methods 2.8.2). Cultured biopsies, termed explants, were washed in sterile PBS supplemented with gentamycin (125 µg/ml) and amphotericin B (1.87 µg/ml) before being added to a 24 well plate containing 500µl EpiLife® media (supplemented with EpiLife™ defined growth supplement, catalogue number S0152, in addition to gentamycin (75 µg/ml), amphotericin B (1.125 µg/ml), and calcium chloride (1.2 mM). Explants were treated as submerged cultures. Additional biopsies were snap frozen on the day in liquid nitrogen or stored in *RNA later* as T-0 samples. In total 6 biopsies were taken for each condition, 3 for RNA extraction, 2 to be snap-frozen, and 1 for wax embedding. Experiments were carried out over a 5-day period (see timeline in Figure 4.1).

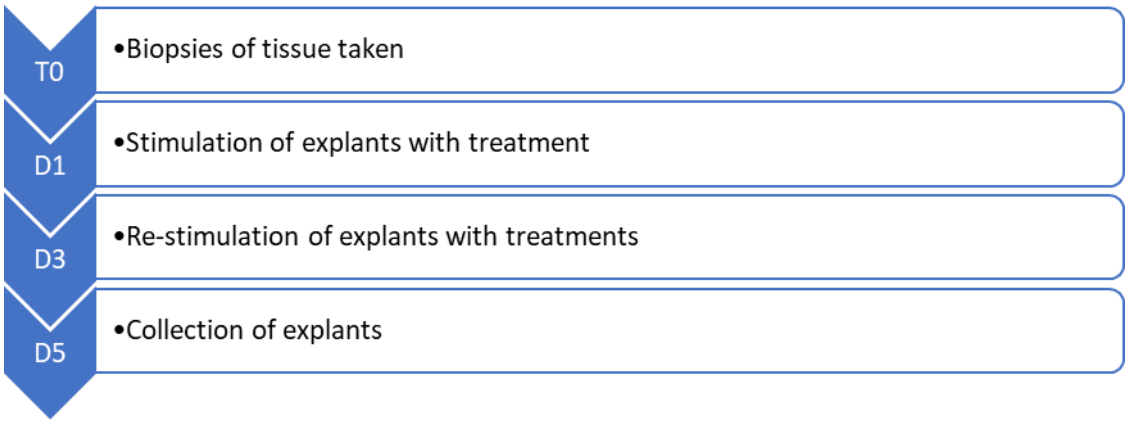

Figure 4.1 Experimental timeline for Ex Vivo skin experiments

4.3.2 Experimental protocol for skin explants

Biopsies were cultured overnight. Medium was removed and replaced with fresh Epilife® medium supplemented as required for the different treatments (D1). For induction of inflammation the two cytokines Interleukin 1 alpha (35 ng/ml) and Oncostatin M (100 ng/ml) were added as required. Tomato juice extracts were added directly to explants in wells as required in a 1 in 10 dilution in culture medium (or at indicated percentages). Explants were cultured for a further two days, before re-stimulation (D3), when the medium was replaced with new media supplemented with required treatments. The explants were again cultured for an additional two days, before collection on Day 5 when explants were stored as stated above. Additionally, conditioned media from wells was also collected at day 5 and snap-frozen at -20°C.

4.3.3 RNA extraction from whole tissue:

Skin explants were stored in RNA later after collection on day 5, before storing at 4°C overnight, and then storing in -80°C until further use. RNA was isolated using Trizol. Skin tissue was cut into

small pieces using scissors before adding to 600 µl Trizol. Tissue was then fully homogenised with ball bearings using the TissueLyser II (Qiagen) at 30Hz. Samples were centrifuged at 14,000 x g for 10 minutes at 4°C and supernatant added to fresh tubes containing 200 µl of chloroform. The samples were mixed thoroughly for a minimum of 15 seconds before centrifuging for 15 minutes at 14,000 x g. The aqueous upper phase containing RNA, was transferred to a new Eppendorf tube containing 200 µl of 95% ethanol, taking care to not disturb the interphase. After thorough mixing, the supernatant was transferred to a RNeasy mini spin column, before centrifuging for 20 seconds at 8000 x g and the supernatant disposed. Following this, the membrane was treated with DNase to degrade any DNA contaminants. To remove all cell contaminants, and to further bind RNA to the membrane a series of washes were performed using buffer RW1 and RPE as according to the manufacturer's instructions. Following the wash steps, the membrane was dried, and purified and RNA was eluted in RNase-free water for storage at -20°C. The quality of RNA was checked (OD 260/280 ratio) by NanoDrop and concentration recorded.

4.3.4 Microarray analysis

RNA Samples were prepared for microarray analysis by Dr Damon Bevan and sent to Source Bioscience. RNA samples for microarray analysis comprised samples from one donor, SPL003, with tomato treatments and inflammatory cytokines as outlined in Table 4:2. Microarray results were analysed, and treatments compared with help from Dr Govind Chandra (Bioinformatics department, JIC). Expression levels from probes were compared across conditions and expressed as fold change. Genes with a fold change ≥+/-1.5-fold change, with $p<0.05$ from DAVID analysis (performed by Govind Chandra, JIC) were considered significant and used for subsequent analysis. Pathway analysis was carried out using InnateDB pathway analysis software (Breuer et al., 2013).

Table 4:2 Skin explant treatments analysed by micro-array.

Cytokine treatment: Addition of Interleukin 1- alpha (35ng/ml) and Oncostatin M (100ng/ml) to stimulate an inflammatory environment. MM: Money Maker Juice (WT tomato juice, acts as a control for tomato juice matrix) ResTom: Resveratrol tomato juice (35S:StSy, 35S:ROMT, E8:MYB12).

SPL003
Control
+ Cytokines
MM
MM + Cytokines
ResTom
ResTom + Cytokines

4.4 Results:

4.4.1 Development of a working assay to study biological activity of tomato juice on human skin.

An unbiased approach was undertaken to investigate the effect of aqueous tomato extracts (ResTom and MM) and cytokines (IL1/OSM) on human skin explants by carrying out microarray analysis of total RNA to identify potentially novel regulated genes or pathways.

Total RNA from SPL003 with the following treatments were prepared by Dr Damon Bevan and sent for microanalysis SPl003_Control, SPL003_MM treated, SPL003_ResTom treated, SPL003_IL1/OSM, SPL003_IL1/OSM +MM, SPL003_IL1/OSM+ ResTom.

4.4.2 Selecting genes for further analysis

From the micro-array data of the above experimental treatment conditions, following bioinformatics analysis by Dr Govind Chandra, JIC, comparisons were made between conditions to investigate several questions

1. What effect does Money Maker juice have on gene regulation in the absence or presence of cytokines? (SPL003_control vs SPL003_MM)
2. What effect does ResTom juice have on gene regulation in the absence of cytokines? (SPL003_control vs SPL003_ResTom) and is this different from MM? (SPL003_MM vs SPL003_ResTom)
3. What effect does cytokine stimulation have on gene regulation? (SPL003_control vs SPL003_IL1/OSM)
4. What effect does Money Maker juice have on gene regulation in the presence of cytokines? (SPL003_IL1/OSM vs SPL003_IL1/OSM_MM) and what additional changes are observed with ResTom treatment? (SPl003_IL1/OSM vs SPl003_IL1/OSM + ResTom)
5. What are the differential effects on gene regulation between MM and ResTom juice in the presence of cytokines (SPl003_IL1/OSM+MM vs SPL003_IL1/OSM + ResTom)

Volcano plots were created based on the above comparisons (Figure 4.3 and Figure 4.2) against p-values. This enabled an overview of genes up and downregulated in the different treatments. Genes up- or downregulated, with a Log2 fold change greater than or equal to 1.5, and with an adjusted p-value of less than 0.05 were highlighted on the volcano plots. For comparison of MM to ResTom (Figure 4.2,C) p-value rather than adjusted p-value was used, as adjusted p-value provided no significantly regulated genes. Therefore, the parameters were widened by using p-values

instead, which allowed for the identification of 26 genes significantly upregulated and 52 significantly downregulated in ResTom compared to MM.

Money-maker juice by itself leads to many changes in gene expression within skin samples (Figure 4.2, A). Although there was little difference in the total number of genes regulated with MM or ResTom juice, ResTom seemed to have a greater activating effect on genes with a greater number of genes up-regulated compared to MM juice, whilst MM juice downregulated a larger proportion of genes compared to ResTom (Table 4.3).

Addition of MM and ResTom juice in the presence of cytokines both caused many genes to be significantly regulated (Table 4.4). Under inflammatory conditions ResTom had a greater effect on gene expression than MM, with 1000 more genes showing a change in expression levels of 1.5-fold or greater compared to MM juice, and 3165 more genes than cytokines alone.

As the ResTom tomatoes have a MM background, we could compare genes regulated with the addition of MM and ResTom (with cytokines) to reveal genes specifically regulated due to the presence of resveratrol in a tomato matrix (Figure 4.3, D). From the volcano plot, 5 genes were identified to be specifically regulated by ResTom juice (Table 4.5) which may be of interest for further investigation.

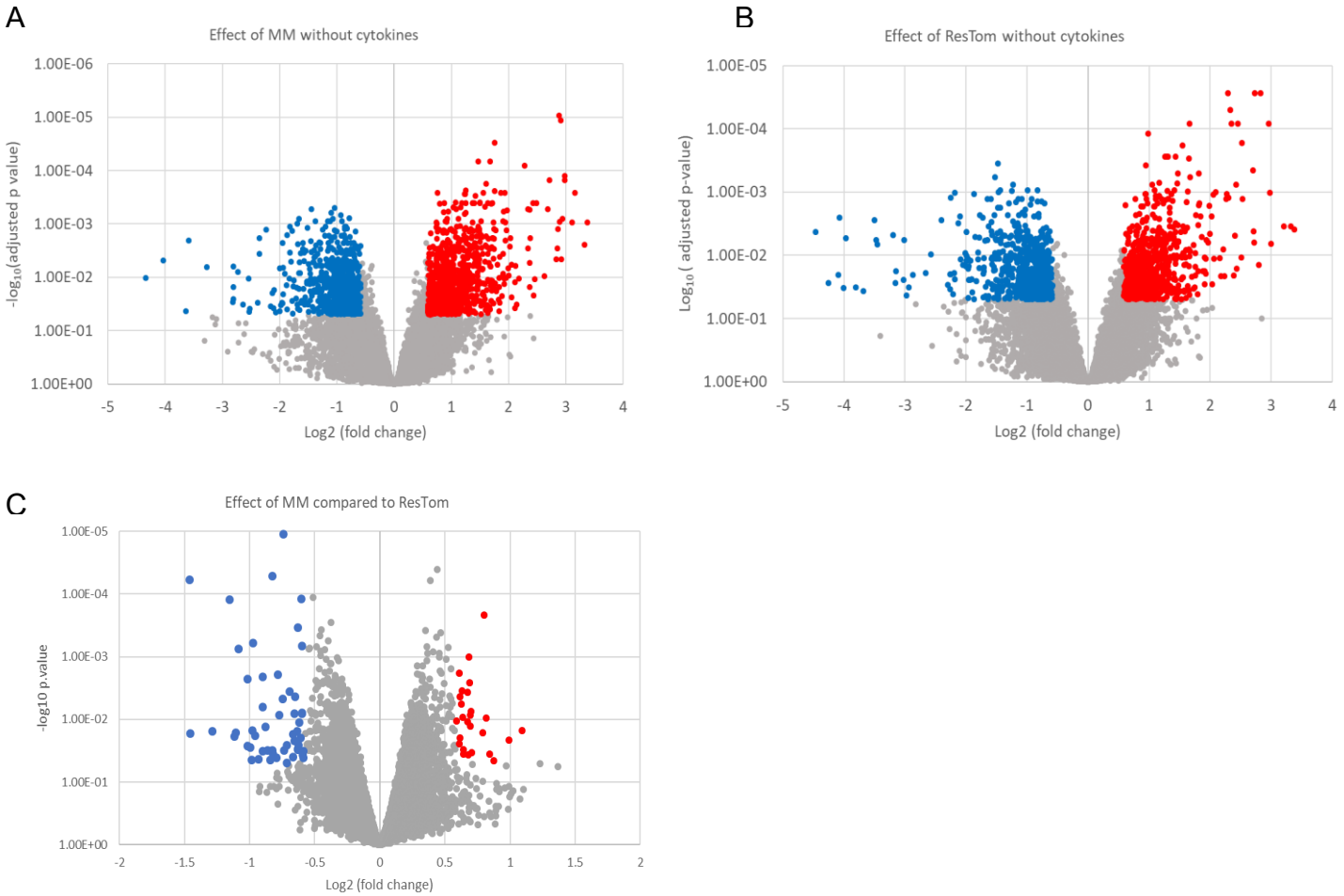

Figure 4.2 Volcano plots showing the effect of tomato juices without cytokine stimulation on gene regulation in skin explants.

(A) MM regulated genes, (B) ResTom regulated genes, (C) comparison of MM to ResTom regulated genes. Genes plotted according to log2 fold change regulation (x-axis) against -log10 adjusted p-value (C, plotted against p-value instead of adjusted p-value) Blue highlighted data points have a fold change ≤-1.5 and adjusted p-value <0.05, red highlighted data points have a foldchange ≥1.5 and adjusted p-value <0.05.

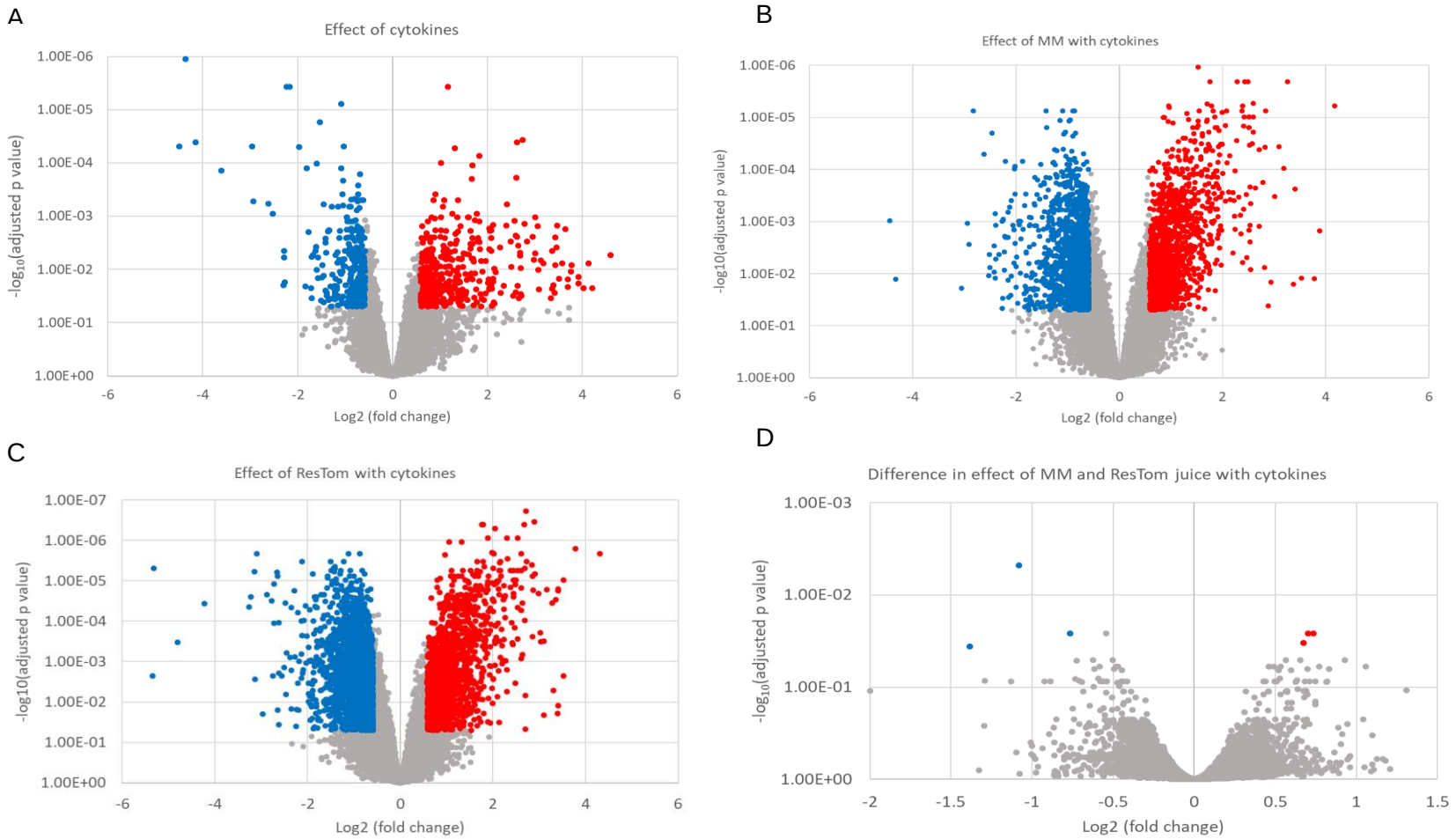

Figure 4.3 Volcano plots showing the effect of tomato juices with cytokine stimulation on gene regulation in skin explants.

(A) genes regulated with cytokine treatment (B) MM regulated genes, (C) ResTom regulated genes, (D) comparison of MM and ResTom regulated genes. Genes plotted according to log2 fold change regulation (x-axis) against -log10 adjusted p-value (C, plotted against p-value instead of adjusted p-value). Blue highlighted data points have a foldchange ≤-1.5 and adjusted p-value <0.05, red highlighted data points have a foldchange ≥1.5 and adjusted p-value <0.05.

Table 4:3 Number of significantly regulated genes, based on absolute fold change greater than or equal to 1.5, and adjusted p-value less than 0.05

	Number of genes regulated		
Effect of	**Up-regulated**	**Down-regulated**	**Total**
MM without cytokines	609	695	1304
ResTom without cytokines	669	628	1297

Table 4:4 Number of significantly regulated genes, based on absolute fold change greater than or equal to 1.5, and adjusted p-value less than 0.05

	Number of genes regulated		
Effect of	**Up regulated**	**Down regulated**	**Total**
Cytokines	421	321	742
MM and cytokines	1363	1619	2982
ResTom and cytokines	2042	1865	3907

Table 4:5 Significantly regulated genes identified by comparison of genes regulated with MM or ResTom treatment with cytokines.

Fold change is greater than or equal to 1.5 and adjusted p-value less than 0.05.

Gene symbol	Gene name	Fold change
CDK5R1	Cyclin dependent kinase 5 regulatory subunit 1	1.626433
RTN3	Reticulon 3	1.593411
EDN1	Endothelin 1	-2.60825
SYT14P1	Synaptotagmin 14 pseudogene	-2.11758
CASP4	Caspase 4	-1.70057

To determine the relationship of genes regulated by different treatments, distribution of regulated genes was compared using Venny online software (http://bioinfogp.cnb.csic.es/tools/venny/). By comparing genes significantly regulated by MM juice and ResTom juice, we were able to identify genes only regulated by addition of ResTom juice. As ResTom shares its background with MM, genes regulated by both MM and ResTom juice may be due to their shared MM background, whereas genes not observed to be significantly regulated by MM juice are most likely ResTom-specific regulated genes.

Figure 4.4,A shows that 820 genes are regulated by both MM and ResTom juice, with 345 genes being differentially expressed by ResTom juice compared to MM juice. In the presence of cytokines, there is an increased proportion of genes regulated only by ResTom juice (Figure 4.5 and Figure 4.4,A). To explore further at the differences in expression distribution between treatments, significantly regulated genes were separated according to whether they were up or down regulated (i.e. Fc ≥1.5 upregulated, Fc ≤ -1.5 downregulated) and again analysed via Venny (Figure 4.4 B-C, and Figure 4.5 B-C).

From the Venn diagrams, we observed that more genes are significantly downregulated with ResTom juice (with and without cytokines) than upregulated. In the presence of cytokines, a greater number of genes are regulated by ResTom than MM, which confirms our observations via volcano plot analysis (Table 4.3 and Table 4.4). Interestingly, comparison of regulated genes shows that as well as regulating a greater number of genes than MM, many of the genes regulated by ResTom were regulated only by ResTom (Figure 4.5,A).

Although the Venn diagram and volcano plot analyses provided insight into the differential regulation of genes by MM and ResTom treatments, we were not able to see differences in expression levels of specific genes. To determine the difference in gene expression between conditions in greater detail, we used the gene lists generated for each segment of the Venn diagram (via Venny online software) and compared fold change values of genes between treatments. Literature review searches were performed on the top regulated genes to identify key candidate genes of interest to pursue via qRT-PCR.

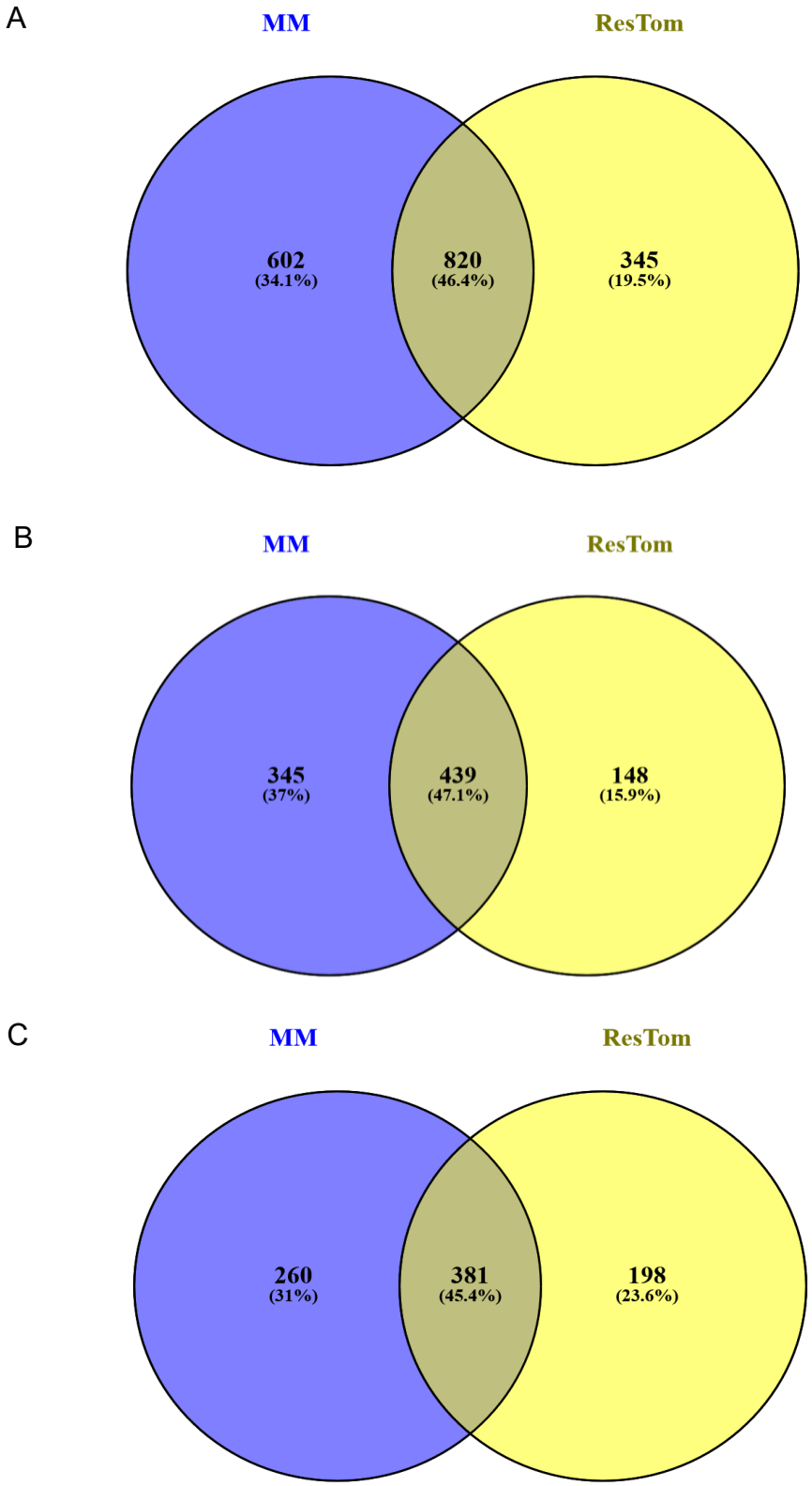

Figure 4.4 Venn Diagrams showing distribution of tomato regulated genes without cytokines.

(A) shows comparison of all genes regulated by MM and ResTom treatments. (B) shows comparison of upregulated genes, and (C) shows comparison of downregulated genes. In all Venn diagrams the percentage of gene changes is indicated. Based on genes shown to be significantly regulated with ≥ 1.5 fold change and an adjusted p-value of 0.05.

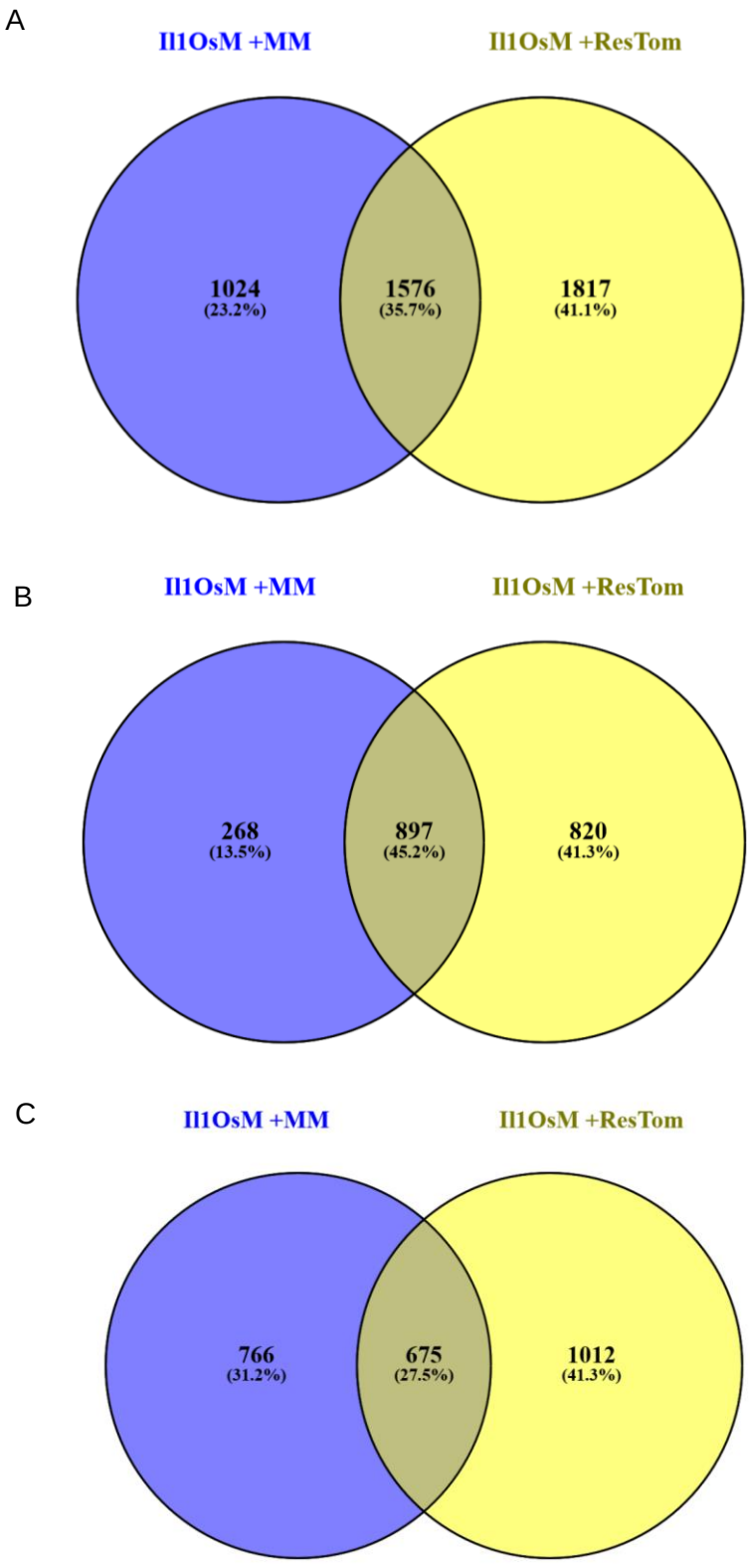

Figure 4.5 Venn Diagrams showing distribution of tomato regulated genes with cytokines.

(A) shows comparison of all genes regulated by cytokines+ MM or ResTom treatments. (B) shows comparison of upregulated genes, and (C) shows comparison of downregulated genes. Based on genes shown to be significantly regulated with a fold change ≥ 1.5 and an adjusted p-value of 0.05.

4.5 Pathway analysis

Significantly regulated genes, with a fold change of ≥1.5 and an adjusted p-value of 0.05 (Identified by data comparisons performed by Dr Govind Chandra, JIC) were entered into functional analysis software to determine pathways which may be regulated by tomato juice treatment, and to identify how significantly regulated genes may be related to each other.

The free online pathway analysis software: InnateDB (Breuer et al., 2013) was used to analyse the data. InnateDB pathway analysis determines which biological pathways are significantly over-represented based upon a gene list with fold change and p-values. A benefit of InnateDB is that it can incorporate pathway annotation from across several databases, therefore giving a comprehensive analysis of enriched pathways. For each pathway, significantly up and downregulated genes are given which allows candidate genes to be easily identified. Pathway enrichment analysis was performed to compare MM and ResTom gene regulation in the absence and presence of cytokines (Tables 4.6 to 4.9).

Comparison of the top up and down regulated pathways across the treatments showed some similar pathways regulated by both MM and ResTom treatment including upregulation of cellular responses to stress, and IL-10 anti-inflammatory signalling (Table 4.6 vs Table 4.7). Comparison of pathways regulated by cytokines (Table 4.8) to cytokines+ tomato juice (Table 4.9 and 4.10) identified pathways which are regulated in different ways. For example, pathways involved in assembly of collagen fibrils are significantly upregulated by cytokines, however downregulated with cytokines plus ResTom treatment (Table 4.9). This suggests that ResTom may be able to effectively prevent cytokine induced activation of certain genes. Both MM and ResTom (with cytokines) significantly downregulate genes related to degradation of the extracellular matrix (Table 4.8, 4.9 and 4.10).

Inflammation, such as that caused by UV damage, is known to lead to the degradation of extracellular matrix components, contributing to the formation of wrinkles. Therefore, the ability of MM and ResTom to downregulate genes involved in the degradation of extracellular matrix is particularly interesting.

Closer inspection of the genes regulated in the extracellular matrix pathways showed that cytokines significantly upregulate several MMPs including MMP-9 and MMP-14 known to be involved in the breakdown of extracellular matrix, in addition to several collagenases associated with degradation of collagen (Table 4:11). Conversely, several matrix metalloproteinases upregulated with cytokines alone, were significantly decreased when treated with cytokines plus ResTom extract (Table 4:11), suggesting a potential protective effect of ResTom juice against negative effects of inflammation on skin structure. As regulation of the extracellular matrix is known to be a factor which is

intrinsically linked to aging, this potential inhibition of extracellular matrix degradation enzymes is of interest.

Using the information provided by the pathway analysis data, in addition to the Venn diagram gene analysis, several candidate genes were identified to investigate in further detail including MMP-12, MMP-1 and MMP-9.

Table 4:6 Effect of MM juice in absence of cytokines on pathway regulation.

Top 10 significantly upregulated and down regulated pathways with the addition of MM juice in the absence of cytokines as determined by InnateDB pathway analysis, ranked by p-values.

Upregulated pathways with MM in absence of cytokines			
Rank	**Pathway Name**	**P-value**	**P-value (corrected)**
1	ATF-2 transcription factor network	2.72E-06	6.28E-03
2	Validated targets of C-MYC transcriptional repression	2.78E-05	3.21E-02
3	Calcineurin-regulated NFAT-dependent transcription in lymphocytes	3.75E-05	2.89E-02
4	Cellular responses to stress	5.63E-05	3.25E-02
5	ATF4 activates genes	1.21E-04	5.58E-02
6	PERK regulates gene expression	1.84E-04	7.09E-02
7	Il-10 anti-inflammatory signalling pathway	1.93E-04	6.38E-02
8	C-MYB transcription factor network	2.31E-04	6.68E-02
9	PRC2 methylates histones and DNA	2.70E-04	6.93E-02
10	Direct p53 effectors	3.99E-04	9.21E-02
Down regulated pathways with MM treatment in absence of cytokines			
Rank	**Pathway name**	**P-value**	**P-value (corrected)**
1	Metabolism	1.21E-04	2.79E-01
2	RNA Polymerase III Transcription Initiation from Type 3 Promoter	2.09E-04	2.41E-01
3	Ubiquinol biosynthesis	2.48E-04	1.91E-01
4	RNA Polymerase III Chain Elongation	3.40E-04	1.96E-01
5	RNA Polymerase III Transcription Initiation	7.29E-04	3.37E-01
6	Cytosolic DNA-sensing pathway	8.77E-04	3.38E-01
7	RNA Polymerase III Transcription Termination	1.10E-03	3.63E-01
8	Respiratory electron transport	1.17E-03	3.39E-01
9	Signalling by NOTCH4	1.39E-03	3.57E-01
10	RNA Polymerase III Abortive and Retractive Initiation	1.47E-03	3.09E-01

Table 4:7 Effect of MM juice in presence of cytokines on pathway regulation.

Top 10 significantly upregulated and down regulated pathways with the addition of MM juice in the presence of cytokines as determined by InnateDB pathway analysis, ranked by p-values

Upregulated pathways with MM in presence of cytokines			
Rank	**Pathway Name**	**P-value**	**P-value (corrected)**
1	ATF-2 transcription factor network	4.37E-09	1.01E-05
2	Canonical NF-kappaB pathway	1.58E-07	1.82E-04
3	MyD88-independent cascade	1.38E-06	6.39E-04
4	TRIF-mediated TLR3/TLR4 signalling	1.38E-06	6.39E-04
5	Toll Like Receptor 3 (TLR3) Cascade	1.38E-06	6.39E-04
6	Activated TLR4 signalling	1.65E-06	6.34E-04
7	MAPK signalling pathway	2.39E-06	7.88E-04
8	TGF_beta_Receptor	3.85E-06	0.001112
9	Calcineurin-regulated NFAT-dependent transcription in lymphocytes	4.85E-06	0.001245
10	Toll Like Receptor 4 (TLR4) Cascade	5.84E-06	0.00135
Down regulated pathways with MM treatment in presence of cytokines			
Rank	**Pathway name**	**P-value**	**P-value (corrected)**
1	The citric acid (TCA) cycle and respiratory electron transport	4.09E-10	9.45E-07
2	Respiratory electron transport, ATP synthesis by chemiosmotic coupling, and heat production by uncoupling proteins.	5.30E-10	6.12E-07
3	Oxidative phosphorylation	1.08E-07	8.35E-05
4	Mitochondrial translation elongation	1.15E-07	5.33E-05
5	Mitochondrial translation initiation	1.15E-07	5.33E-05
6	Mitochondrial translation termination	1.47E-07	5.66E-05
7	Respiratory electron transport	3.93E-07	1.30E-04
8	Mitochondrial translation	5.73E-07	1.66E-04
9	Degradation of the extracellular matrix	1.12E-06	2.88E-04
10	Metabolism	2.38E-06	5.49E-04

Table 4:8 Effect of Cytokines on pathway regulation.

Top 10 significantly upregulated and down regulated pathways with the addition of cytokines as determined by InnateDB pathway analysis, ranked by p-values.

	Pathways upregulated with cytokine treatment		
Rank	**Pathway Name**	**P-value**	**P-value (corrected)**
1	Amoebiasis	2.36E-13	5.46E-10
2	Extracellular matrix organization	5.18E-13	5.98E-10
3	Cytokine-cytokine receptor interaction	1.64E-10	1.27E-07
4	ECM proteoglycans	2.22E-09	1.28E-06
5	Beta1 integrin cell surface interactions	2.55E-09	1.18E-06
6	Collagen formation	1.94E-08	7.47E-06
7	Non-integrin membrane-ECM interactions	2.61E-08	8.63E-06
8	IL23-mediated signalling events	2.65E-08	7.66E-06
9	Assembly of collagen fibrils and other multimeric structures	1.19E-07	3.05E-05
10	Chemokine receptors bind chemokines	5.41E-07	1.25E-04
	Pathways downregulated with cytokine treatment		
Rank	**Pathway name**	**P-value**	**P-value (corrected)**
1	Metabolism	8.97E-10	2.07E-06
2	HIF-1-alpha transcription factor network	6.52E-09	7.53E-06
3	Metabolism of lipids and lipoproteins	1.33E-07	1.03E-04
4	Glucose metabolism	4.28E-06	2.47E-03
5	Cholesterol biosynthesis	1.39E-05	6.43E-03
6	Glycolysis / Gluconeogenesis	2.43E-05	9.37E-03
7	Activation of gene expression by SREBF (SREBP)	6.80E-05	2.25E-02
8	Transcriptional regulation of white adipocyte differentiation	8.10E-05	2.34E-02
9	Gap junction assembly	1.39E-04	3.57E-02
10	Steroid biosynthesis	1.48E-04	3.43E-02

Table 4:9 Effect of ResTom juice without cytokines on pathway regulation.

Top 10 significantly upregulated and down regulated pathways with the addition of ResTom in the absence of cytokines as determined by InnateDB pathway analysis, ranked by p-values.

	Upregulated pathways with ResTom in absence of cytokines		
Rank	**Pathway Name**	**P-value**	**P-value (corrected)**
1	ATF-2 transcription factor network	5.55E-07	1.28E-03
2	Cellular responses to stress	1.20E-06	1.39E-03
3	Cellular Senescence	1.25E-06	9.65E-04
4	DNA Damage/Telomere Stress Induced Senescence	1.77E-06	1.02E-03
5	Calcineurin-regulated NFAT-dependent transcription in lymphocytes	1.10E-05	5.06E-03
6	Senescence-Associated Secretory Phenotype (SASP)	1.34E-05	5.15E-03
7	Packaging of Telomere Ends	3.05E-05	1.01E-02
8	Il-10 anti-inflammatory signalling pathway	9.27E-05	2.68E-02
9	RNA Polymerase I Promoter Opening	2.11E-04	5.42E-02
10	Telomere Maintenance	2.75E-04	6.36E-02
	Down regulated pathways with ResTom treatment in absence of cytokines		
Rank	**Pathway name**	**P-value**	**P-value (corrected)**
1	Metabolism	3.22E-10	7.43E-07
2	Metabolism of lipids and lipoproteins	7.03E-07	8.13E-04
3	Butanoate metabolism	2.22E-05	1.71E-02
4	Fatty acid, triacylglycerol, and ketone body metabolism	2.46E-05	1.42E-02
5	Beta oxidation of hexanoyl-CoA to butanoyl-CoA	4.78E-05	1.84E-02
6	Beta oxidation of lauroyl-CoA to decanoyl-CoA-CoA	4.78E-05	1.84E-02
7	Beta oxidation of decanoyl-CoA to octanoyl-CoA-CoA	1.17E-04	3.39E-02
8	Beta oxidation of octanoyl-CoA to hexanoyl-CoA	1.17E-04	3.39E-02
9	The citric acid (TCA) cycle and respiratory electron transport	1.52E-04	3.90E-02
10	Mitochondrial Fatty Acid Beta-Oxidation	1.68E-04	3.88E-02

Table 4:10 Effect of ResTom juice with cytokines on pathway regulation.

Top 10 significantly upregulated and down regulated pathways with the addition of ResTom in the presence of cytokines as determined by InnateDB pathway analysis, ranked by p-values

Upregulated pathways with ResTom in presence of cytokines			
Rank	**Pathway Name**	**P-value**	**P-value (corrected)**
1	ATF-2 transcription factor network	2.19E-06	5.07E-03
2	Calcineurin-regulated NFAT-dependent transcription in lymphocytes	4.13E-06	4.77E-03
3	MAPK signalling pathway	7.35E-05	5.66E-02
4	SIRT1 negatively regulates rRNA Expression	1.28E-04	7.41E-02
5	Systemic lupus erythematosus	1.71E-04	7.90E-02
6	HDACs deacetylate histones	2.16E-04	8.30E-02
7	PRC2 methylates histones and DNA	7.20E-04	2.38E-01
8	IL12-mediated signalling events	8.64E-04	2.50E-01
9	Amino acid synthesis and interconversion (transamination)	8.69E-04	2.23E-01
10	IFN-gamma pathway	9.13E-04	2.11E-01
Down regulated pathways with ResTom treatment in presence of cytokines			
Rank	**Pathway name**	**P-value**	**P-value (corrected)**
1	Mitochondrial translation elongation	1.30E-10	3.01E-07
2	Mitochondrial translation initiation	7.21E-10	8.33E-07
3	Mitochondrial translation termination	1.00E-09	7.74E-07
4	Mitochondrial translation	1.32E-09	7.65E-07
5	Organelle biogenesis and maintenance	1.43E-07	6.59E-05
6	The citric acid (TCA) cycle and respiratory electron transport	1.49E-07	5.73E-05
7	Respiratory electron transport, ATP synthesis by chemiosmotic coupling, and heat production by uncoupling proteins.	3.50E-07	1.16E-04
8	Degradation of the extracellular matrix	6.94E-07	2.00E-04
9	Assembly of collagen fibrils and other multimeric structures	3.21E-06	8.24E-04
10	Beta3 integrin cell surface interactions	3.35E-06	7.74E-04

Table 4:11 Comparison of gene regulation of some genes of the "extracellular degradation pathway" with cytokine, cytokine+ MM and cytokine +ResTom treatments.

Identification of some of the genes identified via InnateDB pathway analysis to be upregulated and downregulated within the 'degradation of extracellular matrix' pathway with cytokine treatment, cytokine +MM and cytokine +ResTom. Arrows denote up or down regulation of genes respectively. ↓= significantly downregulated, ↑= significantly upregulated.

	IL1/OSM + MM	IL1/OSM +ResTom	Cytokines only
MMP-1	↓	↓	↑
MMP-2	↓	↓	↑
MMP-3	↓	↓	↑
MMP-9	↓	↓	↑
MMP-10	↑	↑	↑
MMP-11	↓	↓	↑
MMP-13	↓	↓	↓
MMP-14	↓	↓	↑
MMP-15	↓	↓	↑
MMP-19	↓	↓	↑
COL1A1	↓	↓	↑
COL1A2	↓	↓	↑
COL5A1	↓	↓	↑
COL5A2	↓	↓	↑
TIMP-1	↓	↓	↑

4.5.1 Validation of gene regulation proposed by microarray analysis

To validate any findings from the microarray, Dr Damon Bevan performed qRT-PCR (in the same RNA samples sent for microarray) for several genes shown to be significantly regulated by the microarray. The qRT-PCR data was then compared back to the microarray data. Table 4:12 and Table 4:13 show that the microarray analysis was largely consistent with qRT-PCR results confirming differences in gene expression found via microarray analysis data could be validated by qRT-PCR analysis.

Table 4:12 Comparisons between microarray analysis and qRT-PCR analysis for MM and ResTom treatment without cytokines.

Genes from microarray analysis were selected and compared to analysis by qRT-PCR in order to validate microarray data analysis. Downregulated genes are represented by "-". Performed by Dr Damon Bevan

	+MM		+ResTom	
	qRT-PCR	Microarray	qRT-PCR	Microarray
TNF-A	2.08	2.6	1.84	3.37
MMP-1	-1.29	-1.29	-1.29	-1.06
MMP-9	-2.77	-2.36	-3.40	-2.80
IL-6	-2.44	-2.27	-2.52	-1.62
MMP-12	-4.57	-3.32	-35.02	-10.94

Table 4:13 Comparisons between microarray analysis and qRT-PCR analysis for MM and ResTom treatment with cytokines.

Genes from microarray analysis were selected and compared to analysis by qRT-PCR in order to validate microarray data analysis. Downregulated genes are represented by "-". Performed by Dr Damon Bevan

	+MM		+ResTom	
	qRT-PCR	Microarray	qRT-PCR	Microarray
TNF-A	2.16	6.06	1.07	3.55
MMP-1	-2.27	-1.03	-3.82	-1.02
MMP-9	-6.50	-3.34	-16.08	-5.87
IL-6	-1.91	-1.17	-6.86	-1.72
COL3A1	-4.25	-3.4	-5.29	-5.12
MMP-12	-10.13	-5.72	-110.28	-39.99

4.5.2 Addition of ResTom reduces steady state mRNA levels of several extracellular matrix proteins

From the above microarray analysis, several candidate genes were assessed further using qRT-PCR using RNA from whole skin explants from - day or 5-day treatment regimes. Difference in gene expression between treatments were compared within donor, and between donors to get an overview of gene expression with treatments. Genes selected for further investigation were

identified as significantly regulated with MM and ResTom treatments, in addition to playing key roles in pathways important in the regulation of skin structure and function.

4.5.2.1 *MMP-1*

Steady state mRNA levels for MMP-1 showed a trend towards down-regulation with MM and ResTom juice after a 5-day treatment regime (Figure 4.6). MMP-1 expression was found to be repressed in 5 of 6 donors treated with MM juice, however one donor did display significant upregulation of MMP-1. ResTom on the other hand consistently downregulated MMP-1 expression across all donors (Table 4:14), however MMP-1 was only significantly downregulated in one donor.

Interestingly, addition of cytokines led to both up and down regulation of MMP-1 in donors, with 3 donors showing an increase in MMP-1 expression, and 2 donors a decrease in expression.

Despite the different donor responses of MMP-1 to cytokines, all donors displayed repression of MMP-1 when MM or ResTom was added in presence of cytokines. Although data analysis did not show a significant difference in gene expression with MM or ResTom treatment, analysis of cycle threshold (C_T) values showed greater repression of MMP-1 by ResTom in 4 of 5 donors (Table 4:15), suggesting higher biological efficacy by ResTom. Overall, these data suggest that tomato juice extracts can effectively repress the induced cytokine response of MMP-1, which could have wide implications in regulation of inflammation in the skin.

A

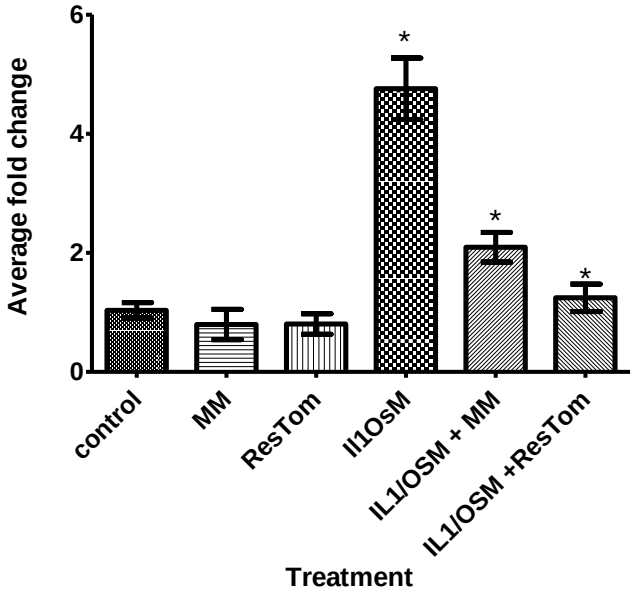

B

Treatment	Average C_T value
Control	20.66
MM	21.04
ResTom	20.82
IL1/OSM	19.38
IL1/OSM +MM	19.95
IL1/OSM +ResTom	20.67

Figure 4.6 Representative example of MMP-1-fold expression change in donor skin explants in response to different treatments.

A) qRT-PCR was performed of 6mm skin biopsies which had been cultured for 5 days (performed in triplicate). Data was analysed by relative quantification and normalised to 18S endogenous control. Each bar represents the mean of 3 samples +/- SEM. For this fold change analysis, the control (unstimulated) was set as 1. (B) Corresponding average C_T values are shown. Statistical difference was determined using ANOVA and Bonferroni multiple comparison test * $p \leq 0.05$, ** $p \leq 0.01$, *** $p \leq 0.001$.

Table 4:14 Summary of change of MMP1 expression levels across multiple skin donors.

qRT-PCR was performed on triplicate samples of 6mm skin biopsies from different donors (performed in triplicate) treated with tomato extracts and purified stilbenes with (A) and without (B) cytokines. Resulting CT values were converted to fold changes and using one way ANOVA and the multiple Bonferroni comparison test significance analysed. Treatments which caused significant changes in MMP1 expression are summarised in the table, showing overall trend of gene expression across different donors, and the number of donors' fold change expression was significant in.

	Vs No cytokines		
	+MM	**+ResTom**	**+IL1/OSM**
Overall trend in expression	↑↓	↓	↑↓
Significant in how many donors?	↑ in 1/6 donors	↓ in 1/6 donors	↑ in 3/6 donors

	Vs Cytokines	
	+MM	**+ResTom**
Overall trend in expression	↓	↓
Significant in how many donors?	in 4/5 donors	in 5/5 donors

Table 4:15 Average MMP1 C_T values for seven donor skin explants after 5 day treatment regime with aqueous tomato extracts with and without cytokines.

qRT-PCR of 6mm whole skin biopsies was performed after a 5 day treatment regime (performed in triplicate). Data was analysed by relative quantification and normalised to 18S for MMP1. Corresponding average C_T values are shown.

Donor	IL1/OSM	IL1/OSM +MM	IL1/OSM +ResTom
SPL003	19.38	19.95	19.95
SPL007	20.57	21.60	23.44
SPL010	21.76	24.78	25.02
SPL015	22.502	23.27	24.18
SPL026	21.64	22.35	23.27

4.5.2.2 *MMP-9*

Steady state mRNA levels for MMP-9 showed a trend towards down-regulation with both MM or ResTom juice after a 5-day treatment regime (Figure 4.7). In the absence of cytokines, treatment with MM and ResTom did not significantly downregulate MMP-9 expression.

Cytokine treatment induced expression of MMP-9, and significantly upregulated MMP-9 expression in 4 out of 7 donors (Table 4:16). Interestingly, cytokine treatment plus either MM or ResTom juice repressed MMP-9 in 4 out of 6 donors, and 4 out of 5 donors respectively showing significant repression of MMP-9. As with MMP-1, this suggests that the tomato extract can reduce the inflammatory cytokine induction of MMP-9 in human skin explants. In addition, there was a trend for ResTom to have a greater repressive effect on MMP-9 expression compared to MM, and although this was not determined to be statistically significant, analysis of C_T values shows a consistent increased repression of MMP-9 by ResTom compared to MM (Table 4:17). As is evident in the C_T values, MM already represses both MMP-1 and MMP-9 to very low expression levels. Therefore, at this concentration of tomato extract (10%) the increased activity of ResTom is not apparent. In future experiments it would be interesting to look at the activity of MM and ResTom at decreased concentrations, for example at 0.5 - 5%, which might show better the differences in repressive activity between the two extracts.

A

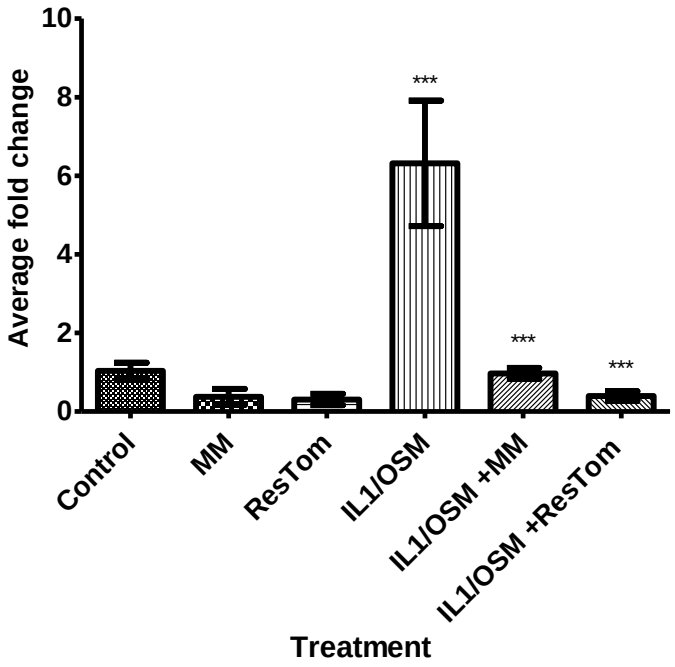

B

Treatment	Average C_T
Control	27.20
MM	28.83
ResTom	28.95
IL1/OSM	25.57
IL1/OSM +MM	27.59
IL1/OSM +ResTom	28.94

Figure 4.7 Representative example of MMP9 fold expression change in donor skin explants in response to different treatments.

A) qRT-PCR of 6mm skin biopsies which had been cultured for 5 days (performed in triplicate). Data was analysed by relative quantification and normalised to 18S endogenous control. Each bar represents the mean of 3 samples +/- SEM. For this fold change analysis, the control (unstimulated) was set as 1. (B) Corresponding average C_T values are shown. Statistical difference was determined using ANOVA and Bonferroni multiple comparison test *p≤ 0.05 **p≤ 0.01. ***p ≤ 0.001, ****p≤0.0001

Table 4:16 Summary of change of MMP9 expression levels across multiple skin donors.

qRT-PCR of triplicate 6mm skin biopsies from different donors treated with tomato extracts and purified stilbenes with (A) and without (B) cytokines. Resulting C_T values were converted to fold changes and using one way ANOVA and the multiple Bonferroni comparison test significance analysed. Treatments which caused significant changes in MMP9 expression are summarised in the table, showing overall trend of gene expression across different donors, and the number of donors' fold change expression was significant in.

	No Cytokines		
	+MM	**+ResTom**	**+IL1/OSM**
Overall trend in expression	↑1/7, ↓6/7	↓	↑
Significant in how many donors?	↑ in 1 donor	n.s.	↑ in 4 donors

	Vs Cytokines	
	+MM	**+ResTom**
Overall trend in expression	↓	↓
Significant in how many donors?	↓ in 4/6 donors	↓ in 4/5 donors

Table 4:17 Average MMP9 C_T values for seven donor skin explants after 5 day treatment regime with water based tomato extracts with and without cytokines.

qRT-PCR of 6mm whole skin biopsies after a 5 day treatment regime, performed in triplicate. Data was analysed by relative quantification and normalised to 18S for MMP9. Corresponding average C_T values are shown.

Donor	IL1/OSM	IL1/OSM +MM	IL1/OSM +ResTom
SPL003	25.57	27.59	28.94
SPL007	27.51	30.69	31.71
SPL010	30.43	33.81	34.48
SPL015	31.26	33.46	34.15
SPL026	30.92	31.06	33.53

4.5.3 Morphological analysis

Morphometry was performed on skin explants, to determine whether treatments led to any changes in epidermal thickness. To calculate epidermal thickness, each image was sectioned into three and the epidermal area and length measured for each section (as illustrated in Figure 4.8,A). Epidermal thickness was then calculated by epidermal area/length and averaged across all three sections.

Upon morphometric analysis of SPL015, it was noticed that cells in the epidermis had started to separate, and in places the dermis and epidermis layers were separated. This impacted upon the epidermal thickness analysis, whereby increases in epidermal thickness were greater due to increased space between cells rather than overall thickening (Figure 4.9 shows example data). As such, measurement of the epidermal layer did not give a true representation of epidermal thickness, so data of other donors have not been included.

Interestingly, separation between cells of the epidermis appeared to occur with ResTom treatments (Figure 4.9), with greater separation observed with cytokines. This was also observed in control tissue, but analysis of further experiments detailed below suggests that in the main, this is seen mainly under inflammatory conditions.

Comparison of samples from an additional 3 donors showed a similar morphology of separating epidermal and dermal layers, associated with IL1/OSM+ ResTom treatment in 2 donors (Figure 4.10). As with the SPL015 control, the SPL008 control showed complete separation between dermal and epidermal layers. Additionally, ResTom treatment alone showed some separation in SPL007. However, separation between cells in the epidermis only seemed to occur with cytokines+ ResTom treatment. From morphological images alone, it was unclear whether this was due to the embedding protocol, or due to the treatment. However, as all tissue samples from a donor were prepared for embedding at the same time, consistent morphological feature across all treatments would be expected, which was not observed, suggesting that separation was due to the treatment.

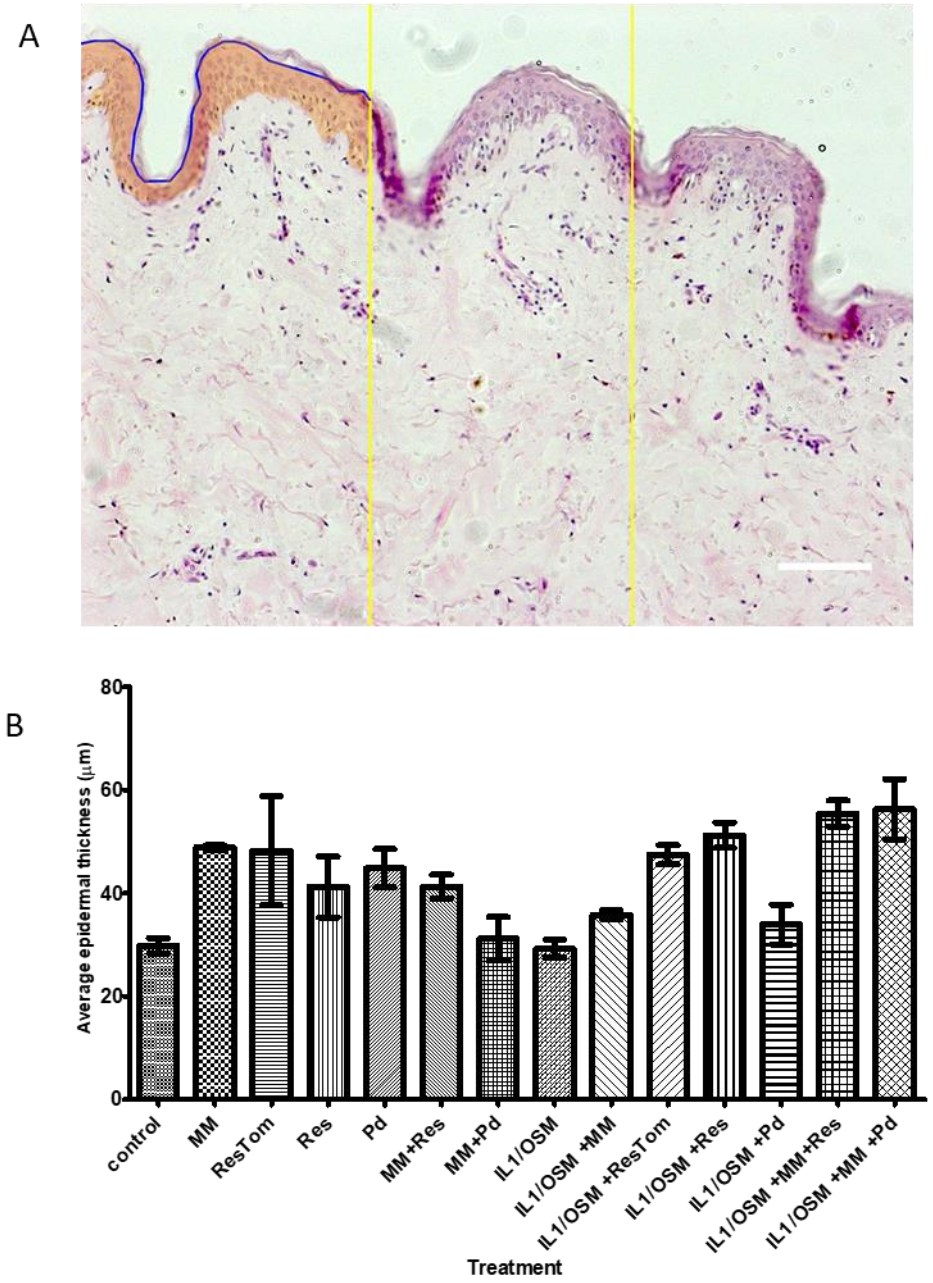

Figure 4.8. Representative example of average epidermal thickness at day 5 in SPL015 for each treatment.

A) Microscopic images were sectioned into three as illustrated, and the area (orange), and epidermal length (Blue) measured for each section. The average was then calculated across all three sections. B) Using the data collected from measurements performed on microscopic images, average epidermal thickness was calculated by area/ epidermal length across the three photo sections.

Res= Resveratrol, Pd= Polydatin

*p≤ 0.05 **p≤ 0.01. ***p ≤ 0.001, ****p≤0.0001

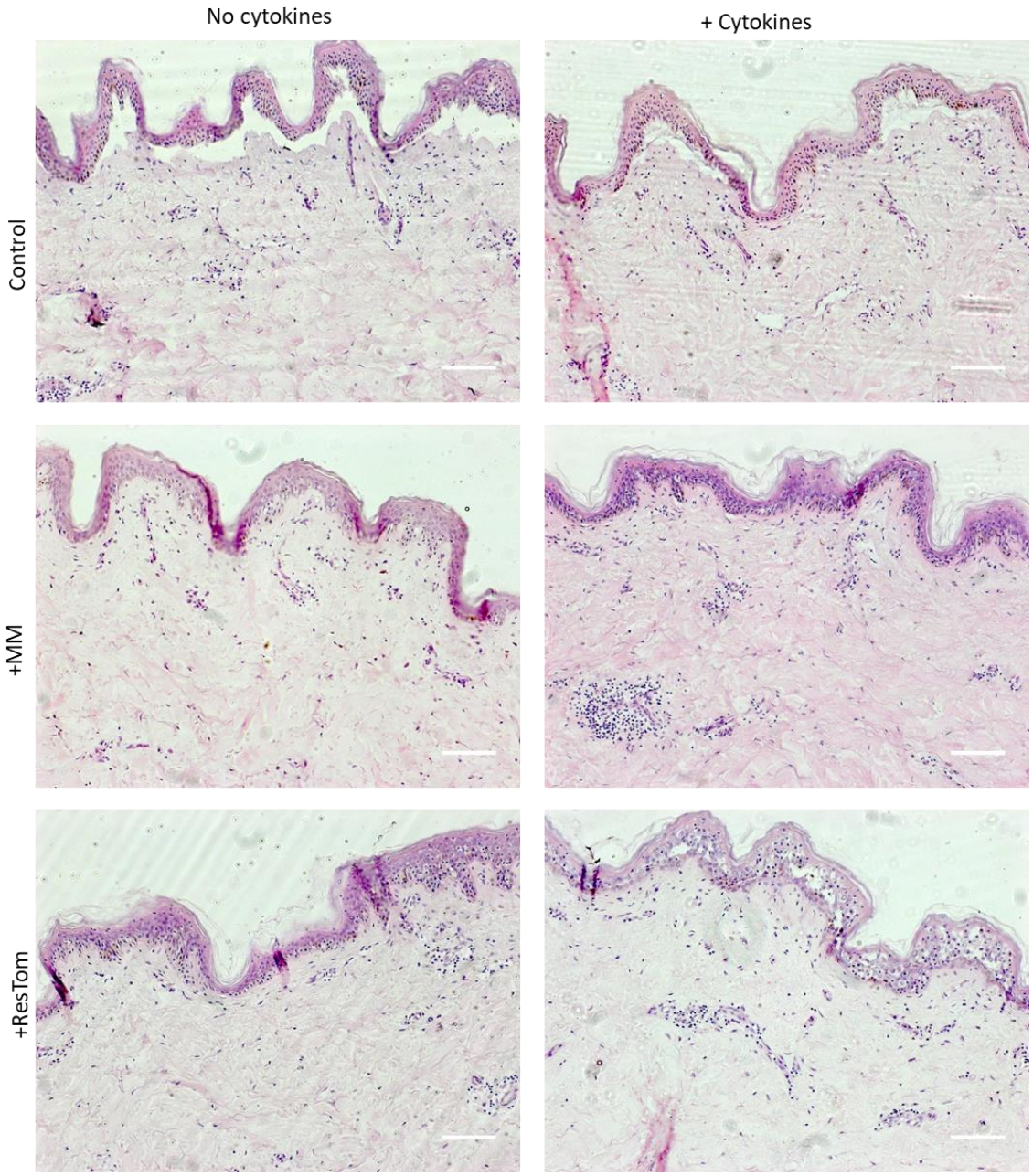

Figure 4.9 Morphology of human skin tissue 5-day post treatment, in SPl015.

6mm skin explants were cultured for 5 days with treatments before collecting. 10µm wax sections were taken for each treatment and stained with H and E to investigate morphological changes. Scale bar = 100µm

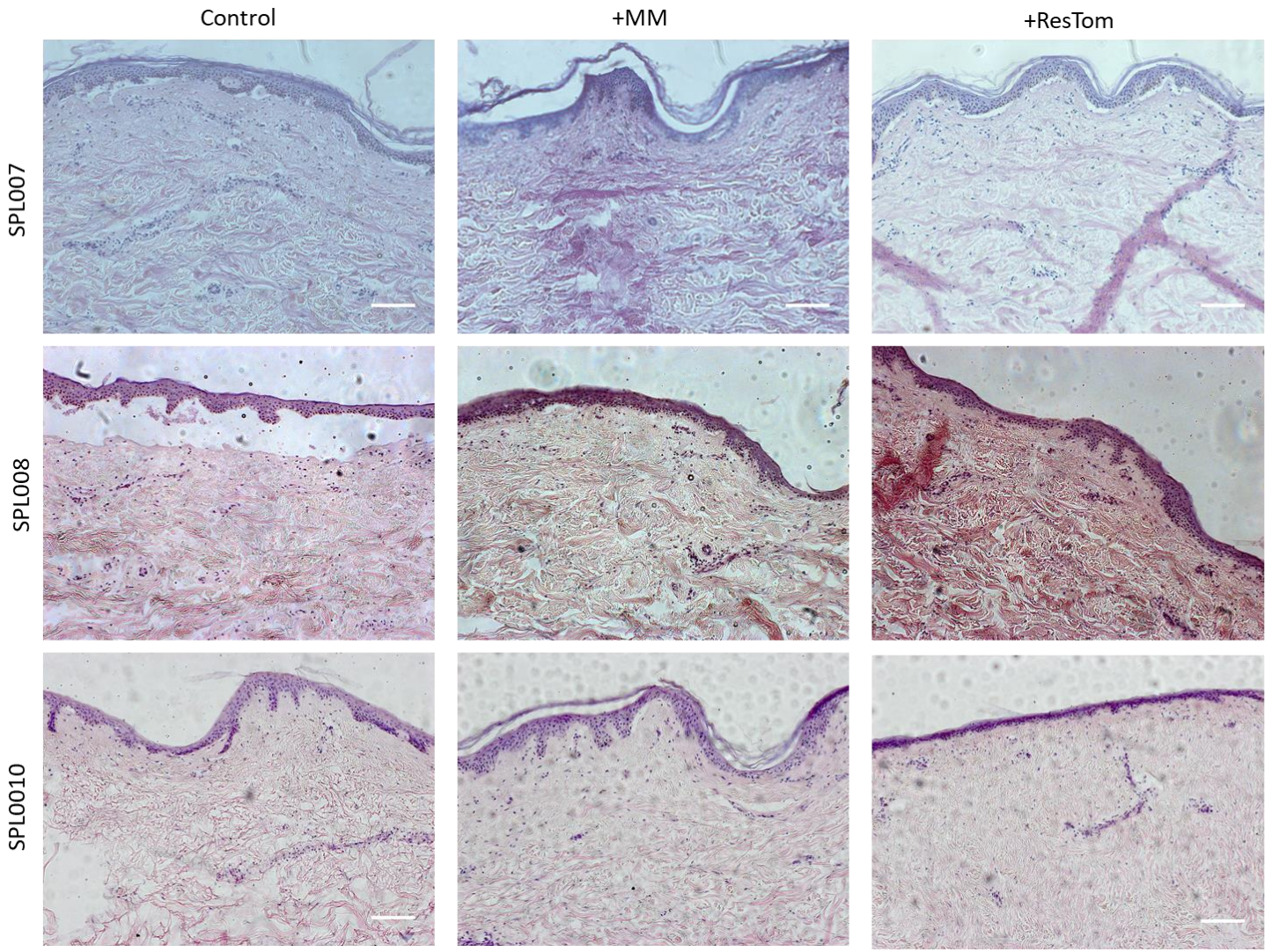
Control
+MM
+ResTom
SPL007
SPL008
SPL0010

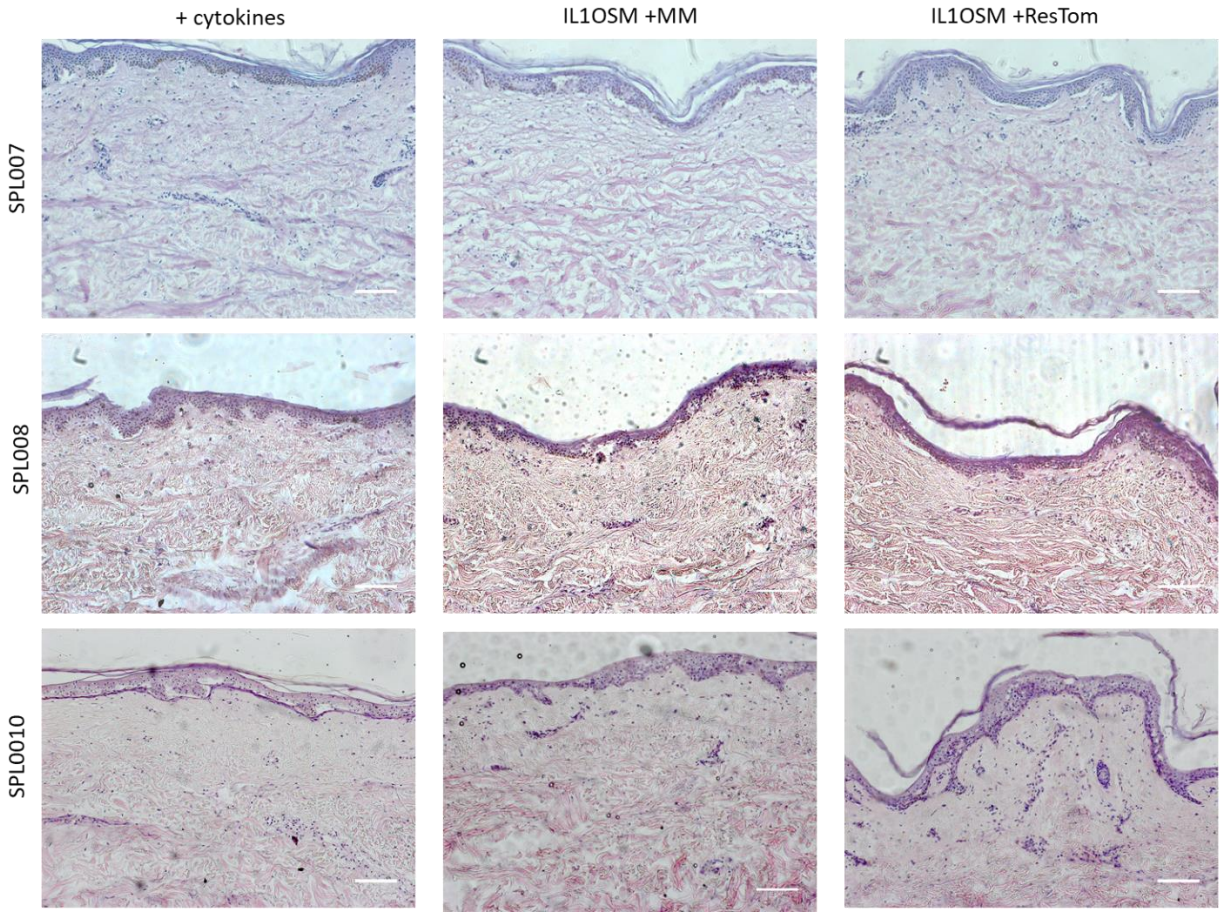

Figure 4.10 Morphology of human skin tissue 5-day post treatment with cytokines and MM/ or ResTom juice extract, in SPl007, SPL008 and SPL010.

6mm skin explants were cultured for 5 days with treatments before collecting. 10µm wax sections were taken for each treatment and stained with H and E to investigate morphological changes. Scale bar = 100µm

4.5.3.1 *COL7A1 and COL17A1*

Following the observation where there was some morphological changes at the dermo epidermal junction, it was interesting that large decreases in fold change of expression were associated with the two genes COL7A1 and COL17A1 when treated with IL1/OSM +ResTom compared to IL1/OSM (Table 4:18). However, adjusted p-values for these two genes were not significant. Both COL7A1 and COL17A1 operate within pathways determined to be significantly downregulated with IL1/OSM +ResTom compared to both IL1/OSM and IL1/OSM +MM.

Table 4:18 Comparison of fold changes of COL7A1 and COL17A1 with IL1/OSM +ResTom treatment compared to IL1/OSM only treatment.

Gene	Fold change	p.value	Adjusted p.value
COL7A1	-6.58983	1.38E-06	0.601799
COL17A1	-5.1157	6.77E-05	0.544418

Collagen VII, (the alpha 1 chain of which is encoded by encoded by COL7A1, is secreted by both keratinocytes and fibroblasts, and is crucial for the anchoring of basal keratinocytes to the dermis (Kuttner et al., 2014). Collagen XVII, (the alpha 1 chain of which is encoded by COL17A1 is an important component of type 1 hemidesmosomes that anchor epithelial cells to the basement membrane (Moilanen et al., 2017). Loss of both collagen VII and collagen XVII have been linked to recessive dystrophic epidermolysis bullosa (RDEB), in which patients suffer from skin blistering caused by separation of the dermis from the epidermis (Kuttner et al., 2014). Additionally, collagen XVII is known to be involved in keratinocyte migration, and is upregulated in several skin-diseases such as actinic keratosis and basal cell carcinomas (Moilanen et al., 2017).

The downregulation of these two collagen genes is therefore interesting and could potentially account for the observed morphology in IL1/OSM + ResTom treated skin samples, and additionally may factor in to changes in wound healing of skin (discussed in the next chapter).

4.5.3.2 *COL7A1*

Analysis of COL7A1 and COL17A1 was initially performed on SPL015, the first sample in which the separation between skin layers was observed. qRT-PCR of COL7A1 showed that expression of this gene was decreased in control skin compared to that of T0 skin, and further repressed by the addition of MM and ResTom juice (Figure 4.11). Although neither MM or ResTom juice showed statistically significant changes in expression of COL7A1 compared to control, the C_T values showed evident repression of expression by both treatments, with MM repressing COL7A1 to a greater degree (Figure 4.11, B).

With cytokine treatment, expression of COL7A1 increased slightly compared to control, but not significantly. Again, addition of MM and ResTom juice showed an increased repressive effect on COL7A1 expression compared to IL1/OSM alone. Interestingly IL1/OSM plus resveratrol or polydatin showed increased COL7A1 expression levels compared to IL1/OSM alone with C_T values near to those observed in control. The large reduction in COL7A1 expression observed using qRT-PCR (Figure 4.10) appeared to correlate with the morphological changes associated with the epidermis and dermis (Figure 4.9), with cytokines plus ResTom having highly repressed levels of COL7A1, and clear separation occurring within cells of the epidermis, or between the epidermis and dermal layers. However, IL1/OSM + MM did not show a high level of separation between cells of the epidermis, despite low COL7A1 expression levels.

To determine whether this trend observed in mRNA expression levels was specific to SPL015, qRT-PCR was repeated on RNA extracted from additional donor skin explants. Comparison of expression levels of COL7A1 across multiple donors did not show a significant repression in COL7A1 with any treatments in the absence of cytokines (Table 4:19), although from comparison of C_T values (Table 4:20) there did appear to be a trend towards the repression of COL7A1 with addition of MM and ResTom juice. With the addition of cytokines, there was a much more definite trend observed. Whereas, addition of IL1/OSM increased expression levels of COL7A1 across all donors, co-treatment of IL1/OSM with tomato juice-based treatments leads to repression of COL7A1. Interestingly, the repressive effect on COL7A1 expression was seen in with both MM and ResTom extracts. Despite this, separation between cells in the epidermal layer, or between dermal and epidermal layers was observed only in IL1/OSM +ResTom treated skin (Figure 4.9 and Figure 4.10). This suggested that COL7A1 is not the important factor underlying the observed morphological change.

A

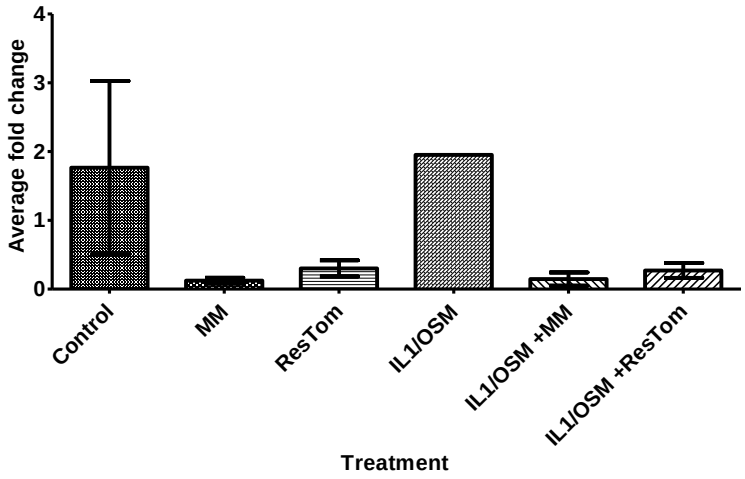

B

Treatment	Average C_T
Ctrl	30.33
MM	32.94
ResTom	32.24
IL1/OSM	†30.09
MM +IL1/OSM	33.66
ResTom +IL1/OSM	32.88

Figure 4.11 Effect of aqueous tomato extracts on relative expression of COL7A1 normalised to 18S in whole skin explants after 5-day treatment regime, from SPL015.

qRT-PCR of 6mm whole skin biopsies after a 5day treatment regime. Data was analysed by relative quantification and normalised to 18S for COL7A1 (A). Corresponding average C_T values are shown (B). Each bar represents the mean fold change of 3 explants ±SEM. Statistical difference was determined using one-way ANOVA with the Bonferroni multiple comparison test *p≤ 0.05 **p≤ 0.01. ***p ≤ 0.001, ****p≤0.0001. †representative of average of two C_T, not included in statistical analysis

Table 4:19 Summary of treatments leading to significant changes in COL7A1 expression in whole skin ex vivo explants, after 5-day treatment regime with and without cytokines.

qRT-PCR of 6mm skin biopsies from different donors treated with tomato extracts and purified stilbenes without with cytokines. Resulting C_T values were converted to fold changes and using one-way ANOVA and the multiple Bonferroni comparison test significance analysed. Treatments which caused significant changes in COL7A1 expression are summarised in the table, showing overall trend of gene expression across different donors, and the number of donors' fold change expression was significant in.

	+ Cytokines		
	+IL1/OSM	**+MM**	**+ResTom**
Overall trend in expression	↑	↓	↓
Significant in how many donors?	sig ↑ 1/5	sig ↓ in 1/4	sig ↓ in 1/3

Table 4:20 Average COL7A1 C_T values for seven donor skin explants after 5 day treatment regime with water based tomato extracts with and without cytokines .

qRT-PCR of 6mm whole skin biopsies after a 5day treatment regime. Data was analysed by relative quantification and normalised to 18S for COL7A1. Corresponding average C_T values are shown.

	SPL010	**SPL013**	**SPL015**	**SPL026**	**SPL028**
Control	30.59	29.82	30.33	29.58	28.60
+MM	30.83	30.78	32.94	30.24	30.00
+ResTom	29.95	32.24	32.24	30.62	-

4.5.3.3 *COL17A1*

qRT-PCR analysis of SPL015 revealed a similar pattern of COL17A1 expression with tomato-extract treatment to that of COL7A1. A significant decrease in COL17A1 was observed with MM extract, but not with ResTom extract (Figure 4.12). Addition of cytokines slightly induced COL17A1 expression, however addition of MM or ResTom together with cytokines acted to inhibit COL17A1 expression. As with COL7A1, these changes in COL17A1 mRNA expression did not correlate fully with the visual morphological changes in skin structure with treatments (Figure 4.9), since MM treated skin showed no separation of between epidermal cells despite very low COL17A1 expression levels.

qRT-PCR of COL17A1 was performed on additional donors (Table 4:21) and showed a definite trend towards repression of COL17A1 with addition of tomato extracts, this effect was also observed under inflammatory conditions, although due to time constraints qRT-PCR was only performed only two donors with these treatment conditions, so definite conclusions cannot be drawn.

Like SPL015, comparison of mRNA expression data from SPL010 and SPL013 did not correlate fully to the observed differences in the morphology of the skin. For example, in SPL010 there was a repression of COL17A1 with IL1/OSM+MM compared to IL1/OSM (Figure 4.13) however H and E staining showed greater separation between the epidermis and dermis in IL1/OSM treated skin (Figure 4.9). Additionally, SPL013 showed a greater repression of COL17A1 with ResTom treatment compared to MM (Figure 4.14), although analysis of the H and E staining showed less separation in skin layers with ResTom treatment compared to MM treatment (Figure 4.15).

Although there was significant repression in expression of both COL7A1 and COL17A1 when treated with tomato extracts, this did not account fully for all the morphological changes observed between the treatments. It is likely that the repression of these two genes is influenced the separation of skin layers observed, although the inconsistencies between mRNA and morphological data in some treatments suggested that there are other mechanisms underlying these morphological changes. Unfortunately, due to time constraints no histochemical, or protein analyses were possible regarding collagen, although it would be interesting to determine how these changes at the mRNA level are being translated in skin.

It was interesting that addition of tomato juice repressed these two genes to such a significant degree, and that this effect seemed to be related to addition of tomato extracts, indicating that tomato juice is affecting expression of these two genes.

The repressive effect of tomato juice on COL7A1 and COL17A1 in inflammatory conditions could be interesting in the treatment of skin cancers. It has been reported in previous studies that COL17A1 is highly upregulated in squamous cell carcinoma, where it helps migration of malignant cells. This

therefore could offer a beneficial topical treatment method for skin carcinomas to help inhibit the invasion and progression of skin cancer cells (Parikka et al., 2006).

A

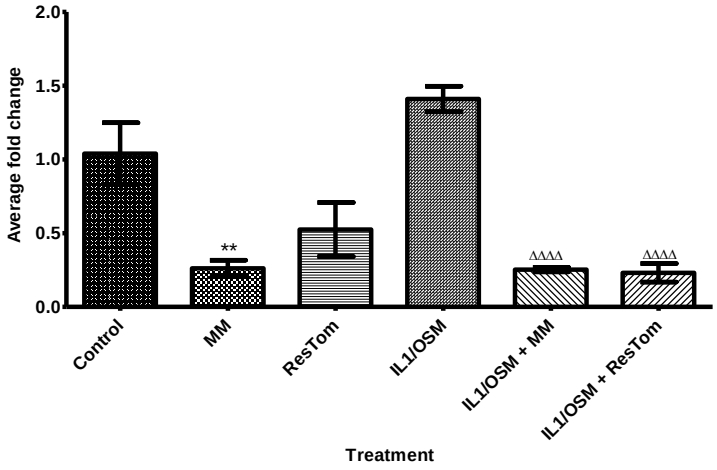

B

Treatment	Average C_T
Ctrl	25.97
MM	27.29
ResTom	26.98
IL1/OSM	26.31
MM +IL1/OSM	27.86
ResTom +IL1/OSM	28.39

Figure 4.12 Effect of aqueous tomato extracts on relative expression of COL17A1 normalised to 18S in whole skin explants after 5-day treatment regime, from SPL015.

qRT-PCR of 6mm whole skin biopsies after a 5day treatment regime. Data was analysed by relative quantification and normalised to 18S for COL17A1(A). Corresponding average C_T values are shown (B). Each bar represents the mean fold change of 3 explants ±SEM. Statistical difference was determined using one way ANOVA with the Bonferroni multiple comparison test *significant compared to control, Δ significant compared to IL1/OSM.

*p≤ 0.05 **p≤ 0.01. ***p ≤ 0.001, ****p≤0.0001

Table 4:21 Summary of treatments leading to significant changes in COL17A1 expression in whole skin ex vivo explants, after 5-day treatment regime with and without cytokines.

qRT-PCR of 6mm skin biopsies from different donors treated with tomato extracts and purified stilbenes without (A) and with (B) cytokines. Resulting C_T values were converted to fold changes and using one-way ANOVA and the multiple Bonferroni comparison test significance analysed. Treatments which caused significant changes in COL17A1 expression are summarised in the table, showing overall trend of gene expression across different donors, and the number of donors' fold change expression was significant in.

	No Cytokines		
	+ResTom	**+MM**	**+IL1/OSM**
Overall trend in expression	↓	↓	↑↓
Significant in how many donors?	sig ↓ in 1/3 donors	sig ↓ in 1/3 donors	sig ↓ in 1/3 donors

	+ Cytokines	
	+ResTom	**+MM**
Overall trend in expression	↓	↓
Significant in how many donors?	sig ↓ in 1/2 donors	sig ↓ in 1/2 donors

A

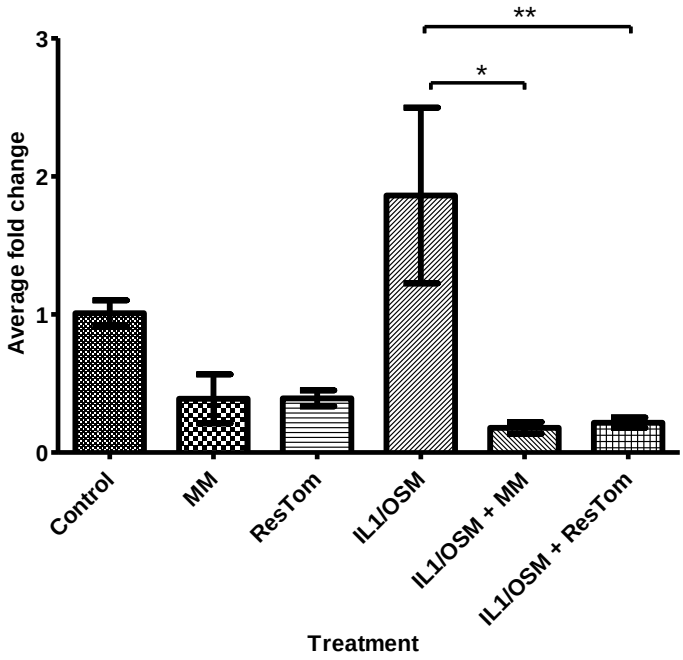

B

Treatment	Average C_T
Control	27.50
MM	29.15
ResTom	28.73
IL1/OSM	27.41
IL1/OSM +MM	29.70
IL1/OSM +ResTom	29.61

Figure 4.13 Effect of aqueous tomato extracts on relative expression of COL17A1 normalised to 18S in whole skin explants after 5-day treatment regime, from SPL010.

qRT-PCR of 6mm whole skin biopsies after a 5day treatment regime. Data was analysed by relative quantification and normalised to 18S for COL17A1 (A). Corresponding average C_T values are shown (B). Each bar represents the mean fold change of 3 explants ±SEM. Statistical difference was determined using one-way ANOVA with the Bonferroni multiple comparison test. *significant compared to control, ϕ significant compared to MM.

*p≤ 0.05 **p≤ 0.01. ***p ≤ 0.001, ****p≤0.0001

A

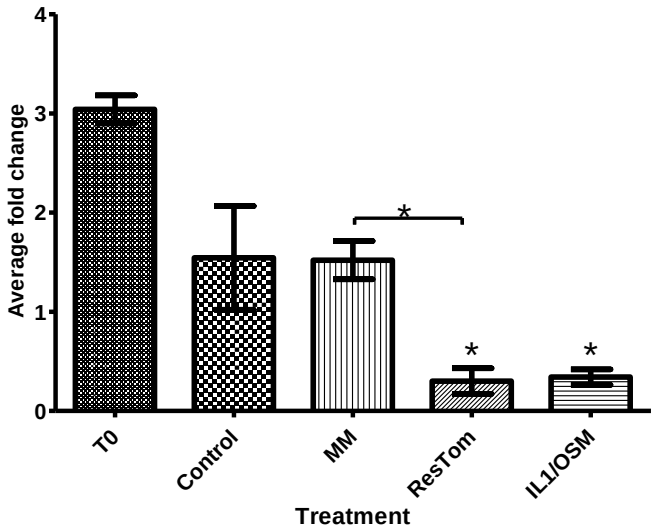

B

Treatment	Average C_T
T0	24.53
Control	26.61
MM	28.18
ResTom	30.08
IL1/OSM	28.25

Figure 4.14 Effect of aqueous tomato extracts on relative expression of COL17A1 normalised to 18S in whole skin explants after 5-day treatment regime, from SPL013.

qRT-PCR of 6mm whole skin biopsies after a 5day treatment regime. Data was analysed by relative quantification and normalised to 18S for COL17A1 (A). Corresponding average C_T values are shown (B). Each bar represents the mean fold change of 3 explants ±SEM. Statistical difference was determined using one-way ANOVA with the Bonferroni multiple comparison test. *significant compared to control, ϕ significant compared to MM.

*p≤ 0.05 **p≤ 0.01. ***p ≤ 0.001, ****p≤0.0001

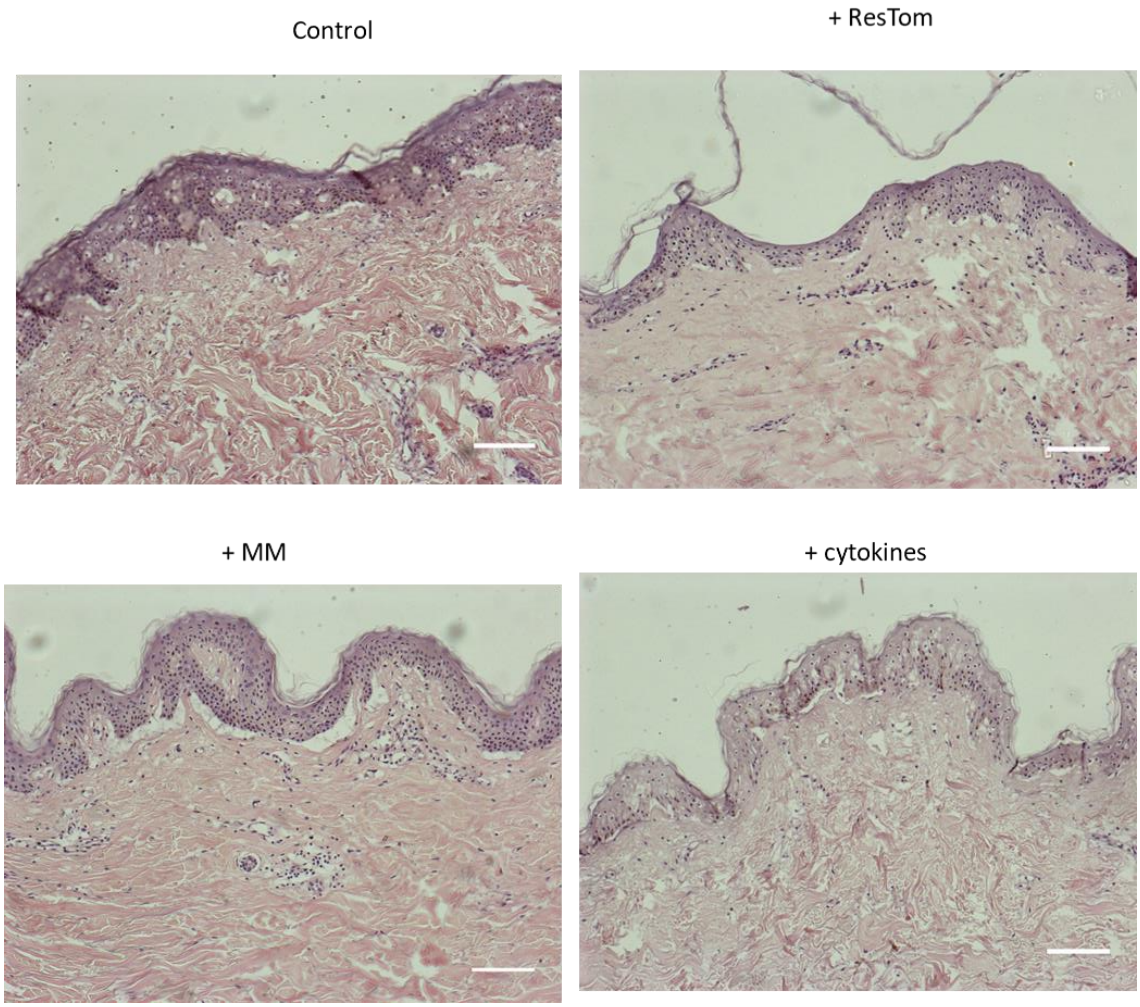

Figure 4.15 Morphology of human skin tissue 5-day post treatment with tomato treatment, and cytokine treatment in SPL013.

6mm skin explants were cultured for 5 days with treatments before collecting. 10µm wax sections were taken for each treatment and stained with H and E to investigate morphological changes.

Scale bar = 100µm

4.5.3.4 *EDN1*

Endothelin 1 (EDN1) was identified before in-depth analysis of the micro-array data has been completed, where EDN1 was identified to be highly downregulated with IL1/OSM +ResTom compared to IL1/OSM. Additionally, pathway analysis identified the "EGFR-dependent Endothelin signalling events pathway" to be significantly downregulated, in which EDN1 plays a role. Endothelin 1 is a key regulator of vasoconstriction and fibrosis and has indirect proinflammatory effects (Kowalczyk et al., 2015), Finally, endothelin 1 has been shown to contribute to the effect of transforming growth factor β1(TGF β1) and associated wound healing acceleration and increased fibrogenesis (Lagares et al., 2010). Therefore, the potential for ResTom to repress EDN1 expression in the presence of inflammatory cytokines was extremely interesting.

qRT PCR of SPL003 confirmed a significant reduction in EDN1 expression with IL1/OSM + ResTom compared to IL1/OSM (Figure 4.16). Although addition of MM to IL1/OSM slightly reduced EDN1 expression, this was not to the same degree as ResTom juice, suggesting that this reduced EDN1 expression was associated with the resveratrol present in the ResTom juice. Further qRT-PCR was performed on additional skin donors and confirmed the repressive action of ResTom juice on IL1/OSM induced expression of EDN1 (Table 4:22), with a significant reduction in 3 of 5 donors. Although a significant difference in EDN1 expression was observed in SPL003 for IL1/OSM +ResTom compared to IL1/OSM +MM, this was not observed in the other donors, which exhibited similar reductions with both treatments.

One donor, SPL007, showed a very different expression pattern of EDN1 (Figure 4.17). In SPL007, expression of EDN1 was highly repressed in response to IL1/OSM treatment and exhibited no change in expression compared to control with ResTom treatment. Additionally, co-treatment of cytokines with MM or ResTom increased EDN1 expression compared to IL1/OSM. The very different expression pattern in SPL007 highlighted donor to donor variation with treatments and gene expression, and the need to look at gene expression changes in multiple donors.

Overall, MM and ResTom treatment reduces the induction of EDN1 by cytokines. This may be beneficial for treatments of chronic skin inflammatory diseases, as a reduction in EDN1 would help reduce vasodilation of blood vessels in the skin and help reduce the inflammatory processes.

A

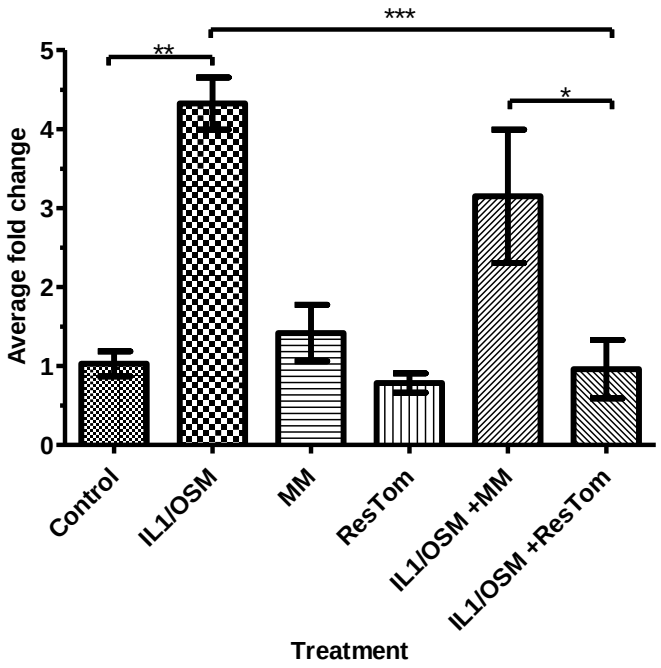

Treatment	Average C_T
Control	29.89
IL1/OSM	28.93
MM	29.42
ResTom	29.74
IL1/OSM + MM	28.57
IL1/OSM + ResTom	30.73

Figure 4.16 Effect of aqueous tomato extracts on relative expression of EDN1 normalised to 18S in whole skin explants after 5-day treatment regime, from SPL003.

qRT-PCR was performed on cDNA extracted from 6mm whole skin biopsies after a 5day treatment regime. Data was analysed by relative quantification and normalised to 18S for EDN1 (A). Corresponding average C_T values are shown (B). Each bar represents the mean fold change of 3 explants ±SEM. Statistical difference was determined using one-way ANOVA with the Bonferroni multiple comparison test. *p≤ 0.05 **p≤ 0.01. ***p ≤ 0.001, ****p≤0.0001

Table 4:22 Summary of treatments leading to significant changes in Endothelin 1(EDN1) expression in whole skin ex vivo explants, after 5-day treatment regime with and without cytokines.

qRT-PCR was performed on triplicate samples of cDNA extracted from 6mm skin biopsies from different donors treated with tomato extracts and purified stilbenes without (A) and with (B) cytokines. Resulting C_T values were converted to fold changes and using one-way ANOVA and the multiple Bonferroni comparison test significance analysed. Treatments which caused significant changes in EDN1 expression are summarised in the table, showing overall trend of gene expression across different donors, and the number of donors' fold change expression was significant in.

	No Cytokines		
	+MM	**+ResTom**	**+IL1/OSM**
Trend in expression	↓	↓	↑
Significant in how many?	ns	ns	↑ in 3 of 5 donors

	+ Cytokines	
	+MM	**+ResTom**
Trend in expression	↓	↓
Significant in how many?	↓ in 3 of 5 donors	↓ in 3 of 5 donors

A

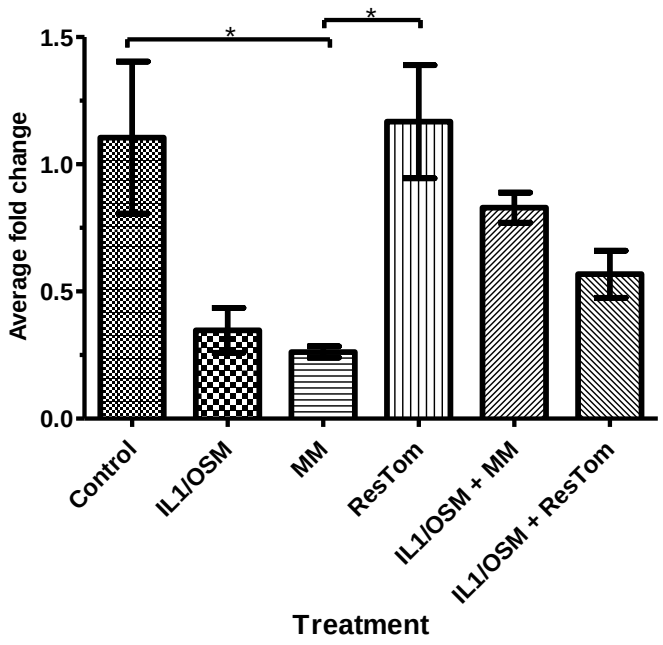

B

Treatment	Average C_T
Control	28.87
IL1/OSM	30.29
MM	30.62
ResTom	29.24
IL1/OSM + MM	29.77
IL1/OSM + ResTom	29.87

Figure 4.17 Effect of aqueous tomato extracts on relative expression of EDN1 normalised to 18S in whole skin explants after 5-day treatment regime, from SPL007.

qRT-PCR was performed on cDNA extracted from 6mm whole skin biopsies after a 5day treatment regime. Data was analysed by relative quantification and normalised to 18S for EDN1 (A). Corresponding average C_T values are shown (B). Each bar represents the mean fold change of 3 explants ±SEM. Statistical difference was determined using one-way ANOVA with the Bonferroni multiple comparison test. *p≤ 0.05 **p≤ 0.01. ***p ≤ 0.001, ****p≤0.0001

4.5.3.5 *MMP-12*

Microarray analysis from donor SPL003, identified a large repressive action of MM on MMP-12 in the presence of cytokines, and even greater repression by ResTom. qRT-PCR of SPL003 (Figure 4.18), confirmed the repressive activity of both MM and ResTom both in the absence and presence of cytokines. Additionally, qRT-PCR confirmed that ResTom supresses MMP-12 to a greater level than MM, although this difference was not statistically significant. Despite this, inspecting differences in CT values show that ResTom is potentially a greater repressor of MMP-12 than MM (Figure 4.18).

The repressive qualities of both MM and ResTom juice on MMP-12 expression were particularly interesting, as MMP-12 is known to be involved with degradation of elastin which is associated with aging of the skin, and sun-associated damage leading to the development of wrinkles. This repression of MMP-12, especially in the presence of inflammatory conditions is therefore an intriguing finding and as such was investigated in further detail in the next chapter.

A

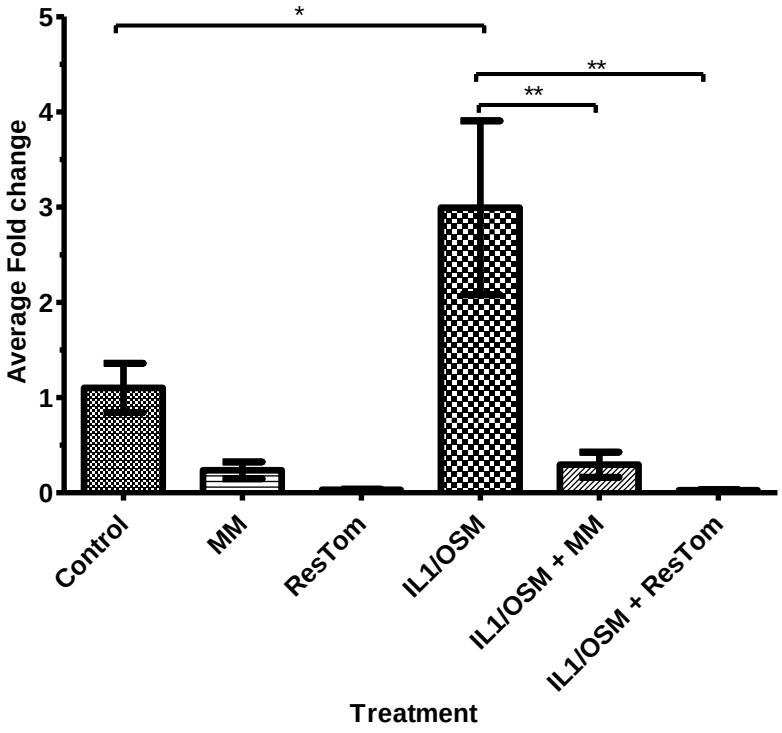

B

Treatment	Average C_T value
Control	29.06
MM	31.41
ResTom	33.68
IL1/OSM	28.81
IL1/OSM + MM	31.72
IL1/OSM + ResTom	34.94

Figure 4.18 Effect of aqueous tomato extracts on relative expression of MMP-12 normalised to 18S in whole skin explants after 5 day treatment regime, from SPL003 (performed by Dr Damon Bevan).

Representative example of MMP-12 fold expression change in donor skin explants in response to different treatments. A) qRT-PCR was performed on cDNA extracted from 6mm skin biopsies which had been cultured for 5 days. Data was analysed by relative quantification and normalised to 18S endogenous control. Each bar represents the mean of 3 samples +/- SEM. For this fold change analysis, the control (unstimulated) was set as 1. (B) Corresponding average C_T values are shown. Statistical difference was determined using ANOVA and Bonferroni multiple comparison test *p≤ 0.05 **p≤ 0.01. ***p ≤ 0.001, ****p≤0.0001.

4.6 Discussion:

Understanding gene regulation in full-thickness skin explants is important for understanding the biological effects of treatments. By comparing gene regulation in skin in response to MM and ResTom juices in both non-inflammatory and inflammatory settings we have been able to identify the effects on several genes which play important roles in the maintenance of skin structure, which could have biological applications in treatment of skin diseases. I used both microarray analysis and qRT-PCR to reveal novel gene regulation in human skin explants in response to tomato juice extracts and identified high biological activity of ResTom juice in an inflammatory environment.

4.6.1 MM juice treatment vs ResTom treatment

Microarray analysis on one donor identified that treatment of skin with MM juice by itself led to many genes being significantly regulated both in the presence and absence of cytokines. Interestingly, in the absence of cytokines, MM juice treatment significantly regulated a greater number of genes than ResTom juice (Table 4:3). This suggested that MM juice itself has high biological activity at 10% *in vitro*.

Comparison of genes significantly regulated by MM compared to ResTom showed that a significant number of genes were specifically regulated by ResTom juice. In the absence of cytokines, a large proportion of genes regulated with ResTom were also regulated with MM treatment (Figure 4.4), although in the presence of cytokines there was a significant increase in the number of genes only regulated only by ResTom (Figure 4.5). This suggests that ResTom has a greater biological effect in the presence of cytokines. An increased biological activity of ResTom compared to MM juice was also shown in the recent study by Scarano et al. (2018). Comparison of the activity of MM and ResTom extracts on the two cytokines IL-1 and TNF-a were shown to be greatly inhibited with ResTom compared to MM juice.

Pathway analysis showed similarities in pathways regulated by both MM and ResTom treatment, for example downregulation of degradation of extracellular matrix components (Table 4.7 and Table 4.10). However, further analysis of these pathways showed that ResTom had a greater effect, significantly regulating more genes than MM (Table 4:11), again suggesting a wider biological effect. Using the combined information from micro-array analysis data and pathway analysis several genes were identified to look at in greater detail on more donors.

4.6.2 MMP-1

Downregulation of MMP-1 was observed with both MM and ResTom treatments in the absence and presence of cytokines. The repressive nature of MM and ResTom juice on MMP-1 was more apparent in the presence of cytokines, where MMP-1 was downregulated with tomato extract treatment in 4/5 and 5/5 donors respectively. Although statistical analysis did not show a significant

difference in gene expression between MM and ResTom juice treatments, it was evident from comparison of CT values that ResTom is able to repress MMP-1 to a greater degree (Table 4:15).

MMP-1 is not expressed in intact adult human epidermis (Kähäri and Saarialho-Kere, 1997), although it is expressed at high levels within cutaneous wounds and photo-damaged skin(Fisher et al., 2002), as well as skin of patients with blistering skin diseases (Kähäri and Saarialho-Kere, 1997), atopic dermatitis, and invasive melanoma cells (Huntington et al., 2004).

Since photodamage of the skin is associated with inflammation (Pillai et al., 2005), and increased expression of MMP-1 leading to degradation of collagen and associated changes in skin structure, the potential for MM and ResTom juice to repress MMP-1 expression under inflammatory conditions could provide to be a therapy to help reduce photo-induced damage of the skin.

4.6.3 MMP-9

MMP-9 was identified as downregulated by both MM and ResTom treatments (Figure 4.7). As with MMP-1 expression, the repressive nature of MM and ResTom on MMP-9 was more apparent in the presence of cytokines, where treatment with tomato extracts effectively prevented induction of MMP-9 expression by cytokines in addition to repressing expression in treated tissues (Table 4:16). ResTom was also shown to suppress MMP-9 to a greater extent than MM juice, although this effect was not statistically significant at the treatment concentrations used.

The ability of ResTom to prevent and reduce expression of MMP-9 in the presence of cytokines offers a lot of potential in terms of treatments of inflammatory skin diseases. MMP-9 is well documented to be highly expressed during inflammation (Manicone and McGuire, 2008) such as UV-damage. As ResTom treatment effectively prevents and reduces expression of MMP-9 even under inflammatory conditions, this could offer an effective treatment to reduce expression of pro-inflammatory mediators after UV-damage, thereby helping to reduce skin structural damage in skin caused by overexpression of MMPs.

4.6.4 Collagen VII and XVII

The two genes COL7A1 and COL17A1 were selected for further investigation after morphological analysis of 6mm skin explants showed significant separation between dermal and epidermal layers. Given this observation, the evidence from micro-array analysis which showed significant upregulation of both COL7A1 and COL17A1 in the separating skin samples was interesting.

qRT-PCR analysis confirmed downregulation of COL7A1 and COL17A1 with MM and ResTom treatments (Figure 4.11), although comparisons of qRT-PCR data with morphological data did not always correlate, suggesting that the down-regulation of these two genes could not provide a full explanation for the observed separation in epidermal and dermal layers. However, in the absence

of data on the expression levels of collagen proteins, it is hard to draw conclusions about the effect of tomato extracts. Therefore, future studies should investigate the protein expression levels of collagen in skin explants, in addition to immunohistochemistry in whole skin explants to fully elucidate how and if tomato extracts are affecting collagen proteins.

The repression of both these genes has several implications regarding migration of cells and wound healing, as both have been implicated in the regulation of keratinocyte migration (Dabelsteen et al., 1998, Löffek et al., 2014). Considering this, the action of these two collagens were investigated further within wound healing models (Chapter 6:).

4.6.5 EDN1

Steady state mRNA levels for EDN1 showed a trend towards down-regulation with both MM or ResTom juice after a 5-day treatment regime (Table 4:22), although the changes in EDN1 expression were significant statistically only in the presence of cytokines.

Plant polyphenols have been widely reported to have an regulatory role on endothelin 1 (Nicholson et al., 2008, Stoclet et al., 2004), with the high polyphenol content of red wine proposed to explain the anti-hypertensive properties linked to red wine consumption (Lopez-Sepulveda et al., 2011). Dietary studies have shown significant decreases in circulating endothelin 1 levels following consumption of high-polyphenol containing feed(Zou et al., 2003, Liu et al., 2005). Additionally, treatment of human endothelial cells with resveratrol significantly decreases endothelin 1 expression (Nicholson et al., 2008, Coppa et al., 2011). The anti-angiogenic effects of polyphenols have been attributed to several different mechanisms, including control of the VEGF pathway, decreasing endothelin-1 expression, reducing recruitment of inflammatory cells (Norata et al., 2007), and regulating nitric oxide synthesis (Yamagata et al., 2015).

Overall, the ability of MM and ResTom to supress induction of EDN1 by cytokines might be beneficial for treatments of chronic skin inflammatory diseases, since a reduction in EDN1 would help reduce vasodilation of blood vessels in the skin and help reduce the inflammatory process. Additionally, endothelin 1 is known to play a significant role in cancer progression, by promoting cellular proliferation, epithelial-mesenchymal transition and neovascularisation (Rosanò et al., 2013). Increased endothelin 1 expression is associated with psoriasis, which is characterised by increased keratinocyte proliferation and neo-angiogenesis (Bonifati et al., 1998) . The inhibitory effect on EDN1 associated with ResTom juice therefore could offer potential as a topical treatment for keratinocyte proliferation-related disorders, in addition to chronic skin disorders.

4.6.6 MMP-12

Microarray analysis identified a large decrease in expression levels of MMP-12 with treatments of MM and ResTom juice. Additionally, there was a clear difference in expression levels with MM and

ResTom treatments, with ResTom suppressing MMP-12 to a greater level (Figure 4.18). Interestingly, in the presence of cytokines, MM and ResTom treatments were able to not only prevent induction of MMP-12 by cytokines, but also repress expression.

MMP-12 encodes an elastase which is important for the maintenance of elastin structural networks in the skin, which are degraded with photo damage and skin aging leading to the characteristic loss of elasticity seen in aged skin. Therefore, the potential for MM and ResTom juice to not only prevent but also repress MMP-12 activity in the presence of cytokines was very interesting, and consequently was investigated in more detail in the following chapters.

4.6.7 Variation in cytokine-mediated gene regulation between experiments

Interestingly, analysis across donors showed that although the addition of cytokines tended to increase expression of genes associated with inflammatory pathways substantially (MMP-1, MMP-9, MMP-12), in some donor's downregulation of these genes was observed. This observation is interesting and highlights the varied responses of individuals to treatments. Even with the differences in expression with cytokine treatment, the genes discussed above still showed significant levels of repression compared to cytokine only treatments. However, this variability highlights the need to replicate experimental treatments across multiple donors to clearly observe clearly the biological effects of treatment.

4.7 Summary

Plant extracts have been used widely for the treatment of skin diseases. Many of the medicinal properties of plant extracts have been attributed to high levels of polyphenols such as resveratrol (Hsu, 2005). Recently a study by Lephart et al. (2014) used microarray analysis to examine the effect of resveratrol on gene expression in human skin, and subsequently identified several genes important in skin-aging and skin-health to be significantly regulated.

Several studies have reported greater biological activity associated with combination treatments of multiple plant phytochemicals (Mertens-Talcott and Percival, 2005, Schlachterman et al., 2008, George et al., 2011). This therefore suggests that whole plant extracts may exhibit high biological activity due to the presence of multiple phytochemicals.

Although the activity of plant extracts, and specific polyphenols has been studied using *in vitro*, *in vivo* and e*x vivo* models (Jensen et al., 2008, Scarano et al., 2018, Lephart et al., 2014), a comprehensive examination of plant extracts on human skin gene expression has not yet been performed. Using microarray analysis in addition to mRNA expression analysis, this thesis has identified several genes in human skin explants which are regulated significantly by the addition of MM and ResTom juice with or without cytokines, which indicate a potential therapeutic use of tomato extracts to treat a range of skin conditions.

A key finding from microarray analysis was the significant repression of MMP-12 by ResTom extract, which has several implications for the use of ResTom extract on skin, and as such was studied in further detail in this project. qRT-PCR analysis was able to confirm the changes in gene expression observed in the micro-array analysis, as well as showing that ResTom juice often has a greater effect on gene expression than MM juice. Unfortunately, the difference in gene expression levels with MM and ResTom was not statistically significant, although analysis of C_T values confirmed the higher regulatory ability of ResTom. MM juice treatment itself leads to a substantial repression of several genes to C_T values as low at 34, although the additional repressive action of ResTom was not as apparent. Future studies using lower concentrations of MM and ResTom juice should establish the differences in regulatory of ability of these two extracts better.

Due to time restrictions in this project I was not able to extend gene expression analysis to earlier and later time points. Experiments over more time points, or longer timescales will provide greater insight into the regulation of genes by MM and ResTom tomato juices.

Additionally, due to the time required to generate PteroTom tomatoes, microarray analysis was not performed to compare PteroTom juice extracts to MM and ResTom. Although the microarray analysis has provided us with information concerning key genes in skin responding to with MM and ResTom juice treatments which could be investigated in future experiments together with PteroTom extract treatments, we may miss key genes responding specifically to PteroTom juice.

Chapter 5: Tomatoes enriched with polyphenols decrease expression of MMP-12 in human skin

5.1 Introduction:

Degradation of the extracellular matrix (ECM) plays an important role in tissue repair and remodelling and under normal physiological conditions, the degradation of ECM components is highly controlled. Dysregulation of ECM turnover and degradation has been associated with a wide range of diseases including fibrosis (Bou-Gharios et al., 1994), cancers (Emery et al., 2009), and photoaging of the skin (Bernstein et al., 1994). One of the major families of enzymes involved in the metabolism of the ECM are Matrix metalloproteinases (Kähäri and Saarialho-Kere, 1997). Human macrophage elastase (MMP-12) is active specifically against elastin, an essential component of skin which allows for recoil and resilience (Taddese et al., 2008). Unusual expression of MMP-12 has been linked to several skin disorders including cutaneous granulomas (Vaalamo et al., 1999), skin cancer (Kerkelä et al., 2000), and dermal photoaging (Saarialho-Kere et al., 1999).

5.2 Elastin and MMP-12

Despite comprising only 2% of total dermal protein, elastin is extremely important for the maintenance of skin structure and integrity. Its major role is to provide elasticity in connective tissues. Elastogenesis, the synthesis of elastin, is performed predominantly by fibroblasts within the superficial dermis (Weihermann et al., 2017). Within connective tissue, elastin fibres form a complex cross-linked network, which is highly stabilised and insoluble. Due to the importance of the elastin network in maintaining the structural integrity and elasticity of the skin, its formation and degradation is highly regulated.

There are two important elastases which promote the degradation of elastin in inflammatory conditions. Neutrophil elastase, a serine proteinase, is secreted by neutrophils and macrophages. Neutrophil elastase has a wide substrate specificity and has been implicated in a wide range of inflammatory diseases including rheumatoid arthritis and cystic fibrosis (Doring, 1994).

MMP-12, macrophage elastase, is a matrix metalloproteinase secreted by keratinocytes, fibroblasts and inflammatory macrophages. Unusual expression of MMPs are associated with several skin disorders including bullous diseases, granulomas and dermal photoaging, and MMP-12 has been found to play an important role in several of these skin disorders, especially in the progression of photoaging (Taddese et al., 2008).

Both intrinsic (normal skin aging) aging and extrinsic aging (photoaging) of skin are characterised by a dysregulation in elastin degradation and formation. Much of the characteristic wrinkling, and sagging of skin aging is due to upregulation of elastin degradation, whereas solar elastosis seen in chronically photoaged skin is caused by dysregulated and downregulated elastin synthesis and network formation as well as elastase activity (Chen et al., 1994).

In vivo and *ex vivo* studies have established a clear link between skin aging and elastin degradation, particularly in relation to photoaging (Bernstein et al., 1994, Fisher et al., 1997, Bissett et al., 1987). Chung et al. (2002) showed that UV exposure of human skin was directly correlated to increased expression of MMP-12 in vivo. This was also confirmed in a later study by Tewari et al. (2014) revealing a significant role of MMP-12 in the process of skin photoaging.

Due to the well-established role of elastin dysregulation leading to reduced skin elasticity and increased wrinkling observed in aged skin, cosmetic treatments which are able to act on the elastin regulatory pathway could offer a new therapeutic treatment in the prevention or reversal of cutaneous aging.

5.3 Aims:

To investigate how tomato extracts, affect expression of the matrix metalloproteinase MMP-12, and determine the structural and morphological implications of any changes.

5.4 Methods:

5.4.1 Protein analysis

5.4.1.1 *Trichloroacetic acid precipitation of proteins from cell culture supernatant*

Precipitation of protein using TCA was performed using standard techniques essentially as previously described for MMPs (Butler et al., 2010). In brief, trichloroacetic acid (TCA) was added to a final concentration of 5% in cell culture media and incubated overnight at 4°C with agitation. The following day, supernatants were centrifuged at 11,000 x g for 10 minutes at 4°C to collect the protein pellet. Following this, protein pellets were washed with cold acetone to remove excess TCA, vortexed, and centrifuged again at 11,000 x g for 10 minutes at 4°C. The acetone was removed, and the pellet allowed to air-dry briefly at room temperature, before adding 0.5M Tris-HCl (pH 9), and centrifuging for 1 minute at 11,000 x g at room temperature. The pellet was resuspended in 1x SDS-PAGE reducing final sample buffer (0.625 M Tris pH 6.8, 2% (v/v) SDS, 10x bromophenol blue, 10% (v/v) glycerol, 15% β-mercaptoethanol).

5.4.1.2 *Extraction of total protein from whole tissue*

Snap frozen tissue sections were immersed in 600 µl cold RIPA lysis buffer (10 mM Tris-HCL, 1 mM EDTA, 0.5 mM EGTA, 1% Triton x-100, 0.1% SDS, 0.1% sodium deoxycholate, 140 mM NaCl) plus 1x phosphatase inhibitor cocktail (Thermo-scientific Halt, EDTA free), and finely cut up with scissors. Tissue was the fully disrupted with ball barings using the Tissue Lyser II (Qiagen). Lysates were left on ice for 15 minutes before centrifugation at 4°C at 11,000 x g for 30 minutes. Lysate was decanted, before centrifugation at 4°C for another 30 minutes at 11,000 x g. Samples were transferred to a fresh tube and stored at -80°C until use.

5.4.1.3 *Protein quantification by Pierce BCA Protein Assay (RIPA-extracted samples)*

Protein concentration of RIPA-extracted samples was quantified using Pierce Bichoninic Acid (BCA) Protein assay kit, following the manufacturer's instructions (Thermo Scientific) for the microplate procedure.

Briefly, protein standards of known concentrations of bovine serum albumin (BSA) were prepared and plated in a 96-well plate ranging from 0-2000 µg/ml. The same volume of unknown protein samples was also plated. A total of 200 µl working reagent at a 1:20 (reagent B: reagent A) concentration was added to each standard and sample before incubating at 37°C for 30 minutes. Absorbance was then measured in a spectrophotometer plate reader at 520 nm. A standard curve was prepared from the known BSA standards, and the equation of the trendline was used to calculate the concentration of unknown samples. Protein extracts were then diluted to allow for equal loading on polyacrylamide gels.

5.4.1.4 *Protein resolution by SDS- Polyacrylamide gel electrophoresis (SDS-PAGE)*

SDS-PAGE separation of proteins was performed using polyacrylamide gels with 10% resolving gel (10% [v/v] acrylamide, 0.5M Tris buffer, pH 6.8) and 5% stacking gel (5% [v/v] acrylamide, 1.5M Tris buffer, pH 8.8), run at a constant 30 mA per gel until the protein was resolved on the gel. A total of 40 μg protein, as quantified by BCA assay, or total TCA precipitates, were mixed with 4x loading buffer (0.625 M Tris pH 6.8, 2% (v/v) SDS, 10x bromophenol blue, 10% (v/v) glycerol, 15% β-mercaptoethanol) and boiled for 5 minutes before loading onto the gel alongside a prestained protein marker, spectra multicolour broad range protein ladder (10 kDa to 260 kDa, Pierce).

5.4.1.5 *Semi-dry transfer*

Proteins were transferred from the gel to a polyvinylidene fluoride (PVDF) membrane. PVDF membranes were activated by incubation in methanol for 10 minutes. Activated PVDF, thick filter paper and the page-gel were equilibrated in semi dry transfer buffer (48 mM Tris-Base pH 8.3, 39 mM Glycine, 20% MeOH, 0.04% SDS) for 15 minutes before protein transfer at 15V for 35 minutes using a transblot SD semi-dry transfer cell (Bio Rad).

5.4.1.6 *Immunoblotting and development*

Depending on the antibody, and sample used, membranes were blocked for 3 hours at room temperature in PBS-Tween (0.1% Tween-20) containing 5% milk and 3% BSA. Membranes were incubated overnight with primary antibody diluted in blocking buffer, at 4°C with rocking, before being washed 3 times in PBS-Tween or PBS-Tween with 1% Milk. Membranes were then incubated with an appropriate secondary antibody conjugated to Alexa Fluor 680, far red (diluted in PBS-Tween, 2% milk, 0.01% SDS, stored in the dark) or, where indicated, horse radish peroxidase (HRP; diluted with PBS-Tween 5% milk) for 1 hour with rocking. For Alexa Fluor-probed membranes, membranes were washed twice in PBS-Tween, and then once in PBS. Membranes were visualised using the Odyssey infrared imaging system at 680 nm. Membranes probed with HRP-conjugated antibodies were washed 3 times in PBS-tween with 1% milk over 30 minutes, before incubating with Pierce ECL western blotting substrate (Thermo scientific). Membranes were then exposed to x-ray film and developed in an autoradiograph film processor (xograph healthcare Ltd.) to quantitatively measure the HRP catalysed chemiluminescent signal. A full list of primary and secondary antibodies can be found in Table 5:1*:*

Table 5:1 Details of antibodies; WB= Western Blotting, IHC= Immunohistochemistry. Immunohistochemistry.

* A sheep antibody to MMP-12 was kindly provided by Prof Gill Murphy (University of Cambridge). This antibody was raised in sheep to the catalytic domain of human MMP-12 and detects MMP-12 protein to 5ng on Western blot (Dr Jelena Gavrilovic and Professor Gillian Murphy, personal communication)

Antibody	Application	Supplier	Concentration/ dilution
Sheep anti-human MMP-12 polyclonal primary	*WB*	*	50µg/ml
Donkey Anti-sheep Alexa-Fluor 680 conjugated secondary	*WB*	*Jackson Immuno Research*	1:50000
Donkey Anti-Sheep HRP conjugated secondary	*WB*	*R+D systems*	1:1000
Sheep anti-human MMP-12 polyclonal primary	*IHC*	*	1:200- 1:50
Biotinylated Donkey Anti-sheep secondary	*IHC*	*R+D systems*	1:500

5.4.1.7 *Elastin staining*

Elastin staining was performed using an Elastin stain kit from Abcam, and performed as outlined in the manufacturer's protocol, with some modifications to improve staining quality and reproducibility. Briefly, an elastic stain solution was prepared containing Haemotoxylin, ferric chloride and lugol iodine (ratios as in manufacturer's instructions). After deparaffinising wax sections, the elastic stain was added dropwise to sections and incubated for 15 minutes before washing off excess dye in running water. Slides were differentiated in the provided differentiation solution, until the background of sections was light grey and elastic fibres black and clearly defined. Slides were added to water to stop the differentiation process. The sections were counterstained with Van Giesons solution that was diluted 1:10, for 1 minute, before washing in 95% ethanol. Slides were then washed in 100% ethanol, cleared with clearene, and mounted with DEPEX mounting medium (Electron Microscopy Science). Analysis of Elastin staining was performed using Image J with the assistance of Fatima Oyaifo.

5.4.1.8 *Frozen sections for Immunohistochemistry*

Frozen sections were cut with Microm HM560 cyrostar cryostat (Thermo Scientific) by Dr Damon Bevan. Sections (10µm) were fixed in ice cold acetone for 10 minutes, before air drying at room temperature. Sections were outlined with a hydrophobic ImmEdge barrier pen (Vector labs). Tissue was washed twice in 1xPBS before incubating at room temperature for 15 minutes in 70% MeOH, 30% PBS, 0.3% (v/v) H_2O_2 solution. The tissue was then washed 3 times with PBS. Tissue was incubated with primary antibody diluted in PBS with 5% serum (as required see Table 5:1) for 60-90 minutes at room temperature, or overnight at 4°C in a hydration chamber. Tissue was washed 3 times with PBS, before incubating for 90 minutes at room temperature with a biotinylated-secondary antibody diluted in PBS. Tissue was washed with PBS, before treating with the VECTASTAIN Elite ABC kit (Vector Lab) for 20 minutes. The VECTASTAIN solution contains an optimised Avidin/Biotinylated HRP enzyme complex (ABC) that irreversibly binds to the biotinylated secondary antibody. Following incubation with VECTASTAIN, tissues were washed 3 times with PBS, before adding DAB (Diaminobenzidine) H_2O_2, and nickel solution as supplied in the DAB peroxidase substrate kit (Vector labs). In the presence of H_2O_2 HRP converts DAB to an insoluble brown precipitate, the addition of nickel solution turns the precipitate to a much darker and more intense precipitate. Optimum incubation times with DAB substrate kit varied, normally requiring 10 minutes of incubation. Tissue was observed during DAB treatment for optimal staining of tissue, and tissues were immersed in water to stop the reaction. Tissue was then dehydrated through a series of Ethanol washes, before mounting onto microscope slides with DEPEX mounting medium (Electron Microscopy Sciences).

5.4.1.9 *Wax sections for Immunohistochemistry*

Wax sections were cut at 10µm and mounted on PolyLysine coated microscope slides. Prior to staining, tissue sections were treated using an antigen-retrieval method to unmask antigenic sites blocked by methylene bridges formed between proteins during tissue fixation by paraformaldehyde. Firstly, tissues were de-paraffinized in clearene, and rehydrated in EtOH. Paraffin sections were incubated in basic-antigen retrieval solution (Abcam) overnight at 60°C. The following day tissues were cooled in the retrieval buffer for 20 mins at room temperature, before proceeding onto the immune cytohistochemistry procedure as described above.

5.5 Results:

5.5.1 The Effect of MM and ResTom juice on MMP-12 expression

Micro-array analysis of day 5 treated skin explants from donor SPL003 identified significant regulation of MMP-12 expression by MM and ResTom juice treatments (see chapter 4, 4.6.6). Initial microarray validation of MMP-12 expression in SPL003 performed by Dr Damon Bevan, UEA, confirmed the suppressive effect of MM and ResTom juice on MMP-12 steady state mRNA levels (see chapter 4, 4.6.6). Although inhibition of MMP-12 by MM and ResTom juice was not statistically significantly lower than the control, the inhibitory effect of both MM and ResTom on MMP-12 expression was evident from C_T values (Chapter 4, 4.6.6). Interestingly, comparison of C_T values revealed a greater inhibition of MMP-12 by ResTom compared to MM treatment, suggesting greater biological efficacy of ResTom.

This inhibitory effect of MM and ResTom juice on MMP-12 was also observed under inflammatory conditions. Treatment of skin with the inflammatory cytokines IL1 and OSM produced significant induction of MMP-12 expression compared to control. In the presence of cytokines MM or ResTom juice treatment again resulted in a significant repression of MMP-12 levels. In addition, C_T values revealed greater suppression of MMP-12 with ResTom juice compared to MM juice.

These data came from a single donor, SPL003, however, and so to explore the effects of MM and ResTom treatments we investigated MMP-12 expression by qRT-PCR across several donors in response to different treatments. the trends determined from these analyses are summarised in Table 5:2 in terms of most significant changes in expression.

Table 5:2 : Summary of treatments leading to significant changes in MMP-12 expression in whole skin ex vivo explants, after 5-day treatment regime with and without cytokines.

qRT-PCR of 6mm skin biopsies from different donors treated with aqueous tomato extracts and purified stilbenes with (A) and without (B) cytokines. Resulting CT values were converted to fold changes and using one-way ANOVA and the multiple Bonferroni comparison test significance analysed. Treatments which caused significant changes in MMP-12 expression are summarised in the table, showing overall trend of gene expression across different donors, and the number of donor's fold change expression was significant in.

(A)

	No cytokines					
	+MM	**+ResTom**	**+Res**	**+MM +Res**	**+MM+Pd**	**+IL1/OSM**
Overall trend in expression	↓	↓	↓	↓	↓	↑↓
Significant in how many donors?	↓ in 4/8	↓ in 4/8	↓ in 1/3	↓ in 1/2	↓ in 1/3	↑ in 1/8 ↓ 3/8

(B)

	+ cytokines				
	+MM	**+ResTom**	**+Resveratrol**	**+Polydatin**	**+Pterostilbene**
Overall trend in expression	↓	↓	↑	↓	↓
Significant in how many donors?	↓ in 2/6	↓ in 2/6	↑ in 1/3	↓ in 1/3	↓ 1/1

5.5.2 A trend to repression of MMP-12 by tomato juice extracts was observed across donors after 5-day treatment.

Skin explants were exposed to different treatments including tomato extracts, and purified stilbenes with and without cytokines over a 5-day treatment regime before total RNA was extracted and quantitative PCR performed. A summary of the treatments which produced significant changes in MMP-12 expression across multiple skin donors are shown in Table 5:3. Overall, a repression of MMP-12 expression by MM and ResTom was observed across all donors, with significant repression observed in 4 out of 7 donors treated with MM vs control and ResTom vs control Table 5:3.

Although both MM and ResTom trended towards repression of MMP-12 under inflammatory conditions, MMP-12 was only observed to be significantly down regulated in 2 out of 6 donors. This could be related to the varying expression levels of MMP-12 in donors in response to IL1/OSM. The comparisons of MMP-12 expression levels across donors highlighted some interesting trends in expression levels which will be discussed in more detail.

Table 5:3 Average MMP-12 CT values for seven donor skin explants after 5-day treatment regime with aqueous tomato extracts with and without cytokines.

qRT-PCR of 6mm whole skin biopsies after a 5day treatment regime. Data was analysed by relative quantification and normalised to 18S for MMP-12. Corresponding average C_T values are shown. ”-” indicates treatments not tested within a donor, †= significant vs control, ¥ =significant vs IL1/OSM

	Average C_T value					
	Control	MM	ResTom	IL1/OSM	IL1/OSM +MM	IL1/OSM +ResTom
SPL003	29.06	31.41	33.68	28.81†	31.72¥	34.94¥
SPL007	30.12	37.83†	33.88†	33.93†	35.84	37.78
SPL008	33.00	37.32†	39.02†	37.92	34.58	36.54
SPL010	31.34	36.43†	36.13†	31.61	35.00¥	34.48¥
SPL012	32.17	30.09	29.99	-	-	-
SPL013	30.18	32.29	36.17	35.25†	-	-
SPL015	28.83	34.20†	34.53†	32.60†	34.27	36.52
SPL026	28.81	29.57	31.82	29.46	29.00	31.30
SPL028	32.95	34.11	-	32.59	32.36	-

5.5.3 Cytokine treatment revealed varying expression of MMP-12 in response to inflammation across donors

A cytokine mixture of interleukin 1 and oncostatin M was added to culture media to mimic an inflammatory environment for the skin explant. Addition of IL1/OSM led to up- (4 donors) and down -regulation of MMP-12 (4 donors) depending on the donor (Figure 5.1 and Figure 5.3 are representative examples of these two trends).

5.5.4 ResTom juice inhibited MMP-12 expression more than MM juice

Comparison of MMP-12 expression across donors showed a trend towards repression of MMP-12 by both MM and ResTom juice (Table 5:2 and Table 5:3). A significant decrease in MMP-12 expression was observed in 4 out of 8 donors with both MM and ResTom treatments when compared to control, as can be seen in Table 5:2.

A trend towards MMP-12 suppression was also observed with both MM and ResTom treatments under inflammatory conditions (Table 5:2). Only 2 out of six donors showed a significant repression of MMP-12 with MM or ResTom treatment + IL1/OSM (SPL003, Figure 4.18, and SPL010, Figure 5.5). This in part may be due to the varied MMP-12 expression response to IL1/OSM, which in some donors such as SPL015 (Figure 5.1) and SPL026 (Figure 5.2) was relatively low. Inspection of C_T values however, showed that MMP-12 expression was inhibited to a much greater degree under inflammatory conditions when also treated with MM or ResTom (Table 5:3). these data showed that both MM and ResTom juice suppressed MMP-12 expression both with and without cytokines. Inhibition of MMP-12 by MM juice was interesting, as this showed that the tomato matrix itself has an inhibitory effect, which could be due to the presence of polyphenols or other phytochemicals within MM juice as described in chapter 3,section 3.6.

A key finding was that ResTom juice had a greater inhibitory effect on MMP-12 than MM juice in most donors (Table 5:3) particularly under inflammatory conditions. Although statistical analysis did not show any significant difference between MM and ResTom treatments, comparison of C_T values shows a large decrease in MMP-12 expression level with ResTom +IL1/OSM compared to MM +IL1/OSM (Table 5:3).

The inhibitory effect of ResTom may purely be due to the presence of resveratrol and its derivatives within ResTom juice or could be the result of synergistic affects between the many polyphenols within the tomato juice.

Since MM alone acted to greatly suppress MMP-12 expression, it could be that the effect of stilbenes in ResTom was masked by MM. However, the inhibitory action of ResTom could not be replicated by spiking MM with Resveratrol or Polydatin.

5.6 Effect of purified stilbenes (with/without tomato juice extract) on MMP-12 expression in skin explants

To investigate whether the inhibitory effect of ResTom was due to its stilbene content, or a more complex interaction based upon synergy between the different stilbenes and other phytochemicals in the ResTom tomato juice, we compared the activity of the individual stilbenes as purified/commercial components, MM juice spiked with a single stilbene, and ResTom juice. MM juice was spiked with either resveratrol or polydatin at a concentration of 50 µM. This concentration was used as this gives a comparable concentration of resveratrol to that found in ResTom juice (chapter 3, section 3.6).

Interestingly addition of purified resveratrol or polydatin had donor-dependent effects on MMP-12 expression compared to control treatments, with a decrease in MMP-12 observed in some donors (Figure 5.1), and little effect on MMP-12 expression observed in others (Figure 5.2) This mixed effect on MMP-12 expression was also observed under inflammatory conditions, with some donors such as SPL026, (Figure 5.2) exhibiting a pronounced increase in MMP-12 expression with IL1/OSM +resveratrol or polydatin, whereas no effect was observed in other donors such as SPL015 (Figure 5.1).

SPl015 and SPL026 also differed in that in SPL015 showed a suppression of MMP-12 by MM in the absence or presence of cytokines, whilst SPL026 exhibited no change in MMP-12 expression with addition of MM. A difference in MMP-12 expression pattern was also seen for MM + Polydatin and MM + resveratrol. In SPL015, greater inhibition of MMP-12 is observed with combination treatment of MM juice + polydatin or resveratrol compared to purified compound alone, but only in the absence of cytokines (Figure 5.1). Whereas, within SPL026 the suppressive effect by MM + Polydatin and MM+ resveratrol was seen only with cytokines (Figure 5.2).

The effects of MM juice spiked with resveratrol or polydatin became even more complex upon examination of the effects on SPL028 and SPL013 skin explants. SPL028 (Figure 5.3) showed decreased expression of MMP-12 in response to both MM + resveratrol and MM + Polydatin treatments in the absence of cytokines, however only MM +resveratrol inhibited MMP-12 in the presence of cytokines (Figure 5.3). Additionally, MM alone supressed MMP-12 expression in SPL028 and addition of resveratrol or polydatin acting to suppress MMP-12 expression, further. This effect was also observed in the presence of cytokines with addition of resveratrol. This potential synergy was also observed in SPL013 with the addition of polydatin to MM further supressing MMP-12 compared to either treatment alone (Figure 5.4). Interestingly these synergistic effects of MM +resveratrol and MM + polydatin were also observed in SPL028 for MMP9 expression (Figure 5.6), and SPL013 for both MMP1 and MMP9 expression (Figure 5.7).

The effects of MM juice spiked with resveratrol or polydatin were extremely complex. However, these data suggested that MM juice and polydatin can interact synergistically to reduce MMP-12 expression, although these effects were skin donor-dependent.

This also suggested that the inhibitory trend observed with ResTom was likely due to a complex synergy occurring between multiple plant bioactivities within the juice, whose effects cannot be replicated by simple addition of a single purified stilbene. Overall, this suggested that the unique matrix of ResTom was crucial for its observed biological activities.

A

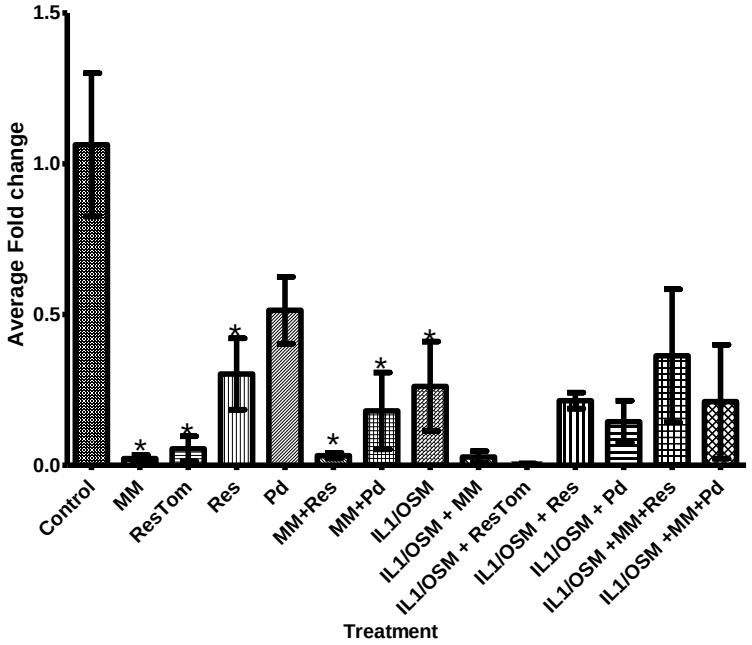

B

	Treatment	Average C_T value
No cytokines	Ctrl	29.67
	MM	34.72
	ResTom	34.67
	Res	31.14
	Pd	31.76
	MM+Res	35.82
	MM+Pd	32.80
+Cytokines	IL1/OSM	33.39
	MM +IL1/OSM	34.36
	ResTom +IL1/OSM	37.27
	Res +IL1/OSM	31.59
	Pd +IL1/OSM	33.15
	MM+Res +IL1/OSM	31.84
	MM+Pd +lL1/OSM	33.99

Figure 5.1 Effect of aqueous tomato extracts on relative expression of MMP-12 normalised to 18S in whole skin explants after 5-day treatment regime, in SPl015.

qRT-PCR of 6mm whole skin biopsies after a 5-day treatment regime was performed. Data was analysed by relative quantification and normalised to 18S for MMP-12 (A). Corresponding average C_T values are shown (B) Each bar represents the mean fold change of 3 explants ±SEM. Statistical difference was determined using one-way ANOVA with the Bonferroni multiple comparison *p≤ 0.05 **p≤ 0.01. ***p ≤ 0.001, ****p≤0.0001.

A

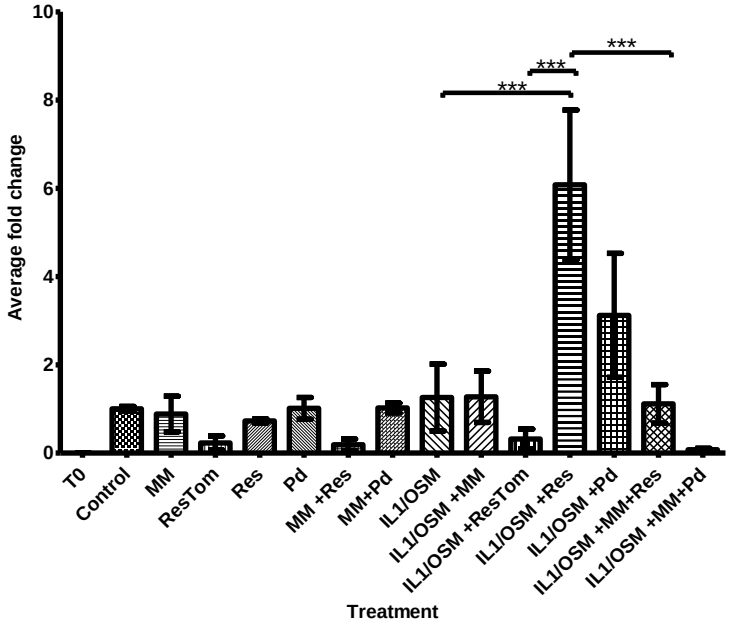

B

	Treatment	Average C_T value
No cytokines	**Ctrl**	28.81
	MM	29.57
	ResTom	31.82
	Res	28.94
	Pd	28.61
	MM+Res	31.47
	MM+Pd	28.64
+Cytokines	**IL1/OSM**	29.46
	MM +IL1/OSM	29.00
	ResTom +IL1/OSM	31.30
	Res +IL1/OSM	26.47
	Pd +IL1/OSM	27.74
	MM+Res +IL1/OSM	29.15
	MM+Pd +IL1/OSM	30.54

Figure 5.2 : Effect of aqueous tomato extracts on relative expression of MMP-12 normalised to 18S in whole skin explants after 5-day treatment regime, and SPL026.

qRT-PCR of 6mm whole skin biopsies after a 5-day treatment regime was performed. Data was analysed by relative quantification and normalised to 18S for MMP-12 (A). Corresponding average C_T values are shown (B) Each bar represents the mean fold change of 3 explants ±SEM. Statistical difference was determined using one-way ANOVA with the Bonferroni multiple comparison *p≤ 0.05 **p≤ 0.01. ***p ≤ 0.001, ****p≤0.0001.

A

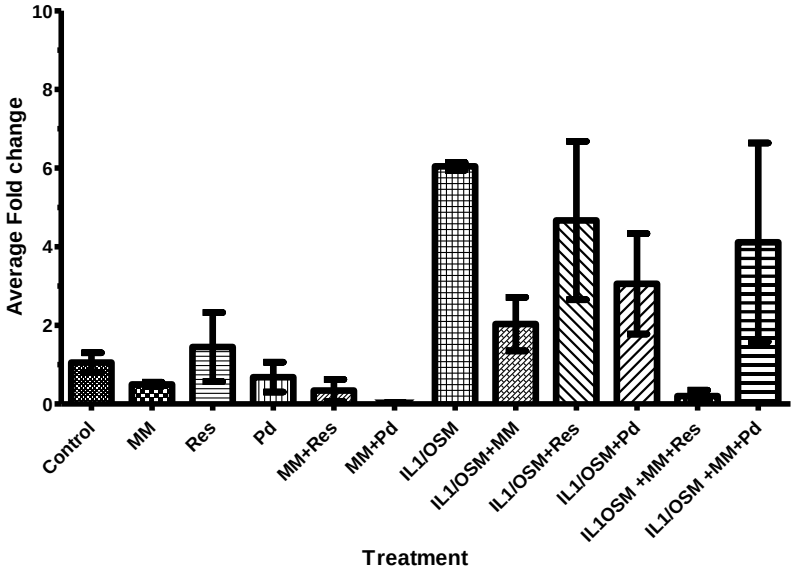

B

	Treatment	Average C_T
No cytokines	Ctrl	32.95
	MM	34.11
	Res	33.36
	Pd	34.11
	MM+ Res	35.35
	MM+ Pd	37.93
+ cytokines	IL1/OSM	32.59
	MM +IL1/OSM	32.36
	Res+ IL1/OSM	32.23
	Pd+ IL1/OSM	32.18
	MM+Res + IL1/OSM	35.78
	MM+ Pd +IL1/OSM	31.16

Figure 5.3 Effect of tomato extract on relative expression of MMP-12 normalised to 18S in whole skin explants after 5-day treatment regime, SPL028.

qRT-PCR of 6mm whole skin biopsies after a 5-day treatment regime was performed. Data was analysed by relative quantification and normalised to 18S for MMP-12 (A). Corresponding average C_T values are shown (B) Each bar represents the mean fold change of 3 explants ±SEM. Statistical difference was determined using one-way ANOVA with the Bonferroni multiple comparison *p≤ 0.05 **p≤ 0.01. ***p ≤ 0.001, ****p≤0.0001

A

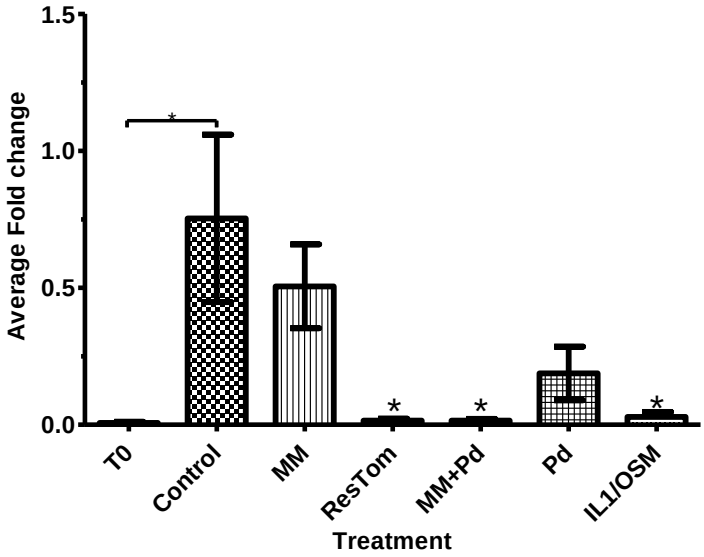

B

Treatment	Average C_T value
T0	36.23
control	30.18
MM	32.29
ResTom	36.17
MM+Pd	36.26
Pd	33.00
IL1/OSM	35.25

Figure 5.4 Effect of aqueous tomato extracts on relative expression of MMP-12 normalised to 18S in whole skin explants after 5-day treatment regime, SPL013.

qRT-PCR of 6mm whole skin biopsies after a 5-day treatment regime was performed. Data was analysed by relative quantification and normalised to 18S for MMP-12 (A). Corresponding average C_T values are shown (B) Each bar represents the mean fold change of 3 explants ±SEM. Statistical difference was determined using one-way ANOVA with the Bonferroni multiple comparison *p≤ 0.05 **p≤ 0.01. ***p ≤ 0.001, ****p≤0.0001

A

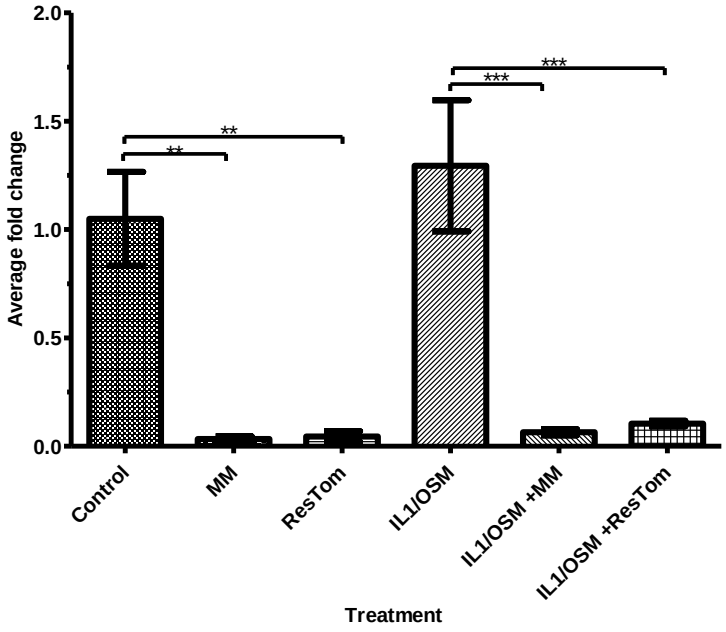

B

Treatment	Average C_T value
Control	31.17
MM	33.31
ResTom	36.06
IL1/OSM	34.44
IL1/OSM + MM	32.55
IL1/OSM + ResTom	35.24

Figure 5.5 Effect of aqueous tomato extracts on relative expression of MMP-12 normalised to 18S in whole skin explants after 5-day treatment regime, SPL010.

qRT-PCR of 6mm whole skin biopsies after a 5-day treatment regime was performed. Data was analysed by relative quantification and normalised to 18S for MMP-12 (A). Corresponding average C_T values are shown (B) Each bar represents the mean fold change of 3 explants ±SEM. Statistical difference was determined using one-way ANOVA with the Bonferroni multiple comparison *p≤ 0.05 **p≤ 0.01. ***p ≤ 0.001, ****p≤0.0001

A

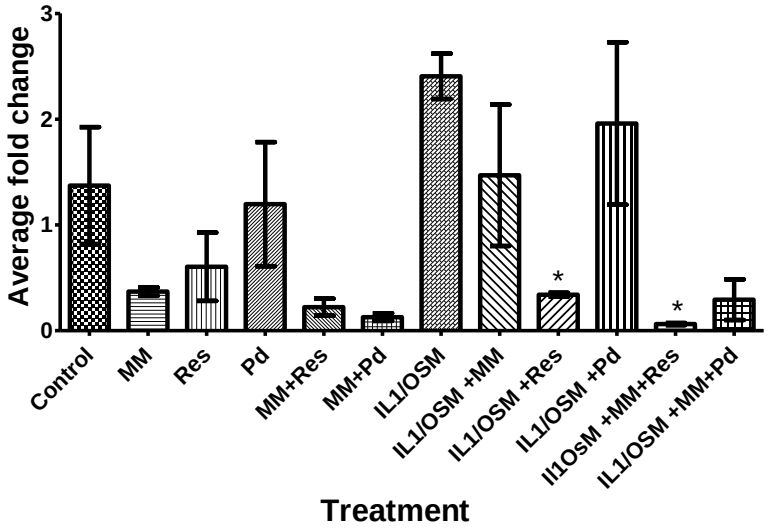

B

	Treatment	Average C_T
No cytoklines	**Ctrl**	28.96
	MM	30.56
	Res	30.27
	Pd	29.39
	MM+ Res	30.89
	MM+ Pd	31.82
+ cytokines	**IL1/OSM**	28.30
	MM +IL1/OSM	29.04
	Res+ IL1/OSM	30.10
	Pd+ IL1/OSM	28.68
	MM+Res + IL1/OSM	32.51
	MM+ Pd +IL1/OSM	31.06

Figure 5.6 Effect of aqueous tomato extract on relative expression of MMP-9 normalised to 18S in whole skin explants after 5-day treatment regime, SPL028.

qRT-PCR of 6mm whole skin biopsies after a 5-day treatment regime was performed. Data was analysed by relative quantification and normalised to 18S for MMP-12 (A). Corresponding average C_T values are shown (B) Each bar represents the mean fold change of 3 explants ±SEM. Statistical difference was determined using one-way ANOVA with the Bonferroni multiple comparison *p≤ 0.05 **p≤ 0.01. ***p ≤ 0.001, ****p≤0.0001

A

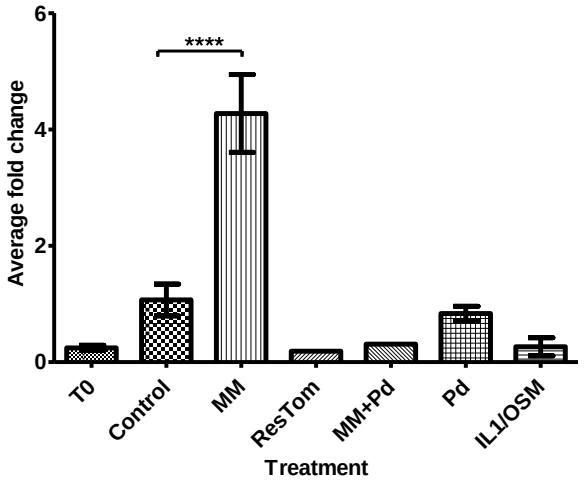

B

Treatment	Average C_T value
T0	31.53
control	29.51
MM	29.87
ResTom†	35.58
MM+Pd†	19.92
Pd	33.07
IL1/OSM	32.64

C

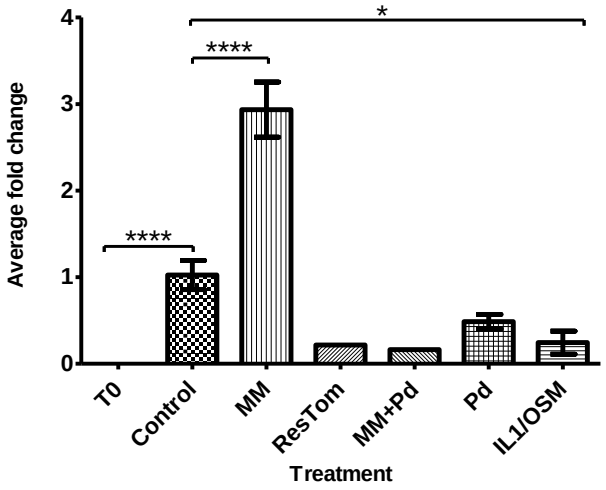

D

Treatment	Average C_T value
T0	38.19
control	22.67
MM	22.85
ResTom†	25.42
MM+Pd†	25.69
Pd†	24.53
IL1/OSM	24.72

Figure 5.7 Effect of aqueous tomato extracts on relative expression of A) MMP-9 and C) MMP-1 normalised to 18S in whole skin explants after 5 day treatment regime, from SPL013.

qRT-PCR of 6mm whole skin biopsies after a 5-day treatment regime was performed. Data was analysed by relative quantification and normalised to 18S for MMP-12. Corresponding average C_T values are shown (B and D). Each bar represents the mean fold change of 3 explants ±SEM. Statistical difference was determined using one-way ANOVA with the Bonferroni multiple comparison test showing significant data points vs Control. Other comparisons highlighted via capped line. *p≤ 0.05 **p≤ 0.01. ***p ≤ 0.001, ****p≤0.0001. †indicates average over 2 C_T values, these data points were excluded from statistical analysis.

5.7 Differential expression of MMP-12 was observed 1-day post-treatment

Effects seen after 5 days of treatment may indicate indirect effects of tomato extracts and/or the individual polyphenols assessed. Thus, some experiments were performed with just 1 day of treatment. In SPL015 we were able to use replicate experimental conditions after both 1-day (Figure 5.8) and 5 days (Figure 5.1) treatments which allowed us to observe progression of MMP-12 expression over time.

At 5 days post-treatment SPL015 skin explants displayed significant suppression of MMP-12 by the majority of treatments, with MM, ResTom and MM +Res suppressing MMP-12 to the greatest degree (Figure 5.1). In addition, at day 5, there was a clear difference in the inhibitory effect of ResTom and MM juice compared to purified polyphenol extracts.

At Day 1 however, although there was a suppression of MMP-12 with treatments compared to controls there was little observable difference in MMP-12 expression between the different treatments (Figure 5.8). It was interesting that whilst MM and ResTom appeared to maintain high levels of MMP-12 inhibition at day 5, the inhibitory effect of Res and Pd seemed to be reduced to approximately 2-fold (without cytokines) and was absent where cytokines were also present (Figure 5.1). This suggested that although these other treatments were able to inhibit MMP-12 expression initially, only ResTom and MM are able to sustain the inhibition of MMP-12 expression over 5 days.

Interestingly between day one and day five, the suppression of MMP-12 by IL1/OSM +Res, and IL1/OSM +Pd appeared to increase.

Due to inconsistent tomato growth, further extracts were not available to allow replication of these experiments in tissue from another donor. However, we were able to investigate the different actions of polydatin, resveratrol and pterostilbene (Figure 5.9) As observed at day 1 in SPL015 (Figure 5.8), polydatin and resveratrol both inhibited MMP-12 expression compared to control. Pterostilbene was also shown to have an inhibitory effect on MMP-12 steady state mRNA levels at day 1 (Figure 5.9). Under inflammatory conditions MMP-12 expression was increased with the addition of all purified polyphenols.

Unfortunately, we were unable to determine whether the inhibitory effects of purified compounds in this donor (Figure 5.9) were sustained across 5 days of treatment, or as observed in SPL015 only inhibit MMP-12 expression in the short term. However, these data did confirm a differential short-term action on MMP-12 expression by purified polyphenols with and without inflammatory cytokines.

A

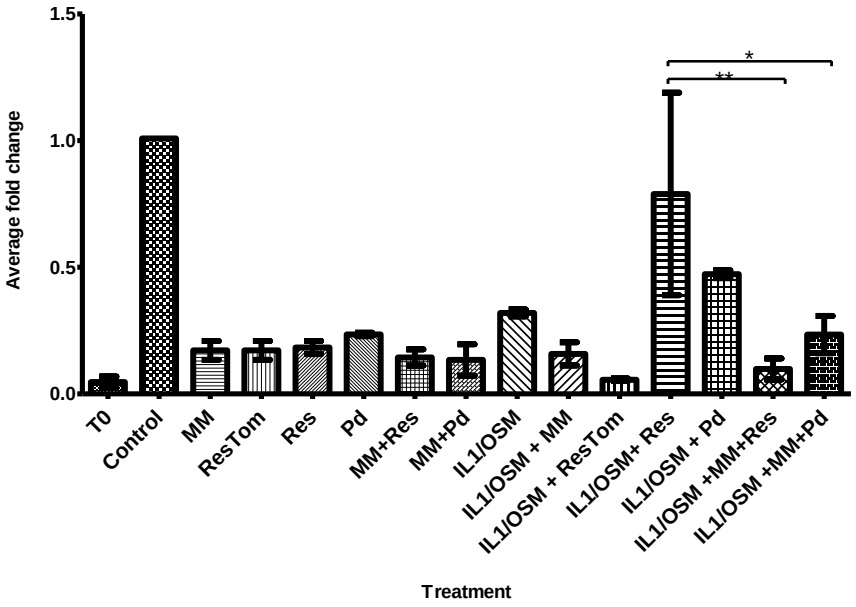

B

	Treatment	Average C_T value
No cytokines	Ctrl†	31.23
	MM	33.89
	ResTom	35.70
	Res	33.09
	Pd	33.02
	MM+Res	34.26
	MM+Pd	34.23
+Cytokines	IL1/OSM	32.54
	MM +IL1/OSM	34.12
	ResTom +IL1/OSM	35.51
	Res +IL1/OSM	31.98
	Pd +IL1/OSM	32.21
	MM+Res +IL1/OSM	35.06
	MM+Pd +IL1/OSM	34.10

Figure 5.8 Effect of aqueous tomato extracts on relative expression of MMP-12 normalised to 18S in whole skin explants after 1-day treatment regime, from SPL015.

qRT-PCR of 6mm whole skin biopsies after a 1-day treatment regime was performed (A). Data was analysed by relative quantification and normalised to 18S for MMP-12. Corresponding average C_T values are shown (B) Each bar represents the mean fold change of 3 explants ±SEM. Statistical difference was determined using one-way ANOVA with the Bonferroni multiple comparison test showing significant data points vs Control. Other comparisons highlighted via capped line. P≤ 0.05 compared to control, *p≤ 0.05 **p≤ 0.01. ***p ≤ 0.001, ****p≤0.0001. †indicates average over 2 C_T values, data points were excluded from analysis due to large variance in 18S C_T value.

A

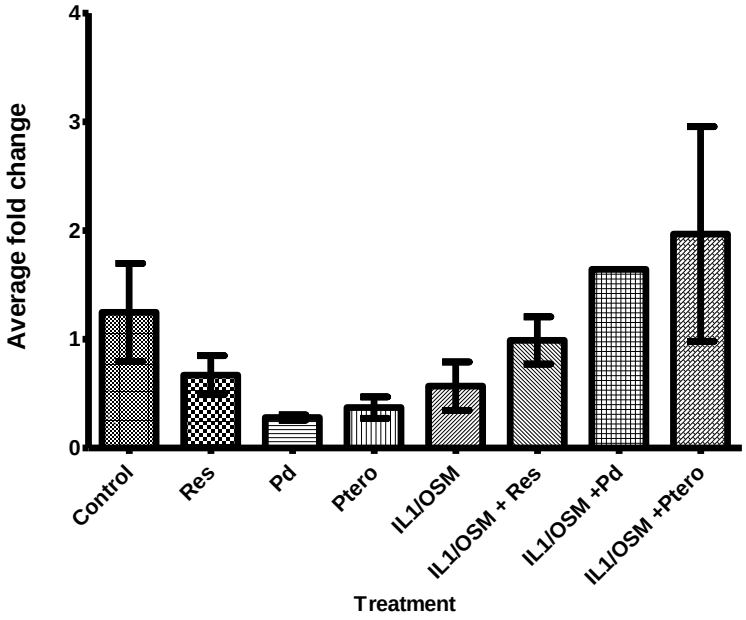

B

Treatment	Average C_T value
Ctrl	35.22
Res	35.55
Pd	36.77
Ptero	35.66
IL1/OSM	34.97
IL1/OSM +Res	34.01
IL1/OSM +Pd	33.40 †
IL1/OSM +Ptero	33.22

Figure 5.9 Effect of single polyphenol purified/commercial components on relative expression of MMP-12 normalised to 18S in whole skin explants after 1-day treatment regime, from SPL029.

qRT-PCR of 6mm whole skin biopsies after a 1-day treatment regime was performed. Data was analysed by relative quantification and normalised to 18S for MMP-12 (A). Corresponding average C_T values are shown (B) †represents average of 2 samples rather than 3. Each bar represents the mean fold change of 3 explants ±SEM. Statistical difference was determined using one-way ANOVA with the Bonferroni multiple comparison test *p≤ 0.05 **p≤ 0.01. ***p ≤ 0.001, ****p≤0.0001. †indicates average over 2 C_T values, data points were excluded from analysis due to large variance in 18S C_T value.

5.8 Effects of PteroTom on expression of MMP-12 at day 1

Once PteroTom had been generated, effects of extracts on MMP-12 steady state mRNA levels were explored (Figure 5.10). This experiment had been designed in parallel to a 5-day experiment also looking at PteroTom activity in conjugation with ResTom, Hi-Resv and MM juice. Unfortunately, the 5-day experiment tissue treated with tomato extracts became contaminated with a bacterial infection (indicating a lack of sterility of extracts).

Analysis of day 1 qRT-PCR (Figure 5.10) revealed a large induction of MMP-12 by PteroTom in comparison to control or MM treatments. Although not directly comparable to other data, this result contrasted dramatically with effects seen with either MM or ResTom treatment in any of the other experiments performed. This may indicate a very different functional effect of PteroTom on MMP-12 expression compared to other tomato extracts and needs to be investigated further.

A

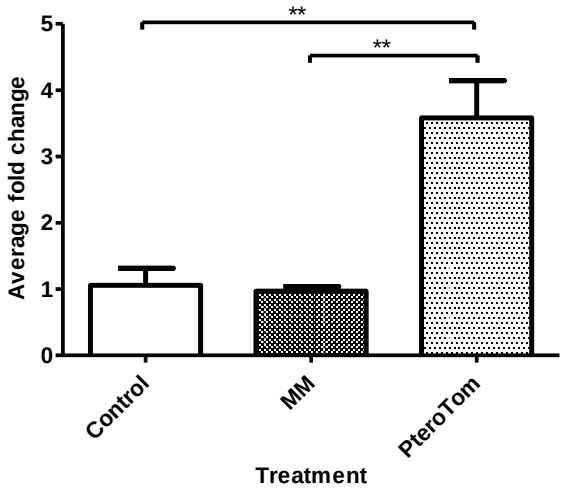

B

Treatment	Average C_T value
Ctrl	34.05
MM	34.09
PteroTom	32.15

Figure 5.10 Effect of aqueous tomato extracts on relative expression of MMP-12 normalised to 18S in whole skin explants after 1-day treatment regime, from SPL032.

qRT-PCR of 6mm whole skin biopsies after a 1-day treatment regime was performed. Data was analysed by relative quantification and normalised to 18S for MMP-12 (A). Corresponding average C_T values are shown (B). Each bar represents the mean fold change of 3 explants ±SEM. Statistical difference was determined using one-way ANOVA with the Bonferroni multiple comparison test, *p≤ 0.05 **p≤ 0.01. ***p ≤ 0.001, ****p≤0.0001.

5.9 Exploring Keratinocyte and Fibroblast expression of MMP-12.

From the above data we observed that MM and ResTom juice both inhibited expression of MMP-12 in whole skin explants, with ResTom suppressing MMP-12 to a greater extent than MM juice. The effects of tomato extracts on MMP-12 steady state mRNA levels seen in skin explants may reflect changes in keratinocytes or fibroblasts (or other cell types). To explore the roles of individual cell types some preliminary experiments were performed on a human keratinocyte cell line.

5.10 Hi Resv and PteroTom juices upregulated expression of MMP-12 in keratinocytes.

RNA from keratinocytes of a scratch wound experiment (described as performed in chapter 6, 6.3.3) was analysed via qRT-PCR (Figure 5.11) The cells were treated for 24 hours with methanol tomato extracts of an equivalent concentration to aqueous extracts. Methanol extracts were used for this experiment to allow for the solubilisation of pterostilbene, and the analysis of effect of this compound, which was not soluble in aqueous extracts. A concentration of 0.5% methanol extract was used in this experiment, the equivalent to 5% aqueous extract, based upon findings from Dr Katharina Bulling (JIC) who had shown high toxicity in breast cancer lines associated with methanol tomato extracts of concentrations higher than 0.5%.

In contrast to the repressed MMP-12 expression observed in whole skin tissue, neither Hi-Resv or PteroTom treatments suppressed MMP-12 expression compared to the MeOH control, and MM treated cells (Figure 5.11). Interestingly, treatment of cells with EGF, a positive promoter of cell proliferation and migration, decreased expression of MMP-12. EGF also decreased MMP-12 expression in the presence of extracts from ResTom and PteroTom.

This suppressive effect of EGF was different to the effects of EGF observed in whole skin. In SPL012 EGF treatment increased expression of MMP-12, with the addition of tomato extracts acting to suppress the effect of EGF (Figure 5.12). RNA from whole skin explants showed expression changes across all cell types. Therefore, the effects of EGF on keratinocytes could indicate different responses to treatments within different cell types of the skin and need to be investigated further.

To determine if there was any difference in biological efficacy between methanol tomato extracts, and aqueous extracts, a second keratinocyte experiment was performed (Figure 5.10) which compared the relative efficacy of these two forms of extract on MMP-12 expression. In this experiment treatment with tomato extracts slightly increased MMP-12 expression compared to control (Figure 5.13, A), although this was not statistically significant. No effect on MMP-12 expression was observed following treatment with methanol extracts (Figure 5.13, B), as in the previous keratinocyte experiment (Figure 5.11). It is important to note that the previous experiment was performed on RNA extracted from scratch wounded cells, whilst cells from this experiment

were not wounded. This may account for the differences in response to MMP-12 and could suggest a wound-specific MMP-12 response within keratinocytes.

These two keratinocyte experiments were run only over a 24-hour period, and since very little change in expression levels were observed across the majority of treatments, this suggested that MMP-12 expression is not altered within the first 24-hour treatment period.

As a concentration of 0.5% methanol extract was used, an equivalent concentration of 5% aqueous extract was also used. However, this concentration was based upon work using breast cancer cell lines and may, of course, not be an optimal concentration to observe effects of tomato extracts on keratinocytes

A

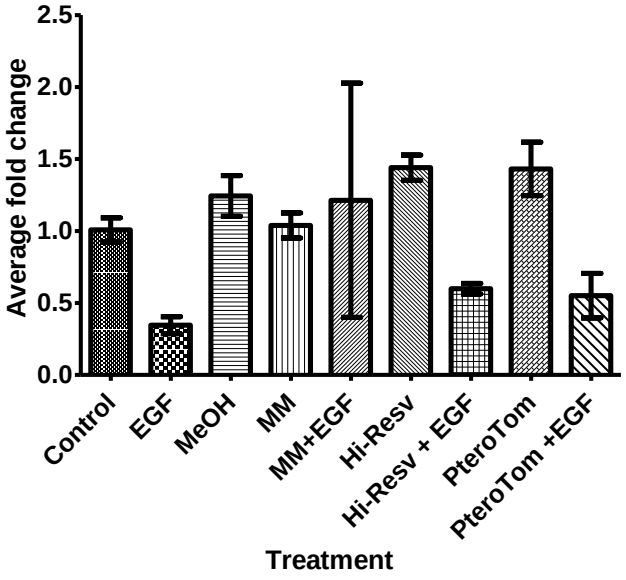

B

Treatment	Average C_T value
Control	30.88
EGF	32.20
MeOH	30.78
MM	30.91
MM +EGF	32.09
Hi-Resv	30.89
Hi-Resv +EGF	31.71
PteroTom	30.97
PteroTom +EGF	31.23

Figure 5.11 Effect of different methanol extracts on relative expression of MMP-12 normalised to 18S in keratinocytes 24 hours post-treatment.

qRT-PCR of wounded cell monolayers was performed 24 hours post- stimulation. Data was analysed by relative quantification and normalised to 18S for MMP-12 (A). Corresponding average C_T values are shown (B). Each bar represents the mean fold change of 3 samples ±SEM. Statistical difference was determined using one-way ANOVA with the Bonferroni multiple comparison test *p≤ 0.05 **p≤ 0.01. ***p ≤ 0.001, ****p≤0.0001.

A

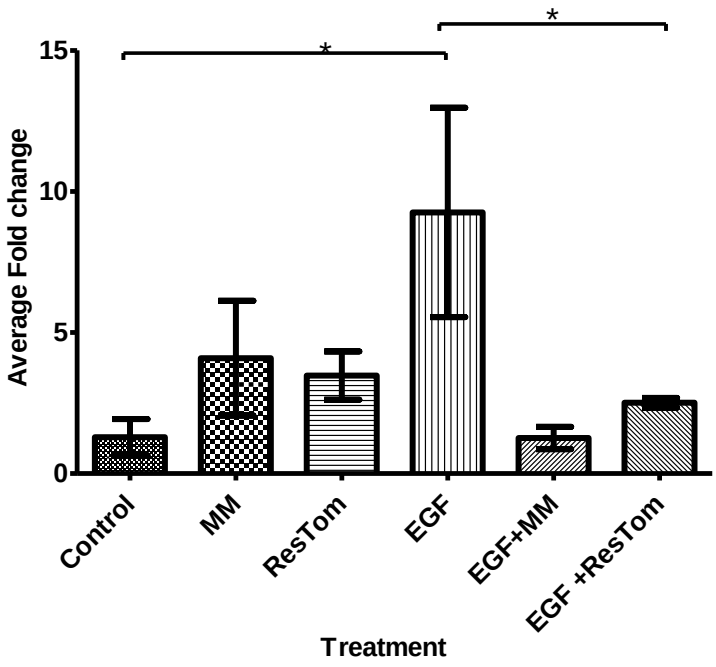

B

Treatment	Average C_T value
Ctrl	32.17
MM	30.09
ResTom	29.99
EGF	30.95
EGF+MM	30.71
EGF+ResTom	30.80

Figure 5.12 Effect of aqueous tomato extracts on relative expression of MMP-12 normalised to 18S in whole skin explants after 5-day treatment regime, SPL012.

qRT-PCR of 6mm whole skin biopsies after a 5-day treatment regime was performed. Data was analysed by relative quantification and normalised to 18S for MMP-12 (A). Corresponding average C_T values are shown (B) Each bar represents the mean fold change of 3 explants ±SEM. Statistical difference was determined using one-way ANOVA with the Bonferroni multiple comparison *p≤ 0.05 **p≤ 0.01. ***p ≤ 0.001, ****p≤0.0001.

A

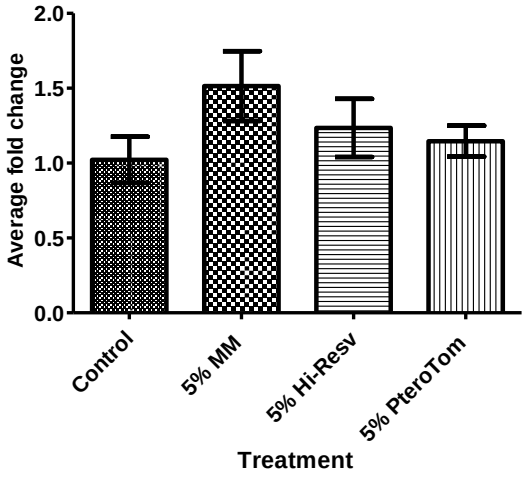

Treatment	Average C_T value
Control	30.61
5% MM juice	30.23
5% Hi-Resv juice	30.67
5% PteroTom juice	30.49

B

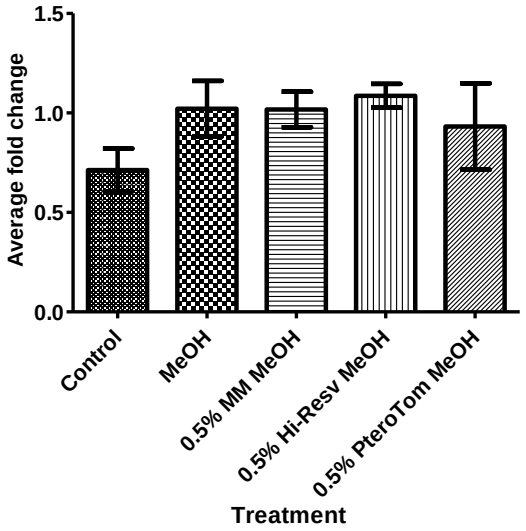

Treatment	Average C_T value
Control	30.61
MeOH	30.41
0.5% MM MeOH	30.46
0.5% Hi-Resv MeOH	30.63
0.5% PteroTom MeOH	30.38

Figure 5.13 Effect of methanol vs aqueous extracts on relative expression of MMP-12 normalised to 18S in keratinocytes 24 hours post-treatment.

qRT-PCR of cell monolayers was performed 24 hours post-stimulation. Data was analysed by relative quantification and normalised to 18S for MMP-12 (A) aqueous extracts, (B) Methanol extracts. Corresponding average C_T values are shown Each bar represents the mean fold change of 3 samples ±SEM. Statistical difference was determined using one-way ANOVA with the Bonferroni multiple comparison test, *p≤ 0.05 **p≤ 0.01. ***p ≤ 0.001, ****p≤0.0001.

.

5.11 PteroTom and Hi-Resv inhibited MMP-12 expression in Fibroblasts

In the complex structure of skin explants, dermal fibroblasts may be the cell type where the greatest effects of tomato extracts are observed (as seen for MMP-12 expression in skin explants). Since human dermal fibroblasts were not available at this time an experiment was performed to explore the effect of methanolic tomato extracts at different concentrations on mouse fibroblasts, using a standard fibroblast cell line (Figure 5.14). All treatment dosages were prepared to contain the same total concentration of methanol, so differences in effects at different tomato concentrations were not due to differing total methanol concentrations.

Interestingly, MM treatment increased expression of MMP-12 in fibroblasts, with a 1% extract increasing MMP-12 expression by two-fold compared to control. In contrast, both Hi-Resv and PteroTom extracts inhibited MMP-12 expression which correlated to what we observed in whole skin tissue analysis. A dose dependent effect was clearly seen with increasing PteroTom concentrations, with the lowest dosage of PteroTom inhibiting MMP-12 to the greatest extent. Although the inhibition of MMP-12 by PteroTom was not statistically significant, the C_T values showed a large inhibition of MMP-12 expression with 0.1% PteroTom treatment (Figure 14,B). It would be interesting to see if concentrations lower than 0.1% lead to greater inhibition of MMP-12.

A 0.1% treatment of PteroTom showed 2-fold greater inhibition of MMP-12 than Hi-Resv, which suggested that PteroTom might have a greater biological efficacy than Hi-Resv, although this difference was not statistically significant. It would be interesting in further studies to see if this difference in inhibition of MMP-12 expression by Hi-Resv and PteroTom was significant in whole tissue.

Overall, these data suggested that PteroTom juice may have a greater biological efficacy than Hi-Resv juice, since inhibition of MMP-12 expression in fibroblasts by PteroTom was greater than Hi-Resv at a 0.1% concentration.

Interestingly, these data showed an inhibitory effect of PteroTom on MMP-12 expression, whereas whole skin expression analysis of PteroTom treatment showed a significant induction of MMP-12 expression by PteroTom (Figure 5.10).

A

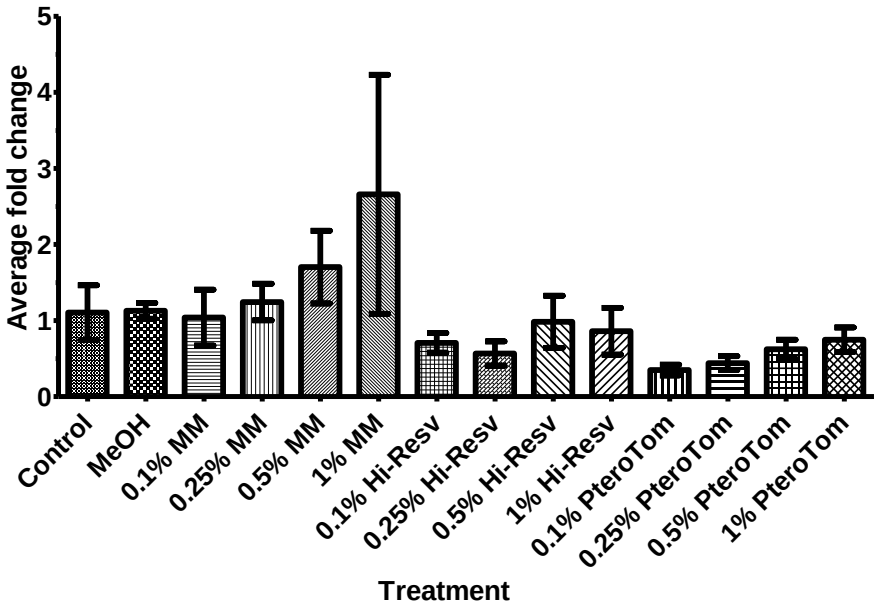

B

Treatment	Average C_T value
Control	35.36
MeOH	35.35
0.1% MM	35.42
0.25% MM	35.38
0.5% MM	34.67
1% MM	34.54
0.1% Hi-Resv	35.80
0.25% Hi-Resv	36.28
0.5% Hi-Resv	35.45
1% Hi-Resv	36.23
0.1% PteroTom	36.95
0.25% PteroTom	36.59
0.5% PteroTom	36.23
1% PteroTom	36.04

Figure 5.14 Effect of different concetrations of methanol-based tomato extracts on relative expression of MMP-12 normalised to 18S in mouse fibroblasts 48 hours post-treatment.

qRT-PCR of wounded cell monolayers was performed 48 hours post- stimulation. Data was analysed by relative quantification and normalised to 18S for MMP-12 (A). Corresponding average C_T values are shown (B). Each bar represents the mean fold change of 3 samples ±SEM. Statistical difference was determined using one-way ANOVA with the Bonferroni multiple comparison test, *p≤ 0.05 **p≤ 0.01. ***p ≤ 0.001, ****p≤0.0001.

5.12 MMP-12 protein levels did not change in accordance with steady state mRNA levels

5.12.1 Protein analysis of conditioned media from skin explants

The above data shows a large change in MMP-12 expression at the RNA level at both day 1 and day 5 with MM and ResTom juice compared to controls. To begin to understand the role of MMP-12 in skin explants it was important next to investigate how this difference might be reflected in MMP-12 protein expression levels.

To analyse secretion of MMP-12, conditioned media from treated skin biopsies in culture were concentrated by TCA precipitation (chapter 5, 5.4.1.1). Equal volumes of conditioned media were used for precipitation, and equal volumes of TCA precipitate loaded into each well. Western blot analysis (Figure 5.15) confirmed that conditioned medium from skin explants treated with MM and ResTom juice contained both proteins of expected Mr, with pro/latent (54 kDa) and processed/active (45 kDa) forms of MMP-12. Bands for MMP-12 in conditioned media matched those of the positive control (THP1 monocytic cell line, generated previously by Dr Megan Murray). MM and ResTom treatments showed a band of pro-MMP-12 at 54 kDa. Of interest, ResTom treatment had a more intense band at approximately 45 kDa, which corresponded to the processed form of MMP-12, suggesting more post-transcriptional cleavage of pro-MMP-12 to active MMP-12 with ResTom treatment.

For mRNA data gained from qRT-PCR of whole skin tissue from the same experiment, ResTom treatment showed a large decrease in MMP-12 steady state mRNA levels at day 5 compared to MM (Figure 5.16). However, it should be noted that the conditioned media samples were collected and pooled from 3 days and 5 days post-treatment, and so the Western blot analysis could reflect early upregulation of MMP-12 protein translation and/or secretion.

As mRNA expression was analysed at day 5, this difference might reflect repression of MMP-12 mRNA at later stages in the experiment due to high levels of MMP-12 protein, through a negative feedback loop. However, as discussed earlier, a substantial decrease in MMP-12 expression was observed as early as day 1 at the mRNA level (Figure 5.8), suggesting early on-set suppression of MMP-12 by MM and ResTom juice, which should be reflected by lower protein production even at early time point. However, this mRNA analysis was of another donor, and response at day 1 for SPL013 may not have been the same as those observed for SPL015.

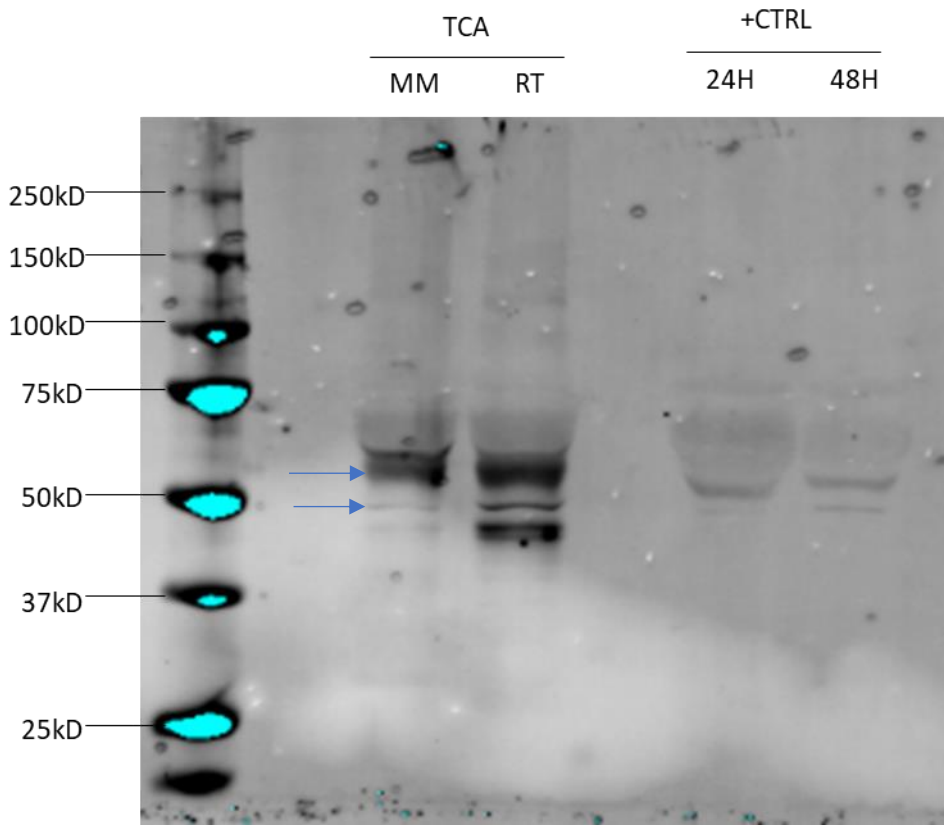

Figure 5.15 ***Western blot for MMP-12 protein expression in conditioned media of SPl013 skin explants.***

Conditioned media of SPL013 skin explants treated with MM and ResTom juice collected after 3 days and 5 days of treatment regime were pooled. The pooled conditioned media was TCA precipitated for western blot analysis. Positive MMP-12 control was TCA precipitated conditioned media from Human THP1 monocytic cell line treated with 10 µg/ml LPS collected at 24 hours and 48hours post treatment (Dr Megan Murray, UEA). Position of BioRad Precision Plus protein standards are as indicated. Pro-MMP-12 is indicated by the arrow at ~54 kDa, Active form of MMP-12 by the arrow at ~48 kDa

No loading control is available for secreted proteins, however equal volumes of TCA precipitates were loaded into each well.

A

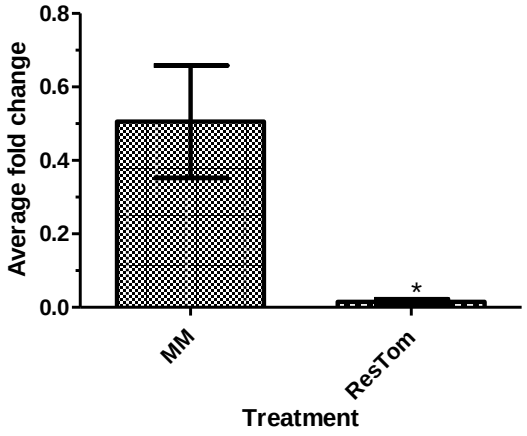

B

Treatment	Average C_T
MM	32.29
ResTom	36.17

Figure 5.16 Effect of aqueous MM and ResTom extracts on relative expression of MMP-12 normalised to 18S in SPL013 whole skin explants after 5-day treatment regime.

qRT-PCR of whole skin tissue after 5-day treatment regime was performed. Data was analysed by relative quantification and normalised to 18S for MMP-12. Corresponding average C_T values are shown (B). Each bar represents the mean fold change of 3 samples ±SEM. Statistical difference was determined using one-way ANOVA with the Bonferroni multiple comparison test *p≤ 0.05 **p≤ 0.01. ***p ≤ 0.001, ****p≤0.0001 (Full data from experiment in Figure 5.4)

.

5.12.2 Protein analysis of MMP-12 in whole tissue

A preliminary experiment was performed to see if changes in MMP-12 expression may be apparent in whole tissue samples (Figure 5.17). An experiment was designed which allowed for T0, T-48h and 5-day tissue samples to be collected for protein analysis after treatment with purified stilbenes. Due to limited amounts of tissue, it was not possible to collect parallel samples for RNA analysis collected from this donor. Additionally, only T-0 and T-48 protein levels were high enough to allow for western blot analysis.

Examination of MMP-12 protein levels in the tissue samples at T0 interestingly showed bands of lower Mr than expected (42 kDa and 38 kDa) in T0 samples. This may be a result of intracellular or within-tissue cleavage, although a proteinase inhibitor cocktail (blocking all classes of proteinase) was included in the extraction buffer. The higher Mr protein of 42 kDa only was detectable in the T48h samples (Figure 5.17). This band corresponds to a molecular weight of approximately 42kDa and therefore could be a cleavage product of the active MMP-12 which has a molecular weight of 44 kDa. From mRNA expression analysis of other donor skin tissue, I commonly observed a significant increase in MMP-12 expression between T-0 and treated control samples after both 1 day and 5 days of treatment (as in SPL015, Figure 5.1 and Figure 5.8). Therefore, it is interesting that there is little difference in MMP-12-band intensity of T-0 or T-48 control samples. If the mRNA of MMP-12 initially dramatically increased after treatment for example at a 12-hour time point, before decreasing again, it is possible that this change in mRNA expression is not observable at the protein level until a later time point or does not result in significant differences in secreted protein.

This western blot shows that analysis of later time points of skin tissue would be beneficial to see how MMP-12 protein expression relates to mRNA expression. Further western blots from whole tissue were not successful, and due to time constraints, it was not possible to perform analysis of MMP-12 protein levels at later time points and with tomato extract treatments. However, we now have a suitable and efficient methodology to be able to do further protein analysis from whole skin tissue in the future.

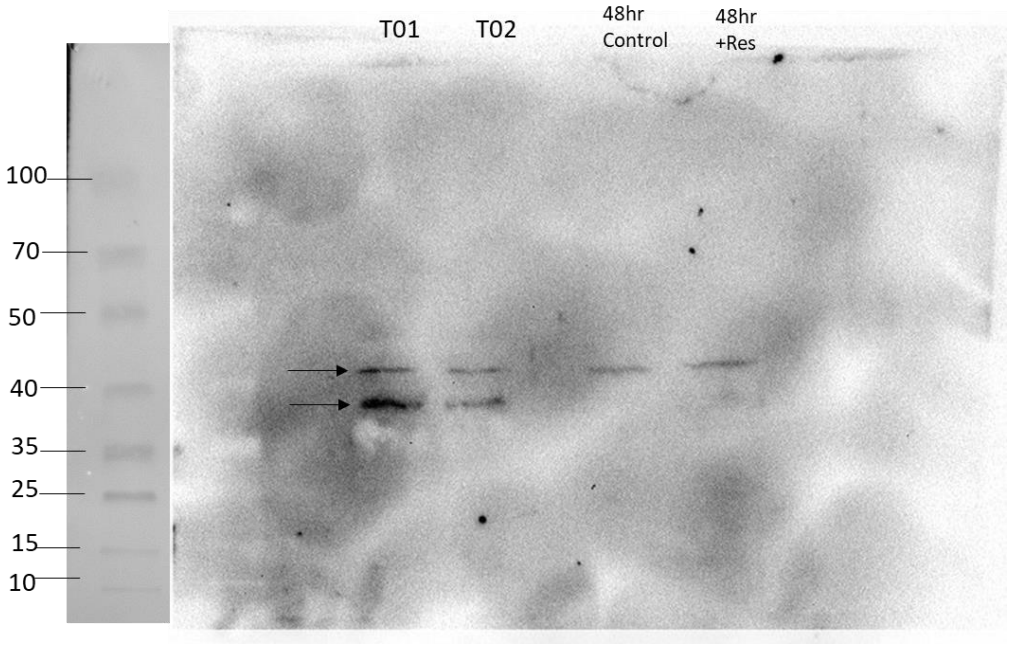

Figure 5.17 ***Western blot for MMP-12 protein expression in SPL031 skin at T0 and after a 48 hours treatment regime.***

Skin was snap frozen at T-0 or at T-48 after treatment. Protein was extracted as described in methods and equal concentrations were loaded into each well. Position of spectra multicolour broad range protein ladder are as indicated. Predicted bands of Mr ~42kDa and ~38kDa are indicated by arrows.

No loading control is available, however equal concentrations of protein were loaded into each well based upon BCA assay results.

5.13 Elastin morphology in response to treatment with tomato extracts

Elastin is a key component of skin dermis, and since MMP-12 is a major elastase it was of interest to investigate whether tomato treatments led to observable morphological changes in elastin in skin. Sections prepared from wax embedded tissue were treated with an elastin stain to visualise the elastic fibres within the skin tissue.

Elastin staining works on the principle of overstaining a slide with a black elastin stain to stain the elastic fibres, before removing the excess stain. The tissue is then counterstained with van Gieson stain to provide a high colour contrast between black elastin fibres and the background tissues. Elastin staining was performed on tissue sections collected from 4 donors: SPL015, SPL026, SPL028 and SPL029, of which SPL029 represented elastin after 1-day culture with treatment. Interestingly, slight differences in morphological structure of elastin was observable with different treatments, however these changes were often donor specific.

The biggest observable changes morphologically occurred in SPL026 (Figure 5.18) Between control and IL1/OSM treated skin sections there appeared to be a marked reduction in the length of elastin fibres in IL1/OSM treated skin. Additionally, comparison of IL1/OSM treatment with IL1/OSM +ResTom showed a pronounced increased number of long bundles of fibres with addition of ResTom. This was indicative that elastin was not being degraded to the same degree when treated with both IL1/OSM and ResTom. This difference in elastin structure corresponded to the mRNA expression data (Figure 5.2), where IL1/OSM + ResTom shows a marked decrease in MMP-12 expression compared to IL1/OSM.

In another donor, shortening of elastin fibres was not observable in SPL028 treated with IL1/OSM despite high mRNA expression of MMP-12 (Figure 5.19 for comparison between SPL028 and SPL026).

Changes in elastin structure appeared to come into effect at later times, so that, comparison of elastin morphology at day 1 (Figure 5.20) showed little effect between treatments suggesting that even if changes in MMP-12 mRNA expression levels were induced by day 1, the effect of these changes would not be observable morphologically until later time points.

Interestingly, there appeared to be large observable changes in morphology at day 5 with IL1/OSM treatment plus tomato extract or purified stilbene. In SPL028 (Figure 5.19) there appeared to be a thickening of elastin fibres within the dermal layer when skin was treated with both IL1/OSM and resveratrol in conjunction, which was not observed in IL1/OSM only treated skin. This contrasted with mRNA expression data which did not show a significant change in MMP-12 expression levels between control and IL1/OSM treatments.

Overall these data suggested that there were visually observable changes in the morphology of elastin in skin between treatments, however the visual changes in elastin morphology did not always seem to link to the mRNA expression data and showed a high degree of donor-to-donor variation.

Although I could observe some differences in morphological structure of elastin, several approaches were taken to try to determine if differences in elastin could be accurately quantified. Firstly, with the help of Dr Paul Thomas (UEA), a thresholding protocol using Image J was trialled for the quantification of Elastin. Unfortunately, there were several problems encountered with this protocol, including an inability of Image J to accurately measure Elastin fibre bundles, and fully differentiate background from fibres.

In a later experiment elastin fibre number, length and area were quantified within 3 randomly assigned 5 x 5 cm boxes of SPL015 images. These data were then analysed to determine any quantitative differences. Quantitative analysis did not show any significant differences in average fibre length, nor area of fibre in the different treatments (Figure 5.21). However, the average length of elastin fibres in MM +Res treated skin were 8 μm shorter than that in Control skin, and a reduced number of fibres were counted per box for MM +Res compared to controls (Figure 5.21). However, this apparent reduction in fibre number and length with MM + Res treatment was opposite to what was expected based upon the mRNA expression data (Figure 5.1) but in keeping with MMP-12 Western blot analysis of another donor (SPL013,Figure 5.4).

For quantification, boxes were randomly assigned three locations on the microscopic image. Although this removed any bias towards measuring fibres in certain areas, it may not have given an accurate portrayal of fibre changes. For example, from Figure 5.22 (A) it is clear to see that the fibres were most dense and long in morphology deeper in the dermis, whereas with other treatments there was not so much of a divide in distribution of fibres in the skin. This could in turn affect the accuracy of quantification.

From elastin staining of samples from several donors, I could see changes in elastin morphology with different treatments, although the amount of morphological change was different between donors. In addition, mRNA expression levels did not always align with the observed morphological changes in elastin. The initial quantification methods I did not quantify changes in elastin effectively in the different treatments and need to be improved to provide a more reliable quantification of morphological changes. From the delayed changes in in mRNA response to treatments, it may be that a 5-day time point is too soon to be able to see significant morphological changes in elastin, and therefore changes in elastin should also be explored at later times after the initial treatment.

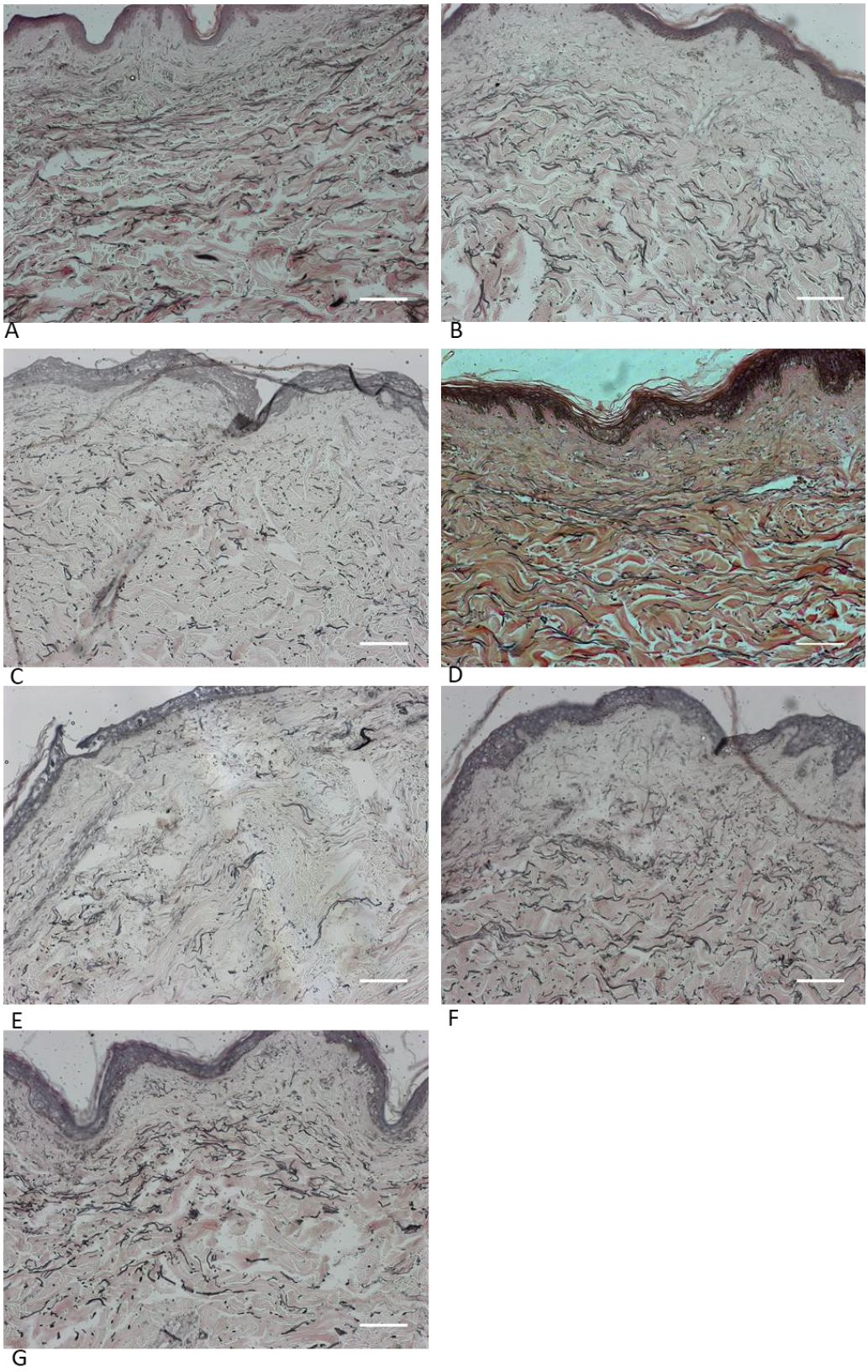

Figure 5.18 ***Elastin morphology of skin tissue from SPL026, day 5.***

Wax sections were fixed and stained for elastin for comparison of different treatments, A) T0 , B) Control, C) Il1OsM, D) MM, E) Il1OsM +MM, F) ResTom, G) Il1OsM +ResTom .

Scale bar = 100µm

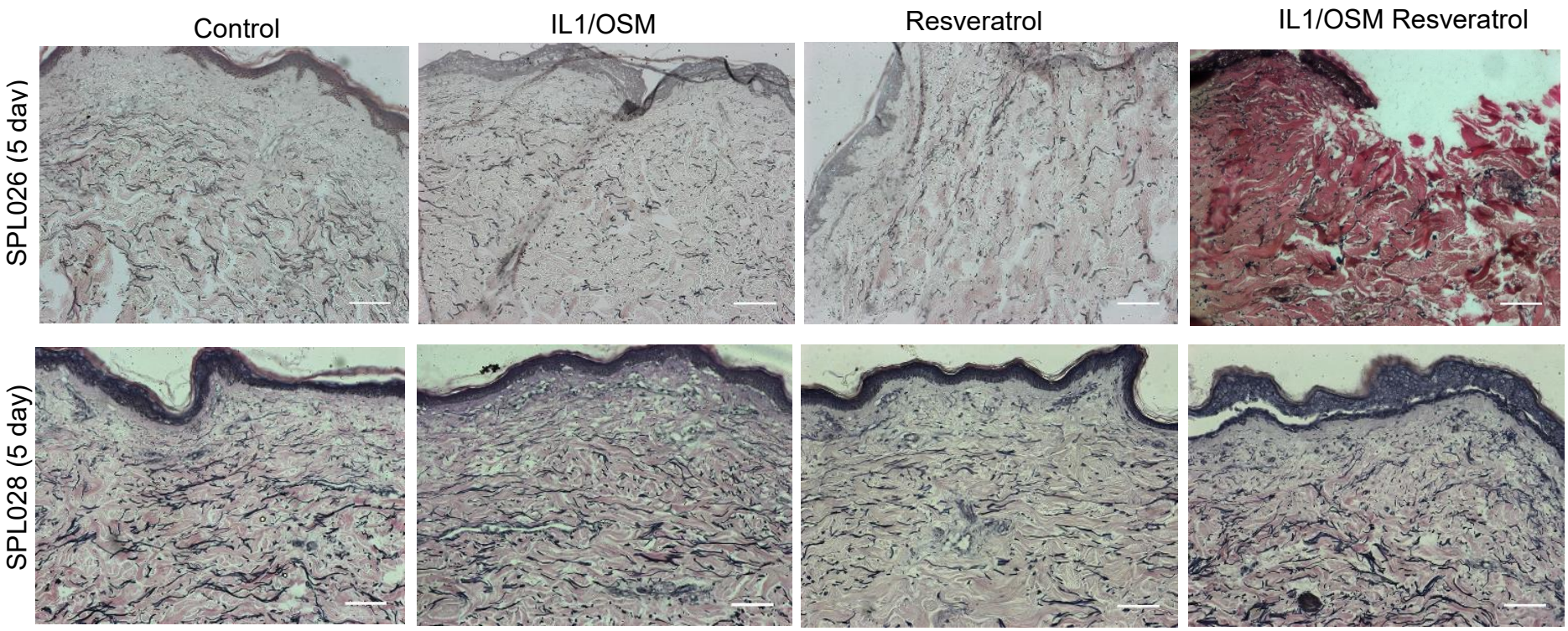

<u>Figure 5.19 Elastin morphology of human skin tissue 5-day post treatment</u>.

Wax sections were fixed and stained for elastin for comparison of different treatments across donors. Scale bar = 100 µm

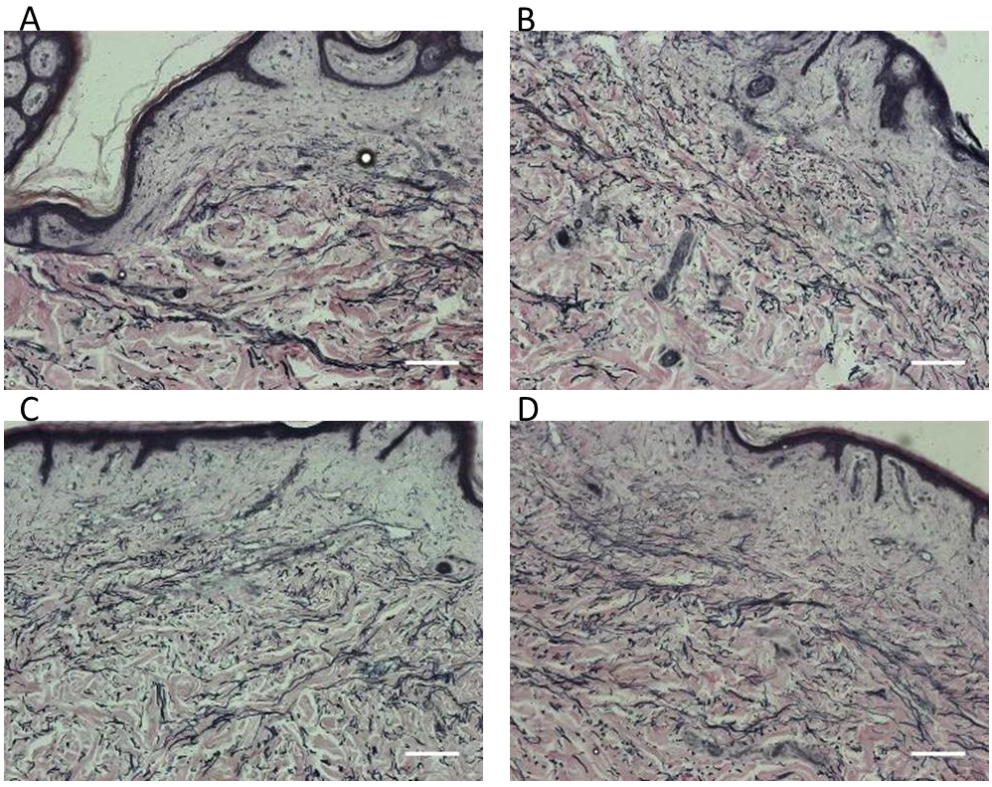

Figure* 5.20 *Elastin morphology of skin tissue from SPL029, Day 1.

Wax sections were fixed and stained for elastin for comparison of different treatments, A) Control, B) IL1/OSM, C) Resveratrol, D) IL1/OSM +Resveratrol

Scale bar = 100µm

A

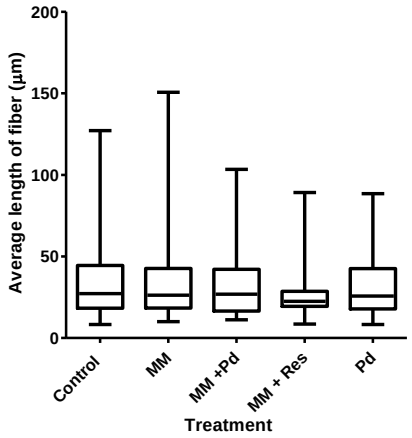

	Control	MM	MM +Pd	MM +Res	Pd
Average length of Elastin (µm)	33.91	33.15	32.52	26.01	30.54
Max strand length (µm)	127.11	150.65	103.36	89.21	88.48
Min strand length (µm)	8.32	10.06	11.18	8.58	8.32
Average number of strand per box	19	16	18	12	20

B

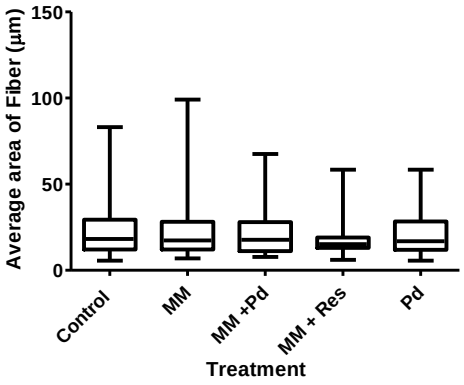

	Control	MM	MM +Pd	MM +Res	Pd
Average area of Elastin (µm)	23.04	22.45	21.71	17.39	20.50
Max strand length (µm)	83.10	99.12	67.52	58.43	58.43
Min strand length (µm)	5.63	6.93	7.79	6.06	5.63
Average number of strand per box	19	16	18	12	20

Figure 5.21 Quantification of morphological changes in Elastin in SPL015.

Wax sections were fixed and stained for elastin for comparison of different treatments. Elastin fibre length (A), number and thickness (B) were analysed in three randomly assigned 5x5 squares using Image J. Analysis performed by Fatima Oyaifo

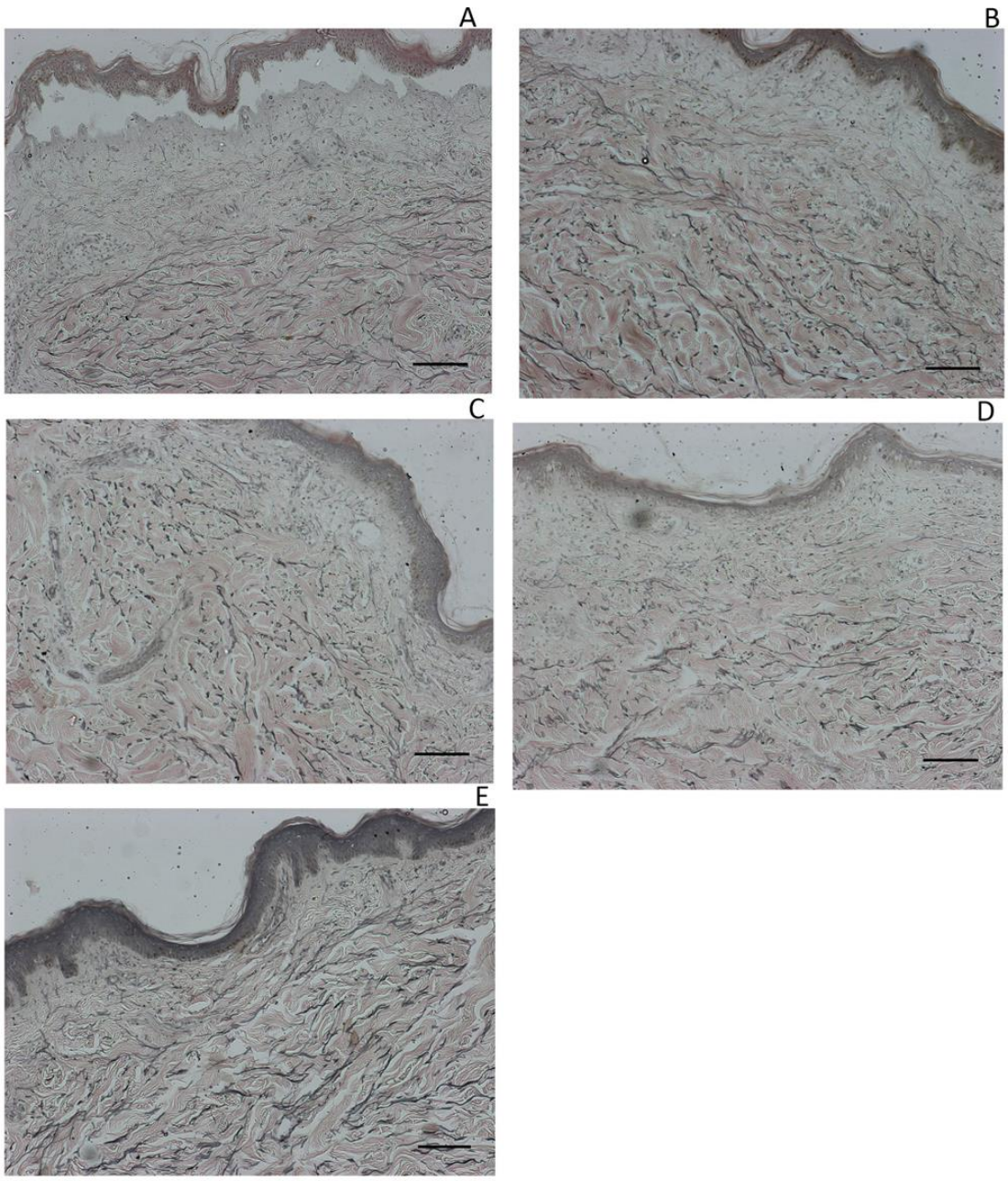

<u>Figure 5.22 Elastin stain in SPL015 samples, with 5-day treatment regime.</u>

10µm sections were fixed and stained with Elastin stain. Images representative of Elastin staining, quantification was performed on these samples by Fatima Oyaifo. A) Control, B) MM, C) MM +Res, D) MM +Pd, E) Pd.

Scale bar= 100 µm

5.14 Immunohistochemistry reveals MMP-12 expression predominantly in the epidermis

ABC (avidin-biotin complex) DAB (diaminobenzidine) peroxidase staining was used to investigate the localisation of MMP-12 in skin. In a combination with nuclear fast red counter-stain, the visualisation of MMP-12 in skin tissue should be clear.

DAB staining revealed little staining of MMP-12 in SPL007 T0 skin tissue, with a slight increase in MMP-12 staining in control skin (Figure 5.23,A). The MMP-12 staining appeared to be diffuse, rather than localising specifically to one skin cell type. With MM treatment, MMP-12 staining was seen clearly in the basal layer of the epidermis. Additionally, in SPL007 donor skin, there appeared to be an increase in MMP-12 staining in MM treated tissue compared to controls (Figure 5.23,A). In contrast, mRNA expression levels showed a significant decrease in MMP-12 expression in MM-treated tissue compared to untreated controls (Figure 5.23,B).

Staining was also performed on SPL013 donor skin sections (Figure 5.24) which, like SPL007, showed a decrease in MMP-12 expression with MM treatment compared to control. As with SPL007 staining, more intense MMP-12 staining was observed within the basal epidermal layer of tissue with MM juice compared to control. Additionally, SPL013 donor skin treated with ResTom juice showed more intense MMP-12 staining compared to MM treatment (Figure 5.24), in contrast to the mRNA expression data (Figure 5.4) where ResTom treatment showed highly supressed MMP-12 expression. Expression of MMP-12 in both SPL007 and SPL013 appeared to be diffuse rather than cell specific, which may have made quantification of MMP-12 difficult.

Melanocytes within SPL013 were much more apparent (Figure 5.24). Melanocytes are brown in colour due to the presence of the pigment melanin. In skin with a high number of melanocytes, this can make differentiation between MMP-12 positively- stained cells, and melanocytes in the basal epidermal layer, difficult.

Histochemical staining of MMP-12 showed increased levels in contrast to the mRNA expression data. The data from western blot analysis showed an increase in MMP-12 in conditioned media of SPL013 skin cultures.

This further suggests that there is a discourse between mRNA expression data and protein expression.

A

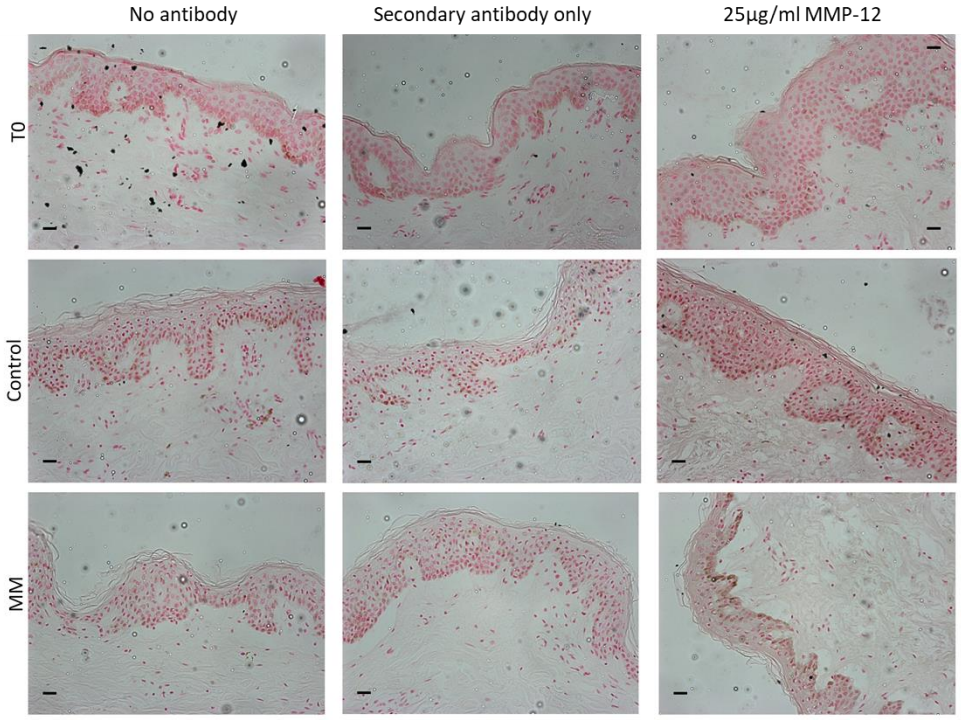

B

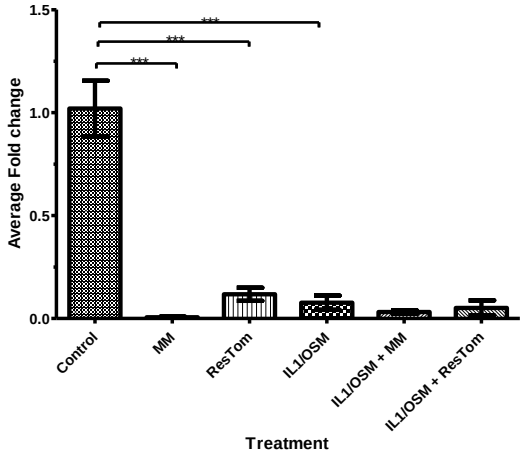

Figure 5.23 ABC DAB staining for MMP-12 in 5 day treated skin explants from donor SPL007.

10µm wax sections were fixed and stained for MMP-12 at 25µg/ml (A). Sections were prepared from skin treated at T0, treated with control culture media, or treated with MM juice extract. Tissue was counterstained with nuclear fast red to emphasise DAB staining which is brown. (B) Corresponding qRT-PCR expression analysis of MMP-12. Data was analysed by relative quantification and normalised to 18S for MMP-12. Corresponding average CT values are shown (B). Each bar represents the mean fold change of 3 samples ±SEM. Statistical difference was determined using one-way ANOVA with the Bonferroni multiple comparison test *p≤ 0.05 **p≤ 0.01. ***p ≤ 0.001, ****p≤0.0001. Scale bar= 200µm

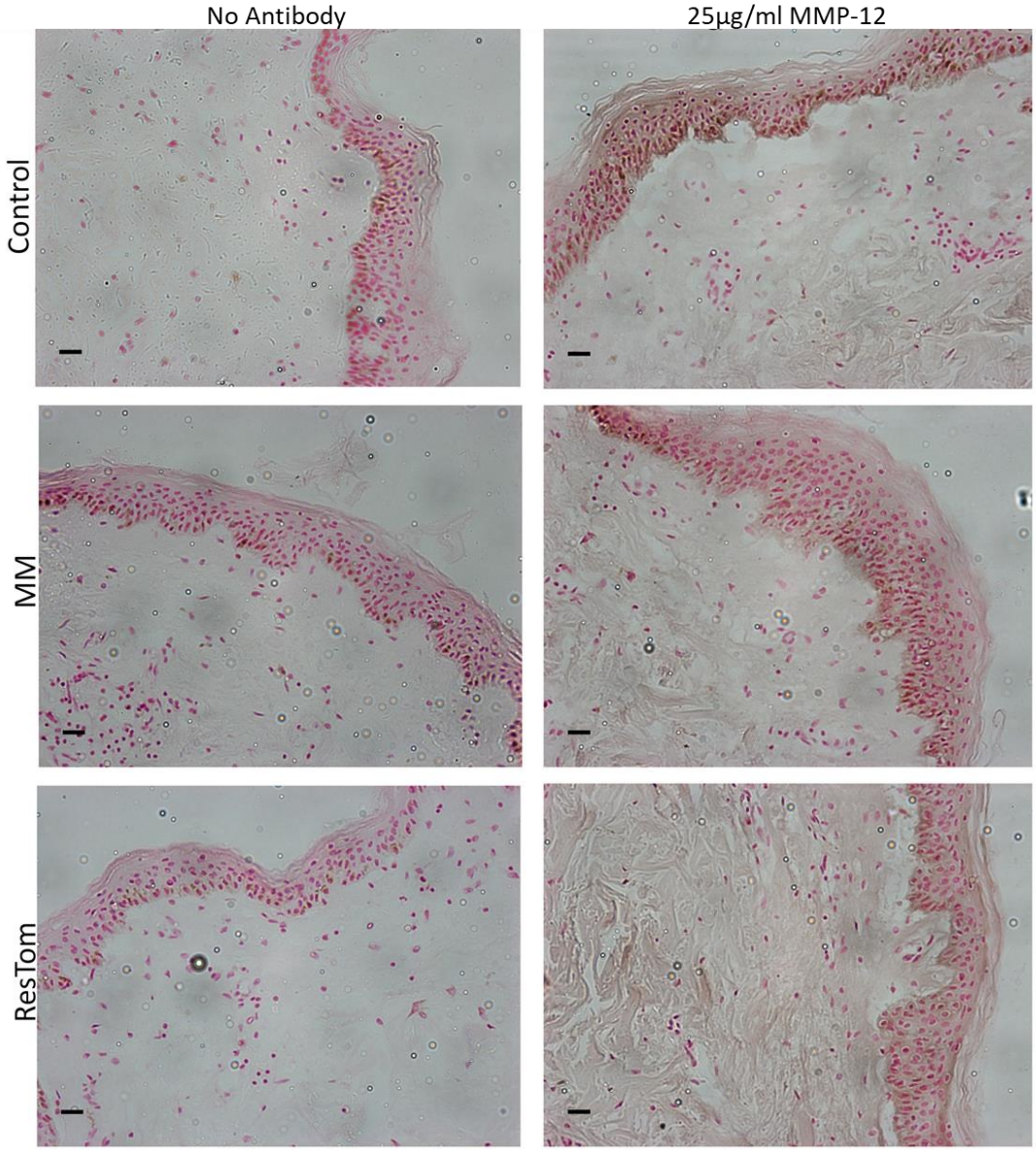

Figure 5.24 ABC DAB staining for MMP-12 in 5 day treated skin explants from donor SPL013.

10µm wax sections were fixed and stained for MMP-12. Sections were prepared from skin treated with control culture media, MM juice extract, or ResTom juice extract. Tissue was counterstained with nuclear fast red to emphasise DAB staining which is brown.

Scale bar= 200µm

5.15 Discussion

Microarray analysis identified MMP-12 as a key gene downregulated by both MM and ResTom juice. MMP-12 acts to degrade elastin, which is a crucial structural component of skin for the maintenance of elasticity. Within skin aging models, dysregulation of elastin has been shown to have a major role in morphological changes associated with both intrinsic and extrinsic aging (Tewari et al., 2014).

UV damage from sun exposure is known to cause an increase in MMP-12 expression and is likely the cause of solar elastosis which is characterised by the development of elastin tangles. In addition, degradation of elastin networks in the skin is known to decrease elasticity leading to the development of wrinkles (Fisher et al., 2002). Considering the importance of elastin in the maintenance of healthy and youthful skin, the potential inhibitory effect on the activity of MMP-12 by MM and ResTom juice identified by microarray analysis was particularly interesting.

It was important to establish whether the inhibition of MMP-12 by MM and ResTom was a common trait across donors or was specific to the donor used for the microarray analysis, SPL003. Analysis of MMP-12 expression across several different donors (Figure 5.2) identified that repression of MMP-12 was a common trait of both MM and ResTom juice, with ResTom juice having a greater inhibitory effect on MMP-12 than MM juice after 5 days of treatment. The repressive effect of MM juice extract itself on MMP-12 expression may have been due to the mix of plant bioactives in the juice. Several plant polyphenols including quercetin are present in MM juice, have been shown to inhibit MMP-12 expression (Ganesan et al., 2010), which might explain the inhibitory effect of MM juice. The further repression of MMP-12 by ResTom juice showed that the addition of resveratrol, and its derivatives had a stronger biological effect on MMP-12 expression than MM juice alone, 5 days after treatment. It is well documented that mixtures of plant compounds can have more potent biological effects than single compounds (Kowalczyk et al., 2010, Herranz-López et al., 2012, Pesakhov et al., 2010), therefore this increased inhibitory effect could be due to a synergistic effect between complex matrix and compounds of ResTom. This interpretation was supported by the absence of repression of MMP-12 expression by pterostilbene, pinostilbene or resveratrol as pure compounds in a number donor skin samples.

Statistical analysis did not reveal statistically significant decreases in expression levels of MMP-12 with MM or ResTom treatments, but comparison of C_T values showed that ResTom had a greater repressive effect. As MM acted to greatly suppress MMP-12 expression, substantially, it could be that much of the effect of ResTom was masked by MM treatment. To investigate the differences in biological efficacy between MM and ResTom juices, different concentrations of these two tomato treatments should be tested and compared.

It was particularly interesting that neither addition of resveratrol or polydatin by themselves led to substantial decreases in MMP-12 expression, which added to the evidence suggesting synergy between the stilbenes and compounds in the tomato juice matrix was a key factor in the observed biological effects.

In inflammatory conditions addition of ResTom led to significant inhibition of MMP-12 expression beyond that observed with MM juice treatment, suggesting greater biological activity for ResTom than MM. This observation correlated with those in the recent study by Scarano et al. (2018), in which mice were fed a diet supplemented with freeze-dried powder from different tomato fruits, including MM and ResTom to compare activity of different dietary polyphenols in the same tomato background. Mice with DSS-induced colitis and fed a ResTom diet showed significantly reduced levels of inflammation compared to those fed MM, with associated reduced secretion of inflammatory cytokines and correspondingly lower disease indices, indicating higher biological activity associated with ResTom fruits than regular MM tomato fruit.

When MM juice was spiked with resveratrol or polydatin, only MM juice spiked with resveratrol repressed MMP-12 to the level of ResTom, suggesting that it is the presence of resveratrol rather than polydatin that drives inhibition of MMP-12 expression (Figure 5.1). Interestingly, under inflammatory conditions, MM spiked with resveratrol or polydatin led to both upregulation and down regulation of MMP-12 expression in skin samples from different donors. However, Inhibition of MMP-12 expression by MM +Res was not as great as for ResTom, suggesting that the tomato matrix of ResTom cannot be wholly replicated by simply adding resveratrol or polydatin to MM juice. This may have been due to the presence of other stilbenes in ResTom with bioactivities in repressing MMP-12 expression.

Due to constraints on availability of tissue and tomato juice extracts for experiments, only a single whole skin experiment was conducted that examined the effect of PteroTom extract treatment on MMP-12 expression (Figure 5.10). Interestingly, the effect of PteroTom was to increase MMP-12 expression greatly, an effect which was not observed with either MM or ResTom treatment. This could indicate a very different biological effect of PteroTom on MMP-12 expression compared to the other tomato extracts, if confirmed in skin explants from other donors. It would be interesting, in future studies to see whether the inductive effect of PteroTom was also observable at later time points after treatment. Increased MMP-12 expression is known to help promote the migration of macrophages through epidermal and vascular structures, and consequently the effects of PteroTom extracts could potentially offer a useful treatment for inflammatory skin disorders (Vaalamo et al., 1999).

The effects of tomato extracts on MMP-12 steady state mRNA seen in explants may represent changes in any of the different cell types in skin. To explore the roles of tomato extracts on different

individual cells, preliminary experiments were carried out on a human keratinocyte cell line. Cells were wounded with a scratch to investigate the effect of tomato juice treatment on wound healing (discussed in Chapter 6:), and the RNA extracted from cells for qRT-PCR. In contrast to expression of MMP-12 in skin explants, neither MM nor ResTom treatment suppressed MMP-12 activity. Additionally, EGF acted to suppress the expression of in contrast to observations in whole skin explants. However, in SPL012, addition of EGF greatly increased MMP-12 expression , and the addition of tomato extract to EGF acted to suppress the inducing activity of EGF on MMP-12.

A second keratinocyte experiment compared the effect of methanol-based tomato extracts and aqueous extracts. In this experiment there was little difference in MMP-12 expression in response to the different tomato extracts. However, as this experiment was only performed over a 24-hour period, it would be informative to run the experiment over longer time periods to observe whether there are any changes in MMP-12 expression at later time points following treatment.

Additionally, the tomato-extract concentrations used were based upon work using breast cell lines (Dr Katharina Bulling, JIC) and may not be optimal for keratinocytes. Therefore, additional experiments should be performed looking at dose response curves of keratinocytes to methanol and aqueous extracts to determine the optimal concentration of juice for use in keratinocyte-based experiments.

Using a mouse fibroblast line, biological activity associated with different concentrations of methanol tomato extracts was investigated. Both ResTom and PteroTom extracts had suppressive effects on MMP-12 expression in fibroblasts, with PteroTom exhibiting greater suppression (Figure 5.14). It is interesting that lower dosages of Hi-Resv and PteroTom juice led to greater inhibition of MMP-12 expression. This indicated that Hi-Resv and PteroTom may have different functionalities at different dosages. Dose-dependent health benefits have been associated with resveratrol, with low doses shown to be beneficial for maintenance of human health by promoting anti-inflammatory effects in addition to providing cardio-protection by acting as an anti-apoptotic agent. At high doses however, resveratrol is known to act as a pro-apoptotic agent, hindering tumour growth, but also inhibiting synthesis of RNA, DNA and protein, decreasing wound healing and decreasing cell proliferation (Mukherjee et al., 2010). Further analysis is needed to elucidate the different biological functions of Hi-Resv and PteroTom at different concentrations, and not only on specific cell lines but also on whole skin to optimise the concentrations required for different beneficial, biological effects.

In contrast to the inhibitory effect of ResTom observed in mRNA expression data, western blot analysis displayed an increase in MMP-12 protein levels with ResTom juice compared to MM juice (Figure 5.15) . This was interesting, as it showed a discordance in expression of MMP-12 mRNA and protein. Although not widely observed, the relationships between mRNA expression and protein

are not always correlated, as observed in several studies (Chen et al., 2002, Blake et al., 1990, Guo et al., 2008) . Similar disparities between mRNA expression and protein levels have been observed for MMP-2 and MMP-9 (Lichtinghagen et al., 2002), with the suggestion that MMPs may be differentially influenced at the protein level, especially in pathological conditions. For example, activated pathways may serve to increase the stability of protein, therefore preventing the degradation of activated protein. Under these circumstances it could be possible that a low level of mRNA translation could result in high total protein concentration due to highly stable protein (Guo et al., 2008).

However, changes in mRNA expression are not usually translated immediately into changes in protein levels, particularly because protein levels are determined by both synthesis and turnover. Therefore, lower levels of MMP-12 mRNA at 5 days after treatment may well result in lower levels of protein only later. Consequently, effects of treatments on MMP-12 protein levels, and on levels of its substrate, elastin, need to be assessed over longer time courses following treatment of skin samples.

In future experiments, it would be beneficial to compare MMP-12mRNA and protein levels over several time points and for longer than 5 days following treatment to understand better the relationship between MMP-12 mRNA and protein levels.

To investigate how changes in MMP-12 expression levels might impact upon elastin morphology of skin, elastin histological stains were performed on several donors. Changes in morphology of elastin were observable across some of the treatments, in particularly IL1/OSM and IL1/OSM + tomato extract or stilbene extract (Figure 5.18). In skin from donor SPL026 there was a observable difference in elastin morphology of IL1/OSM treated skin compared to IL1/OSM +ResTom, with longer elastic fibres present with the addition of ResTom (Figure 5.18). This correlated to a reduced expression of MMP-12 mRNA with IL1/OSM +ResTom treatment compared to IL1/OSM (Figure 5.2,B), suggesting that inhibition of MMP-12 expression by ResTom juice can result in changes in elastin. Additionally, comparison of IL1/OSM and IL1/OSM +Resveratrol treatments in SPL028 showed an increase in fibre thickness with addition of resveratrol (Figure 5.19), again suggesting a positive effect of the ResTom tomato juice on elastin, which appeared to offer protection against the degradative effects on elastin seen with IL1/OSM treatment. These data potentially show a protective effect of polyphenols on elastin in skin under inflammatory conditions.

A previous study by Jimenez et al. (2006) demonstrated a similar protective effect, and thickening of elastin fibres in skin treated with two polyphenols ellagic acid and tannic acid. In addition, the polyphenols pentagalloyll glucose, epigallocatechin gallate and catechin have been shown to promote elastogenesis in aortas (Sinha et al., 2014). Both studies showed an increase in elastin production with polyphenol treatments as well as an increase in crosslinking, increasing the overall

elastic structure. Similar effects could account for the changes in elastin morphology observed with ResTom and resveratrol treatments.

Within my experimental design although changes in elastin morphology could be visualised, quantification was not accurate and did not give a clear indication of any changes in elastin in skin samples between treatments (Figure 5.21). For my experiments, skin was treated over a 5 day period, whereas in the study by Jimenez et al. (2006) skin was cultured for 10 days. The lack of observable, significant changes in elastin after 5 days, coupled with the lack of changes in protein levels may indicate that changes at the morphological level do not become apparent until several days after alterations in MMP-12 mRNA expression levels. It would be informative to visualise and quantify changes in elastin at later time points as performed in the study by Jimenez et al. (2006).

Finally, we investigated differences in MMP-12 protein levels in whole skin tissue using immunohistochemistry. MMP-12 expression appeared diffuse in expression within epidermis, with more expression surrounding basal epidermal cells (Figure 5.23 and Figure 5.24). This diffuse expression of MMP-12 correlated with that observed in other studies (Tewari et al., 2014). However, MMP-12 levels did not correlate with observed changes in mRNA expression levels. For example, in the skin of the SPL013, greater MMP-12 staining was observed with ResTom treatment compared to control (Figure 5.24), despite reduced MMP-12 mRNA seen in ResTom treated skin (Figure 5.4).

These data combined with the data from elastin staining, protein expression and mRNA expression studies showed that the activity of MMP-12 may lag changes in MMP-12 gene expression. This may be due to a lag in protein expression levels following changes in mRNA expression. In addition, analysis on Western blots showed some evidence for post-translational regulation of MMP-12 levels. This showed that MMP-12 should be investigated using mRNA, protein and immunohistochemical assays to fully understand the underlying changes in MMP-12 expression and activity. In addition, since elastin is modified by MMP-12 through its elastase activity, effects of treatments on elastin may need to be investigated over even longer time courses. In future experiments, it may be beneficial to culture skin explants overextended time periods, after which effects of treatments on protein expression and activity may be better evaluated.

Overall my data have shown differential effects on MMP-12 between different treatments, with mRNA and elastin data suggesting a potential inhibitory and protective effect of ResTom juice on maintenance of elastin. These effects need to be investigated over longer treatment times, where the effects of treatments on MMP-12 and elastin protein levels may become more apparent.

Elastin promoting treatments would need to be tightly managed, since too much elastin degradation could be extremely detrimental. The elastic-fibre disease Cutis Laxa exemplifies the

negative effects associated with severe elastin degradation in the skin. Cutis Laxa is characterised by loose and sagging skin, with reduced recoil as a result of loss of elastic fibres (Uitto, 2001), due to inflammation in the skin, or mutations in the elastin gene. Additionally, individuals with Marfans syndrome, a disease caused by a mutation in fibrillin-1 required for the correct formation of the extracellular matrix, and maintenance of elastin fibres, show a wide range of clinical manifestations related to disrupted elastin networks including musculoskeletal, cardiac and ocular defects (Milewicz et al., 2000), highlighting the importance of correct maintenance of elastin networks. Interestingly, the treatment of human skin samples with tomato juice, and more significantly with stilbene enriched tomato juice appears to reduce inflammation and the transcript levels of MMP-12 encoding an elastase, both of which may be beneficial effects for the maintenance of healthy skin.

5.16 Summary

The results presented in this chapter showed that both MM and ResTom juice inhibited mRNA levels of MMP-12 in whole skin tissue. Analysis of two cell lines, HaCaT keratinocytes and 3T3 fibroblasts showed a differential response in MMP-12 expression, with inhibition of MMP-12 observed in fibroblasts but not in keratinocytes, indicating tomato extracts may act differentially on different cell types. In addition, limited results on cell mono-cultures suggested that PteroTom juice might have a higher biological activity than ResTom juice.

Thus far, I have been unable to confirm the impact of downregulated MMP-12 mRNA expression on the morphological characterisation of skin, or on protein levels. Although changes in elastin morphology were observed in some explants, an accurate method by which to quantify elastin levels is still required. Elastin levels should also be investigated at later time points following treatment of skin.

It is important that in future studies the changes in MMP-12 gene expression in response to treatments observed in this study are verified at the protein level. During this thesis, protein expression levels were investigated in two donors, using conditioned media collected from a skin explant experiment, and whole tissue, after 48 hours of treatment. However, an increase in MMP-12 protein levels was observed with ResTom treatment compared to MM (Figure 5.15), contrary to MMP-12 mRNA expression levels. Although RNA was extracted from whole tissue explants treated for 5 days, protein levels were too low to be able to use for western blots. With optimisation of the protein extraction protocol, such as a reduction of total volume of buffer used for extraction, it should be possible to extract higher levels of protein allowing levels to be studied at a later time points following treatment.

An initial experiment with PteroTom juice treatment on human skin showed a large increase in MMP-12 compared to that observed with other tomato extracts (Figure 5.10), however cell culture experiments did not confirm these results. It is unclear, at this stage, whether these data reflected a donor-specific response seen in full skin or were indicative of differential responses in different cells of the skin. Further work will be needed to clarify these findings, although the differential activity of PteroTom is intriguing and could give rise to further applications of tomato extracts in cosmetics.

Chapter 6: Investigating wound healing modulation by stilbenes

6.1 Introduction:

Plant polyphenols have been shown to have effects on inflammatory and reparative processes of skin *in vitro*. It has been suggested that plant polyphenols can regulate wound healing via modulation of the inflammatory pathway, particularly through interaction with the EGF receptor (Pastore et al., 2012a). The two polyphenol glycosides verbascoside and teupoliside, for example, have been shown to significantly accelerate wound healing in full thickness wounds of rats when applied topically (Korkina et al., 2007). It was hypothesised that these two plant polyphenols increase wound healing by activating the EGF pathway. However, some oral studies of resveratrol have shown inhibition of endothelial cell growth, and delayed angiogenesis-dependent wound healing in mice (Brakenhielm et al., 2001), suggesting that resveratrol may in fact have an inhibitory effect on wound healing.

Most of the current work on the topical functionality of polyphenols has been derived from studies looking at the topical application of a single polyphenol to full thickness wounds in rat models. However, differences in the structure and permeability of rodent skin compared to human skin means that extrapolation of these data to human responses is unreliable (van Ravenzwaay and Leibold, 2004).

A known problem with resveratrol is low bioavailability, although several studies have suggested that overall bioavailability and activity of resveratrol can be increased by combination treatments with other plant polyphenols. Despite most of these studies have been focused on the bioavailability of resveratrol via oral intake, they suggest possible synergistic effects between different plant phytochemicals. A study which looked at the difference of combined phytochemicals on murine skin tumorigenesis showed significant differences compared to single compound treatments, and showed that combinations of phytochemicals often led to an additive response, increasing overall biological activity of the applied phytochemicals (Kowalczyk et al., 2010).

Consequently, I wanted to investigate how tomato extracts composed of different biologically interesting compounds act on wound healing.

6.2 Aims:

- To identify how tomato extracts containing different key biologically active compounds impact wound healing, and to determine whether there are any differences in overall biological efficacy between these tomato extracts.
- To investigate the use of *ex-vivo* human skin explants as a model for wound healing in full thickness skin.

6.3 Methods:

Table 6:1 Table of tomato abbreviations used in the chapter with corresponding details of tomato lines.

Name	
MM	Wild type tomato
ResTom	Original resveratrol producing tomato 35S:StSy/ E8:MYB12
Hi-Resv	New resveratrol tomato E8:StSy/E8:MYB12
PteroTom	Pterostilbene tomato E8:StSy/E8:ROMT/E8:MYB12

6.3.1 *Ex-vivo* model of wound healing

All *ex vivo* skin wounding procedures ("doughnut" model) were carried out by Dr Damon Bevan essentially as described in Olivera and Tomic-Canic (2013).

In brief, using a sterile 3 mm punch tool, a shallow biopsy was made in the epidermis of human skin (surplus to surgery and donated with ethical approval as described in 2.8.2), and the epidermal core, with a small part of the dermal layer of skin removed with dissecting scissors, was extracted to leave a shallow 3 mm wound. An 8 mm full thickness punch biopsy was made around the 3 mm wound (Figure 6.1) and the explant was placed in culture media at the air-liquid interface with an 8 day, or 11-day treatment regime. For 8-day regimes, explants were stimulated initially on day 1, and re-stimulated with treatments on day 4 and 6, before collecting samples on day 8. 11-day treatment regimens were initially stimulated on day 1 and re-stimulated on day 4 and 7 before collection on day 11. Extracts were applied topically by pipetting onto the wound bed.

A

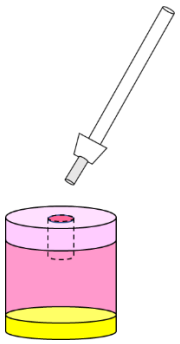

B

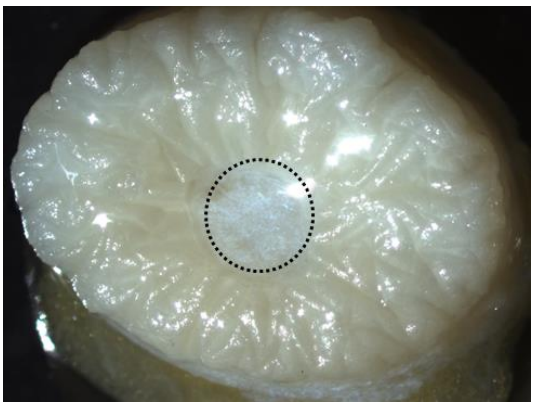

Figure 6.1 Diagram to illustrate the Ex vivo wound healing explant.

A 3mm punch biopsy was used to make a shallow wound, and the epidermal and small part of dermal layer was removed with dissecting scissors (A), (B) shows the 8mm full thickness explant, with the 3mm wound outlined. Image collected after initial wounding (photo by Stuart Keppie).

6.3.2 Tissue embedding and sectioning.

Cultured skin explants were collected at day 8 or 11 and fixed in 4% paraformaldehyde. The fixed tissues were then embedded in paraffin and cut into 10 µm sections with the Microm HM355S automatic microtome (Thermo Scientific) and mounted on poly-lysine microscope slides (Thermo Scientific) prior to H&E staining and immunohistochemistry.

6.3.3 Scratch wound assay

Cells for scratch assays were plated by or under the supervision of Dr Damon Bevan. Cells were plated into a 24 well plate at a density of 100,000 cells per well and cultured in high glucose DMEM + 10% FCS at 37°C, 5% CO_2 until confluency. Once confluent, the cell media was changed to DMEM + 0% FCS prior to generation of a "wound". Changing media from 2% FCS to 0% FCS was to prevent cells from proliferating to ensure that any wound healing observed was due purely to migration of cells, rather than to cell proliferation. Before wounding, a line was drawn horizontally through the centre of each well to use as a landmark when taking photos of the scratch above or below the line. Cells were wounded with a yellow pipette tip by scratching across the diameter of each well. Once

the scratch had been performed, the medium was changed to DMEM+ 2% FCS containing the required supplements and images were collected (T= 0h). The cells were incubated for 24- 48 hours, with photographs taken at T=24h and T=48h timepoints (depending on the rate of scratch closure). After incubation, conditioned media (for Western blotting) and cell lysates (for RNA analysis) were collected. Analysis of wound closure was performed using Image J.

6.3.4 Analysis of wound closure in skin explants

Images were taken of both edges of the wound (left and right) and using Image J, several measurements of wound closure were made including length of epidermal tongue, thickness of the wound edge, and overall area of wound re-epithelialisation (Figure 6.2). Epidermal Growth Factor (EGF) was included as a positive control for wound closure (Nanney, 1990).

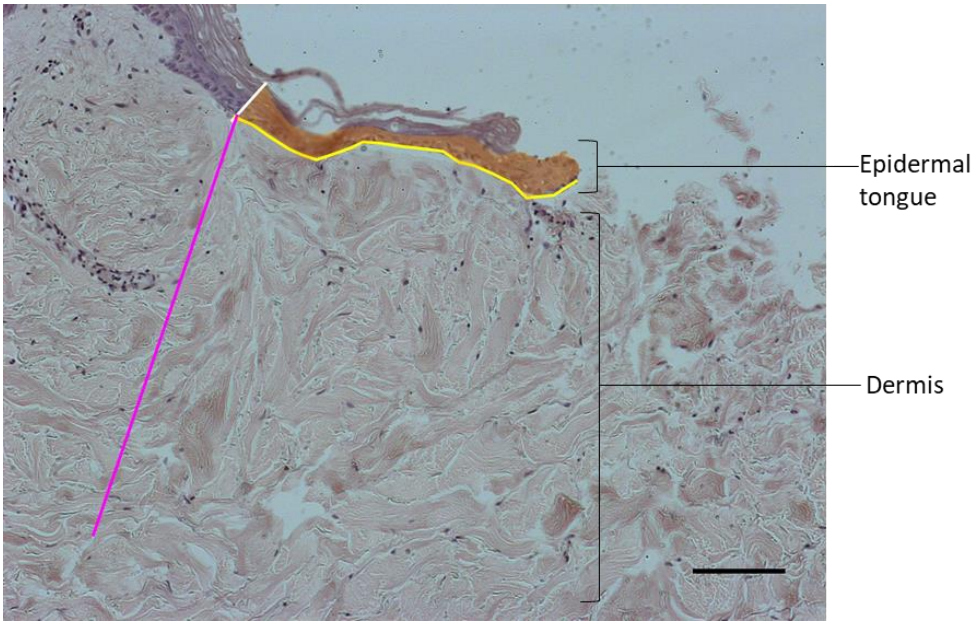

Figure 6.2 Diagrammatic representation of wound healing analysis using Image J.

Three measurements were taken for left and right sides of wounds. Thickness of the wound edge (white), Length of epidermal tongue (yellow) and overall area of wound re-epithelialisation (orange). Average tongue thickness was calculated from wound edge thickness and area. Note that the original wound edge was determined by the change observed in the underlying dermis (magenta line). Scale bar= 100µm

6.3.5 Methanolic tomato extract preparation for cell studies.

Methanol extracts of tomatoes were made (as outlined in chapter 2, 2.9.3), a small quantity (100 µl) was taken for use in LCMS IT-TOF analysis, and the remainder concentrated using a rotary evaporator. The solvent was evaporated until the extracts were almost dry and had reached a gel-like composition. The tomato derived extracts were then re-dissolved at a 1:10 dilution in 50% MeOH (v/v). The resolubilised extracts were then stored at -20°C. Stilbenes and flavonol content was quantified (as described in chapter 3, 3.5). A final concentration of between 0.1% and 1% of the methanolic tomato extract was used in cell cultures. A 1% methanol tomato extract is the equivalent dosage as the 1:10 dilution of aqueous tomato extract used in cell culture media.

6.3.6 Preparation of commercial purified resveratrol and polydatin

Plant polyphenols were purchased from Sigma and dissolved in DMSO to a final concentration of 50 mM. All plant polyphenols were added to cell cultures at a final concentration of 50 µM unless otherwise stated (Pastore et al., 2011a).

6.4 Results:

6.4.1 *Ex vivo* skin wound assays.

The wound healing properties of several plant compounds have been studied *in vitro* and *in vivo*. Healing of dermal wounds has been shown to be accelerated with green tea extract (Asadi et al., 2013), and grape seed pro-anthocyanidins (Khanna et al., 2002), suggesting wound-healing properties associated with the phytochemicals in these extracts. Additionally, several plant polyphenols have been shown to accelerate scratch wound healing, and exert anti-inflammatory effects *in vitro (*Pastore et al., 2012a*)*. There are few data concerning the effect of topical resveratrol on wound healing, and oral studies conducted with resveratrol in murine models have shown both inhibition (Brakenhielm et al., 2001) and acceleration of wound healing (Yaman et al., 2013). Given these varied properties associated with plant polyphenols, we investigated the effect of tomato juice enriched with resveratrol on full thickness wounds in human skin, by adapting the *ex vivo* skin model (described in 2.8.2).

The method used for creating wounds required a smaller shallow biopsy to be taken from the skin, and removal of the epidermis within this wounded section (Figure 6.1). Each explant needed to be wounded individually, and as such this has led to some variation in the size, depth and angle of the wound in the explant. In addition, in some cases, it appears that there may have not been a completely clean-cut wound edge, or complete removal of all the epidermal skin from the wound. This resulted in some of the wound explants containing additional wound artefacts, as can be seen in Figure 6.3, control 1. This made analysis of the new epidermal layer, and the site of the wound difficult and additionally, may have affected overall wound healing.

The wound edge and subsequent reepithelialisation was identified by using both the wound outline in the dermal layer of the skin, and the absence of the stratum corneum (Figure 6.3). Wound measurements were performed on both the left and the right-hand side of the wound. Unfortunately, not all wounds were able to be used for wound analysis due to the technical difficulties described above, or problems emerging from microtome sectioning.

Tissue from donor SPL013 was used for a preliminary experiment of the wound-healing methodology, and as such was analysed 8-days post-healing as recommended in the methodology by Olivera and Tomic-Canic (2013). As full wound healing was not observed by day 8 in SPL013, the following wound experiments using donor tissue SPL014 and SPL016 were collected at the later time point of 11 days post wound healing.

Between-experiment as well as donor-to-donor variation was particularly apparent in these wound studies. As such, analysis of SPL013 highlights some of the problems initially encountered using this method of *ex-vivo* skin healing. EGF is a well-established promoter of wound healing, stimulating

the migration of keratinocytes and fibroblasts (Chen et al., 1993, Lembach, 1976). Treatment of wounds with EGF showed increased wound healing compared to control wounds, in donors SPL014 and SPL016 (Figure 6.7,Figure 6.11) but not in donor SPL013 (Figure 6.3). In the SPL013 control it was observed that not all of the wound epidermal layer has been removed, which could have affected the reepithelialisation mechanism (Figure 6.3). This showed that within this methodology of *ex vivo* skin healing it was important to have a clean wound, and no remaining debris within the wound itself which might interfere with the healing process.

Measurements taken from the right and left side of the wound were averaged to give an overview of the wound healing response with each treatment (Figure 6.4, Figure 6.9, Figure 6.12). However, it was noticed during analysis that often one out of two wound edges in each explant displayed greater wound healing than the other (as in Figure 6.5). One possible explanation may be a lack of level positioning of the explants within the well. In some cases, this led to very different levels of re-epithelialisation on the two wound edges, making any effects of the different treatments difficult to ascertain. Consequently, the average wound healing response did not always give an inaccurate portrayal of wound healing. To try and help alleviate this problem, the maximal value of each measurement from the two wound edges was used (Figure 6.6, Figure 6.10, Figure 6.14), which enabled me to determine how treatments may affect the maximal wound healing achieved.

6.4.2 Wound healing in response to tomato treatment varies across donors

Across all wounds, there was little difference in wound edge thickness between treatments, however differences in epidermal tongue length were observed. The effect of ResTom and MM treatments varied between donors. With MM and ResTom treatment, maximal epidermal tongue length in both SPL013 and SPL014 was reduced compared to control (Figure 6.6 and Figure 6.10). As results for donor SPL013 were collected at an earlier time point than for donor SPL014 this could in part be due to assays made over a reduced healing time.

In contrast to SPL014, SPL016 appeared to show increased healing with MM and ResTom (Figure 6.14). However, SPL016 showed widely different tongue length measurements within MM and ResTom treated wounds (Figure 6.13) and therefore it was difficult to determine accurately its wound healing response.

Both SPL014 and SPL016 explants displayed similar trends in wound healing between control, EGF and IL1/OSM treatments, with EGF treatment increasing wound healing (Figure 6.10, Figure 6.14), and IL1/OSM treatment supressing wound healing (Figure 6.10, Figure 6.14). Interestingly, SPL014 displayed an increase in wound edge thickness with IL1/OSM treatment (Figure 6.10), whereas the SPL016 wound edge was not greatly increased compared to control (Figure 6.14).

MM tomato juice enhanced wound healing under inflammatory conditions in SPL014 (Figure 6.10), although this effect was not seen in SPL016, and since this result was seen in only one donor further analysis of future donor skin samples is required.

Unfortunately, due to donor availability and time constraints I was unable to do further *ex-vivo* wound experiments to compare the effects of MM, ResTom and PteroTom juices, or to look at the potential inhibitory effect of ResTom and PteroTom on the action of EGF.

A summary of treatments tested across the different models can be found in Table 6:2.

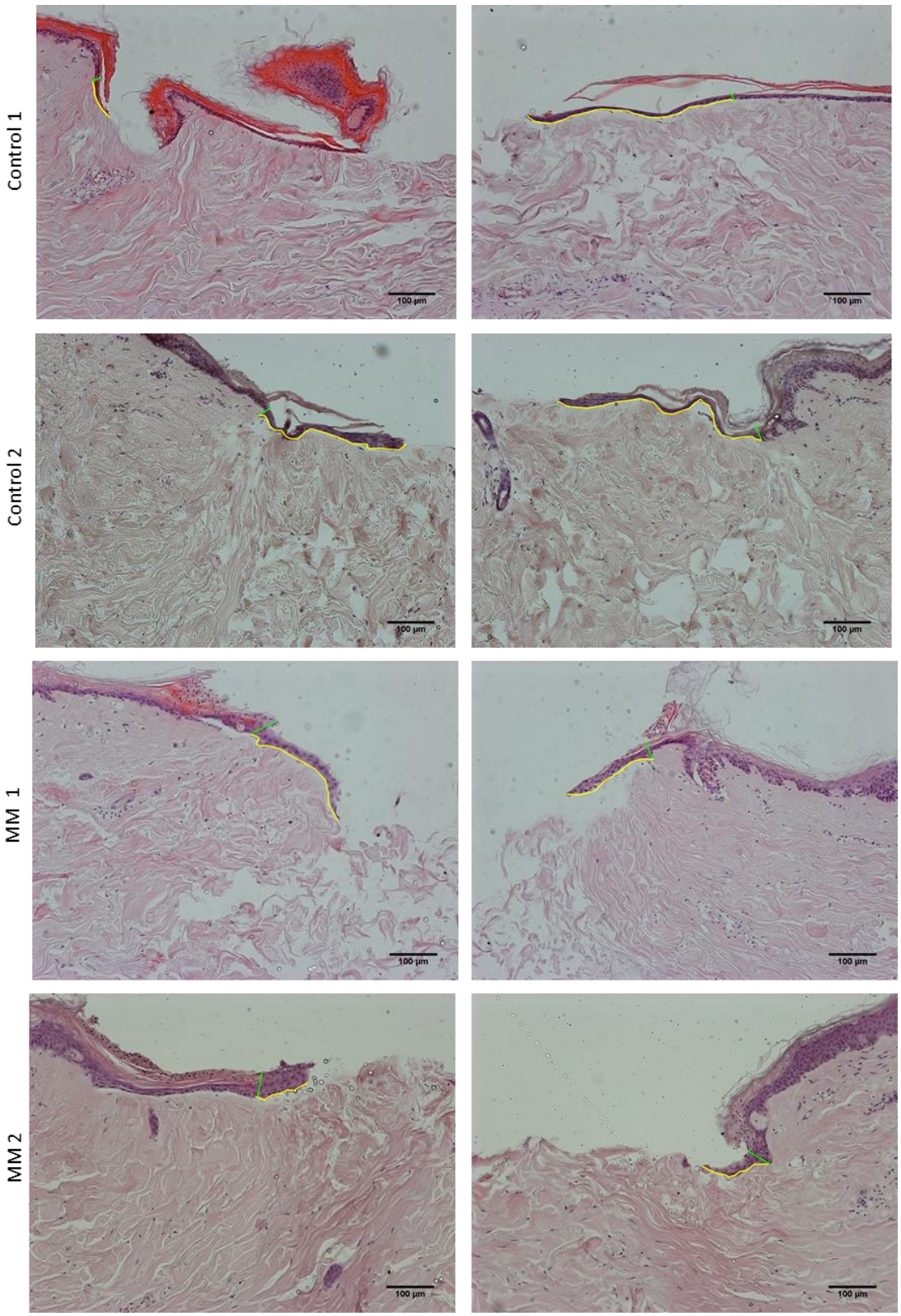
Control 1
Control 2
MM 1
MM 2
100 µm

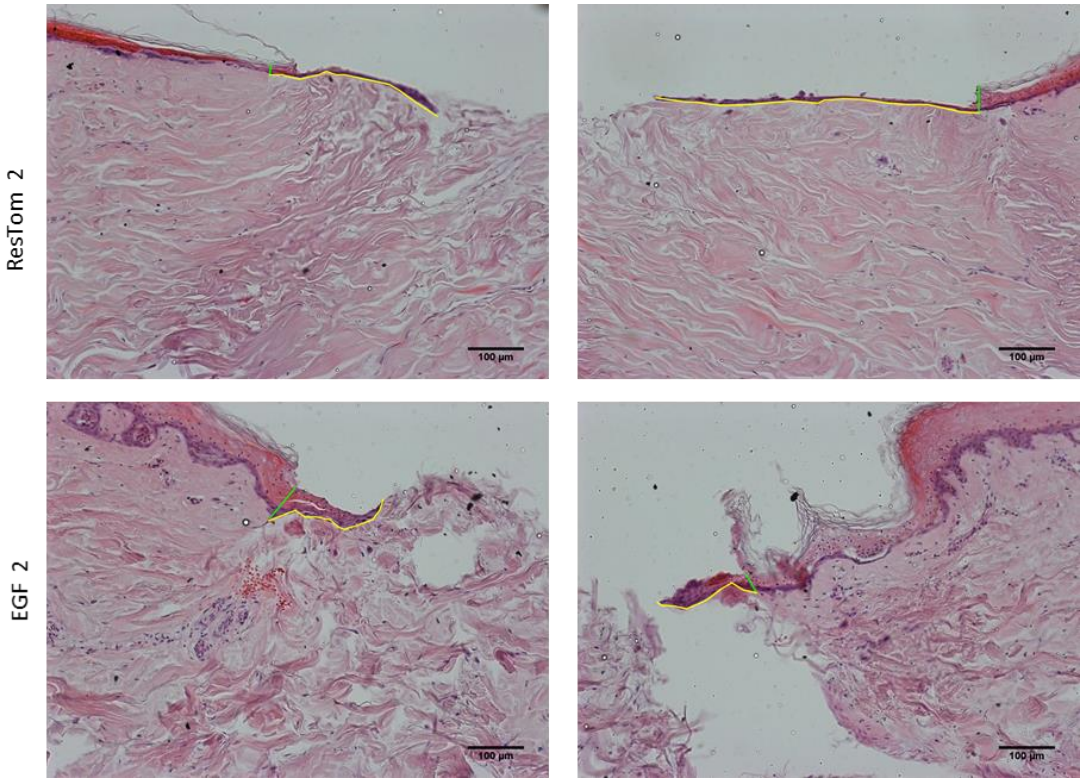

Figure 6.3 Analysis of SPL013 ex vivo skin wounds.

10 µm sections were fixed and stained with haematoxylin for comparison of normal wound healing, 8 days post wounding. Note that these wounds appeared to have lost some underlying dermis in some instances.

Scale bar= 100µm

A

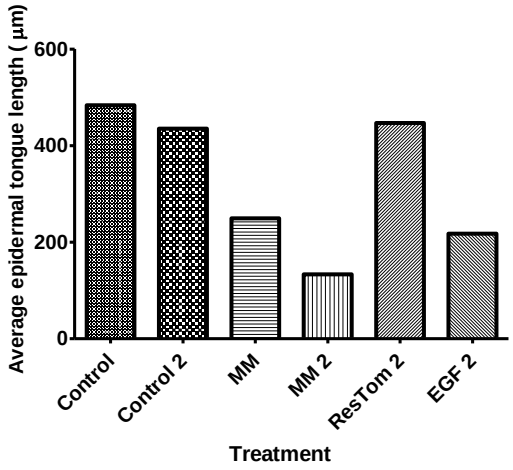

B

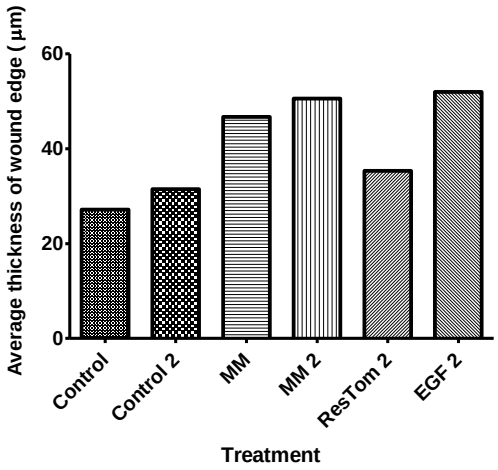

C

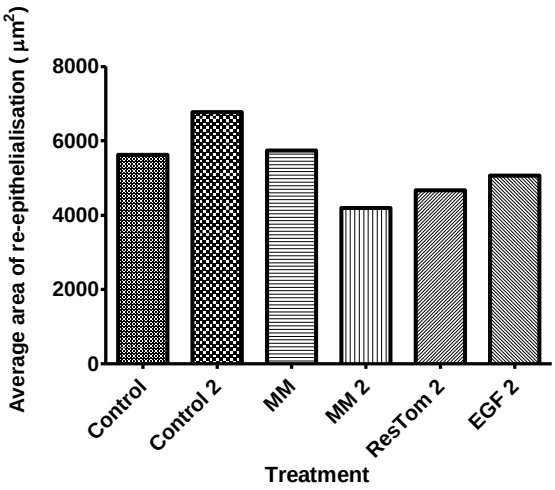

Figure 6.4 Average wound healing of SPL013

A) Epidermal tongue length, B) wound edge thickness, C) and area of re-epithelialisation were analysed using Image J software. Each bar represents average of left and right wound measurements for each treatment.

A

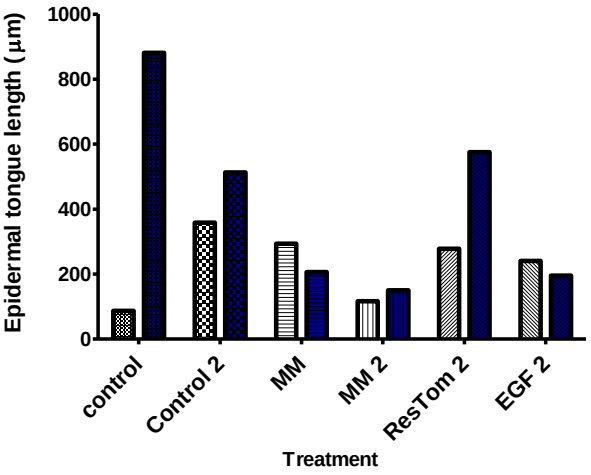

B

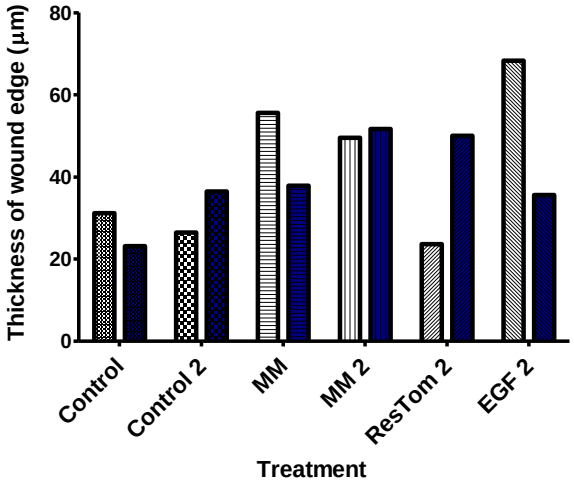

C

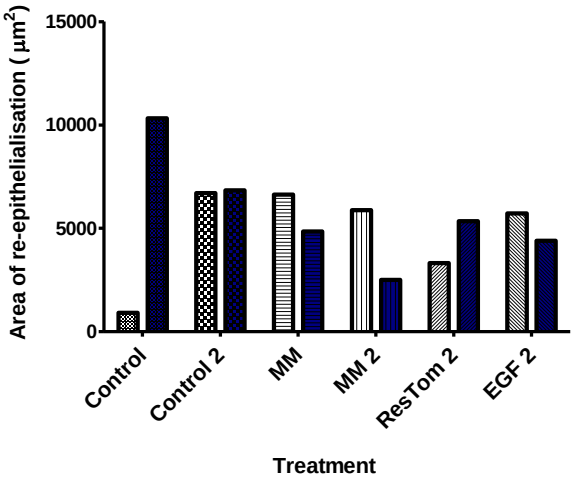

Figure 6.5 SPL013 wound analysis.

A) Epidermal tongue length, B) wound edge thickness, C) and area of reepithelialisation were analysed using Image J software. The two bars for each treatment represent measurements taken from the left and right side of the wound as depicted in images (Figure 6.3).

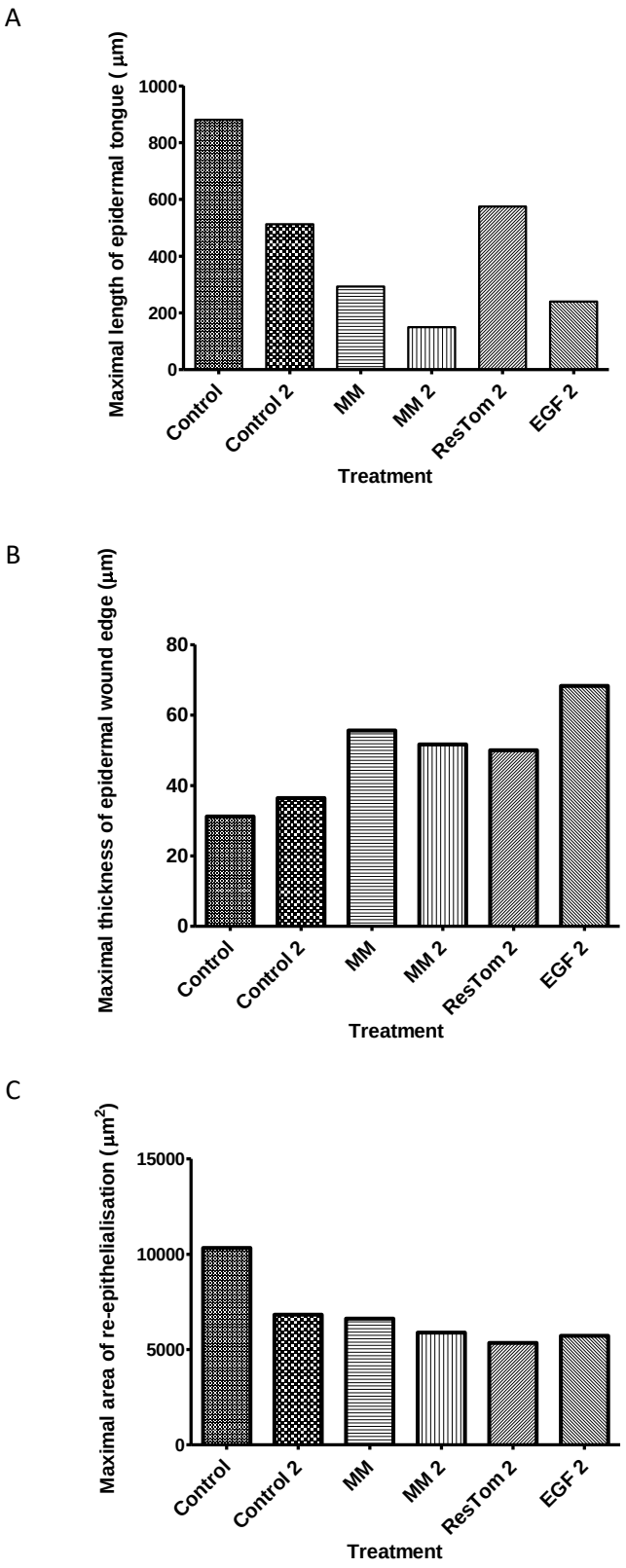

Figure 6.6 Maximal wound healing of SPL013

A) Maximal epidermal tongue length, B) maximal epidermal wound edge thickness, C) and maximal area of reepithelialisation were analysed using Image J software. Each bar represents the maximal value measured for each wound.

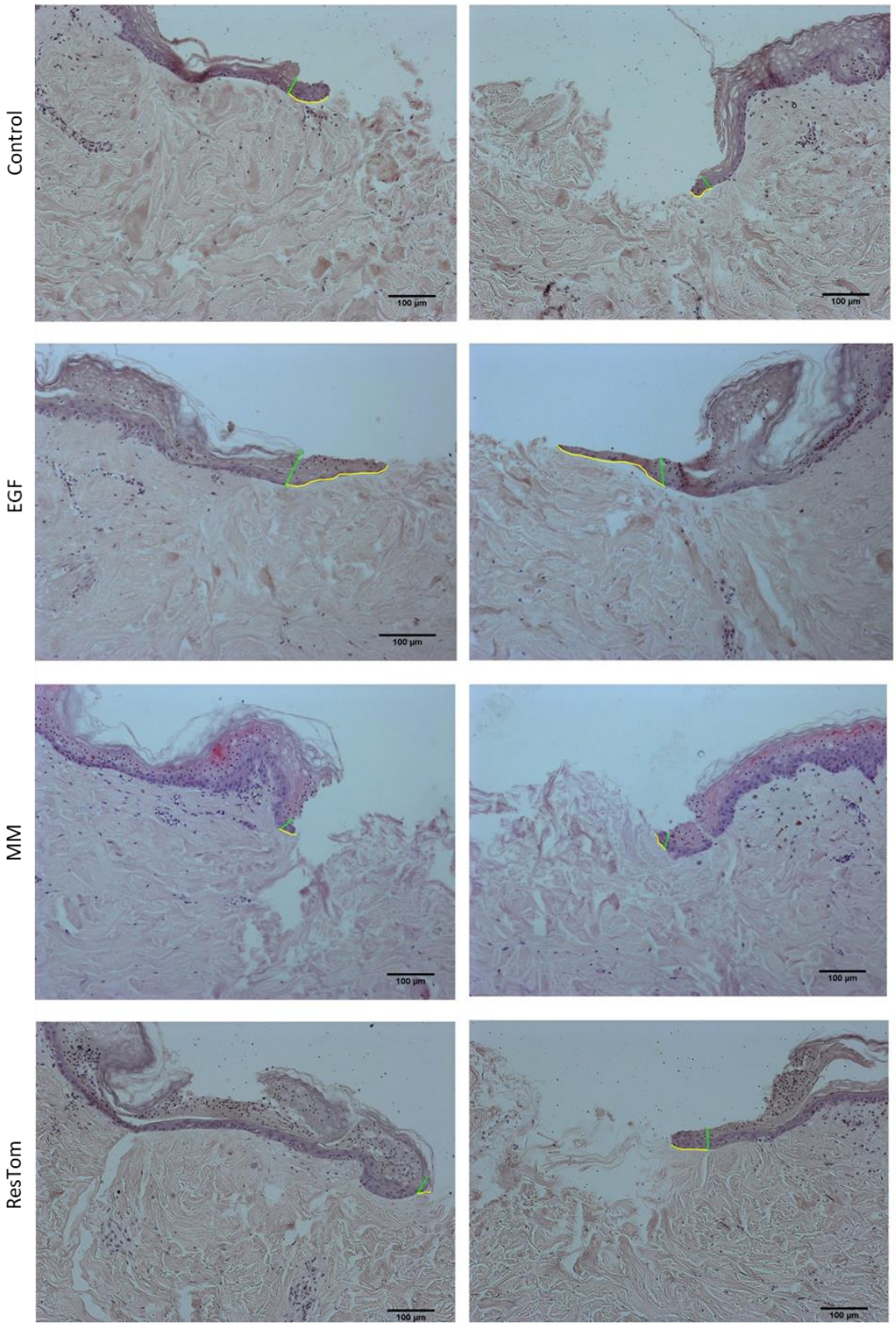
Control
EGF
MM
ResTom
100 µm

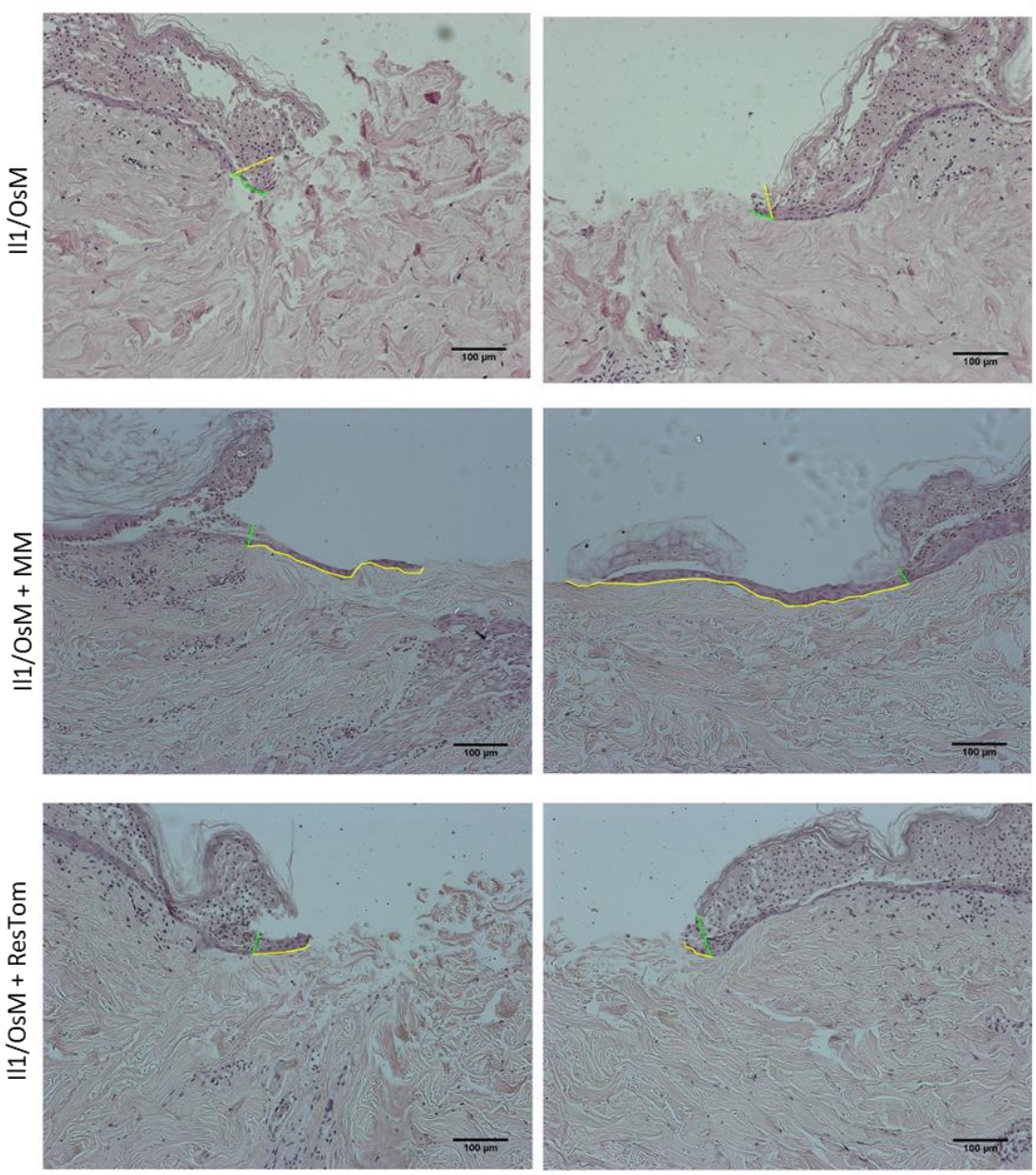

Figure 6.7 Analysis of SPL014 ex vivo skin wounds.

10µm sections were fixed and stained with haematoxylin for comparison of normal wound healing to EGF treatment, tomato juice extracts and healing in an inflammatory environment (IL1/OSM. 11 days post-wounding. Scale bar= 100µm

A

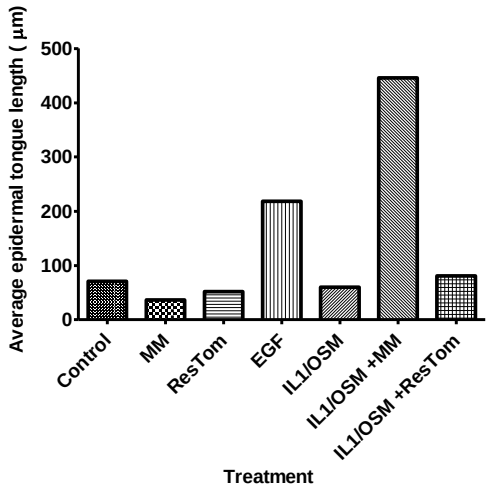

B

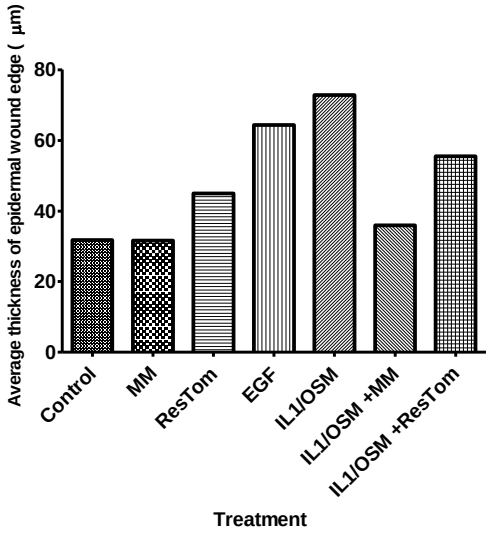

C

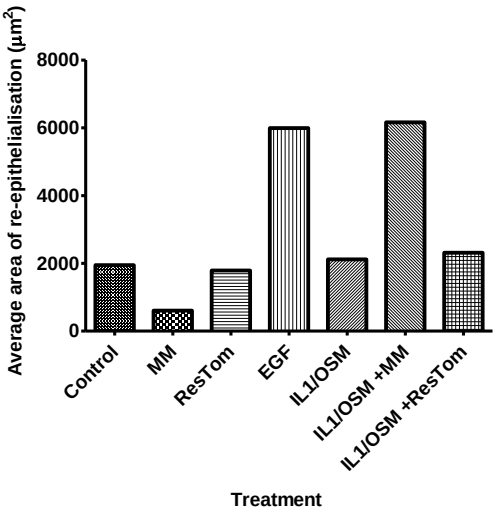

Figure 6.8 Average wound healing of SPL014

A) Epidermal tongue length, B) wound edge thickness, and C) area of reepithelialisation were analysed using Image J software. Each bar represents average wound measurements for each treatment.

A

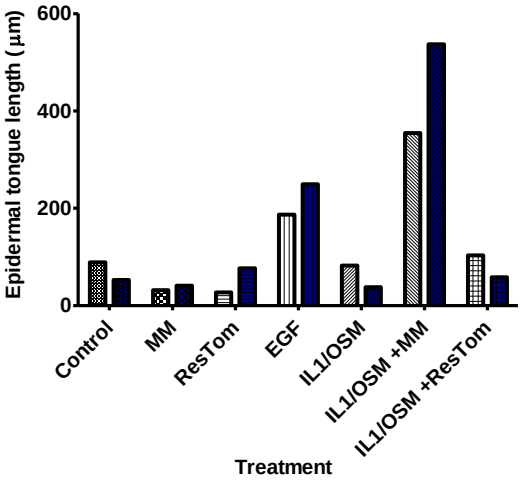

B

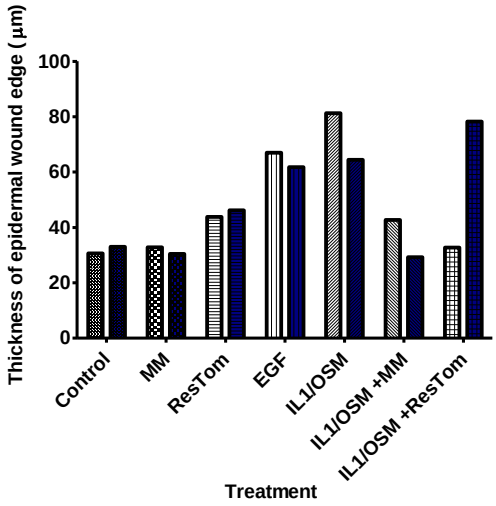

C

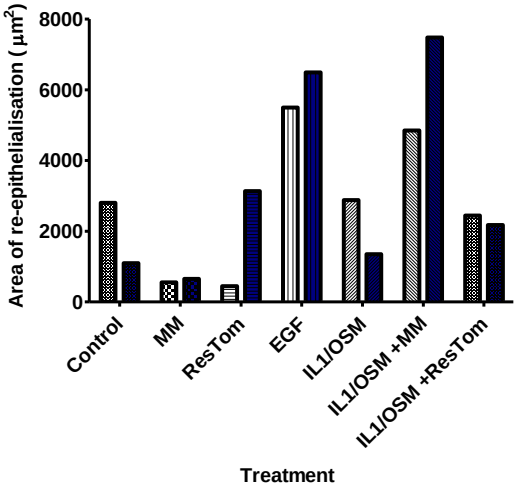

Figure 6.9 SPL014 wound analysis

A) Epidermal tongue length, B) wound edge thickness, and C) area of re-epithelialisation were analysed using Image J software. The two bars for each treatment represent measurements taken from the left and right side of the wound as depicted in Figure 6.7.

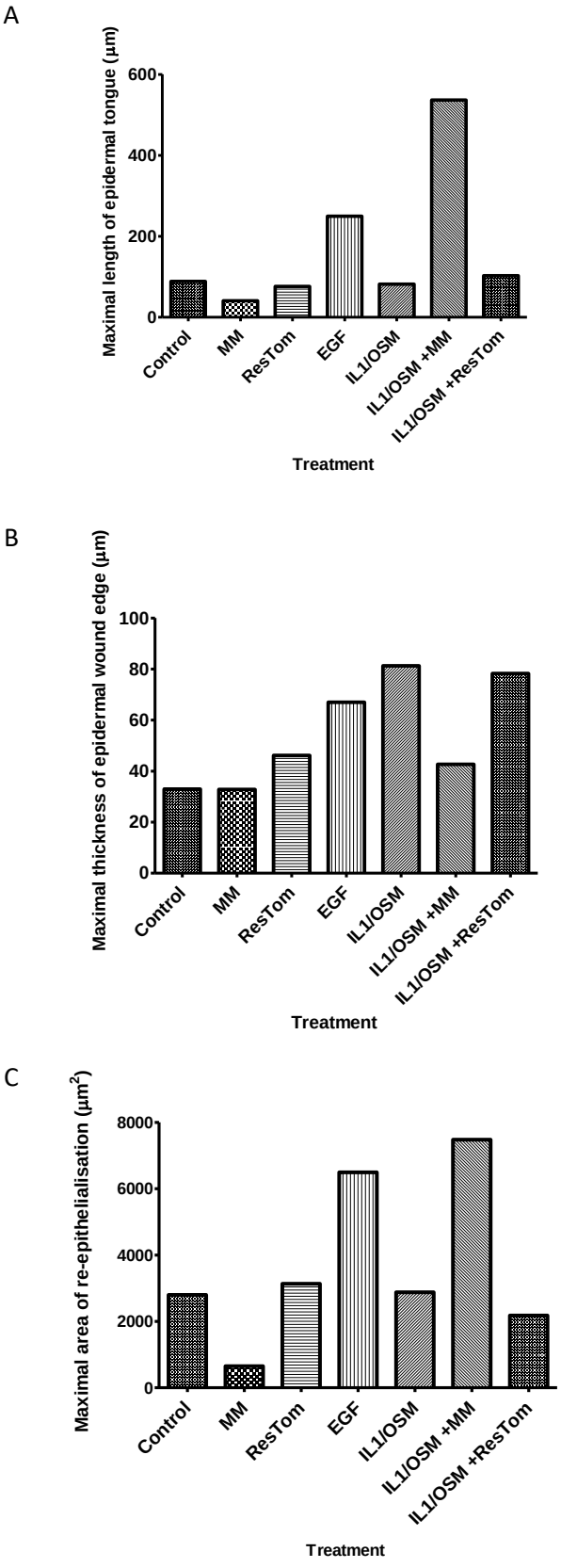

Figure 6.10 Maximal wound healing of SPL014

A) Epidermal tongue length, B) wound edge thickness, and C) area of reepithelialisation were analysed using Image J software. Each bar represents the maximal value measured for each wound.

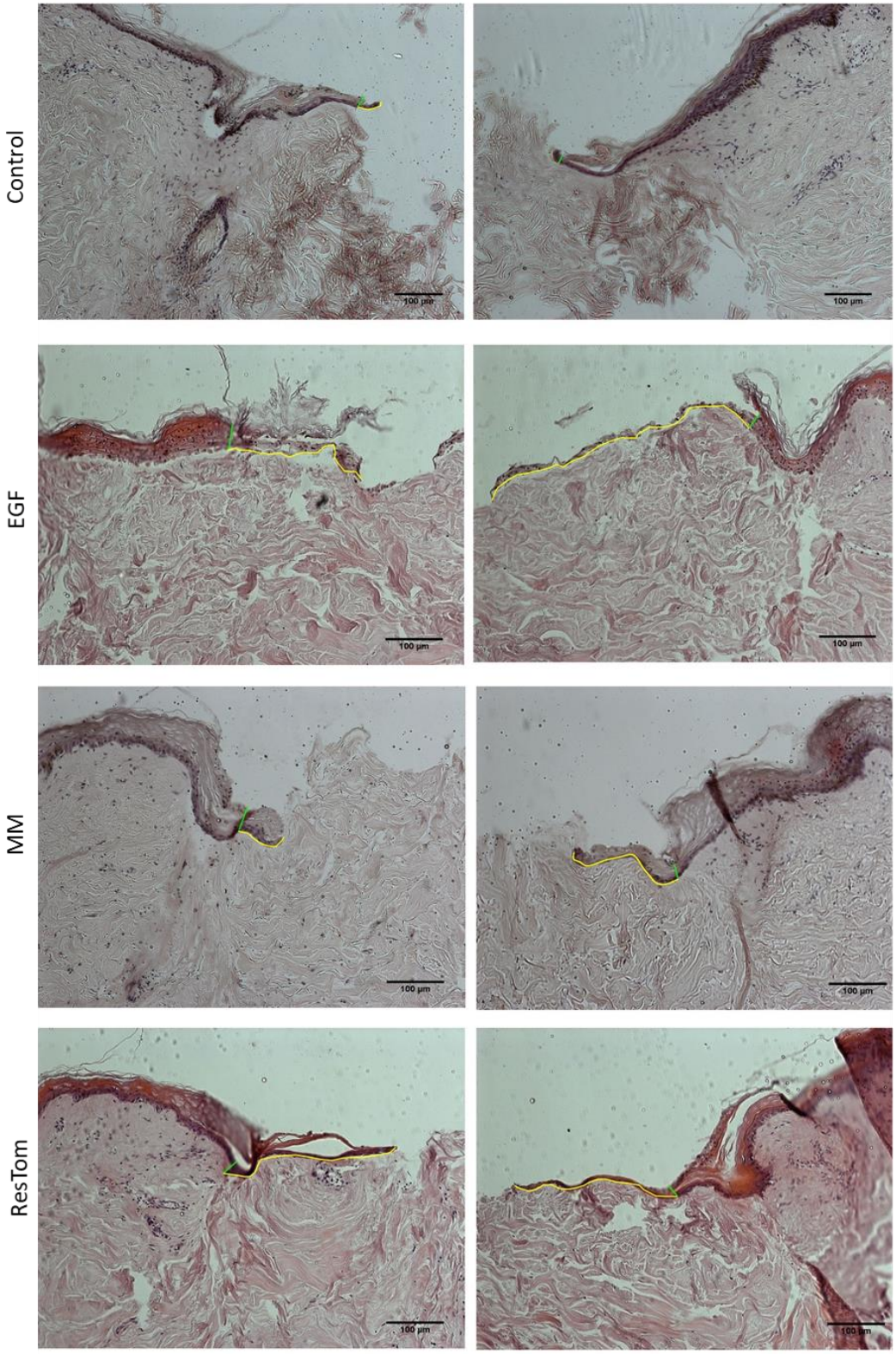
Control
EGF
MM
ResTom
100 µm

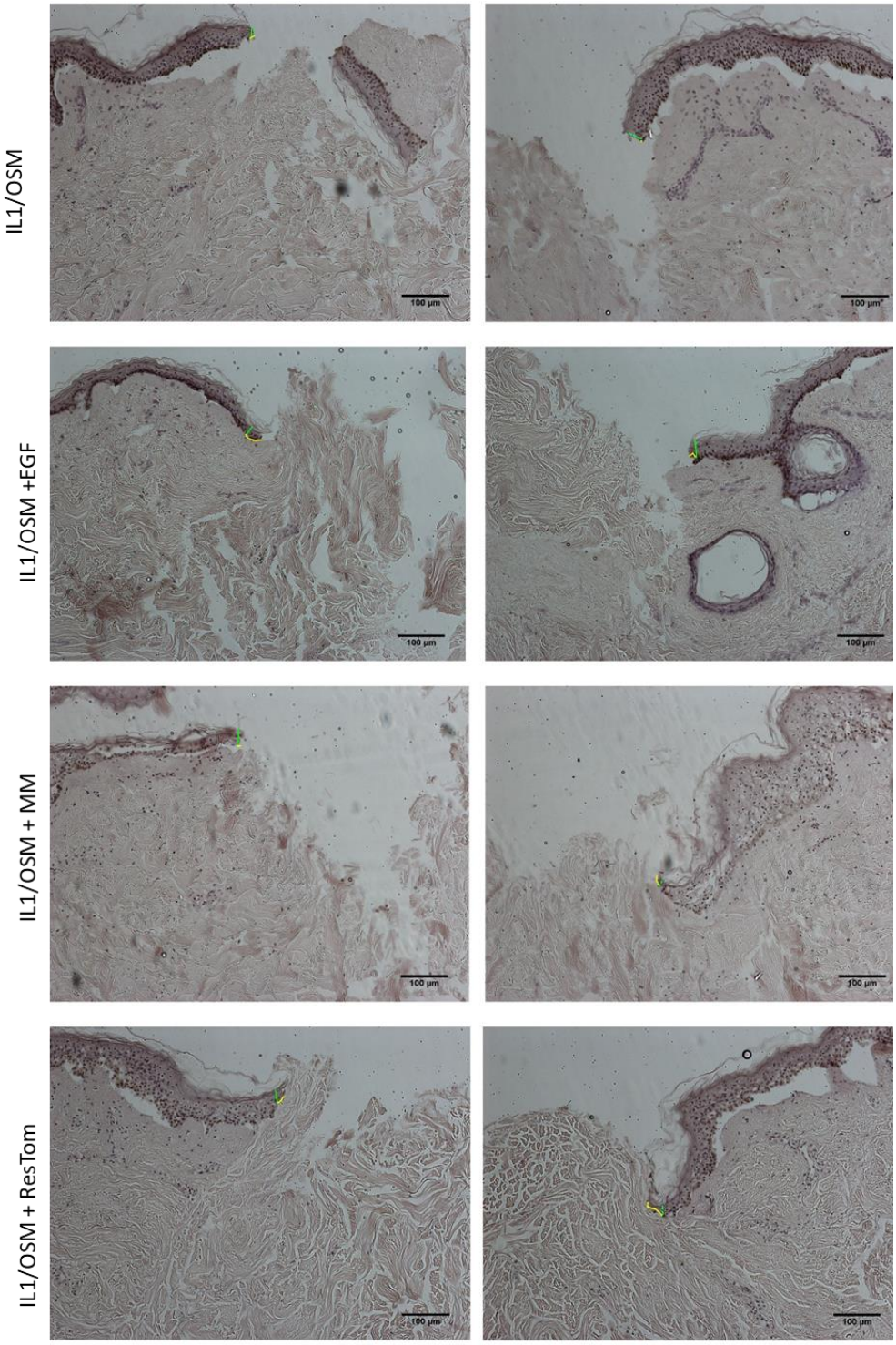

Figure 6.11 Representative analysis of SPL016 ex vivo skin wounds.

10µm sections were fixed and stained with haematoxylin for comparison of normal wound healing to EGF treatment, tomato juice extracts and healing in an inflammatory environment (IL1/OSM 11 days post-wounding). Each treatment was performed in duplicate, example images from 1 of the two explants are shown above. Scale bar = 100µm

A

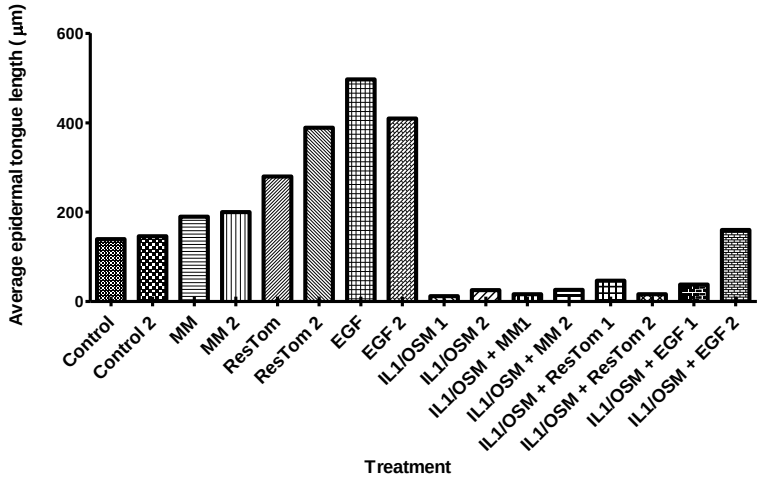

B

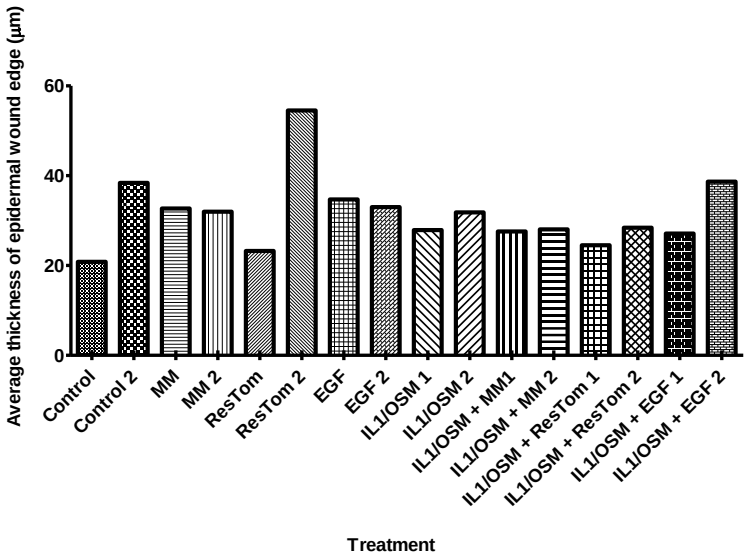

C

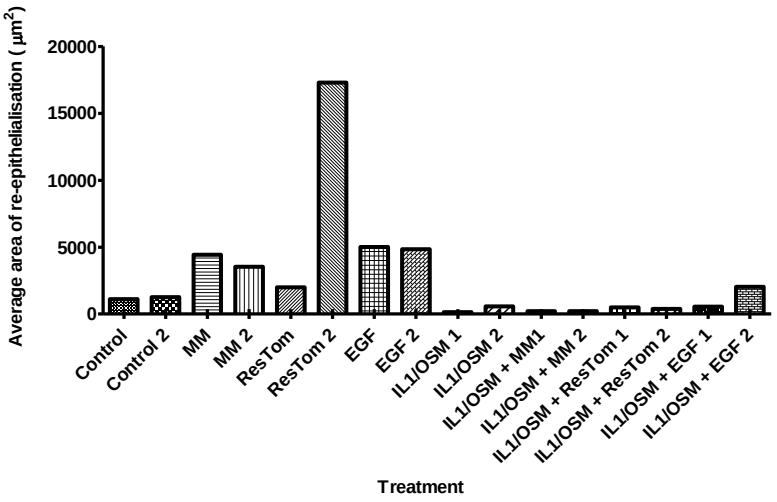

Figure 6.12 Average wound healing of SPL016.

A) Epidermal tongue length, B) wound edge thickness, and C) area of reepithelialisation were analysed using Image J software. Each bar represents average left and right wound measurements for each treatment.

A

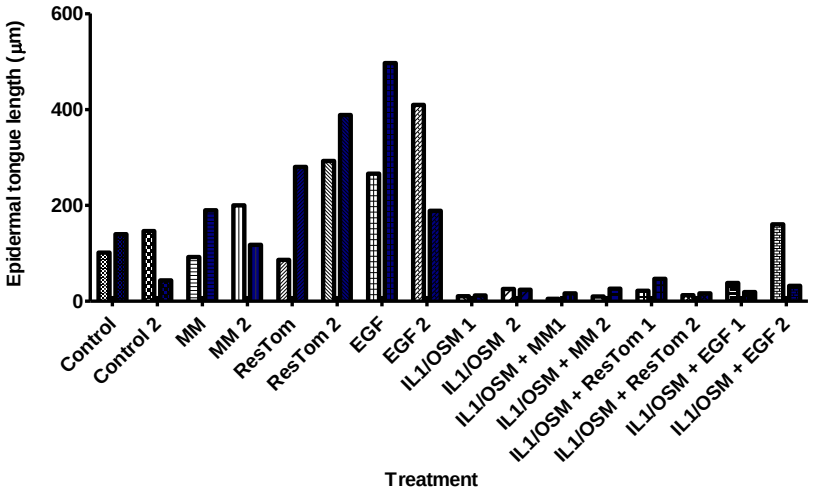

B

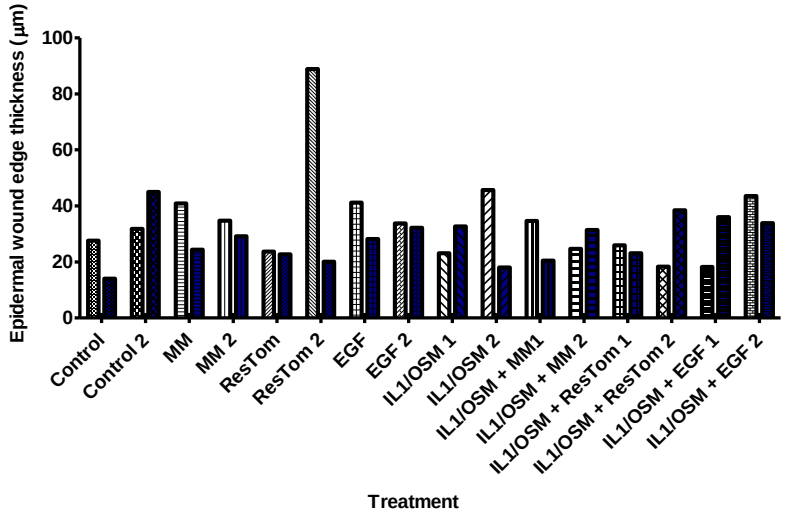

C

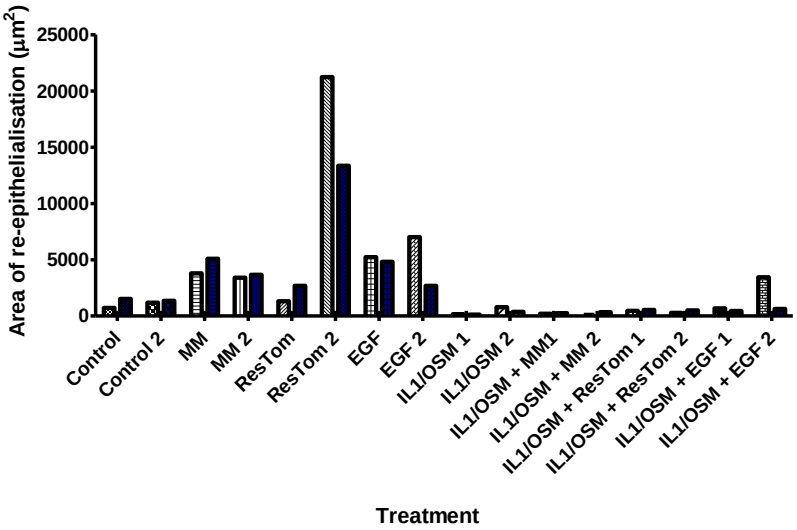

Figure 6.13 SPL016 wound analysis.

A) Epidermal tongue length, B) wound edge thickness, C) area of reepithelialisation were analysed using Image J software. The two bars for each treatment represent the left and right side of the wound.

A

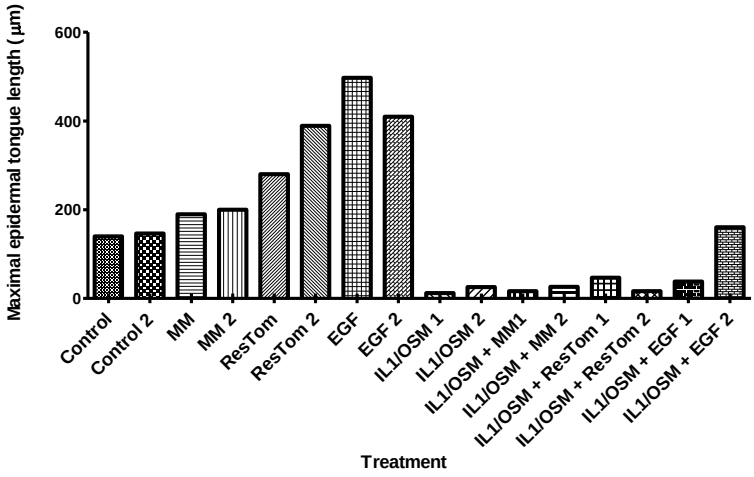

B

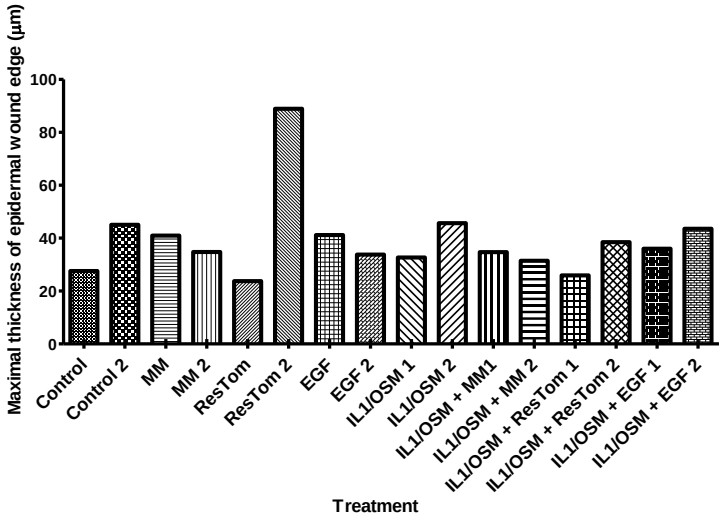

C

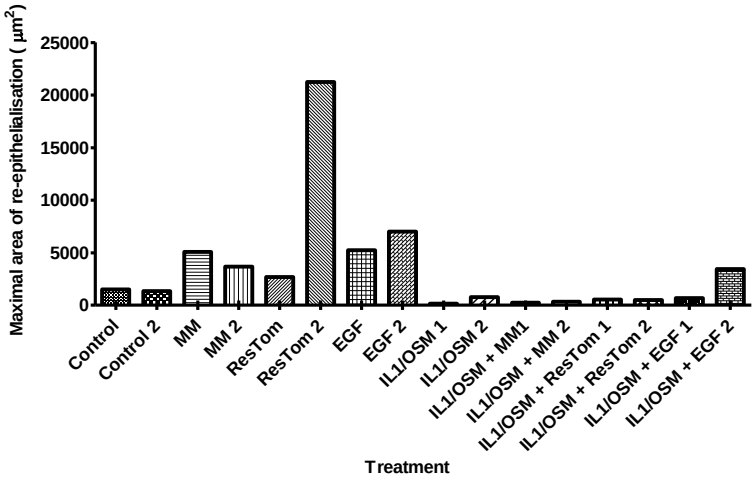

Figure 6.14 Maximal wound healing of SPL016

A) Epidermal tongue length, B) wound edge thickness, and C) area of reepithelialisation were analysed using Image J software. Each bar represents the maximal value measured for each wound.

Table 6:2 Summary of treatments tested across the different wounding-models

Treatments tested	Model		
	Skin	**Keratinocytes**	**Fibroblasts**
Tomato extract	MM ResTom	MM ResTom	No
Methanol extract	No	MM (0.5%) Hi-Resv (0.5%) PteroTom (0.5%)	MM (0.1-1%) Hi-Resv (0.1-1%) PteroTom (0.1-1%
Purified polyphenols	No	Resveratrol (5-50 µM) Polydatin (5-50 µM)	No
EGF	Yes (5ng/ml)	Yes (5ng/ml)	No
Cytokines	Yes	No	No

6.4.3 Purified resveratrol inhibits wound closure of keratinocytes at high concentration whereas polydatin promotes wound closure.

Whilst re-epithelialisation of skin explant wounds is mediated by keratinocytes, it was also possible that underlying dermal fibroblasts may play a role. In order to begin to explore keratinocyte and fibroblast roles in the wound healing response, the effects of purified polyphenols and tomato extracts were investigated using individual cell lines.

LCMS IT-TOF analysis determined that whilst both ResTom and PteroTom juice contains high levels of resveratrol, polydatin, the glycosylated form of resveratrol, is the predominant form in extracts. Therefore, we investigated whether there was a difference in biological efficacy between resveratrol and polydatin.

Using the stilbene content of the tomato extracts as a guide (chapter 4, 4.4), I used levels of resveratrol and polydatin *in vitro* experiments at 50 µM, the equivalent of resveratrol concentration found in a 1:10 dilution of tomato extract.

An initial experiment looking at the effect of resveratrol on HaCaT keratinocyte wound healing (Figure 6.15), showed an inhibitory effect of resveratrol on overall wound closure by 24 hours. In this experiment control untreated cells had closed the wound completely, such that cells treated with EGF, a positive regulator of wound healing did not show any increase in wound closure (Figure 6.16). Resveratrol caused a decrease in overall wound closure compared to untreated cells. Additionally, a decrease in wound closure was seen in cells treated with EGF + Resveratrol compared to EGF alone, suggesting that resveratrol may be able to inhibit the EGF response in cells (Figure 6.16), although, this decrease was not significant. From this experiment, it was evident that resveratrol is able to inhibit wound closure at a concentration of 50µM.

The above experiment was only performed only over a 24-hour period, and as such, I was unable to see if the resveratrol treatment led to a delayed healing response or prevented full wound closure.

Reports on resveratrol treatment from other cell lines showed higher biological effect at lower dosages (Bai et al., 2017). Therefore, the dose response of keratinocytes to different concentrations of resveratrol were investigated. Additionally, comparison to polydatin was made, in order to observe how glycosylation effects biological activity of resveratrol.

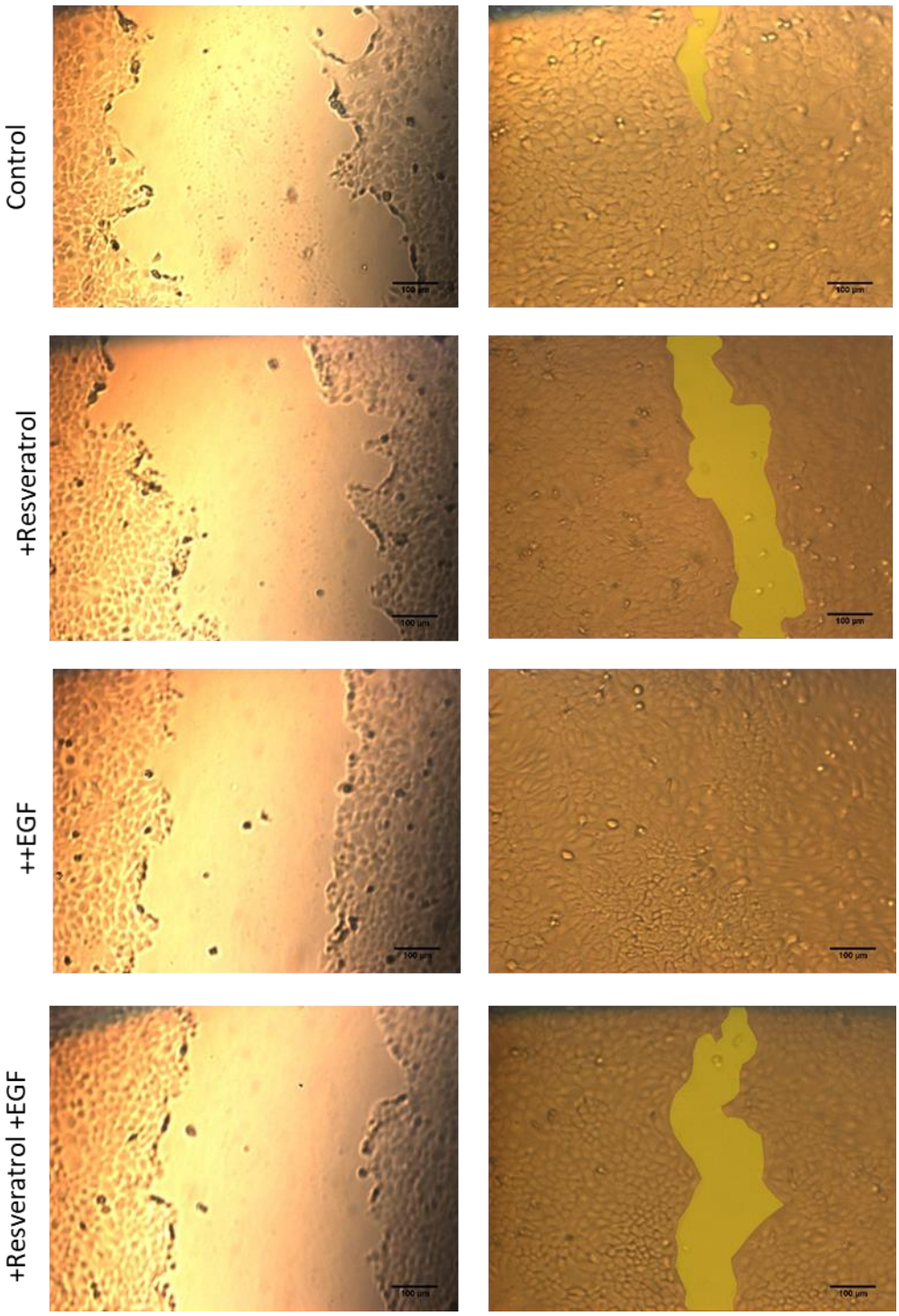

Figure 6.15 : Keratinocyte scratch assay.

Phase contrast images representative of keratinocyte scratch wounds at T-0 and T-24 after treatment in control culture media (DMEM +2% FCS), in addition to EGF (5ng/ml), Resveratrol (50 µM) or Resveratrol +EGF. Percentage wound closure was calculated by comparison of wound area at T-0 to T-24. Total wound analysis was performed using Image J, wound area is highlighted. Scale bar= 100 µm.

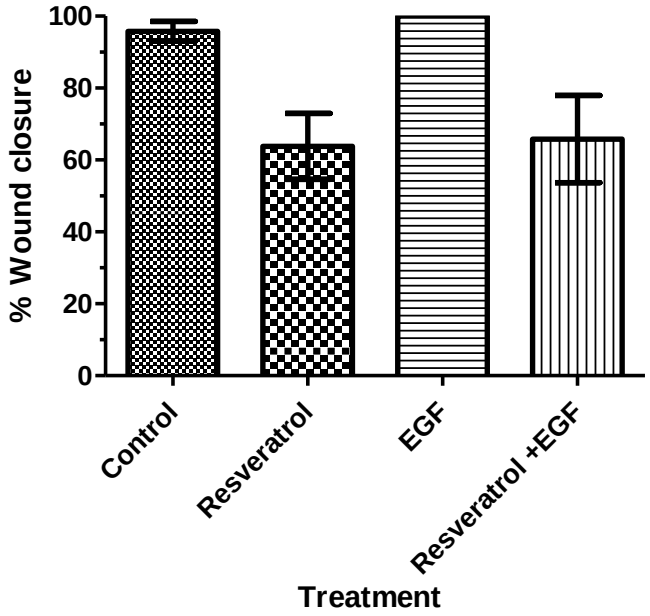

Figure 6.16 Resveratrol inhibits wound closure of keratinocytes.

Percentage wound closure for the experiment depicted in Figure 6.15, over 24 hours was calculated for each treatment using image J. Each bar represents the mean wound healing in 3 scratches +/- SEM. Statistical difference was determined using one-way ANOVA with the Bonferroni multiple comparison test, *p≤ 0.05 **p≤ 0.01. ***p ≤ 0.001, ****p≤0.0001.

The effects of resveratrol and polydatin were investigated over a concentration range of 5µM to 50 µM (Figure 6.17 and Figure 6.18). In this experiment complete wound closure by control cells was not observed, with control cells only closing the wound by only 25% at 24h and 50% at 48h. It was unclear as to why control cells exhibited low wound closure in this experiment. This may have been a result of the passage number at which these cells were used, or biological variation. Despite this, several clear differences were able to be seen between resveratrol and polydatin treated cells.

Up to a concentration of 20 µM resveratrol displayed a beneficial effect on wound closure, with significant increases in overall wound closure observed at 48 hours compared to control (Figure 6.18), although at a concentration of 50 µM resveratrol treatment appeared to show an inhibitory effect on wound closure. This suggested that resveratrol could potentially have two effects on wound closure depending on the concentration at which it is applied at; it could have either a wound healing, or a wound inhibiting effect.

Whereas resveratrol appears to have these two effects on wound healing based on its concentrations, polydatin promoted wound closure, only. The wound healing promoting effect of polydatin appeared to be dose dependent, with an increase in wound closure observed with increasing dosages of polydatin. This however, was not the case for a 20 µM concentration, which led to less wound healing than 10 µM (Figure 6.19 and Figure 6.20). While a concentration of 50 µM resveratrol appeared to have an inhibitory effect on wound closure (Figure 6.18), polydatin at the same concentration promoted wound closure (Figure 6.20).

From these experiments, purified resveratrol and polydatin were shown to affect the regulation of wound healing and to demonstrate the effects that chemical modifications have on the biological activity of resveratrol. However, these results showed the effects of these compounds only in isolation. The tomato extracts from ResTom and PteroTom have a complex matrix composed of different concentrations of many polyphenolic compounds which may work synergistically with each other. Therefore, I wanted to investigate how the addition of compounds such as resveratrol and polydatin translate when within the complex tomato extract background. In addition, PteroTom contains high levels of a methylated derivative of resveratrol, pterostilbene, which has been suggested to have increased biological activity compared to resveratrol, and therefore it would be interesting to see if this leads to a similar inhibitory effect on wound healing as resveratrol shows *in vitro*.

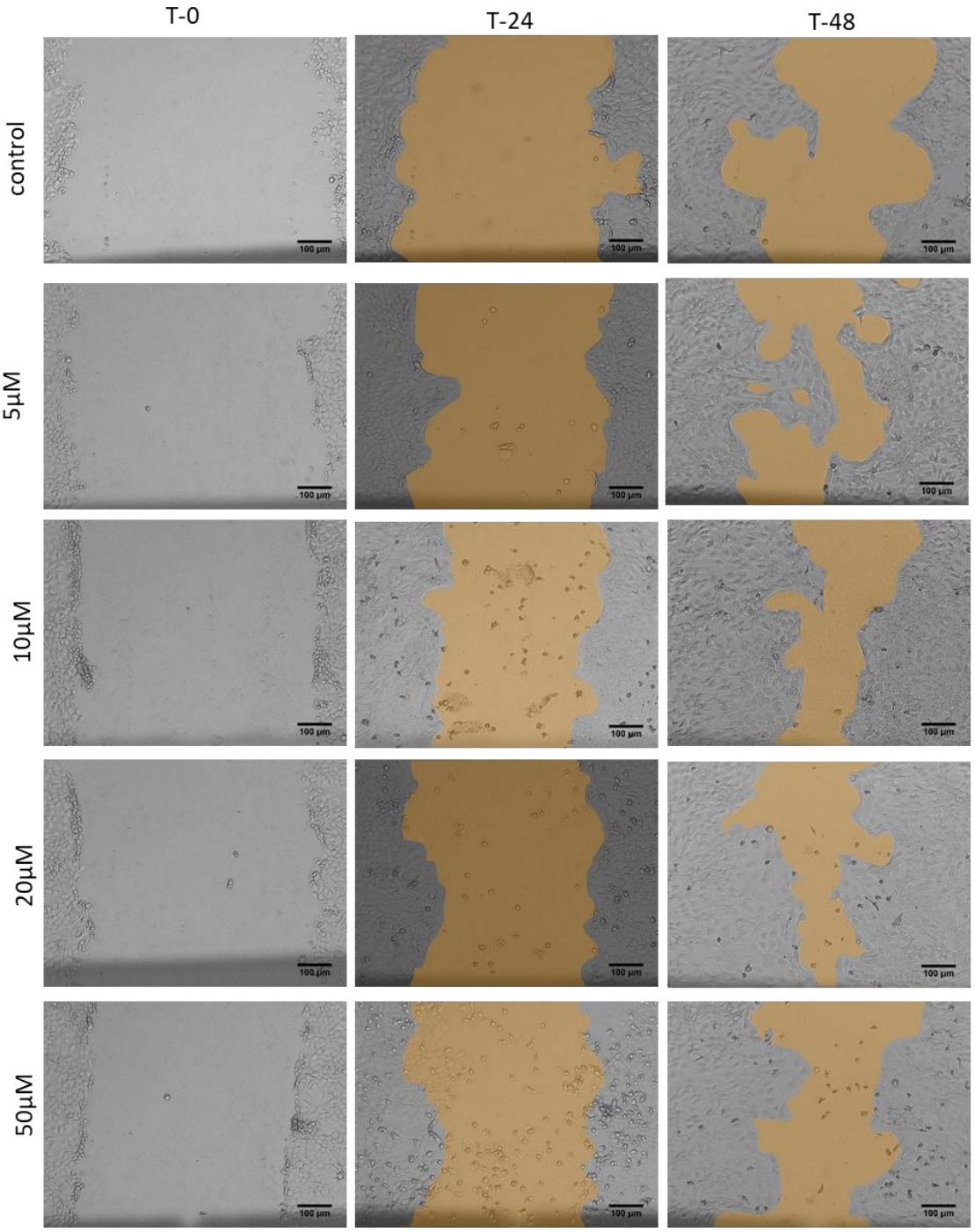

Figure 6.17 Wound closure of keratinocytes in response to increasing concentrations of Resveratrol.

Phase contrast images representative of keratinocyte scratch wounds at T-0, T-24 and T-48 after treatment in control culture media (DMEM +2% FCS), in addition resveratrol from 10-50 µM. Total wound analysis was performed using Image J, wound area is highlighted. Scale bar= 100 µm.

A

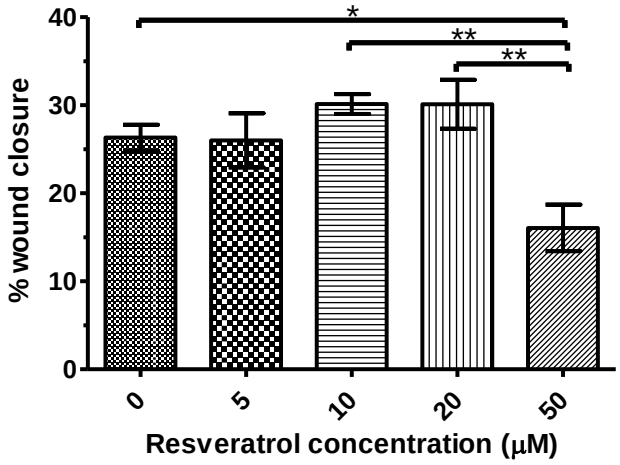

B

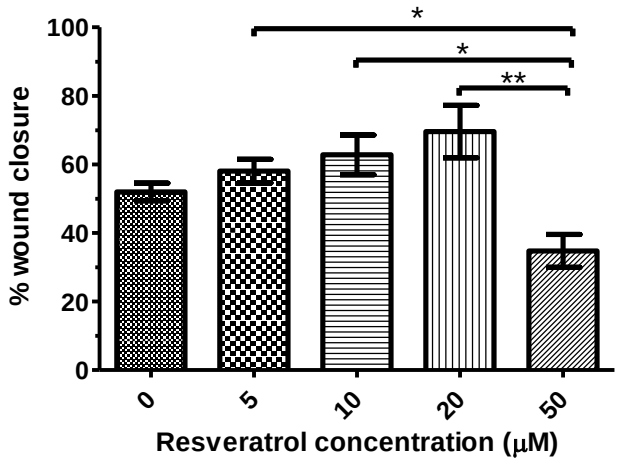

Figure 6.18 Resveratrol has a dose response effect on wound closure of keratinocytes.

Percentage wound closure over 24 (A), and 48 hours (B) was calculated for the experiment depicted in Figure 6.17, using Image J. Each bar represents the mean wound closure in 3 wells of cells ±SEM. Percentage wound closure was calculated by comparison of wound area at T-0 to T-24, and T-48. Statistical difference was determined using one-way ANOVA with Tukeys multiple comparison test, *P≤ 0.05, **P≤ 0.01, ***P≤ 0.001, ****P ≤0.0001.

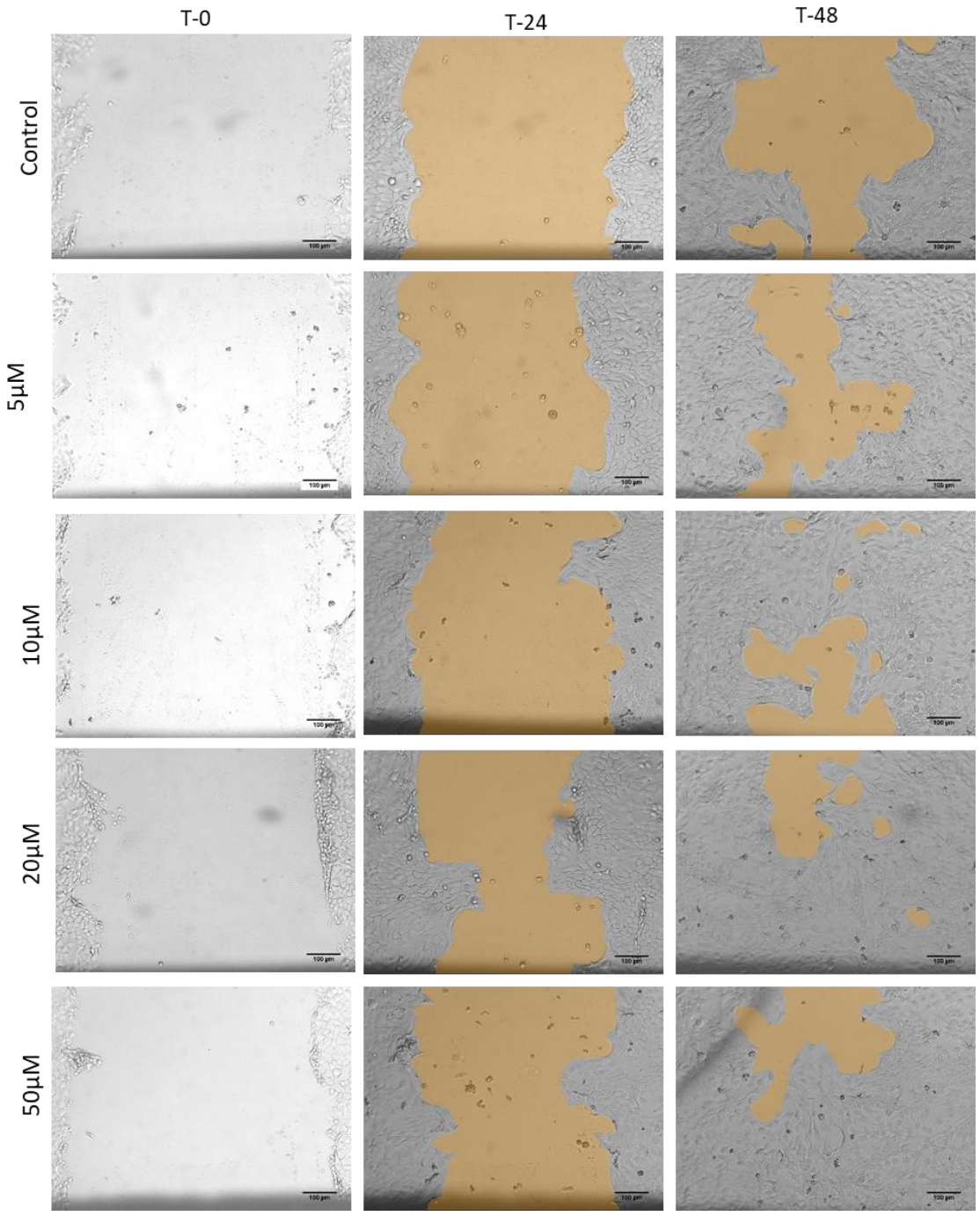

Figure 6.19 Wound closure of keratinocytes in response to increasing concentrations of Polydatin.

Phase contrast images representative of keratinocyte scratch wounds at T-0, T-24 and T-48 after treatment in control culture media (DMEM +2% FCS), in addition polydatin from 10-50 µM. Scale bar= 100 µm. Total wound analysis was performed using Image J, wound area is highlighted.

A

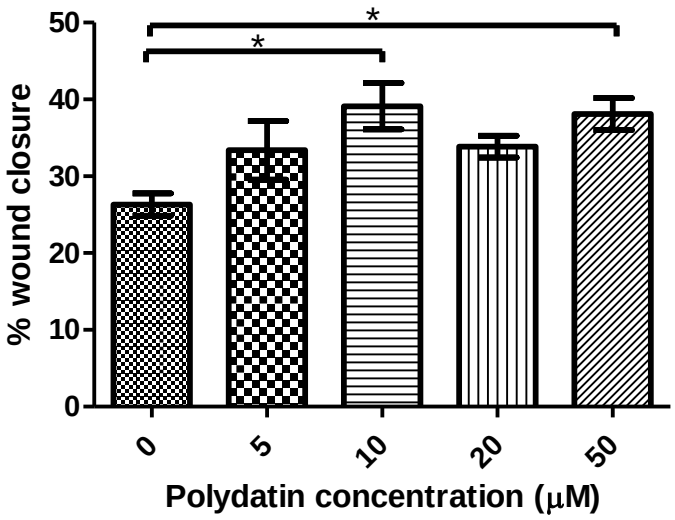

B

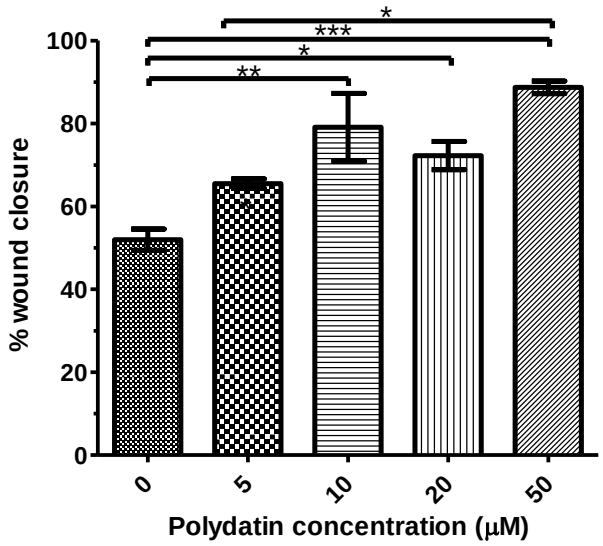

Figure 6.20 Polydatin promotes scratch wound closure of keratinocytes in a dose dependent manner.

Percentage wound closure over 24 (A), and 48 hours (B) was calculated for the experiment depicted in Figure 6.19, using Image J. Each bar represents the mean wound closure in 3 scratches ± SEM. Percentage wound closure was calculated by comparison of wound area at T-0 to T-24, and T-48. Statistical difference was determined using one-way ANOVA with Tukeys multiple comparison test, *p≤ 0.05 **p≤ 0.01. ***p ≤ 0.001, ****p≤0.0001.

6.4.4 Methanol tomato extracts

LCMS IT-TOF analysis (tomato chapter) identified that pterostilbene was not present within aqueous PteroTom extracts due its poor solubility in water. Therefore, since I wanted to compare the biological activity of the ResTom extract with the PteroTom extract, I prepared methanol-based extracts. Since pterostilbene is highly soluble in methanol, these extracts would enable me to observe any effects of the presence of pterostilbenes and derivatives in the complex background of the tomato. However, the use of methanol extracts was not ideal, as methanol can be highly toxic to cells, and could potentially mask any affects due to the tomato compounds through its toxicity. Therefore, it was important to include methanol controls in all experiments at the same concentration as that found in the highest methanolic tomato extract being tested.

6.4.5 Methanol tomato extracts inhibit wound healing of HaCaTs

The effects of MoneyMaker (control), Hi-Resv (resveratrol containing) and PteroTom (Pterostilbene containing) methanol extracts on wound healing of HaCaTs was investigated over 24 hours (Figure 6.21). Methanol tomato extracts were added to a final concentration of 0.5%. This extract concentration was chosen from previous work completed by Dr Katharina Bulling, which showed high levels of toxicity in the two breast cancer cell lines MCF-7 and MDA-MB-231 when treated with ResTom extracts higher than 0.5% (Bulling and Martin, personal communication).

In this experiment, methanol extracts were made from the two tomato lines Hi-Resv and PteroTom. The high resveratrol tomato line is the new resveratrol producing tomato line, using the E8 promoter to drive StSy expression, and produces less resveratrol and polydatin than the original ResTom tomatoes where StSy was driven by the CaMV 35S promoter (chapter 4, 4.4). However, since the PteroTom tomato is based upon the same construct as the High-Resv tomato, it makes for a good comparison between the biological effectiveness of these two tomato lines.

Crucially, this experiment showed that addition of methanol to cells, at the same concentration of that in tomato methanolic extracts, did not cause toxicity within cells, or any difference in overall wound healing compared to controls (Figure 6.22). This meant that any observable changes in wound healing could be attributed to the action of the tomato extracts.

This experiment displayed very little wound closure overall by 24 hours (Figure 6.22), especially compared to previous experiments conducted with HaCaTs (Figure 6.15, Figure 6.17, Figure 6.19). This may be due to biological variation between the cells, or the passage number at which the cells were used for the wound experiment. There was a large accumulation of cell debris associated with these cells by 24 hours which suggested that the health of the keratinocytes was sub-optimal and might account for the poor healing observed in this experiment.

Whilst overall wound closure rates were very low in this experiment (approx. 2% for control, untreated cells and approx. 5% for EGF treated cells) wild type tomato (MM), and Hi-Resv extract both caused a slight reduction in overall wound closure compared to control (Figure 6.22). This slight inhibitory effect on wound closure by MM extract was interesting, as it suggested that the compounds found within normal tomato juice themselves influence wound healing.

Interestingly, PteroTom extract increased inhibition of wound closure compared to both MM and Hi-Resv extracts, and in fact, wounds were observed to increase slightly in size with PteroTom treatment. This observation was apparent only with the PteroTom treatment, suggesting that this effect was due to a compound specific to this tomato juice extract, and there may also be a slight toxicity to cells associated with PteroTom extract.

When EGF was applied in addition to MM juice, wound healing increased to a greater level than that observed with only EGF. However, EGF in the presence of Hi-Resv or PteroTom extracts exhibited reduced wound healing compared to EGF treatment alone, with PteroTom inhibiting wound closure to a greater degree than Hi-Resv (Figure 6.8) This may suggest that these two tomato extracts are able to inhibit the action of EGF, and as this was not observed with the addition of MM, it was likely to be an effect of one of the stilbenes synthesised in these tomatoes. In addition, it suggested that PteroTom extract may have a higher biological activity than Hi-Resv extract.

However, it is important to note that over a 24-hour period these HaCaTs did not show high levels of healing even with EGF treatment. Unfortunately, data from this experiment was not able to be collected at 48 hours, due to high levels of cell debris in the media by 24 hours which required removal before photographing. At a later time point a better difference in wound closure between the treatments might have been observed. At these low levels of healing, it is hard to confirm the effects of these extracts and as such, this experiment needs to be repeated over a 48-hour time period. Despite this, these data are suggestive that both Hi-Resv and PteroTom extracts inhibit migration of HaCaTs, with PteroTom exhibiting a greater inhibitory effect.

Unfortunately, due to a long-term tissue culture facility problem with bacterial contamination, further scratch assays with HaCaTs were not able to be performed. However, we were able to investigate further wound healing via the mouse fibroblast line 3T3 using neighbouring tissue culture facilities (see section 6.4.10).

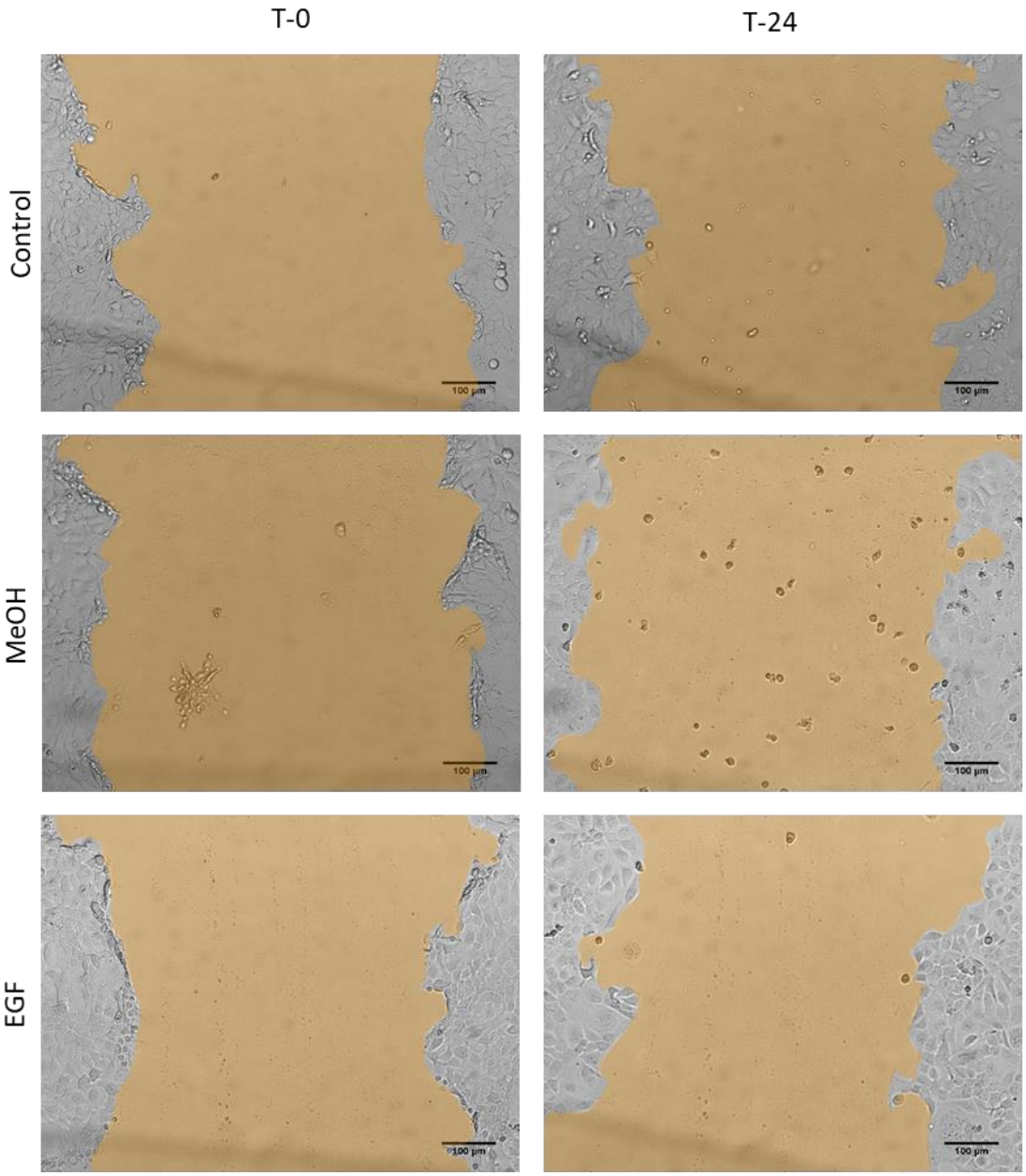
T-0
T-24
Control
MeOH
EGF
100 µm

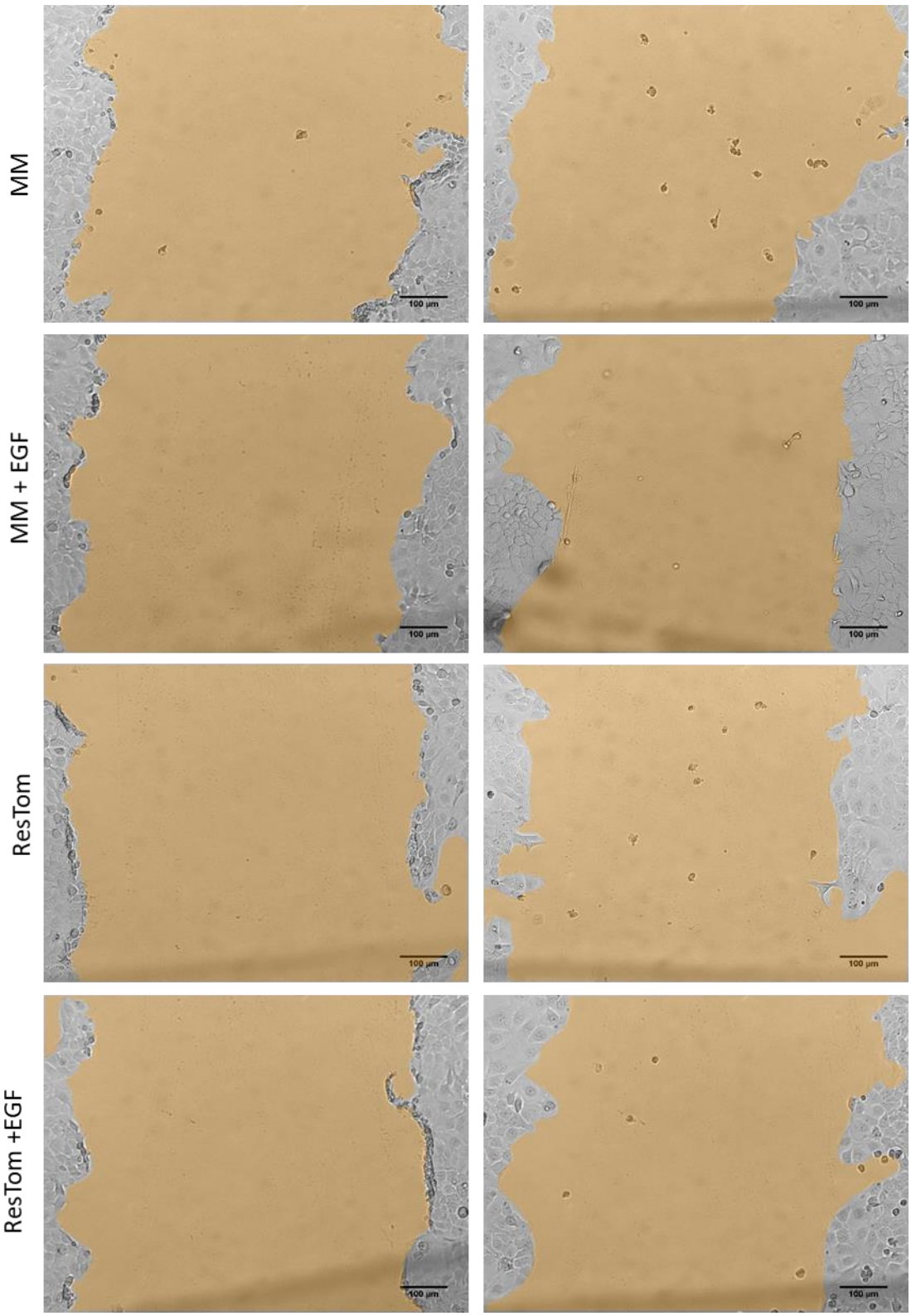
MM
MM + EGF
ResTom
ResTom +EGF
100 µm

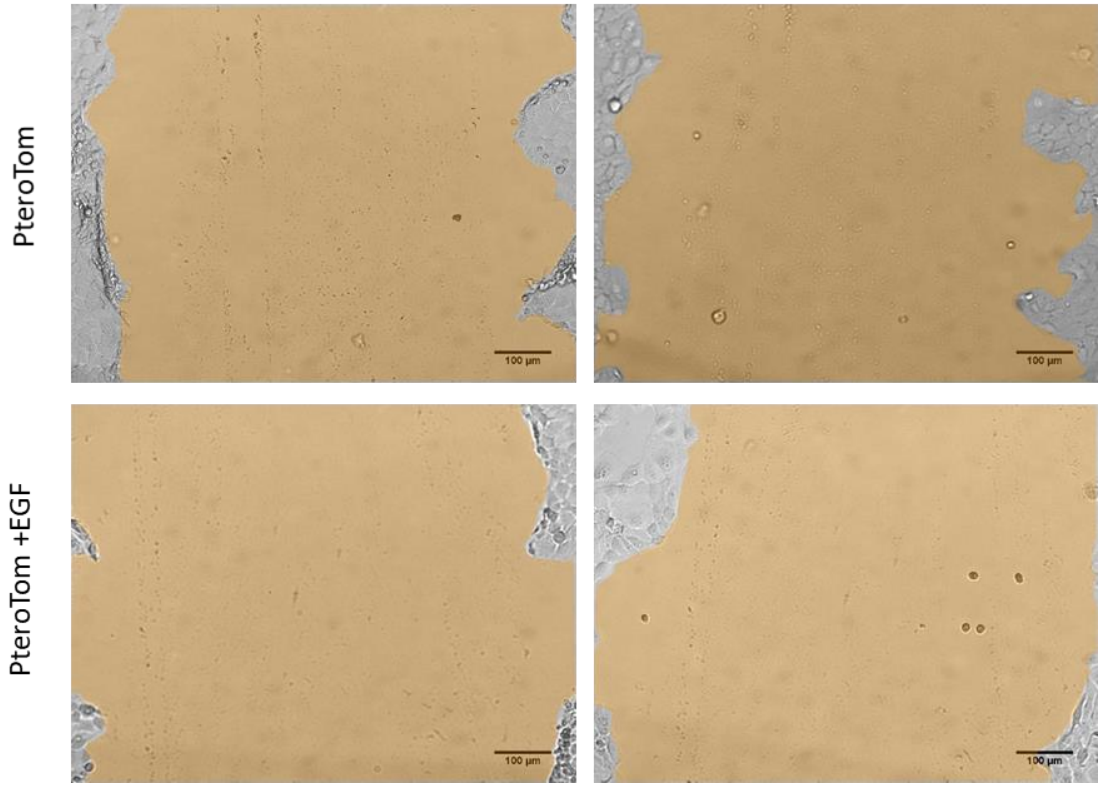

Figure 6.21 Wound closure of keratinocytes in response to methanolic tomato extracts.

Phase contrast images representative of keratinocyte scratch wounds at T-0 ,and T--24 treatment in culture media (DMEM +2% FCS) with EGF (5ng/ml), MeOH (50% MeOH at 0.5% v/v), MM (0.5% v/v), MM (0.5% v/v) + 5ng/ml EGF, Hi-Resv (0.5% v/v), Hi-Resv (0.5% v/v) + EGF (5ng/ml), PteroTom (0.5% v/v), PteroTom (0.5% v/v) + EGF (5ng/ml). All methanol tomato extracts were prepared in 50% MeOH.

Total wound analysis was performed using Image J, wound area is highlighted. Scale bar= 100 µm.

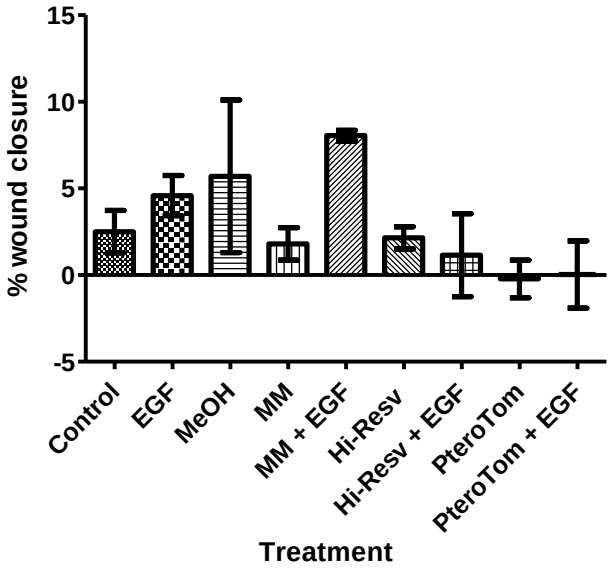

Figure 6.22 Wound healing analysis of keratinocytes in response to methanol tomato extracts.

Percentage wound closure over 24 (A), was calculated for the experiment depicted in Figure 6.21, using Image J. Percentage wound closure was calculated by comparison of wound area at T-0 to T-24. Each bar represents the mean wound closure in 3 scratches ± SEM. Statistical difference was determined using one-way ANOVA with the Bonferroni multiple comparison test, *p≤ 0.05 **p≤ 0.01. ***p ≤ 0.001, ****p≤0.0001.

6.4.6 Methanol tomato extracts inhibit MMP-1 activity and can supress MMP-1 induction by EGF in keratinocytes

Matrix metalloproteinases function in re-epithelialisation and wound repair. In injured human skin, MMP-1 expression is induced, which is crucial for the migration of keratinocytes. Due to the inhibition of wound healing and migration of keratinocytes by Hi-Resv and PteroTom extracts (Figure 6.22), expression of MMP-1 was investigated (Figure 6.23).

There was no significant difference in expression levels of MMP-1 between control, and methanol treated keratinocytes, which means that any associated change in MMP-1 activity could be attributed to the treatment with methanolic extracts of tomato.

Treatment of keratinocytes with EGF led to significant upregulation of MMP-1 (Figure 6.23), which correlates to the slight increase in wound closure observed with this treatment (Figure 6.22). Neither Hi-Resv or PteroTom showed differences in MMP-1 expression compared to control.

Interestingly, there was a trend towards reduced steady state mRNA levels of MMP-1 when cells were co-treated with EGF and either MM, Hi-Resv or PteroTom compared to EGF alone. The inhibition of MMP-1 by Hi-Resv and EGF is not as great as that by PteroTom which could reflect a greater biological activity by PteroTom.

These data suggested that tomato extracts are able to inhibit MMP-1 induction by EGF, which may be linked to the observed decrease in wound closure. The greater inhibitory action of PteroTom on EGF compared to Hi-Resv suggested an increased biological activity of this tomato extract. As MM extract was also able to inhibit EGF mediated MMP-1 induction, this suggested that the other components of the background compounds of the tomato extracts including flavonoids possibly have an inhibitory effect on EGF, and that PteroTom may gain its increased inhibitory power via synergistic effects of its active compounds.

Within a preliminary experiment on non-wounded keratinocytes the different effects of methanol and aqueous extracts on MMP-1 expression levels were investigated (Figure 6.24). Interestingly in this experiment treatment with MeOH slightly increased expression of MMP-1 compared to control cells. The inducing effect of MeOH on MMP-1 expression was reduced with MM and PteroTom methanol extracts, with PteroTom methanol extract decreasing expression of MMP-1 compared to Hi-Resv methanol extract, and methanol alone (Figure 6.24,A).

Contrasting to the MeOH extracts, treatment with aqueous extracts of the Hi-Resv tomato extract statistically increased MMP-1 expression (9-fold) compared to control (Figure 6.24,B). These data showed statistical differences in aqueous extract activity compared to methanol-based extracts.

Although the relative levels of stilbenes were quantified within primary aqueous-extracts, and methanol extracts, the concentration of stilbenes reconstituted into methanol after evaporation was not quantified. The difference in activity between methanol and aqueous extract suggest that after evaporation of methanol, and resuspension, not all compounds which have an effect on MMP-1 expression were resuspended. Therefore, quantitative analysis should be performed on the reconstituted methanol extracts to confirm levels of stilbenes before their use in cell experiments.

A

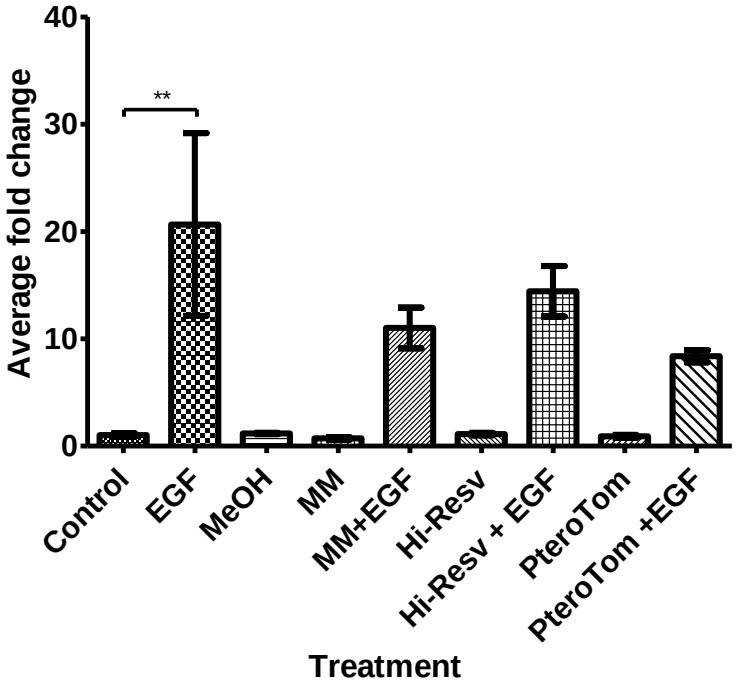

B

Treatment	Average C_T value
Control	30.85
EGF	26.47
MeOH	30.82
MM	31.45
MM +EGF	28.25†
Hi-Resv	31.23
Hi-Resv +EGF	31.23
PteroTom	31.62
PteroTom +EGF	27.17

Figure 6.23 Effect of different methanolic extracts on relative expression of MMP-1 normalised to 18S in keratinocytes 24 hours post-treatment.

qRT-PCR of wounded cell monolayer were performed 24-hours post-stimulation. Data was analysed by relative quantification and normalised to 18S for MMP-1. Corresponding average C_T values are shown (B). Each bar represents the mean fold change of 3 samples ±SEM. Statistical difference was determined using one-way ANOVA with the Bonferroni multiple comparison test *p≤ 0.05 **p≤ 0.01. ***p ≤ 0.001, ****p≤0.0001. † represents data excluded from analysis, as one 18S C_T value varied more than 1.5 C_Ts from the mean.

A

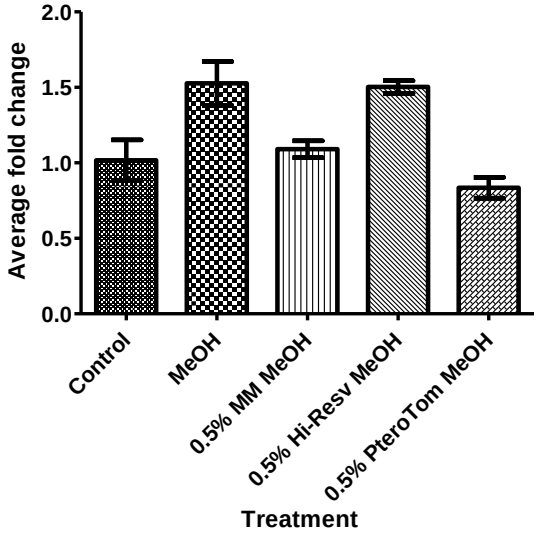

	Average C_T
Control	30.30
MeOH	30.02
0.5% MM MeOH	30.56
0.5% Hi-Resv MeOH	30.36
0.5% PteroTom MeOH	30.68

B

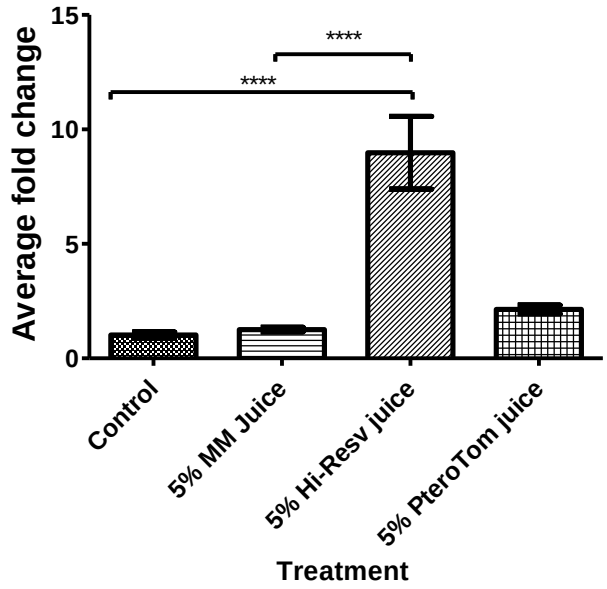

	Average C_T
Control	30.30
5% MM juice	30.16
5% Hi-Resv juice	27.50
5% PteroTom juice	29.28

Figure 6.24 Effect of methanolic vs aqueous extracts on relative expression of MMP-1 normalised to 18S in keratinocytes 24 hours post-treatment.

Data shown is from one experiment, with data separated over two graphs for simplicity, (A) methanol tomato extracts and (B) aqueous tomato extracts. qRT-PCR of cell monolayers were performed 24-hours post-stimulation. Data was analysed by relative quantification and normalised to 18S for MMP-1. Each bar represents the mean fold change of 3 samples ±SEM. Statistical difference was determined using one-way ANOVA with the Bonferroni multiple comparison test, *p≤ 0.05 **p≤ 0.01. ***p ≤ 0.001, ****p≤0.0001. Corresponding average C_T values are shown.

6.4.7 Methanol tomato extracts inhibit induction of MMP-9 by EGF in keratinocytes

Another MMP which is key to the progression of wound healing is MMP-9. MMP-9 degrades type IV collagen and laminin in the basement membrane, allowing cells at the edge of the wound to detach from the basement membrane and migrate across the wound. The expression of MMP-9, like other MMPs is induced during wound repair in response to inflammatory molecules such as cytokines (Li et al., 2007). Tight regulation of MMP-9 expression levels is crucial for wound healing. Although a high initial expression of MMP-9 after wounding is crucial for the progression of wound closure, prolonged high expression of MMP-9 has been associated with chronic wounds. In addition, low levels of MMP-9 expression during the initial response to wound healing has been linked to delayed wound healing (Wall et al., 2002).

HaCaTs showed a significant increase in MMP-9 expression with EGF treatment, as expected (Figure 6.25). Interestingly, although MeOH tomato extracts by themselves did not significantly alter MMP-9 expression, the addition of tomato extract to EGF appeared to inhibit the activation of MMP-9 by EGF. Significantly lower levels of MMP-9 were observed with MM+EGF treatment, with Hi-Resv +EGF showing a further reduction in MMP-9 expression, and PteroTom +EGF showing the greatest reduction in MMP-9 expression. The reduction in MMP-9 expression with methanolic tomato extracts +EGF could, in part, account for the observed reduction in wound closure observed (Figure 6.22).

Comparison of methanol and aqueous tomato extracts showed some differences in MMP-9 expression levels in non-wounded keratinocytes. Within this experiment, addition of MeOH slightly decreased expression of MMP-9 compared to that observed in control cells, however this was not significant. Addition of MM MeOH extract acted to slightly inhibit expression of MMP-9 compared to MeOH alone, whereas both Hi-Resv and PteroTom extracts increased expression of MMP-9. Although expression of MMP-9 was not increased compared to that of control cells, it was compared to MeOH treated cells (Figure 6.26).

An increase in MMP-9 expression compared to control was also observed in cells treated with aqueous extracts. MMP-9 was upregulated to a much higher degree in cells treated with aqueous compared to methanol extracts. It is interesting that methanol extracts of PteroTom and Hi-Resv showed similar levels of MMP-9 expression, but aqueous extracts showed significantly different expression levels. This may reflect the solubility of pterostilbene in methanol extracts compared to aqueous. It would be interesting to determine in the future whether aqueous extract have the same inhibitory effect on EGF-induced MMPs as these observed with the methanol tomato extracts.

A

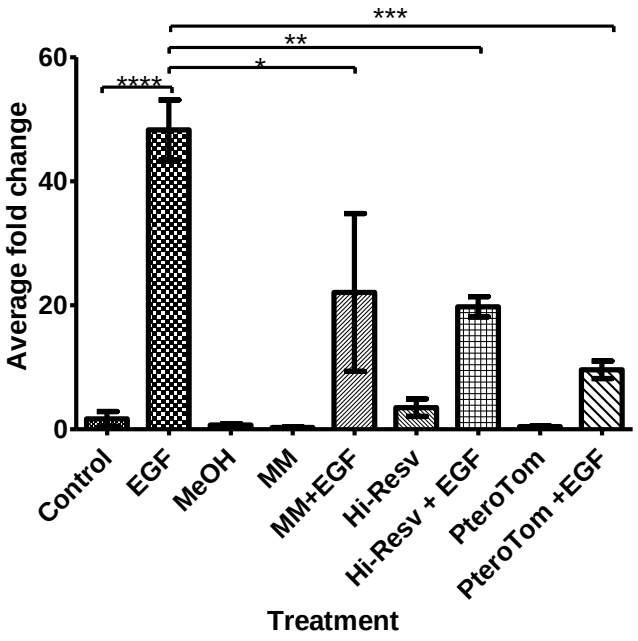

B

Treatment	Average C_T value
Control	33.53
EGF	27.70
MeOH	34.36
MM	35.51
MM +EGF	30.34†
Hi-Resv	32.73
Hi-Resv +EGF	32.73
PteroTom	35.48
PteroTom +EGF	29.68

Figure 6.25 Effect of different methanol extracts on relative expression of MMP-9 normalised to 18S in keratinocytes 24 hours post-treatment.

qRT-PCR of wounded cell monolayers were performed 24-hours post-stimulation. Data was analysed by relative quantification and normalised to 18S for MMP-9. Corresponding average C_T values are shown. (B). Each bar represents the mean fold change of 3 samples ±SEM. Statistical difference was determined using one-way ANOVA with the Bonferroni multiple comparison test, *P≤ 0.05, **P≤ 0.01, ***P≤ 0.001, ****P ≤0.0001. † represents data excluded from analysis, as one 18S C_T value varied more than 1.5 C_Ts from the mean

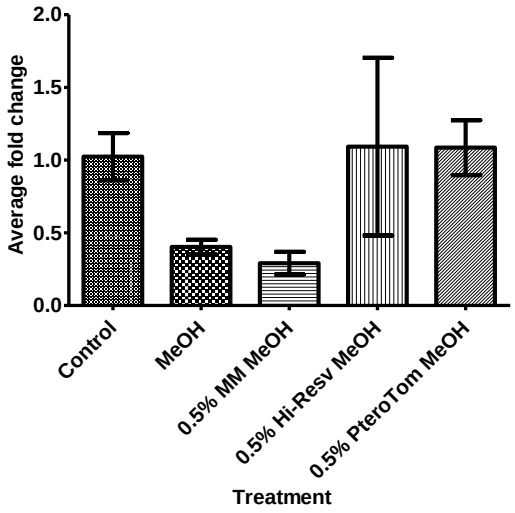

	Average C_T
Control	31.12
MeOH	32.77
0.5% MM MeOH	33.37
0.5% Hi-Resv MeOH	32.23
0.5% PteroTom MeOH	31.16

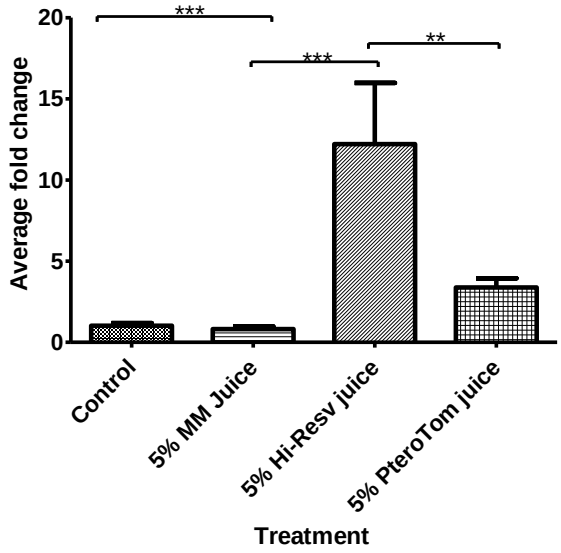

	Average C_T
Control	31.12
5% MM juice	31.65
5% Hi-Resv juice	27.99
5% PteroTom juice	29.47

Figure 6.26 Effect of methanol vs aqueous extracts on relative expression of MMP-9 normalised to 18S in keratinocytes 24 hours post-treatment.

Data shown is from one experiment, with data separated over two graphs for simplicity A) methanol tomato extracts (B) aqueous tomato extracts. qRT-PCR of cell monolayers were performed 24-hours post-stimulation. Data was analysed by relative quantification and normalised to 18S for MMP-9. . Statistical difference was determined using one-way ANOVA with the Bonferroni multiple comparison test, *P≤ 0.05, **P≤ 0.01, ***P≤ 0.001, ****P ≤0.0001. Each bar represents the mean fold change of 3 samples ±SEM. Corresponding average C_T values are shown.

6.4.8 COL7A1

As discussed in Chapter 4: MM and ResTom juice have been shown to significantly repress the expression of COL7A1 in whole skin explants. Although the main role of Collagen VII is in the anchoring of fibrils and the binding of basal keratinocytes to the dermis, recent research has also suggested that a reduction in COL7A1 expression reduces re-epithelialisation of wounds (Nystrom et al., 2013). Given the reduction in wound closure with tomato extract (Figure 6.22), and the repression of COL7A1 (which encodes the alpha chain of Collagen VII) in whole skin explants (chapter 4, 4.6.4), qRT-PCR was used to analyse expression levels in wounded keratinocytes (Figure 6.27).

Analysis of wounded keratinocytes showed only slight changes in COL7A1 expression levels across treatments (Figure 6.27). EGF treatment reduced expression of COL7A1 compared to control, with addition of PteroTom further increasing the repression of COL7A1. Interestingly, neither MM, ResTom, or PteroTom showed the highly repressive effect on COL7A1 as was observed in whole skin explants. This might be due to application of the different tomato extracts as methanol-extracts, or might be due to the difference in timepoints, since analysis of RNA from this experiment was at T-24, which could be too soon to see effects at the mRNA level.

A second preliminary experiment on non-wounded keratinocytes allowed for the comparison of methanol and aqueous extracts (Figure 6.28). There was little difference in COL7A1 expression in control compared to MeOH treated cells, suggesting that methanol had no detrimental effects on cell health. A trend towards repression of COL7A1 was observed for all methanol-tomato extracts, with PteroTom supressing COL7A1 expression to the greatest degree, however this reduced expression was not statistically significant.

Treatment of cells with aqueous extracts showed a very similar trend in COL7A1 expression compared to treatment with methanol-extracts. However, aqueous Hi-Resv juice displayed the greatest levels of suppression, with a significant decrease in COL7A1 expression compared to control.

A

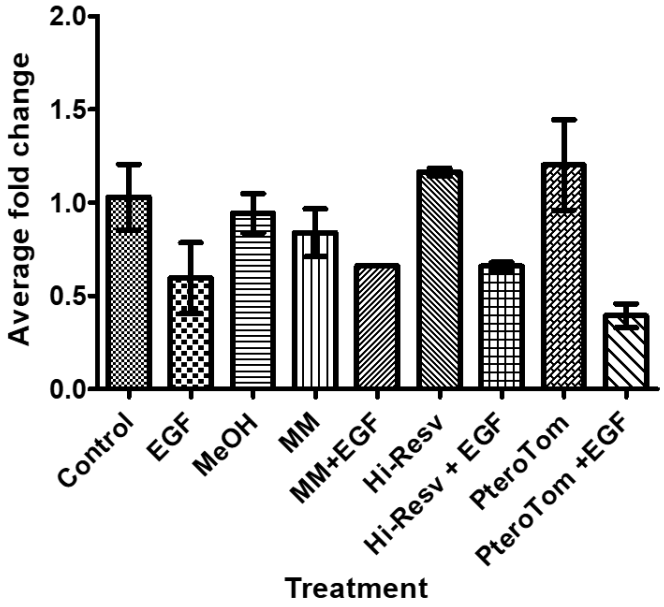

Treatment	Average C_T
Control	25.61
EGF	26.24
MeOH	25.91
MM	25.98
MM +EGF	27.62†
ResTom	25.92
ResTom +EGF	26.29
PteroTom	25.98
PteroTom +EGF	26.37

Figure 6.27 Effect of methanol tomato extracts on relative expression of COL7A1 normalised to 18S in wounded keratinocytes 24 hours post wounding and treatment.

qRT-PCR of wounded cell monolayer were performed 24-hours post-stimulation. Data was analysed by relative quantification and normalised to 18S for COL7A1 (A). Corresponding average C_T values are shown (B). Each bar represents the mean fold change of 3 samples ±SEM. † represents data excluded from analysis, as one 18S C_T value varied more than 1.5 C_Ts from the mean. Statistical difference was determined using one-way ANOVA with the Bonferroni multiple comparison test, *P≤ 0.05, **P≤ 0.01, ***P≤ 0.001, ****P ≤0.0001.

A

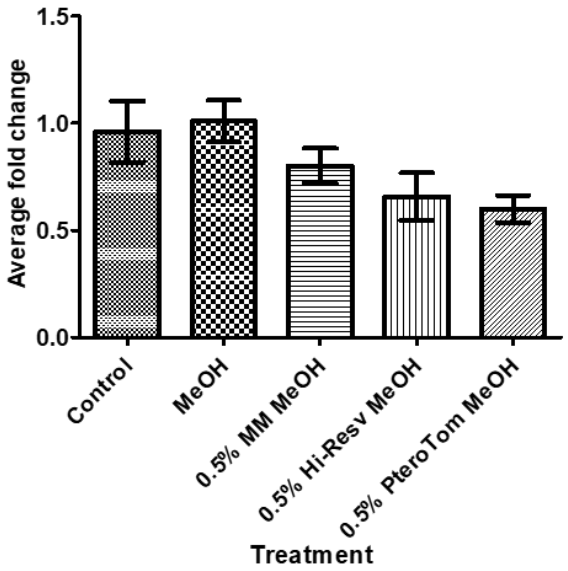

Treatment	Average C_T
Control	25.47
MeOH	25.69
0.5% MM MeOH	26.09
0.5% ResTom MeOH	26.67
0.5% PteroTom MeOH	26.24

B

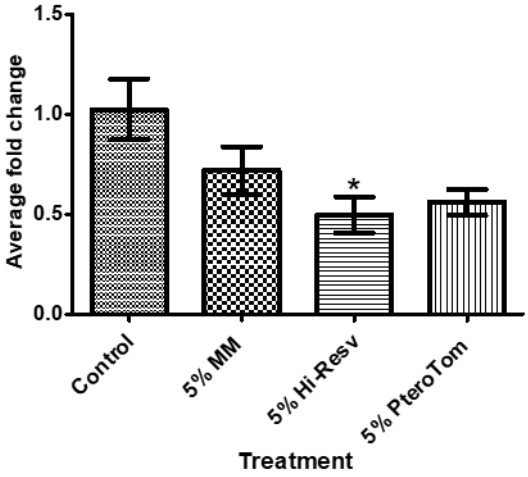

Treatment	Average C_T
Control	25.47
MeOH	25.69
5% MM juice	26.17
5% ResTom juice	26.84
5% PteroTom juice	26.39

Figure 6.28 : Effect of methanol vs aqueous extracts on relative expression of COL7A1 normalised to 18S in keratinocytes 24 hours post-treatment.

Data shown is from one experiment, with data separated over two graphs for simplicity A) methanol tomato extracts (B) aqueous tomato extracts. qRT-PCR of cell monolayers were performed 24-hours post-stimulation. Data was analysed by relative quantification and normalised to 18S for COL7A1. Each bar represents the mean fold change of 3 samples ±SEM. . Statistical difference was determined using one-way ANOVA with the Bonferroni multiple comparison test, *P≤ 0.05, **P≤ 0.01, ***P≤ 0.001, ****P ≤0.0001. Corresponding average C_T values are shown.

6.4.9 COL17A1

Collagen XVII is implicated in regulation of keratinocyte migration, with expression upregulated within keratinocytes during re-epithelialisation (Dabelsteen et al., 1998, Löffek et al., 2014), and high expression correlated with increased invasiveness of squamous cell carcinoma (Moilanen et al., 2017). Additionally, keratinocytes lacking Collagen XVII have a non-directory migration phenotype, further contributing to the evidence that Collagen XVII is important in keratinocyte migration. Given the decreased migration of keratinocytes observed with tomato treatment (Figure 6.22), and suppression of COL17A1 (which encodes the alpha chain of Collagen XVII) observed in whole skin explants (chapter 4, 4.5.3.1), qRT-PCR was performed on wounded keratinocytes to determine if changes in expression levels of COL17A1 correspond to the inhibitory effect of tomato extract on wound closure (Figure 6.29).

qRT-PCR data seemed to fit with what is known in the literature surrounding COL17A1 expression and wound healing, in that EGF and MM +EGF which exhibited the greatest levels of healing (Figure 6.22), also have the greatest expression of COL17A1 (Figure 6.29). Additionally, MM and Hi-Resv both have decreased levels of COL17A1 and gave reduced levels of wound closure. However, the mRNA data did not correlate as well for other treatments, but this in part is due to the large error margins in wound closure assays.

Using non-wounded keratinocytes (Figure 6.30), the difference in biological activity of methanol-extracts compared to aqueous extracts was compared. Between the different tomato methanol-extracts there was little change in COL17A1 expression levels as observed in wounded cells. Interestingly however, both PteroTom and Hi-Resv aqueous extracts significantly increased COL17A1 expression levels compared to control. Cells treated with Hi-Resv extract exhibited a significantly larger increase in COL17A1 levels compared to both PteroTom and MM extracts. This is contrary to expression level data from whole skin data analysis (4.5.3.1) in which a decrease in COL17A1 was observed with both MM and ResTom juice. This may reflect the different response of different skin cell types to tomato juice.

Due to the different expression levels observed for COL17A1 with methanol and aqueous extracts, scratch-wound experiments with both types of tomato extracts should be performed, to allow for comparison of activity between the two extracts and determine how the form of tomato-treatment given affects gene expression response.

A

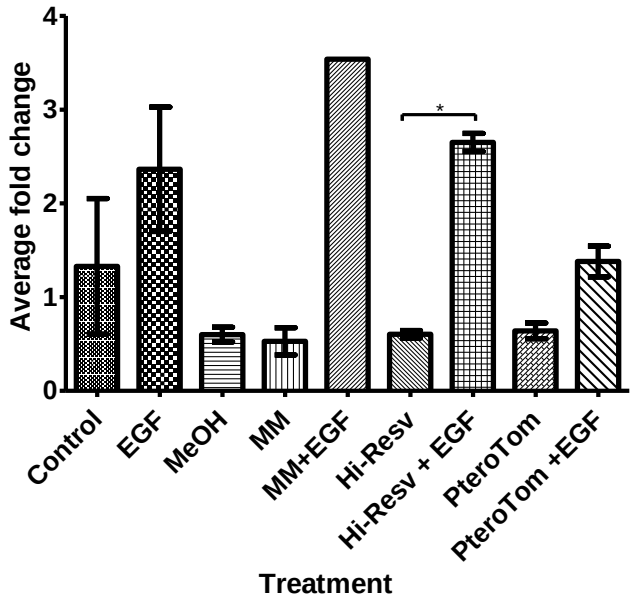

B

Treatment	Average C_T
Control	24.72
EGF	23.33
MeOH	25.68
MM	25.86
MM +EGF	24.54†
Hi-Resv	25.98
Hi-Resv +EGF	23.39
PteroTom	25.97
PteroTom +EGF	23.65

Figure 6.29 Effect of methanol tomato extracts on relative expression of COL17A1 normalised to 18S in wounded keratinocytes 24 hours post wounding and treatment.

qRT-PCR of wounded cell monolayers were performed 24-hours post-stimulation. Data was analysed by relative quantification and normalised to 18S for COL17A1 (A). Corresponding average C_T values are shown (B). Each bar represents the mean fold change of 3 samples ±SEM. † represents data excluded from analysis, as one 18S C_T value varied more than 1.5 C_Ts from the mean . Statistical difference was determined using one-way ANOVA with the Bonferroni multiple comparison test, *P≤ 0.05, **P≤ 0.01, ***P≤ 0.001, ****P ≤0.0001

A

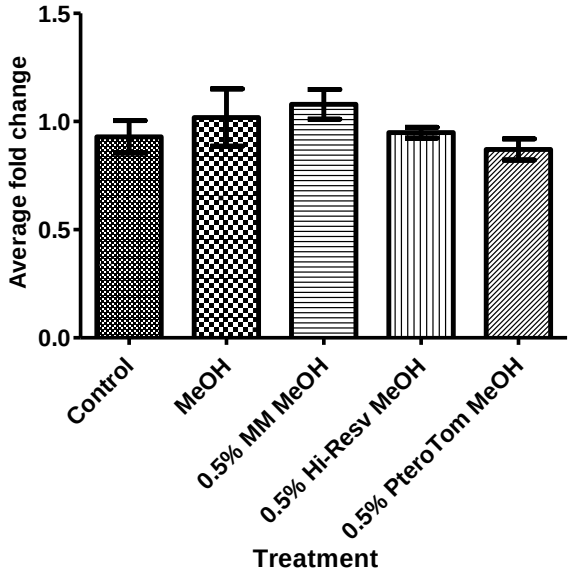

	Average C_T
Control	25.88
MeOH	26.08
0.5% MM MeOH	26.04
0.5% Hi-Resv MeOH	26.49
0.5% PteroTom MeOH	26.08

B

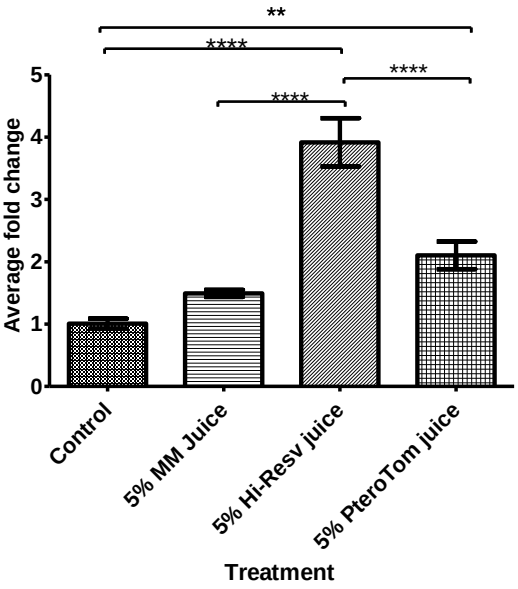

	Average C_T
Control	25.88
5% MM juice	25.49
5% Hi-Resv juice	24.24
5% PteroTom juice	24.89

Figure 6.30 Effect of methanol vs aqueous extracts on relative expression of COL17A1 normalised to 18S in keratinocytes 24 hours post-treatment.

Data shown is from one experiment, with data separated over two graphs for simplicity (A) methanol tomato extracts, and (B) aqueous tomato extracts. qRT-PCR of cell monolayers were performed 24-hours post-stimulation. Data was analysed by relative quantification and normalised to 18S for COL17A1 Each bar represents the mean fold change of 3 samples ±SEM. . Statistical difference was determined using one-way ANOVA with the Bonferroni multiple comparison test, *P≤ 0.05, **P≤ 0.01, ***P≤ 0.001, ****P ≤0.0001. Corresponding average C_T values are shown

6.4.10 Methanol Hi-Resv extracts inhibited wound healing of mouse fibroblasts, but PteroTom extracts did not.

An initial experiment was performed to look at the effect of methanol extracts on a mouse fibroblast cell line (3T3). Mouse 3T3 cells have been used extensively in research into skin health and disease and will help to give insight into biological activity of tomato extracts on fibroblasts, which may be different from those observed in keratinocytes.

To investigate the relative biological activity of MM, ResTom and PteroTom extracts on fibroblasts, an experiment was performed to look at the effect of several different concentrations of methanol tomato extract (Figure 6.31). Concentrations of 0.1%, 0.25%, 0.5% and 1% methanol tomato extracts were used. A concentration of 1% MeOH extract was comparable to 10% aqueous tomato extract. The total concentration of methanol was made to the equivalent of 1% tomato extract across all treatments, to account for any affects additional methanol levels may have on cells.

A higher level of methanol did not have any adverse effects on cell health (Figure 6.32), or wound closure capability, meaning that any changes in wound healing associated with tomato juice extracts could be attributed to the compounds within the tomato extract.

Addition of methanolic MM extract or PteroTom extract caused no significant changes in total wound healing at any concentration level, with wounds near completely healed by 48 hours (Figure 6.32). This contrasts with observations of HaCaT cell response to PteroTom, which appeared to show a slight inhibition of wound healing (Figure 6.22). This could potentially show a difference in response to the tomato extract by skin cell types and should be investigated more in the future.

Addition of Hi-Resv methanol extract did lead to delayed wound closure at all concentrations, with a trend towards greater delay in wound closure with higher Hi-Resv concentrations (Figure 6.32), the exception being for treatment with 0.25% Hi-Resv which showed a greater reduction in wound closure than either 0.5% or 1% extract at 24 hours. By 48 hours, cells treated with Hi-Resv extracts had still not completely healed, with cells treated with 1% Hi-Resv extract showing the greatest reduction in overall wound closure (Figure 6.32), although no Hi-Resv treatment allowed for complete wound closure by 48 hours. This suggested that Hi-Resv extract had an inhibitory effect on fibroblast migration.

It is interesting that this effect was not seen in the cells treated with PteroTom, which also contained resveratrol at low concentration, and pterostilbene which has been suggested to be a more biologically active compound than resveratrol. This may indicate that synergy between several compounds present in the tomato juice leads to different biological responses, and that the presence of pterostilbene in addition to resveratrol is able to help negate negative effects on wound healing by resveratrol.

Data from HaCaT and fibroblast wound healing assays have shown several differing effects of resveratrol, and polydatin, as well as between Hi-Resv and PteroTom juice. It is interesting that in HaCaTs both ResTom Hi-Resv PteroTom appeared to have an inhibitory effect on wound closure (Figure 6.22), with PteroTom having a greater inhibitory effect than HI-Resv, whereas in fibroblasts only Hi-Resv extracts displayed this inhibitory affect (Figure 6.32). These two cell lines are from different organisms, human and mouse, which may, in part, account for this difference in cellular response to tomato extracts. However, it may also suggest a differential response between skin cell types to different extracts of tomato.

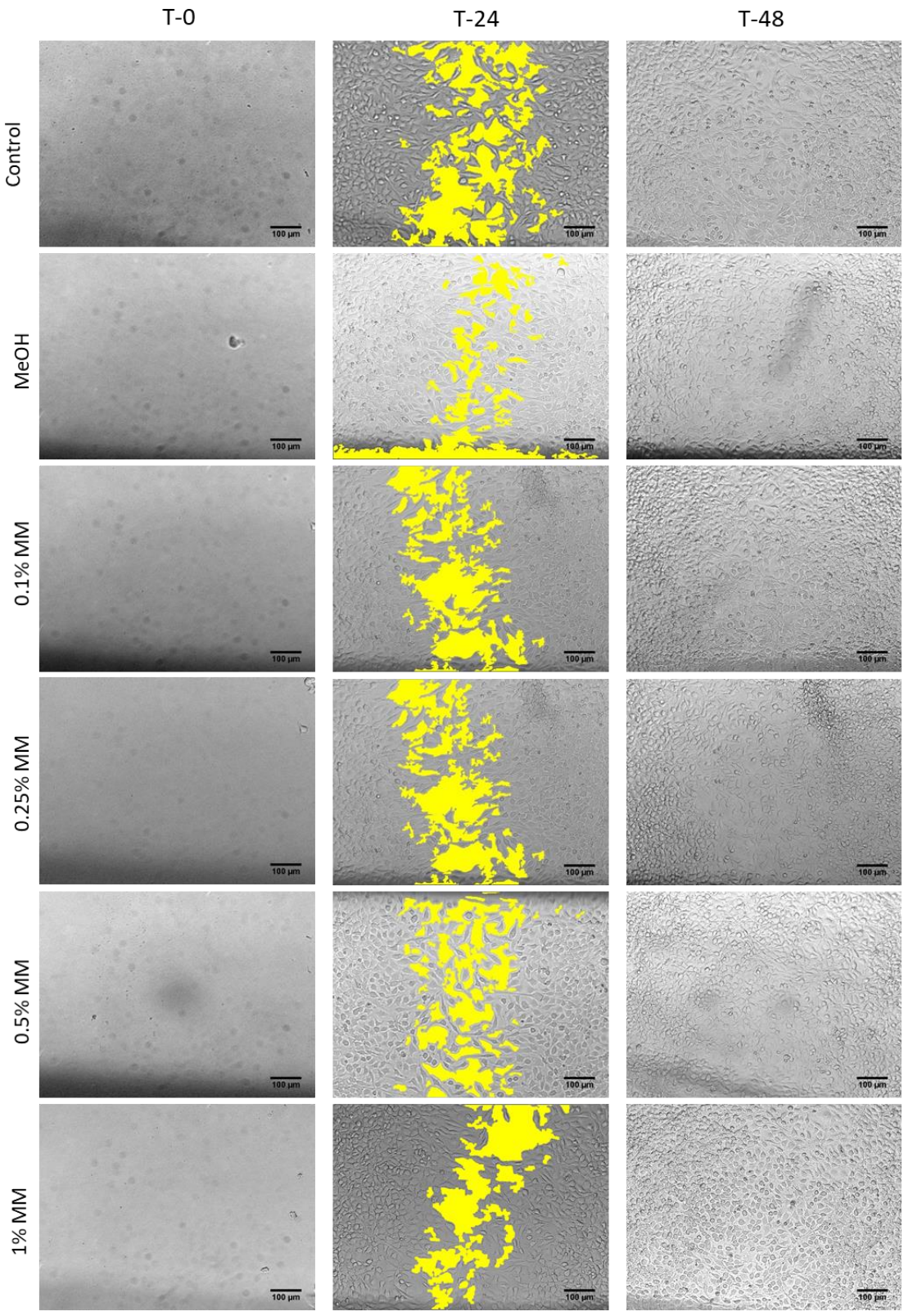
T-0
T-24
T-48
Control
MeOH
0.1% MM
0.25% MM
0.5% MM
1% MM
100 µm

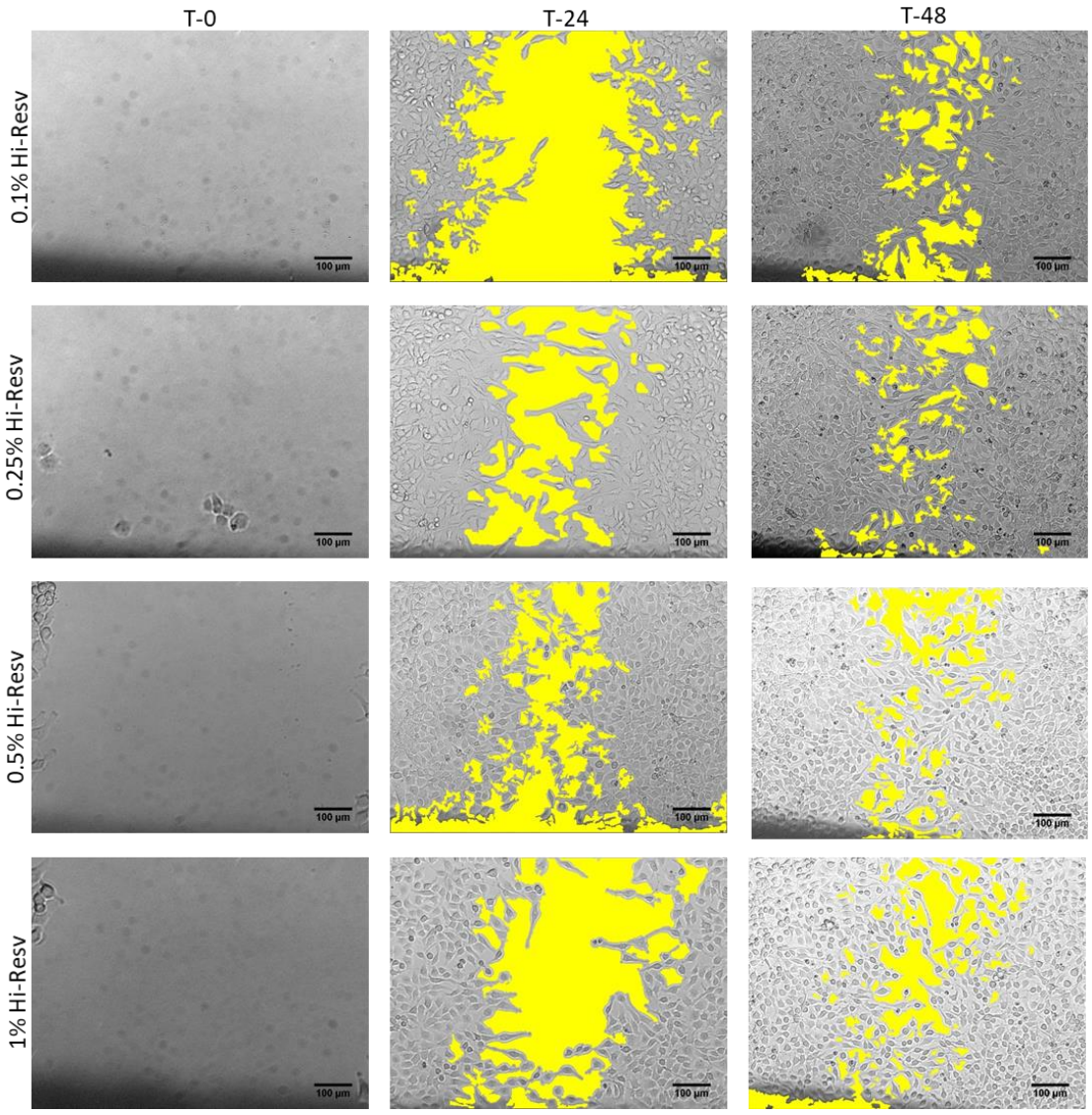
T-0
T-24
T-48
0.1% Hi-Resv
0.25% Hi-Resv
0.5% Hi-Resv
1% Hi-Resv
100 µm

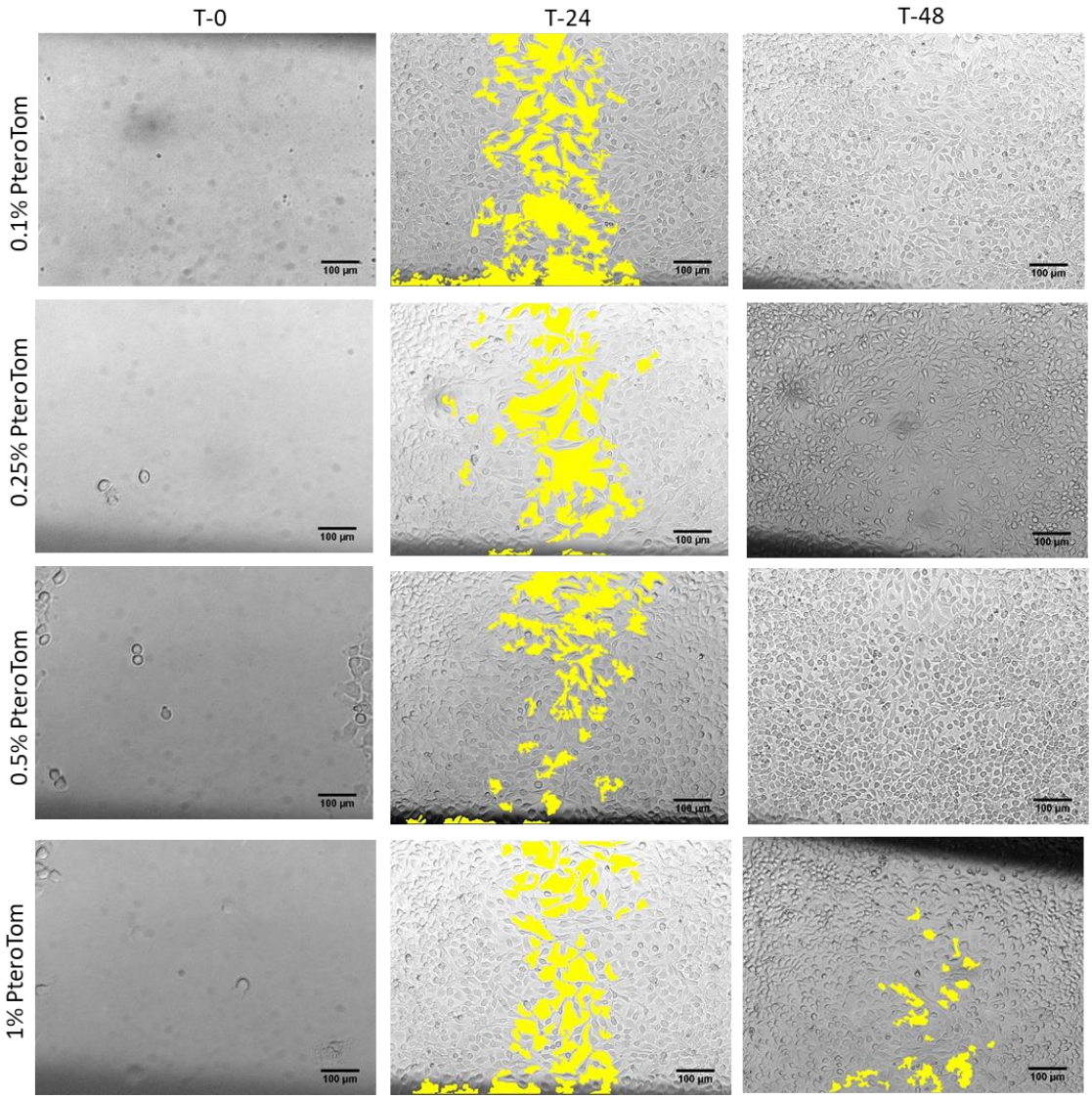

Figure 6.31 Wound closure of fibroblasts in response to different dosages of methanol tomato extracts.

Phase contrast images representative of fibroblast scratch wounds at T-0, T--24 and T-48 post treatment in culture media (DMEM +2% FCS) with 0.1%- 1% v/v methanol-tomato extract. All methanol tomato extracts were prepared in 50% MeOH. Percentage wound closure was calculated by comparison of wound area at T-0 to T-24, and T-48. Total wound healing was quantified with the ImageJ plugin: MRI Wound Healing Tool (Bäcker, 2012). Wound area is highlighted in yellow. Scale bar= 100µm.

Cells were seeded for scratch assay by Dr Damon Bevan at a density of 100,000

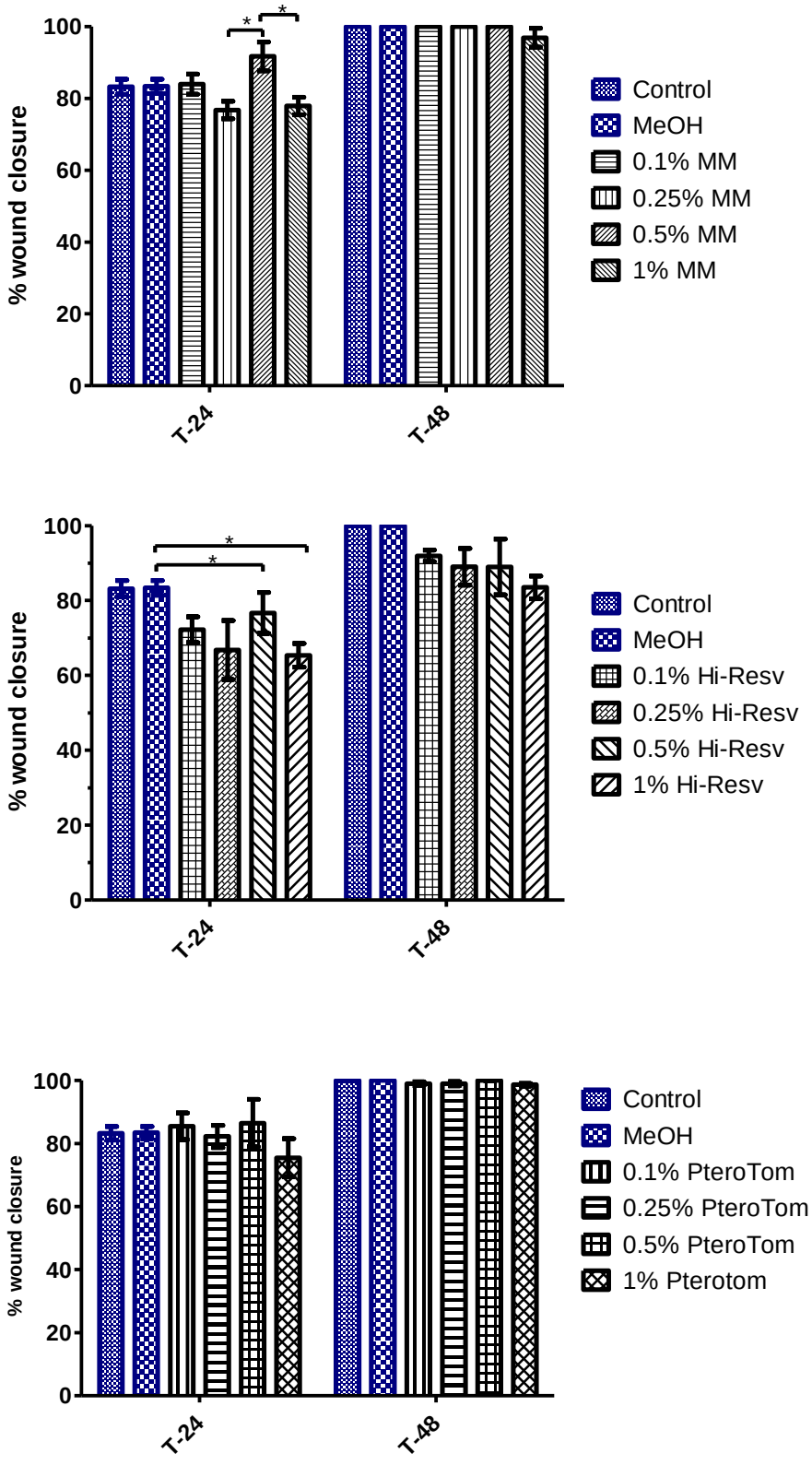

Figure 6.32 Wound closure analysis of fibroblasts in response to increasing concentrations of methanol tomato extracts

Percentage wound closure over 24 and 48 hours was calculated for A) MM, B) Hi-Resv and C) PteroTom methanolic extracts using image J. Each bar represents the mean wound closure in 3 scratches ± SEM. Statistical difference was determined using one-way ANOVA with the Bonferroni multiple comparison test, *P≤ 0.05, **P≤ 0.01, ***P≤ 0.001, ****P ≤0.0001

6.5 Discussion

6.5.1 *Ex vivo* model of wounding

Under normal physiological conditions wound healing occurs in a defined temporal-spatial manner. The wound healing process is a complex response requiring the activation of several different cell types, including keratinocytes and fibroblasts (Li et al., 2007), which is difficult to replicate *in vitro.*

Using an *ex vivo* wound healing model we were able to investigate the response of skin wound healing to tomato extracts in an environment representative of that found in non-inflammatory and inflammatory conditions *in vivo*.

The *ex vivo* wounding model provided insight into wound healing of skin, showing that IL1/OSM is associated with greatly reduced wound closure, and treatment with EGF increased wound closure (Figure 6.6, Figure 6.8, Figure 6.12). The observable reduction in wound closure under inflammatory conditions may suggest that this model could be used for modelling impaired wound closure under inflammatory conditions. Currently, investigation of impaired wounding is commonly performed using biopsies from chronic wounds such as diabetic foot wounds (Nunan et al., 2014) or animal wound models. However, both of these models have inherent problems, with animal models displaying differences in skin structure compared to humans, and chronic wounds such as diabetic wounds often having no single classifiable cause making investigations of therapeutics difficult (Nunan et al., 2014). Therefore, the *ex vivo* wound model could offer an informative alternative.

Overall it was not possible to conclude whether tomato extracts can promote or impair skin explant wound closure as results were variable even within one donor which may be a consequence of methodological complications. Several issues with the current methodology used for *ex vivo* wounding were encountered, such as variation in wound sizes which could impact upon overall wound healing, and the trend for one side of the wound to display much greater healing than the other (Figure 6.16, Figure 6.19, Figure 6.22). Other studies with partial thickness, and full-thickness *ex vivo* skin models have used techniques including pinning of the skin (Xu et al., 2012) , the use of a mesh support in plate wells (Glinos et al., 2017), and embedding in a collagen gel (Sebastian et al., 2015) to help support and level skin. In the future we may be able to utilise one of the above methods to enable level positioning of the explants. Additionally, complete removal of fat tissue and levelling of each individual explant may also help to achieve explants that are consistently level. Another possibility is that there is a variable degree of damage to the underlying dermis at different points across the wound. Future studies could determine changes in protein expression in relevant regions of the dermis.

Despite the problems discussed above, this method shows great promise for the study of wound healing in full thickness skin. Currently, the main way in which to study human skin wound healing

is using single cell skin cultures, as we have performed with keratinocytes and fibroblasts, or through *in vitro* co-cultures of fibroblasts and keratinocytes (Oberringer et al., 2007, Oh et al., 2013). Although these methods provide good insight into how these cell lines individually respond to different treatments, they are not able to represent the complex environment of skin and the important interactions between different cell types (Semlin et al., 2011, Werner et al., 2007). Mouse and rat models have also commonly been used for *in vivo* full thickness wound experiments, although again they do not give a true representation of human skin due to structural difference in the skin as well as mechanistic differences in wound healing (Dunn et al., 2013). In addition, the differences in skin structure can lead to different absorption rates of treatments than would be obtained in human skin (van Ravenzwaay and Leibold, 2004).

As such, this method holds promise for the analysis of full thickness wounds, and given the complex nature of skin, and the interactions between the many cells in its makeup, this could offer more insight into the response of wound healing to different topical treatments. With a few adjustments to the current protocol to ensure higher level of wound size reproducibility in multiple wounds, this could represent a unique way to study wound healing in human skin.

6.5.2 Insights from single cell cultures

Resveratrol studied in the context of wound healing has previously be shown to inhibit proliferation and migration of several cell types and has been hypothesised to be able to inhibit the EGFR pathway (Lee et al., 2011, Vergara et al., 2011). However, little has been studied concerning the action of the glycosylated derivative of resveratrol, polydatin. As this is a major stilbene constituent of the ResTom, Hi-Resv and PteroTom tomato lines, the biological effects of polydatin on keratinocyte wound healing were explored.

A preliminary experiment which looked at the activity of 50 µM of resveratrol on wound HaCaT wound healing showed a reduction in wound closure with resveratrol treatment (Figure 6.18). In addition, a combination treatment of EGF and resveratrol displayed reduced wound closure compared to EGF treatment alone, which corresponded to observations cited in the literature. We had chosen an initial concentration of 50µM resveratrol to correspond to resveratrol concentration in ResTom extracts. Further analysis of ResTom extracts showed that tomato extracts contained even higher levels of the glycosylated derivative of resveratrol, polydatin (Chapter 3:).

Whereas polydatin was observed to significantly increase wound closure at a concentration of 10 µM - 50 µM (Figure 6.20), resveratrol was found to slightly increase wound closure between 10-20 µM, although at a concentration of 50 µM it inhibited wound closure significantly (Figure 6.18). The differential effects of resveratrol on wound closure, and therefore cell migration by resveratrol at different concentrations was particularly interesting and could potentially be exploited in medicinal treatments to achieve different purposes. Many of the factors induced within the wound healing

responses are also involved in pathological mechanisms such as migration of cancer cells which drives metastatic cancer. Therefore, the ability of high concentrations of resveratrol to inhibit cell migration support the use of plant polyphenols for inhibition of metastasis. The anti-migratory action of phytochemicals has been shown on breast cancer cells (Ham et al., 2015, Adams et al., 2010), therefore it would be interesting in, future studies, to investigate the action of phytochemicals on skin cell lines such as human basal cell carcinoma cell lines.

On the other hand, low concentrations of resveratrol, which acts to promote cell migration, could help in the treatment of wounds with impaired healing such as diabetic skin wounds, where keratinocytes at the wound edge display a reduced ability for re-epithelialisation (Galkowska et al., 2006).

From these preliminary data we were able to see a potential inhibitory effect of resveratrol on the action of EGF in wound healing, and a difference in the biological effects of resveratrol and polydatin. The next step was to see how these data translated into the effects of complex tomato matrix extracts, and whether these properties of single compound treatments of polydatin and resveratrol were observed in complex tomato extracts or if, within a complex matrix, different biological effects would be seen. In addition, we wanted to investigate how differences in tomato extract composition could affect wound healing.

LCMS IT-TOF analysis of PteroTom juice had identified a lack of pterostilbene in aqueous extracts (Chapter 3:), and in order to be able to compare different activities of ResTom and PteroTom tomatoes on wound healing, we used methanolic based tomato extracts which had been shown to contain high levels of pterostilbene.

One of the problems associated with the use of methanol is its associated toxicity. However at the low levels which were used in our scratch wound assays no toxicity was observed with addition of methanol (Figure 6.21), and methanol did not cause any significant differences in wound healing compared to controls (Figure 6.22). This meant that any change in wound healing with methanolic tomato extracts could be associated with the plant polyphenols present in the extracts.

Interestingly, treatment with all tomato extracts led to a decrease in wound closure compared to the controls (Figure 6.22). This suggests that the tomato matrix itself, may have an inhibitory effect on the process of wound healing, which may be due to the presence of compounds such as flavanols naturally found in tomato juice.

The major difference in gene expression was associated with tomato extract co-treatment with EGF. Treatment of wounds with EGF led to increased wound closure compared to controls (Figure 6.22). When wounds were treated with a combination of MM juice and EGF, wound closure increased even further than EGF treatment alone, but co-treatment with EGF and Hi-Resv or

PteroTom showed a decrease in overall wound closure, with PteroTom exhibiting inhibition to the highest degree. The downregulation of MMP-1 and MMP-9 in EGF + Hi-Resv and EGF + PteroTom cells (Figure 6.23, Figure 6.25) compared to EGF correlated with the observations of wound closure with these treatments (Figure 6.22). However, MM + EGF which showed an increase wound closure compared to EGF only, also showed a decrease in MMP-1 expression.

Inhibition of MMP-9 by resveratrol has previously been observed in other cell types (Hu et al., 2007, Woo et al., 2003), particularly cancer cells. MMPs have a well-established link to the progression of cancer, with their role in the breakdown of extracellular-matrix components an important step in invasion and metastasis (Gialeli et al., 2011). Additionally, MMPs are known to contribute to cancer cell-proliferation by modulating signalling pathways involved in cell growth, angiogenesis and inflammation (Kessenbrock et al., 2010). Skin melanomas are known to express elevated levels of several MMPs, including MMP-1 and MMP-9 (Varani et al., 2000). Mouse-knock out studies have shown the importance of MMP-9 in metastasis and invasion of cancer cells (Itoh et al., 1999), whilst MMP-1 has been associated with tumour progression (Iida and McCarthy, 2007).

Growth factors such as EGF, have been shown to play an important role in the induction of MMPs such as MMP-9, in tumour cells, (Nutt et al., 2003, Liu and Klominek, 2003). Therefore, the ability of Hi-Resv and PteroTom to suppress MMP-9 induction by EGF could potentially have several medicinal applications, especially in topical treatments of skin melanomas to help reduce proliferation and migration of melanoma cells.

In addition, from these data PteroTom has been shown to inhibit wound closure, and expression of wound healing genes such as MMP-1 and MMP-9 to a higher degree than Hi-Resv, suggesting greater biological effectiveness of PteroTom extracts and, by implication, pterostilbene compared to resveratrol.

Interestingly, qRT-PCR of HaCaTs treated with comparable concentrations of aqueous tomato extract compared to methanol-based extract showed very different effects on MMP-9 expression, with Hi-Resv juice significantly increasing MMP-9 expression, and methanol extracts showing little effect on MMP-9 expression (Figure 6.26). It would be interesting in the future to determine if aqueous extracts and methanol-based extracts also show a differential response with EGF co-treatment. This observed action of Hi-Resv aqueous extract could be suggestive that the compounds within the matrix interact in a different way when in the tomato water matrix or could be an effect of the associated properties of the aqueous tomato extract.

Comparison of biological activity of methanol and aqueous extracts showed some differences in gene expression responses to these two extracts, which was particularly apparent in gene expression analysis of MMP-1 (Figure 6.28) and COL17A1 (Figure 6.30). However, interestingly

different expression responses between methanol and aqueous extracts were not seen for all genes. The different gene expression levels observed with methanol compared to aqueous extracts may be indicative that upon reconstitution of evaporated methanol extracts not all compounds were fully re-solubilised. Quantitative analysis was not performed on the reconstituted methanol extracts, and given these observable differences in biological activity, additional analyses should be performed. It is also possible that important constituents of the tomato matrix, such as sugar levels or pH are important in associated biological activity and cannot be fully replicated in methanol extracts. As such, further experiments should be conducted in the future in order to determine the differences in gene expression by methanol and aqueous extracts. Due to the insolubility of Pterostilbene in water, this may be something that needs to be considered in future analysis.

From the previous Chapter (MMP-12) it has been established that juice extracts of MM and ResTom have major effects on gene expression in skin explants. Keratinocytes are just one cell type present in skin, therefore to see how Hi-Resv and PteroTom extracts affect other skin cells we also investigated activity of fibroblasts in response to methanol tomato extracts.

Contrary to my observations on keratinocyte scratch wounds (Figure 6.22), fibroblast wounds treated with PteroTom did not display any inhibition of wound closure, even when treated with an increased concentration of PteroTom of 1% (Figure 6.32, C). Fibroblasts however did display a reduction in wound closure of approximately 20% with treatment of Hi-Resv. By monitoring wound closure over a 48-hour period, we were able to observe that Hi-Resv treatment does not prevent wound closure but does delay wound closure. In addition, even at a low concentration of 0.1% Hi-Resv delayed wound closure was observed (Figure 6.32,B).

The contrasting activity of the PteroTom extract on wound healing between fibroblasts and keratinocytes was interesting and suggested a differential response to some plant polyphenols between different skin cell types. This should be considered when looking at the response to different tomato treatments in whole skin explants. However, this response may also be due to the murine origin of these fibroblasts. It would be interesting to observe whether there is a difference in response to wound healing with Hi-Resv and PteroTom extracts in human fibroblasts.

6.6 Summary

The data from this chapter showed a complex interaction between tomato extracts and wounding healing responses within skin and begins to show how the overall wound healing response in whole skin relates to effects observed in individual cell types. Overall, the data from this chapter suggests that tomato juice both, MM and ResTom, do not improve wound healing, and may in fact act to inhibit wound closure.

This chapter investigated the use of a full thickness *ex vivo* wound healing model to study the effects of tomato extracts on wound healing. Unfortunately, analysis of wounded explants identified a problem associated with the methodology of wounding, which led to uneven healing of wounds which made analysis difficult. Despite this, we were able to observe clear differences in wound healing with EGF and IL1/OSM, which indicated that with further development this model could be used to effectively study wound healing with different treatments.

Using two cell lines we were able to begin investigating the effect of tomato extracts in the individual cells of skin. Preliminary data from cell wound assays indicated greater activity associated with PteroTom extracts than Hi-Resv extracts, and the potential ability of both extracts to not only inhibit wound healing, but also inhibit action of EGF. Gene expression analysis reinforced EGF-inhibiting activity of Hi-Resv and PteroTom juice which showed significant inhibition of MMP-1 and MMP-9 in cells treated with both EGF and tomato extract compared to EGF alone, together with inhibitory trends displayed in other genes including COL7A1 and COL17A1. These data also correlated with literature reports of resveratrol function, which in several studies, have shown that resveratrol is able to inhibit EGF (Vergara et al., 2011, Lee et al., 2011). This could indicate potential use of Hi-Resv and PteroTom extracts for the treatment of inflammatory skin diseases such as psoriasis.

Psoriasis, is categorised by thickening of the epidermis due to increased keratinocyte proliferation and differentiation as reviewed in Lowes et al. (2007). EGF plays a major role in pathogenies of psoriasis, with high EGF serum levels found in psoriatic scales (Flisiak et al., 2014). Additionally, levels of EGF appear to correlate with disease severity. Therefore, the ability of tomato extracts to inhibit EGF responses could offer potential for use in therapeutic treatments of inflammatory skin disorders characterised by keratinocyte over-proliferation, and further research should be conducted in this area.

Additionally, the reduced migration of keratinocytes observed with both Hi-Resv and PteroTom extracts, in addition to inhibitory action on MMPs could indicate potential to inhibit migration of cancer cells and prevent metastasis. It would therefore be an interesting avenue of research to study the effect of tomato extract on human basal cell carcinoma cell lines.

However, it is important to note that a number of differences have been identified between normal human epidermal keratinocytes (Primary cell line) and HaCaT cell lines (immortalised cell line) (Liu et al., 2012). For example, Pastore et al. (2011b) noted that treatment of HaCaT cells with plant polyphenols elicited a much stronger up-regulation of stress responses than in normal human epidermal keratinocytes (NHEK) cells. In addition, molecular differences have been observed between HaCaT and NHEK cells. A study by Lewis et al. (2006) showed that aberrant NF-κB activity occurs in HaCaT cells, altering the response of HaCaT cells to UVB irradiation, with differences in

the activation of key upstream signalling pathway components such as AKT phosphorylation observed. Finally, Liu et al. (2012) noted that HaCaT cells are more sensitive to hydrogen peroxide induced oxidative stress, and subsequently have much higher levels of intracellular superoxide dismutase, than NHEK cells. These results suggest that HaCaT cells are not comparable to *in vivo* skin as once thought, and caution should be used when analysing biological responses of HaCaT cells in isolation of other cell models. Therefore, it would be beneficial to perform repeats of these experiments using primary keratinocytes, which may more accurately represent how individual cell lines would respond i*n vivo*.

Finally, we began to investigate the differences in biological activity of different tomato extracts. As pterostilbene is not soluble in aqueous extracts, methanol extracts were prepared to allow for comparison of the relative biological activity of tomatoes. Despite large changes observable in gene expression analysis from scratch wounded keratinocytes treated with methanol extracts, comparison of methanol to aqueous extracts identified significant differences in biological activity between these two extract types. This may be indicative that other factors in the tomato matrix such as sugar levels and acidity, which may not be effectively replicated in methanol extracts, are important for biological activity. Additionally, although methanol extracts were quantified before evaporation and resuspension into a reduced volume of methanol, the resulting methanol extract was not quantified. It may be possible that during resuspension, not all compounds were fully reconstituted, and therefore quantification analysis should be performed to confirm relative levels of stilbenes.

Chapter 7: General Discussion and Future directions

7.1 Discussion

Plant stilbenes are reported to have a many biological activities which may be beneficial for human health and/or for treatment of disease including anti-inflammatory (Potapovich et al., 2011, Pastore et al., 2012b), anti-aging (Farris et al., 2014) and anti-carcinogenic properties (Rimando et al., 2002, Tang et al., 2008, Ham et al., 2015). Several studies have been published reporting beneficial effects of plant polyphenols on skin health and prevention of disease (Wittenauer et al., 2015, Zhao et al., 2009, Khanna et al., 2002). Despite a number of studies looking at the activity of plant polyphenols on skin health, the effect of stilbenes on gene expression in skin has not been widely studied. Lephart et al. (2014) showed that resveratrol treatment acts to significantly downregulate gene expression of inflammatory and skin aging molecules, whilst upregulating extracellular matrix proteins and anti-oxidant markers. Therefore, plant stilbenes represent an interesting avenue of research for human dermal applications to maintain and improve skin health

However, a lack of model systems for the efficient and high production of stilbenes impedes the further development of medicinal/anti-ageing treatments. Additionally, due to problems with tissue availability as well as ethical considerations for in-human trials, many experimental studies investigating the biological activity of plant stilbenes have been based upon cell cultures, or animal models such as mouse. Yet, these models lack the complexity or specific features of human skin, and as such may not be a true representation of the biological responses that would be observed in humans (discussed in Chapter 1:).

Data in this thesis showed the use of a tomato bio-factory for high-level production of plant stilbenes, and the use of an ex *vivo* skin explant model to test biological activity of tomato extracts on human skin.

7.2 Metabolic engineering to produce pterostilbene in tomato

A major barrier in the development of resveratrol as a biological treatment is its low bioavailability (Azachi et al., 2014, Walle et al., 2004). The di-methylated derivative of resveratrol, pterostilbene, offers an attractive alternative to resveratrol as it has a much higher bioavailability (Kapetanovic et al., 2011, Lin et al., 2009). However, the few plants which synthesise pterostilbene do so in low concentrations, making extraction direct from plants an unviable option. Additionally, current microbial factories require more optimisation before they can synthesise pterostilbene at high yield and low cost (Heo et al., 2017).

Metabolic engineering of tomato for stilbene synthesis using stilbene synthase from *Vitis vinifera* in addition to the Arabidopsis transcription factory AtMYB12, resulted in high accumulation of resveratrol in tomato fruits. These tomatoes produced up to 6 mg/g dry weight (DW) resveratrol and resveratrol derivatives, that is 100-fold higher than levels found in red grapes (Zhang et al.,

2015). These data showed that tomato provide an excellent bio factory to produce stilbenes. However, this expression system resulted in poor plant health due to the use of the promoter (35S) used to express resveratrol, which caused expression of resveratrol throughout the plant. Therefore, this project aimed to improve the current tomato production system for resveratrol by exchanging the 35S promoter for the fruit-specific E8 promoter, thereby resulting in expression of StSy only in tomato fruit. Additionally, a new tomato was engineered based upon this tomato production system to produce pterostilbene, by the introduction of a grape resveratrol-o-methyltransferase gene.

Tomatoes from the new tomato line PteroTom (E8:StSy,E8:ROMT, E8:MYB12) were found to produce up to 16 µg/g DW pterostilbene, in addition to 5 µg/g pinostilbene, 5µg/g resveratrol and 19.5 µg/g polydatin. At levels of 16 µg/g DW pterostilbene, this was 30 times greater than that produced in *Vaccinium stamineum* (deerberry) berries (up to 520 ng/g DW) (Rimando et al., 2004).

These levels of pterostilbene are representative of first generation tomato fruits and may improve over generations as the transgenes are brought to homozygosity. Crossing of E8:ROMT,E8:Myb12 plants with the bronze tomato by Dr Eugenio Butelli, produced the PteroBronze tomato able to produce anthocyanins in addition to pterostilbene and resveratrol. This tomato had increased levels of pterostilbene compared to the original PteroTom fruits, suggesting production of pterostilbene within PteroTom fruits is currently suboptimal. Crossing with E8:MYB12 plants and 35S:StSy should allow us to further improve pterostilbene production.

7.3 Development of a working human skin explant assay to investigate the effect of tomato extracts

Research models frequently employed for skin studies do not provide a true representation of the complexity of human skin. With the development of an *ex vivo* skin explant model, we have been able to establish a robust experimental platform to investigate the effects of tomato juice extracts on human skin health and wound healing.

Ex vivo full thickness human skin constitutes a model close to *in vivo* human skin, with the cellular and extracellular matrix spatial distribution largely conserved, providing an appropriate system for the testing of topical treatments.

In this thesis, data have been obtained identifying changes in gene regulation in skin explants modulated by cytokines and different tomato extracts, summarised in Figure 7.1.

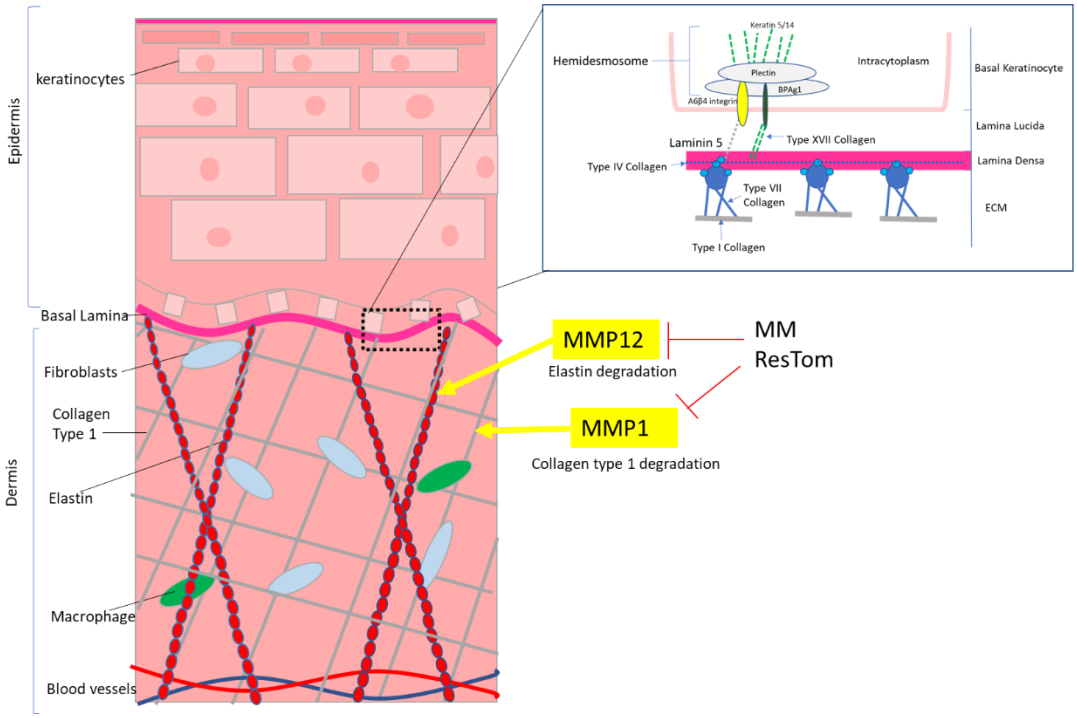

Figure 7.1 Summary of findings within ex vivo skin model under inflammatory conditions

Cytokines induce inflammation in skin explants leading to upregulation of several genes related to inflammation and skin degradation including MMP1, MMP9 and EDN1. Addition of MM and ResTom juice acts to suppress expression of MMP12 and MMP1. Preliminary data from PteroTom juice treatment shows significant induction of MMP12. Addition of ResTom juice was observed to reduce expression levels of COL7A1 and COL17A1 which encode alpha chains of collagen VII and collagen XVII respectively, which act to connect the extracellular matrix to cells in the basal layer. Reduction in these two collagens results in separation of epidermal and dermal layers. Information for this diagram from (Nishie, 2014, Sorrell et al., 2004)

Wound healing represents a complex response within skin. Due to the ethics surrounding *in vivo* wound healing in humans, the majority of wound healing experiments are either performed using cell cultures or animals. However, neither of these experimental procedures are able to accurately portray the complexities of wound healing in human skin as discussed in Chapter 1:. Isolated plant polyphenols or grape extracts have previously been shown to have a positive on wound healing in mouse, human and rat *in vivo* models (Khanna et al., 2002, Hemmati et al., 2014, Wu et al., 2012), however the underlying mechanistic and morphological changes associated with increased healing have not been well studied.

Therefore, the development of the *ex vivo* skin assay offers a method in which we can investigate wound healing on full thickness skin, and the effect that tomato treatments have on wound healing alongside examination of gene expression levels and morphological changes. Although the methodology used in this thesis requires further development to ensure more consistent wound healing, this approach showed a lot of promise for analysis of full thickness wounds, which could offer better insight into the response of wound healing to different treatments compared to cell culture wounds.

An additional benefit of this methodology was the ability to investigate *ex vivo* skin explants from several different donors and across a variety of ages. This allowed us to observe trends with treatments both within donors, and across donors. This is especially beneficial for determining if a response to treatment is donor-specific or more widely observable.

Overall the use of an *ex vivo* skin model in conjunction to cell culture experiments can be used to show in depth changes in skin with different tomato treatments under different pathological conditions.

7.4 Regulation of molecular pathways by tomato extract

The biological activity of several tomato extracts, including MM and ResTom, have been studied very recently using dietary models, and cell-based models in relation to inflammatory bowel disease (Tomlinson et al., 2017, Scarano et al., 2018). Mouse dietary studies showed that polyphenol-enriched tomatoes changed the gut microbiota of healthy mice and suppressed production of pro-inflammatory interleukins (Scarano et al., 2018). Additionally, ResTom juice has been shown to significantly inhibit expression of several proinflammatory cytokines and chemokines, including IL-6, TNFa, and CCL5 compared to MM extract in gut epithelial cells (Tomlinson et al., 2017). However, the biological effects of tomato extract on human skin up until now has not been investigated.

In Chapter 4:microarray analysis revealed that the tomato matrix itself (MM juice) had a significant effect on gene regulation, with several genes involved in anti-inflammatory responses and the maintenance of skin structure showing differential expression from control skin. These data also

correlate with those in the recent study by Tomlinson et al. (2017), which demonstrated suppression of pro-inflammatory signalling pathways with MM juice extracts in isolated colonic epithelial cells. Interestingly, p38 MAPK phosphorylation was observed to be significantly inhibited by tomato extracts (Tomlinson et al., 2017). Inhibition of p38 MAPK has also been observed with topical application of green tea polyphenols in mouse skin and in human epidermal cells treated with pomegranate extract (Katiyar et al., 2001, Zaid et al., 2007). p38 MAPK has several roles in the immune response including induction of pro-inflammatory mediators such as cytokines and MMPs (Cho et al., 2000, Chi et al., 2006). Additionally, p38 activation and feedback is important in the inflammatory response to ultraviolet B-induced skin damage (Brancho et al., 2003). Stress-activated MAP kinase activities are also known to be upregulated in aged human skin and have been indicated to play a key role in pathophysiology of human skin (Chung et al., 2000). Therefore, the associated effects of tomato extracts observed in skin could be due to changes in MAPK activity.

In order to investigate the effect of MM and ResTom juice treatment in a pathological setting, an inflammatory environment was stimulated by treatment with interleukin 1 and oncostatin M. Interestingly, addition of MM and ResTom juice appeared to have a greater effect on gene regulation in the presence of cytokines. Pathway analysis identified several genes including MMP-1, MMP-9, EDN1, and MMP-12 which were significantly down-regulated with MM and ResTom. Interestingly, greater suppression was observed by ResTom compared to MM extracts. qRT-PCR analysis of these genes confirmed the downregulation in expression reported by the micro-array, with ResTom showing greater repressive effects.

Several plant actives have been shown to have regulatory effects on MMPs. Additionally, isolated resveratrol has been investigated in relation to its activity on MMPs, however the reported effect of resveratrol on MMP expression are variable, depending on the cell type studied (Gweon and Kim, 2013, Li et al., 2003).

Several plant compounds including pro-cyanidins (Caton et al., 2010), green tea polyphenols (Maiti et al., 2003) and Quercitin (Tan et al., 2003) have been reported to have repressive effects on angiogenesis, with resveratrol cited as a suppressor of EDN1 (Schmitt et al., 2010, Ruef et al., 2001), correlating with our data.

Within skin explant experiments a tomato juice extract of 10% was used. Although ResTom treatment often exhibited a greater suppressive effect on gene expression levels than MM, this was often not statistically different. As MM juice treatment itself represses several genes to C_T values as low as 34, the further repressive action is not as apparent. Therefore, future studies should investigate the effect of juice extracts at lower concentrations, which may allow for a greater differentiation in gene expression levels to be observed between treatments.

7.5 MMP-12 is significantly repressed with ResTom juice treatment

MMP-12 is an elastase important for the regulation and maintenance of elastic networks in skin (Chen et al., 2005). During skin aging, elastin is known to be degraded leading to the reduced elasticity associated with intrinsically aged skin, and elastosis observed in sun-aged skin (Fisher et al., 2002).

Additional evidence for the critical role of MMP-12 in inflammation and tissue repair mechanisms has been provided by knock-out mice. MMP-12 KO mice have shown a clear involvement of MMP-12 in inflammatory pulmonary diseases (Hautamaki et al., 1997) with MMP-12 shown to be crucial in the recruitment of macrophages, degradation of extracellular matrix in lung tissue (Shapiro et al., 2003), and matrix invasion by macrophages (Shipley et al., 1996). These data suggest that MMP-12 can act to contribute to pathology in inflammation, however there is experimental evidence suggesting protective qualities of MMP-12. For example, MMP-12 has been shown to have a protective effect on corneal fibrosis during wound repair through its inhibition of angiogenesis which helps to promote corneal clarity (Chan et al., 2013).

Microarray analysis identified that MMP-12 expression was significantly inhibited with MM and ResTom treatment in the presence of cytokines. qRT-PCR analysis confirmed the strong downregulation of MMP-12 by both MM and ResTom in the presence of cytokines, and further identified a greater suppressive effect of ResTom on MMP-12 expression.

There is a small amount of evidence of plant polyphenols exhibiting MMP-12 suppression in the literature. Demeule et al. (2000) reported the inhibition of MMP-12 activity by the plant polyphenols epicatechin, epicatechin gallate and epigallocatechin gallate. In the study by Long et al. (2015) mice induced with respiratory syncytial virus (RSV) displayed high expression levels of MMP-12 in addition to significant airway inflammation. However, pre-treatment with resveratrol, markedly reduced MMP-12 expression levels and alleviated airway inflammation. As yet there is apparently no evidence of inhibitory effects associated with topical polyphenol treatment on MMP-12 in skin.

Protein expression analysis of MMP-12 did not correlate with the mRNA expression data, with protein levels appearing to increase with ResTom treatment, at the time-points studied. Similar disparities between mRNA expression and protein levels have been with other MMPs (Lichtinghagen et al., 2002). This suggests that there may be mechanisms such as post-translational modification, or transcriptional splicing affecting protein levels of MMP-12. There have also been reports of post transcriptional regulation of MMPs by microRNAs. MicroRNAs are a family of small, non-coding RNA molecules, which function in post-transcriptional regulation by translational repression or degradation of mRNA. The microRNA miR-452 has been implicated to target MMP-

12 in alveolar macrophages (Graff et al., 2012), however the role of microRNAs in MMP-12 regulation is not well established. As such, MMP-12 protein expression will need to be investigated in more detail, potentially at later time points, to fully understand the mechanisms underlying activity induced by MM and ResTom juice. Therefore, the presence of resveratrol in tomato juice could potentially account for the changes in elastin morphology observed with ResTom and resveratrol treatment.

Finally, to investigate how the change in MMP-12 expression effects the morphology of skin, skin explants were stained with elastin. Several morphological changes in elastin were observable across treatments, with a slight thickening of elastin fibres observed in IL1OSM +ResTom treated skin compared to IL1OSM. These data potentially show a protective effect of polyphenols to inflammatory conditions. Plant polyphenols have been associated with a protective effect on elastic fibre structure, in addition to promotion of elastogenesis, by increasing cross-linking in elastin and promoting a thickening of fibres (Jimenez et al., 2006, Sinha et al., 2014, Wang et al., 2015).

The findings from the microarray analysis have identified differential expression of several genes important in the maintenance of skin structure with MM and ResTom treatment. Additionally, ResTom juice extract often displayed a greater regulatory effect on gene expression levels compared to MM juice and control treatments suggesting a higher biological activity and a synergetic effect between plant actives in ResTom juice.

7.6 PteroTom vs ResTom

Due to the timescale required to produce PteroTom tomatoes, only a small number of experiments were conducted to investigate differences in the biological activity between PteroTom and ResTom. These preliminary experiments do indicate potential differences in activity of the two tomato juices and are discussed below.

In full skin explants, a preliminary experiment revealed that 1-day treatment PteroTom resulted in a significant induction of MMP-12 steady state mRNA levels, compared to levels seen in either control or MM treated skin. This high induction had not previously been observed in any other donors with tomato extract treatment. Although no definite conclusions can be drawn, this data is extremely interesting and suggests a very different response with PteroTom treatment. If these findings are substantiated in the future, PteroTom juice may have future roles in treatment of skin fibrosis where elastin has been identified as an important component (Nakasaki et al., 2015).

LCMS IT-TOF analysis identified a lack of pterostilbene in aqueous tomato extracts, therefore in order to be able to fully determine differences in biological activity of PteroTom and Hi-Resv extracts, methanol extracts were prepared for use in cell mono-cultures. From these experiments,

PteroTom was shown to have potentially higher biological activity than Hi-Resv ResTom. qRT-PCR analysis showed greater suppression of MMP-9 and MMP-1 with PteroTom compared to Hi-Resv, and effective repression of EGF induced gene expression (Findings are summarised in Figure 7.2).

This correlates with numerous cancer studies which have reported a significant inhibitory effect of Pterostilbene on MMP-9 expression (Pan et al., 2011, Li et al., 2016a). Additionally, a strong synergistic effect has been observed between pterostilbene combined with other polyphenols such as quercetin (Ferrer et al., 2005, Kostin et al., 2012), which could account for the higher activity of PteroTom observed. Pterostilbene has been shown to be a strong inhibitor of MMP-9, by blocking protein-kinase C/MAPK/PI_3/NF-$_K$B and AP-1 signalling pathways (Pan et al., 2009). However, it is also known that EGF is one of several inflammatory cytokines that induce MMP-9 expression (Pan et al., 2009), therefore the ability of PteroTom to suppress EGF activity may in part account for the inhibition of MMP-9 observed.

PteroTom treatment of both whole skin and keratinocytes showed an inducing effect on MMP-12 expression, with a much more pronounced effect seen in whole-skin than keratinocytes. However, treatment of fibroblasts with PteroTom resulted in inhibition of MMP-12, suggesting a differential effect of pterostilbene on different cell types. In the study by Dewi et al. (2015) pterostilbene was shown to have anti-proliferative effects on rat hepatoma cells, however showed little effect on the proliferation of either rat myoblasts or skin fibroblasts. This highlights how the effect of an extract treatment can be different overall in skin compared to isolated cells, and the importance of testing extracts on whole skin explants to observe the true effect of a compound. Finally, this data may suggest that the observed MMP-12 inhibition in whole skin correlates to expression of keratinocytes, however as MMP-12 in relation to PteroTom skin was only analysed in one donor, further experiments need to be performed to validate this finding.

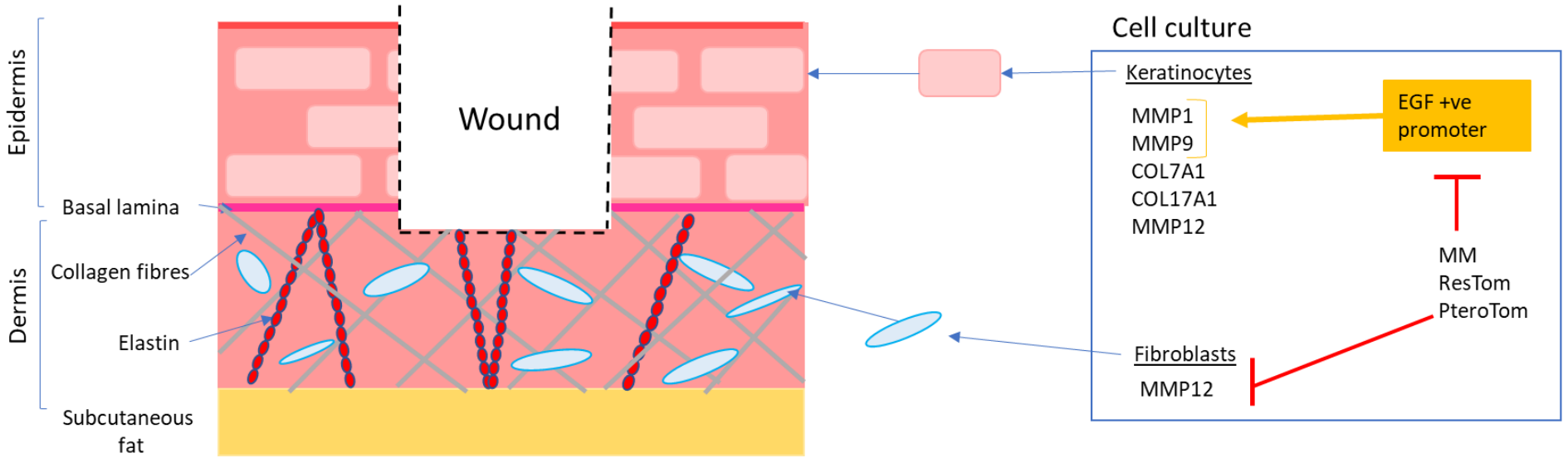

Figure 7.2 Summary of key findings from wound healing studies

Wound healing of full thickness skin leads to varied wound healing responses, with IL1/OSM treatment inhibiting wound healing. Keratinocyte and Fibroblast monocultures were used to investigate affect of tomato extract on individual skin cell types. Keratinocytes showed reduced levels of wound closure with EGF and ResTom/PteroTom treatment.Keratinocytes displayed increased MMP1 and MMP9, with EGF treatment, and decreased expression of MMP12. Co-treatment of wounds with EGF+ MM/ResTom repressed gene induction by EGF.Fibroblast treatment with ResTom and PteroTom treatment repressed MMP12, with PteroTom extract showing enhanced inhibition of MMP12 compared to ResTom.

7.7 Future work

7.7.1 Investigating mechanisms underlying changes in gene expression in whole skin

Microarray analysis, and pathway analysis showed significant changes in the regulation of several different pathways in whole skin. Although this methodology allows us to see gene changes in a model representative of human skin, understanding the mechanisms underlying these effects are difficult to uncover. For example, gene expression analyses are performed using RNA extracted from whole skin explants, therefore RNA expression is representative of all the cells within the skin explants. Although this enables to see the overall changes in gene expression across skin, we are not able to determine the cells in which the gene expression changes are taking place. In order to fully understand the responses to ResTom and PteroTom juice, it is therefore important to do parallel experiments of mono-cultures and full thickness experiments. Whilst initial attempts at such comparisons were made here due to the time restrictions of my research, I was not possible able to explore gene expression changes in all cell types individually and how this may relate to the observations in whole skin

Future studies in primary human skin keratinocytes, fibroblasts and dermal endothelial cells as well as resident immune system cells would be appropriate. In addition, immunocytochemistry in skin explants of proteins whose gene expression was altered would help to define the contribution of different cell types to changes observed.

7.7.2 Developing PteroTom juice for treatments

Initial experiments comparing the biological activity of ResTom to PteroTom are highly suggestive that PteroTom has an alternative biological activity compared to ResTom, however further experiments are required to confirm these observations. Additionally, comparison experiments of PteroTom compared to ResTom should be performed on *ex vivo* skin explants. Due to the observation that PteroTom juice does not contain quantifiable levels of pterostilbene, future experiments should be conducted using methanol-based tomato extracts in addition to aqueous extracts. This would provide us with important information concerning the biological activity of PteroTom aqueous extracts vs methanol-based extracts, as well as comparisons to ResTom biological activity. The determination of aqueous and methanol-based extract activity and LCMS IT-TOF evaluation of concentration, will be crucial in considerations when developing treatments utilising tomato extracts.

7.7.3 Further investigating biological activity of tomato

With the development of a robust experiment for analysis of treatments on full thickness skin, in culture, there are several opportunities to further develop the research platform. Previous studies have suggested possible synergistic effects between multiple plant phytochemicals, leading to an

overall biological activity in models where mixtures of phytochemicals are added compared to individual compounds (Kowalczyk et al., 2010). Therefore, tomato extract containing several biologically active phytochemicals offers a unique opportunity to investigate biological activities associated with tomatoes containing different combinations of biologically active compounds.

With the production of a working system for the synthesis of pterostilbene, in addition to tomato lines producing high levels of anthocyanin and flavanols we have an effective toolbox which we can use for the development of new tomato lines synthesising different combinations of biologically active phytochemicals. Current research has shown high biological activity associated with stilbenes, flavonols and anthocyanins, however, as yet it is unclear how these compounds act together, and the overall biological activity. Using the *ex vivo* skin explant model it is possible to investigate several different tomato extracts, and the how different compositions of plant phytochemicals interact with human skin.

Appendices

Table S 1: Primer sequences used for Plant research.

Primers were designed using Primer3Plus open webs software, unless stated, and purchased via Sigma Aldrich. Underlined primer sequences indicate gateway specific sequence.

Gene	Primer Name	Purpose	Primer sequence (5'-3')
ROMT	ROMT-F	Gene amplification from *Vitis vinifera* (Jeong et al., 2014)	GATACATGGATTTGGCAAACGGTGTGA
ROMT	ROMT-R	Gene amplification from *Vitis vinifera* (Jeong et al., 2014)	ATAGAGCATCAAGGATAAACCTCAATGA
ROMT	ROMT-Bis F	Gene amplification from *Vitis vinifera*	GATACATGGATTTGGCAAACGGTGTGA
ROMT	ROMT-BIS R	Gene amplification from *Vitis vinifera*	ATAGAGCATCAAGGATAAACCTCAATGA
StSy	Res-F	genotyping	ACCCCCGACCACTGTGTCTACCA
StSy	Res-R	genotyping	GATTACAGCTGCAGACCCATCACCA
ROMT	ROMT end FORWARD	Genotyping	ATTCTTGGATGCTGGTTTCAGT
ROMT	ROMT end REVERSE	Genotyping	ATGATTCCAGACATGAGCTTGA
StSy	END-STSY-F	Genotyping	GAAGGATTGGATTGGGGAGTATTA

StSy	END STSY-R	Genotyping	GTGCTCGCTCTTAGTGACCC
E8 promoter	E8 I FORWARD	Genotyping	GCCACTTGTCCAATTGTTGA
AtMYB12	Myb-Pb-F	Genotyping	CGAGTAGGTCCGCTATGAAACCA
AtMYB12	Myb-Pb-R	Genotyping	TGTTATGCAACTCCCCATCACCA
Kanamycin resistance	NPTII REV	Genotyping	TATTCGGCAAGCAGGCATCG
Kanamycin resistance	NPTII- FOR	Genotyping	GGATTGCACGCAGGTTCTCC
ROMT	GW-ROMT F	GW cloning	GGGGACAAGTTTGTACAAAAAAGCAGGCT TAATGGATTTGGCAAACGGTGTGATATCA
ROMT	GW-ROMT R	GW cloning	GGGGACCACTTTGTACAAGAAAGCTGG GTAGAGCATCAAGGATAAACCTCAATGA
ROMT	PROLINE-F	Site-directed mutagenesis	GTGTTAGATCTCCCCCACGTGGGTTGCTGGC
ROMT	PROLINE-R	Site directed mutagenesis	GCCAGCAACCACGTGGGGGAGATCTAACAC

Table S 2 : Sequences and efficiency values of primers for real time PCR used to investigate Stilbene synthase and Resveratrol-o-methyltransferase gene expression.

Gene	Primer	Sequence (5' to 3')	Efficiency
ROMT	F	ACTCAAGTGGATACTGCACGA	105.44
	R	CTACCCGGGGCGAAAATCAT	
StSy	F	ACCATCCTAGCCATTGGCAC	101.84
	R	TTGTCACATATGCGATTGAACTTCT	

Table S 3 Human primer and probe sequences for genes studied by qRT-PCR.

Primers and probes for MMPs and 18S were designed using primer express software (Applied Biosystems) by Dr Caroline Pennington. Primers and probes were designed using the UPL assay design centre. Primers for TNF-a and EDN1 were designed by Dr Damon Bevan. All given probes are labelled with FAM (5') and tetramethylrhodamine (TAMRA) (3').

Symbol	Primer probes and sequences (5'-3')	
18S	Forward Primer	GCCGCTAGAGGTGAAATTCTTG
	Reverse Primer	CATTCTTGGCAAATGCTTTCG
	Probe	ACCGGCGCAAGACGGA
MMP-1	Forward Primer	AAGATGAAAGGTGGACCAACAATT
	Reverse Primer	CCAAGAGAATGGCCGAGTTC
	Probe	CAGAGAGTACAACTTACATCGTGTTGCGGCTC
MMP-9	Forward Primer:	AGGCGCTCATGTACCCTATGTAC
	Reverse Primer:	GCCGTGGCTCAGGTTCA
	Probe:	CATCCGGCACCTCTATGGTCCTCG
MMP-12	Forward Primer:	CGCCTCTCTGCTGATGACATAC
	Reverse Primer:	GGTAGTGACAGCATCAAAACTCAAA
	Probe:	TCCCTGTATGGAGACCCAAAAGAGAACCA
BNC1	Forward Primer	TGGAGGGCTGTAATGCTACC
	Reverse Primer	GGTGGAGGTTTAGGTTTGAGC
	UPL probe #	68
Col7a1	Forward Primer	GCTGGTGCTGCCTTTCTCT
	Reverse Primer	TCCAGGCCGAACTCTGTC
	UPL Probe #	71
Col17a1	Forward Primer	CTGCTCTTCGGCCTCATT
	Reverse Primer	GGCAGTATGCTCCTCCTGAT
	UPL probe #	78
EDN1	Forward Primer	GCTCGTCCCTGATGGATAAA
	Reverse Primer	GTTGACCCAAATGATGTCCA
	UPL Probe #	29
LTB	Forward Primer	GGCGGTGCCTATCACTGT
	Reverse Primer	TTCTGAAACCCCAGTCCTTG
	UPL probe #	76
TNF-A	Forward Primer	CGCTCCCCAAGAAGACAG
	Reverse Primer	CTGCCACGATCAGGAAGG
	UPL probe #	57

Table S 4 Mouse primer and probe sequences for genes studied by qRT-PCR.

Primers and probes for MMPs and 18S were designed using primer express software (Applied Biosystems) by Dr Caroline Pennington. All given probes are labelled with FAM (5') and tetramethylrhodamine (TAMRA) (3').

Symbol	Primer probes and sequences (5'-3')	
MMP12	Forward Primer	GAAACCCCCATCCTTGACAA
	Reverse Primer	TTCCACCAGAAGAACCAGTCTTTAA
	Probe	AGTCCACCATCAACTTTCTGTCACCAAAGC

Recipes of Media

Lysogeny Broth

Tryptone	10
Yeast Extract	5
NaCl	10
Distilled water	1 L (total volume)
+ Agar (for LB agar)	15g/L

MMA

Tryptone	10
Yeast Extract	5
NaCl	10
Distilled water	1 L (total volume)
+ Agar (for LB agar)	15g/L

Tomato transformation growth media and supplements

Seed germination medium

1x Murashige and skoog (MS) medium + Vitamins (Melford)

6 g/l Agarose

adjusted to pH 5.8 with KOH before autoclaving.

Cell suspension

1x MS+vitamins medium	1x (4.4g)
10g Sucrose	10g
6g Agarose	6g

Adjusted to pH 5.7 with KOH before autoclaving. After autoclaving filter sterilised and add 0.5mg 2,4-D (in ethanol, prepared by Matthew Smoker, Sainsbury Lab)

Regeneration-1

1x MS +Nitch's vitamins (Melford)

100mg myo inositol

20g sucrose

4g Agargel

Adjusted to pH 6 with KOH before autoclaving. After autoclaving filter sterilise and add 2mg Zeatin riboside (Melford), 320mg Timentin (Melford), 100mg Kanamycin.

Regeneration 2

1x MS +Nitch's vitamins (Melford)

100mg myo inositol

20g sucrose

4g Agargel

Adjusted to pH 6 with KOH before autoclaving. After autoclaving filter sterilise and add 2mg Zeatin riboside (Melford), 320mg Timentin (Melford), 100mg Kanamycin, and 250mg Cefotaxime (Melford)

Rooting media (1L)

0.5 x MS + vitamins (Melford)

5g Sucrose

2.25g Gelrite

Adjusted to pH 6 with KOH before autoclaving. After autoclaving filter sterilise and add 320mg Timentin (Melford) and 100mg Kanamycin.

References

ADAMS, L. S., PHUNG, S., YEE, N., SEERAM, N. P., LI, L. & CHEN, S. 2010. Blueberry Phytochemicals Inhibit Growth and Metastatic Potential of MDA-MB-231 Breast Cancer Cells through Modulation of the Phosphatidylinositol 3-Kinase Pathway. *Cancer Research,* 70**,** 3594-3605.

ADHAMI, V. M., AFAQ, F. & AHMAD, N. 2003. Suppression of ultraviolet B exposure-mediated activation of NF-kappaB in normal human keratinocytes by resveratrol. *Neoplasia,* 5**,** 74-82.

AFAQ, F., ADHAMI, V. M. & AHMAD, N. 2003. Prevention of short-term ultraviolet B radiation-mediated damages by resveratrol in SKH-1 hairless mice. *Toxicology and Applied Pharmacology,* 186**,** 28-37.

ASADI, S. Y., PARSAEI, P., KARIMI, M., EZZATI, S., ZAMIRI, A., MOHAMMADIZADEH, F. & RAFIEIAN-KOPAEI, M. 2013. Effect of green tea (Camellia sinensis) extract on healing process of surgical wounds in rat. *International Journal of Surgery,* 11**,** 332-337.

ASCENSIÓN, M.-M., A., M.-C. J., KARLA, R.-E., M., C. R., JAVIER, P. & ROQUE, B.-M. 2016. Production of highly bioactive resveratrol analogues pterostilbene and piceatannol in metabolically engineered grapevine cell cultures. *Plant Biotechnology Journal,* 14**,** 1813-1825.

AVCI, P., SADASIVAM, M., GUPTA, A., DE MELO, W. C. M. A., HUANG, Y.-Y., YIN, R., RAKKIYAPPAN, C., KUMAR, R., OTUFOWORA, A., NYAME, T. & HAMBLIN, M. R. 2013. Animal models of skin disease for drug discovery. *Expert opinion on drug discovery,* 8**,** 331-355.

AZACHI, M., YATUV, R., KATZ, A., HAGAY, Y. & DANON, A. 2014. A novel red grape cells complex: health effects and bioavailability of natural resveratrol. *International Journal of Food Sciences & Nutrition,* 65**,** 848-855.

BÄCKER, V. 2012. *ImageJ Macro Tool Sets for Biological Image Analysis*.

BACKVALL, H., WASSBERG, C., BERNE, B. & PONTEN, F. 2002. Similar UV responses are seen in a skin organ culture as in human skin in vivo. *Experimental Dermatology,* 11**,** 349-356.

BAI, Y., YANG, H., ZHANG, G., HU, L., LEI, Y., QIN, Y., YANG, Y., WANG, Q., LI, R. & MAO, Q. 2017. Inhibitory effects of resveratrol on the adhesion, migration and invasion of human bladder cancer cells. *Mol Med Rep,* 15**,** 885-889.

BARRIENTOS, S., STOJADINOVIC, O., GOLINKO, M. S., BREM, H. & TOMIC-CANIC, M. 2008. PERSPECTIVE ARTICLE: Growth factors and cytokines in wound healing. *Wound Repair and Regeneration,* 16**,** 585-601.

BASTIANETTO, S., MENARD, C. & QUIRION, R. 2014. Neuroprotective action of resveratrol. *Biochim Biophys Acta*.

BATCHELDER, R. J., CALDER, R. J., THOMAS, C. P. & HEARD, C. M. 2004. In vitro transdermal delivery of the major catechins and caffeine from extract of Camellia sinensis. *International Journal of Pharmaceutics,* 283**,** 45-51.

BENFEY, P. N. & CHUA, N. 1990. The cauliflower mosaic virus 35S promoter: Combinatorial regulation of transcription in plants. (Cover story). *Science,* 250**,** 959.

BERNSTEIN, E. F., CHEN, Y. Q., TAMAI, K., SHEPLEY, K. J., RESNIK, K. S., ZHANG, H., TUAN, R., MAUVIEL, A. & UITTO, J. 1994. Enhanced elastin and fibrillin gene expression in chronically photodamaged skin. *Journal of investigative dermatology,* 103**,** 182-186.

BHULLAR, S., DATTA, S., ADVANI, S., CHAKRAVARTHY, S., GAUTAM, T., PENTAL, D. & BURMA, P. K. 2007. Functional analysis of cauliflower mosaic virus 35S promoter: re-evaluation of the role of subdomains B5, B4 and B2 in promoter activity. *Plant Biotechnology Journal,* 5**,** 696-708.

BISSETT, D., HANNONAND, D. & ORR, T. 1987. AN ANIMAL MODEL OF SOLAR-AGED SKIN: HISTOLOGICAL, PHYSICAL, and VISIBLE CHANGES IN UV-IRRADIATED HAIRLESS MOUSE SKIN*. *Photochemistry and Photobiology,* 46**,** 367-378.

BLAKE, M. J., GERSHON, D., FARGNOLI, J. & HOLBROOK, N. J. 1990. Discordant expression of heat shock protein mRNAs in tissues of heat-stressed rats. *Journal of Biological Chemistry,* 265**,** 15275-9.

BONIFACE, K., DIVEU, C., MOREL, F., PEDRETTI, N., FROGER, J., RAVON, E., GARCIA, M., VENEREAU, E., PREISSER, L., GUIGNOUARD, E., GUILLET, G., DAGREGORIO, G., PENE, J., MOLES, J. P., YSSEL, H., CHEVALIER, S., BERNARD, F. X., GASCAN, H. & LECRON, J. C. 2007. Oncostatin M secreted by skin infiltrating T lymphocytes is a potent keratinocyte activator involved in skin inflammation. *J Immunol,* 178**,** 4615-22.

BONIFATI, C., MUSSI, A., CARDUCCI, M., PITTARELLO, A., D'AURIA, L., VENUTI, A., BAGNATO, A., SALANI, D., FAZIO, M. & AMEGLIO, F. 1998. Endothelin-1 levels are increased in sera and lesional skin extracts of psoriatic patients and correlate with disease severity. *ACTA DERMATOVENEREOLOGICA-STOCKHOLM-,* 78**,** 22-26.

BOOCOCK, D. J., FAUST, G. E., PATEL, K. R., SCHINAS, A. M., BROWN, V. A., DUCHARME, M. P., BOOTH, T. D., CROWELL, J. A., PERLOFF, M., GESCHER, A. J., STEWARD, W. P. & BRENNER, D. E. 2007. Phase I dose escalation pharmacokinetic study in healthy volunteers of resveratrol, a potential cancer chemopreventive agent. *Cancer Epidemiol Biomarkers Prev,* 16**,** 1246-52.

BOU-GHARIOS, G., OSMAN, J., BLACK, C. & OLSEN, I. 1994. Excess matrix accumulation in scleroderma is caused partly by differential regulation of stromelysin and TIMP-1 synthesis. *Clinica Chimica Acta,* 231**,** 69-78.

BOUKAMP, P., PETRUSSEVSKA, R. T., BREITKREUTZ, D., HORNUNG, J., MARKHAM, A. & FUSENIG, N. E. 1988. Normal keratinization in a spontaneously immortalized aneuploid human keratinocyte cell line. *J Cell Biol,* 106**,** 761-71.

BRAKENHIELM, E., CAO, R. & CAO, Y. 2001. Suppression of angiogenesis, tumor growth, and wound healing by resveratrol, a natural compound in red wine and grapes. *Faseb j,* 15**,** 1798-800.

BRANCHO, D., TANAKA, N., JAESCHKE, A., VENTURA, J.-J., KELKAR, N., TANAKA, Y., KYUUMA, M., TAKESHITA, T., FLAVELL, R. A. & DAVIS, R. J. 2003. Mechanism of p38 MAP kinase activation in vivo. *Genes & Development,* 17**,** 1969-1978.

BREUER, K., FOROUSHANI, A. K., LAIRD, M. R., CHEN, C., SRIBNAIA, A., LO, R., WINSOR, G. L., HANCOCK, R. E., BRINKMAN, F. S. & LYNN, D. J. 2013. InnateDB: systems biology of innate immunity and beyond--recent updates and continuing curation. *Nucleic Acids Res,* 41**,** D1228-33.

BUTELLI, E., TITTA, L., GIORGIO, M., MOCK, H.-P., MATROS, A., PETEREK, S., SCHIJLEN, E. G. W. M., HALL, R. D., BOVY, A. G., LUO, J. & MARTIN, C. 2008. Enrichment of tomato fruit with health-promoting anthocyanins by expression of select transcription factors. *Nature Biotechnology,* 26**,** 1301-1308.

BUTLER, G. S., DEAN, R. A., MORRISON, C. J. & OVERALL, C. M. 2010. Identification of Cellular MMP Substrates Using Quantitative Proteomics: Isotope-Coded Affinity Tags (ICAT) and Isobaric Tags for Relative and Absolute Quantification (iTRAQ). *In:* CLARK, I. M. (ed.) *Matrix Metalloproteinase Protocols.* Totowa, NJ: Humana Press.

CASAGRANDE, R., GEORGETTI, S. R., VERRI, W. A., JABOR, J. R., SANTOS, A. C. & FONSECA, M. J. V. 2006. Evaluation of functional stability of quercetin as a raw material and in different topical formulations by its antilipoperoxidative activity. *AAPS PharmSciTech,* 7**,** E64-E71.

CATON, P. W., POTHECARY, M. R., LEES, D. M., KHAN, N. Q., WOOD, E. G., SHOJI, T., KANDA, T., RULL, G. & CORDER, R. 2010. Regulation of Vascular Endothelial Function by Procyanidin-Rich Foods and Beverages. *Journal of Agricultural and Food Chemistry,* 58**,** 4008-4013.

CHAN, M. F., LI, J., BERTRAND, A., CASBON, A. J., LIN, J. H., MALTSEVA, I. & WERB, Z. 2013. Protective effects of matrix metalloproteinase-12 following corneal injury. *J Cell Sci,* 126**,** 3948-60.

CHANG, J., RIMANDO, A., PALLAS, M., CAMINS, A., PORQUET, D., REEVES, J., SHUKITT-HALE, B., SMITH, M. A., JOSEPH, J. A. & CASADESUS, G. 2012. Low-dose pterostilbene, but not resveratrol, is a potent neuromodulator in aging and Alzheimer's disease. *Neurobiology of Aging,* 33**,** 2062-2071.

CHEN, G., GHARIB, T. G., HUANG, C.-C., TAYLOR, J. M. G., MISEK, D. E., KARDIA, S. L. R., GIORDANO, T. J., IANNETTONI, M. D., ORRINGER, M. B., HANASH, S. M.

& BEER, D. G. 2002. Discordant Protein and mRNA Expression in Lung Adenocarcinomas. *Molecular & Cellular Proteomics,* 1**,** 304-313.
CHEN, J. D., KIM, J. P., ZHANG, K., SARRET, Y., WYNN, K. C., KRAMER, R. H. & WOODLEY, D. T. 1993. Epidermal growth factor (EGF) promotes human keratinocyte locomotion on collagen by increasing the alpha 2 integrin subunit. *Exp Cell Res,* 209**,** 216-23.
CHEN, Y. Q., BERNSTEIN, E. F., TAMAI, K., SHEPLEY, K. J., RESNIK, K. S., ZHANG, H. U. I., TUAN, R., MAUVIEL, A. & UITTO, J. 1994. Enhanced Elastin and Fibrillin Gene Expression in Chronically Photodamaged Skin. *Journal of Investigative Dermatology,* 103**,** 182-186.
CHEN, Z., SEO, J. Y., KIM, Y. K., LEE, S. R., KIM, K. H., CHO, K. H., EUN, H. C. & CHUNG, J. H. 2005. Heat Modulation of Tropoelastin, Fibrillin-1, and Matrix Metalloproteinase-12 in Human Skin In Vivo. *Journal of Investigative Dermatology,* 124**,** 70-78.
CHI, H., BARRY, S. P., ROTH, R. J., WU, J. J., JONES, E. A., BENNETT, A. M. & FLAVELL, R. A. 2006. Dynamic regulation of pro- and anti-inflammatory cytokines by MAPK phosphatase 1 (MKP-1) in innate immune responses. *Proceedings of the National Academy of Sciences,* 103**,** 2274-2279.
CHIOU, Y.-S., TSAI, M.-L., NAGABHUSHANAM, K., WANG, Y.-J., WU, C.-H., HO, C.-T. & PAN, M.-H. 2011. Pterostilbene Is More Potent than Resveratrol in Preventing Azoxymethane (AOM)-Induced Colon Tumorigenesis via Activation of the NF-E2-Related Factor 2 (Nrf2)-Mediated Antioxidant Signaling Pathway. *Journal of Agricultural and Food Chemistry,* 59**,** 2725-2733.
CHO, A., GRAVES, J. & REIDY, M. A. 2000. Mitogen-activated protein kinases mediate matrix metalloproteinase-9 expression in vascular smooth muscle cells. *Arterioscler Thromb Vasc Biol,* 20**,** 2527-32.
CHONG, J. L., POUTARAUD, A. & HUGUENEY, P. 2009. Metabolism and roles of stilbenes in plants. *Plant Science,* 177**,** 143-155.
CHUNG, J. H., KANG, S., VARANI, J., LIN, J., FISHER, G. J. & VOORHEES, J. J. 2000. Decreased Extracellular-Signal-Regulated Kinase and Increased Stress-Activated MAP Kinase Activities in Aged Human Skin In Vivo. *Journal of Investigative Dermatology,* 115**,** 177-182.
CHUNG, J. H., SEO, J. Y., LEE, M. K., EUN, H. C., LEE, J. H., KANG, S., FISHER, G. J. & VOORHEES, J. J. 2002. Ultraviolet Modulation of Human Macrophage Metalloelastase in Human Skin In Vivo. *Journal of Investigative Dermatology,* 119**,** 507-512.
COLLIVER, S., BOVY, A., COLLINS, G., MUIR, S., ROBINSON, S., DE VOS, C. H. R. & VERHOEYEN, M. E. 2002. Improving the nutritional content of tomatoes through reprogramming their flavonoid biosynthetic pathway. *Phytochemistry Reviews,* 1**,** 113-123.
COPPA, T., LAZZE, M. C., CAZZALINI, O., PERUCCA, P., PIZZALA, R., BIANCHI, L., STIVALA, L. A., FORTI, L., MACCARIO, C., VANNINI, V. & SAVIO, M. 2011. Structure-activity relationship of resveratrol and its analogue, 4,4'-dihydroxy-trans-stilbene, toward the endothelin axis in human endothelial cells. *J Med Food,* 14**,** 1173-80.
DABELSTEEN, E., GRØN, B., MANDEL, U. & MACKENZIE, I. 1998. Altered Expression of Epithelial Cell Surface Glycoconjugates and Intermediate Filaments at the Margins of Mucosal Wounds. *Journal of Investigative Dermatology,* 111**,** 592-597.
DANSO, M. O., BERKERS, T., MIEREMET, A., HAUSIL, F. & BOUWSTRA, J. A. 2015. An ex vivo human skin model for studying skin barrier repair. *Exp Dermatol,* 24**,** 48-54.
DE LA LASTRA, C. A. & VILLEGAS, I. 2005. Resveratrol as an anti-inflammatory and anti-aging agent: mechanisms and clinical implications. *Mol Nutr Food Res,* 49**,** 405-30.
DEMEULE, M., BROSSARD, M., PAGÉ, M., GINGRAS, D. & BÉLIVEAU, R. 2000. Matrix metalloproteinase inhibition by green tea catechins. *Biochimica et Biophysica Acta (BBA) - Protein Structure and Molecular Enzymology,* 1478**,** 51-60.
DEWI, N. I., YAGASAKI, K. & MIURA, Y. 2015. Anti-proliferative effect of pterostilbene on rat hepatoma cells in culture. *Cytotechnology,* 67**,** 671-680.

DEYRIEUX, A. F. & WILSON, V. G. 2007. In vitro culture conditions to study keratinocyte differentiation using the HaCaT cell line. *Cytotechnology,* 54**,** 77-83.
DINARELLO, C. A. 1988. Biology of interleukin 1. *The FASEB Journal,* 2**,** 108-115.
DINARELLO, C. A. 2011. Interleukin-1 in the pathogenesis and treatment of inflammatory diseases. *Blood,* 117**,** 3720-3732.
DORING, G. 1994. The role of neutrophil elastase in chronic inflammation. *Am J Respir Crit Care Med,* 150**,** S114-7.
DUNN, L., PROSSER, H. C., TAN, J. T., VANAGS, L. Z., NG, M. K. & BURSILL, C. A. 2013. Murine model of wound healing. *J Vis Exp***,** e50265.
EMERY, L. A., TRIPATHI, A., KING, C., KAVANAH, M., MENDEZ, J., STONE, M. D., DE LAS MORENAS, A., SEBASTIANI, P. & ROSENBERG, C. L. 2009. Early Dysregulation of Cell Adhesion and Extracellular Matrix Pathways in Breast Cancer Progression. *The American Journal of Pathology,* 175**,** 1292-1302.
FARRIS, P., YATSKAYER, M., CHEN, N., KROL, Y. & ORESAJO, C. 2014. Evaluation of efficacy and tolerance of a nighttime topical antioxidant containing resveratrol, baicalin, and vitamin e for treatment of mild to moderately photodamaged skin. *J Drugs Dermatol,* 13**,** 1467-72.
FERRER, P., ASENSI, M., SEGARRA, R., ORTEGA, A., BENLLOCH, M., OBRADOR, E., VAREA, M. T., ASENSIO, G., JORDÁ, L. & ESTRELA, J. M. 2005. Association between Pterostilbene and Quercetin Inhibits Metastatic Activity of B16 Melanoma. *Neoplasia,* 7**,** 37-47.
FISHER, G. J., KANG, S., VARANI, J., BATA-CSORGO, Z., WAN, Y., DATTA, S. & VOORHEES, J. J. 2002. Mechanisms of photoaging and chronological skin aging. *Archives Of Dermatology,* 138**,** 1462-1470.
FISHER, G. J., WANG, Z., DATTA, S. C., VARANI, J., KANG, S. & VOORHEES, J. J. 1997. Pathophysiology of Premature Skin Aging Induced by Ultraviolet Light. *New England Journal of Medicine,* 337**,** 1419-1429.
FLISIAK, I., SZTERLING-JAWOROWSKA, M., BARAN, A. & ROGALSKA-TARANTA, M. 2014. Effect of psoriasis activity on epidermal growth factor (EGF) and the concentration of soluble EGF receptor in serum and plaque scales. *Clin Exp Dermatol,* 39**,** 461-7.
GALIANO, R. D., MICHAELS, V., JOSEPH, DOBRYANSKY, M., LEVINE, J. P. & GURTNER, G. C. 2004. Quantitative and reproducible murine model of excisional wound healing. *Wound Repair and Regeneration,* 12**,** 485-492.
GALKOWSKA, H., WOJEWODZKA, U. & OLSZEWSKI, W. L. 2006. Chemokines, cytokines, and growth factors in keratinocytes and dermal endothelial cells in the margin of chronic diabetic foot ulcers. *Wound Repair Regen,* 14**,** 558-65.
GANESAN, S., FARIS, A. N., COMSTOCK, A. T., CHATTORAJ, S. S., CHATTORAJ, A., BURGESS, J. R., CURTIS, J. L., MARTINEZ, F. J., ZICK, S., HERSHENSON, M. B. & SAJJAN, U. S. 2010. Quercetin prevents progression of disease in elastase/LPS-exposed mice by negatively regulating MMP expression. *Respiratory Research,* 11**,** 131.
GAYLARDE PM FAU - SARKANY, I. & SARKANY, I. Cell migration and DNA synthesis in organ culture of human skin.
GEORGE, J., SINGH, M., SRIVASTAVA, A. K., BHUI, K., ROY, P., CHATURVEDI, P. K. & SHUKLA, Y. 2011. Resveratrol and Black Tea Polyphenol Combination Synergistically Suppress Mouse Skin Tumors Growth by Inhibition of Activated MAPKs and p53. *PLOS ONE,* 6**,** e23395.
GIALELI, C., THEOCHARIS, A. D. & KARAMANOS, N. K. 2011. Roles of matrix metalloproteinases in cancer progression and their pharmacological targeting. *The FEBS journal,* 278**,** 16-27.
GLINOS, G. D., VERNE, S. H., ALDAHAN, A. S., LIANG, L., NOURI, K., ELLIOT, S., GLASSBERG, M., CABRERA DEBUC, D., KORU-SENGUL, T., TOMIC-CANIC, M. & PASTAR, I. 2017. Optical coherence tomography for assessment of epithelialization in a human ex vivo wound model. *Wound Repair and Regeneration,* 25**,** 1017-1026.
GRAFF, J. W., POWERS, L. S., DICKSON, A. M., KIM, J., REISETTER, A. C., HASSAN, I. H., KREMENS, K., GROSS, T. J., WILSON, M. E. & MONICK, M. M. 2012. Cigarette

Smoking Decreases Global MicroRNA Expression in Human Alveolar Macrophages. *PLOS ONE,* 7**,** e44066.
GUO, Y., XIAO, P., LEI, S., DENG, F., XIAO, G. G., LIU, Y., CHEN, X., LI, L., WU, S., CHEN, Y., JIANG, H., TAN, L., XIE, J., ZHU, X., LIANG, S. & DENG, H. 2008. How is mRNA expression predictive for protein expression? A correlation study on human circulating monocytes. *Acta Biochimica et Biophysica Sinica,* 40**,** 426-436.
GUY, P., DARIO, B., NOAM, G., ALEJANDRO, S.-P., EFRAT, W., MARGARITA, P., DIEGO, O., ANTONIO, G., ILANA, R. & ASAPH, A. 2016. Elucidation of the first committed step in betalain biosynthesis enables the heterologous engineering of betalain pigments in plants. *New Phytologist,* 210**,** 269-283.
GWEON, E. J. & KIM, S. J. 2013. Resveratrol induces MMP-9 and cell migration via the p38 kinase and PI-3K pathways in HT1080 human fibrosarcoma cells. *Oncol Rep,* 29**,** 826-34.
HAM, S. L., NASROLLAHI, S., SHAH, K. N., SOLTISZ, A., PARUCHURI, S., YUN, Y. H., LUKER, G. D., BISHAYEE, A. & TAVANA, H. 2015. Phytochemicals potently inhibit migration of metastatic breast cancer cells. *Integr Biol (Camb),* 7**,** 792-800.
HARPER, C. E., PATEL, B. B., WANG, J., ARABSHAHI, A., ELTOUM, I. A. & LAMARTINIERE, C. A. 2007. Resveratrol suppresses prostate cancer progression in transgenic mice. *Carcinogenesis,* 28**,** 1946-1953.
HAUTAMAKI, R. D., KOBAYASHI, D. K., SENIOR, R. M. & SHAPIRO, S. D. 1997. Requirement for macrophage elastase for cigarette smoke-induced emphysema in mice. *Science,* 277**,** 2002-4.
HEMMATI, A. A., FOROOZAN, M., HOUSHMAND, G., MOOSAVI, Z. B., BAHADORAM, M. & MARAM, N. S. 2014. The topical effect of grape seed extract 2% cream on surgery wound healing. *Glob J Health Sci,* 7**,** 52-8.
HEO, K. T., KANG, S.-Y. & HONG, Y.-S. 2017. De novo biosynthesis of pterostilbene in an Escherichia coli strain using a new resveratrol O-methyltransferase from Arabidopsis. *Microbial Cell Factories,* 16**,** 30.
HERMANNS, H. M. 2015. Oncostatin M and interleukin-31: Cytokines, receptors, signal transduction and physiology. *Cytokine Growth Factor Rev,* 26**,** 545-58.
HERRANZ-LÓPEZ, M., FERNÁNDEZ-ARROYO, S., PÉREZ-SANCHEZ, A., BARRAJÓN-CATALÁN, E., BELTRÁN-DEBÓN, R., MENÉNDEZ, J. A., ALONSO-VILLAVERDE, C., SEGURA-CARRETERO, A., JOVEN, J. & MICOL, V. 2012. Synergism of plant-derived polyphenols in adipogenesis: Perspectives and implications. *Phytomedicine,* 19**,** 253-261.
HICHRI, I., BARRIEU, F., BOGS, J., KAPPEL, C., DELROT, S. & LAUVERGEAT, V. 2011. Recent advances in the transcriptional regulation of the flavonoid biosynthetic pathway. *Journal of Experimental Botany*.
HIRAI, T., KIM, Y.-W., KATO, K., HIWASA-TANASE, K. & EZURA, H. 2011. Uniform accumulation of recombinant miraculin protein in transgenic tomato fruit using a fruit-ripening-specific E8 promoter. *Transgenic Research,* 20**,** 1285-1292.
HSU, S. 2005. Green tea and the skin. *Journal of the American Academy of Dermatology,* 52**,** 1049-1059.
HU, Y., SUN, C. Y., HUANG, J., HONG, L., ZHANG, L. & CHU, Z. B. 2007. Antimyeloma effects of resveratrol through inhibition of angiogenesis. *Chin Med J (Engl),* 120**,** 1672-7.
HUANG, M. T., HO, C. T., WANG, Z. Y., FERRARO, T., FINNEGAN-OLIVE, T., LOU, Y. R., MITCHELL, J. M., LASKIN, J. D., NEWMARK, H., YANG, C. S. & ET AL. 1992. Inhibitory effect of topical application of a green tea polyphenol fraction on tumor initiation and promotion in mouse skin. *Carcinogenesis,* 13**,** 947-54.
HUESO, E. L., DIEGO, O., LUCAS, L.-P., BENITO, P., TERESA, A. M., VICENTE, M. & ANTONIO, G. 2009. A multisite gateway-based toolkit for targeted gene expression and hairpin RNA silencing in tomato fruits. *Plant Biotechnology Journal,* 7**,** 298-309.
HUNG, C. F., LIN, Y. K., HUANG, Z. R. & FANG, J. Y. 2008. Delivery of resveratrol, a red wine polyphenol, from solutions and hydrogels via the skin. *Biol Pharm Bull,* 31**,** 955-62.

HUNG, L. M., CHEN, J. K., HUANG, S. S., LEE, R. S. & SU, M. J. 2000. Cardioprotective effect of resveratrol, a natural antioxidant derived from grapes. *Cardiovasc Res,* 47**,** 549-55.

HUNTINGTON, J. T., SHIELDS, J. M., DER, C. J., WYATT, C. A., BENBOW, U., SLINGLUFF, C. L. & BRINCKERHOFF, C. E. 2004. Overexpression of Collagenase 1 (MMP-1) Is Mediated by the ERK Pathway in Invasive Melanoma Cells: ROLE OF BRAF MUTATION AND FIBROBLAST GROWTH FACTOR SIGNALING. *Journal of Biological Chemistry,* 279**,** 33168-33176.

IIDA, J. & MCCARTHY, J. B. 2007. Expression of collagenase-1 (MMP-1) promotes melanoma growth through the generation of active transforming growth factor-beta. *Melanoma Res,* 17**,** 205-13.

INGROSSO, I., BONSEGNA, S., DE DOMENICO, S., LADDOMADA, B., BLANDO, F., SANTINO, A. & GIOVINAZZO, G. 2011. Over-expression of a grape stilbene synthase gene in tomato induces parthenocarpy and causes abnormal pollen development. *Plant Physiology and Biochemistry,* 49**,** 1092-1099.

ITOH, T., TANIOKA, M., MATSUDA, H., NISHIMOTO, H., YOSHIOKA, T., SUZUKI, R. & UEHIRA, M. 1999. Experimental metastasis is suppressed in MMP-9-deficient mice. *Clinical & Experimental Metastasis,* 17**,** 177-181.

ITOH, Y. 2015. Membrane-type matrix metalloproteinases: Their functions and regulations. *Matrix Biology,* 44-46**,** 207-223.

JANG, M., CAI, L., UDEANI, G. O., SLOWING, K. V., THOMAS, C. F., BEECHER, C. W. W., FONG, H. H. S., FARNSWORTH, N. R., KINGHORN, A. D., MEHTA, R. G., MOON, R. C. & PEZZUTO, J. M. 1997. Cancer Chemopreventive Activity of Resveratrol, a Natural Product Derived from Grapes. *Science,* 275**,** 218-220.

JEANDET, P., BESSIS, R. & GAUTHERON, B. 1991. The Production of Resveratrol (3,5,4'-trihydroxystilbene) by Grape Berries in Different Developmental Stages. *American Journal of Enology and Viticulture,* 42**,** 41-46.

JEANDET, P., BESSIS, R., SBAGHI, M. & MEUNIER, P. 1995. Production of the Phytoalexin Resveratrol by Grapes as a Response to Botrytis Attack Under Natural Conditions. *Journal of Phytopathology,* 143**,** 135-139.

JEANDET, P., CLÉMENT, C., TISSERANT, L.-P., CROUZET, J. & COUROT, É. 2016. Use of grapevine cell cultures for the production of phytostilbenes of cosmetic interest. *Comptes Rendus Chimie,* 19**,** 1062-1070.

JEANDET, P., DELAUNOIS, B., CONREUX, A., DONNEZ, D., NUZZO, V., CORDELIER, S., CLEMENT, C. & COUROT, E. 2010. Biosynthesis, metabolism, molecular engineering, and biological functions of stilbene phytoalexins in plants. *Biofactors,* 36**,** 331-41.

JEANDET, P., DOUILLET-BREUIL, A.-C., BESSIS, R., DEBORD, S., SBAGHI, M. & ADRIAN, M. 2002. Phytoalexins from the Vitaceae: Biosynthesis, Phytoalexin Gene Expression in Transgenic Plants, Antifungal Activity, and Metabolism. *Journal of Agricultural and Food Chemistry,* 50**,** 2731-2741.

JENSEN, G. S., WU, X., PATTERSON, K. M., BARNES, J., CARTER, S. G., SCHERWITZ, L., BEAMAN, R., ENDRES, J. R. & SCHAUSS, A. G. 2008. In Vitro and in Vivo Antioxidant and Anti-inflammatory Capacities of an Antioxidant-Rich Fruit and Berry Juice Blend. Results of a Pilot and Randomized, Double-Blinded, Placebo-Controlled, Crossover Study. *Journal of Agricultural and Food Chemistry,* 56**,** 8326-8333.

JEONG, Y. J., AN, C. H., WOO, S. G., JEONG, H. J., KIM, Y. M., PARK, S. J., YOON, B. D. & KIM, C. Y. 2014. Production of pinostilbene compounds by the expression of resveratrol O-methyltransferase genes in Escherichia coli. *Enzyme Microb Technol,* 54.

JEONG, Y. J., WOO, S. G., AN, C. H., JEONG, H. J., HONG, Y. S., KIM, Y. M., RYU, Y. B., RHO, M. C., LEE, W. S. & KIM, C. Y. 2015. Metabolic engineering for resveratrol derivative biosynthesis in Escherichia coli. *Mol Cells,* 38**,** 318-26.

JIMENEZ, F., MITTS, T. F., LIU, K., WANG, Y. & HINEK, A. 2006. Ellagic and Tannic Acids Protect Newly Synthesized Elastic Fibers from Premature Enzymatic Degradation in Dermal Fibroblast Cultures. *Journal of Investigative Dermatology,* 126**,** 1272-1280.

KÄHÄRI, V.-M. & SAARIALHO-KERE, U. 1997. Matrix metalloproteinases in skin. *Experimental Dermatology,* 6**,** 199-213.
KAPETANOVIC, I. M., MUZZIO, M., HUANG, Z., THOMPSON, T. N. & MCCORMICK, D. L. 2011. Pharmacokinetics, oral bioavailability, and metabolic profile of resveratrol and its dimethylether analog, pterostilbene, in rats. *Cancer Chemother Pharmacol,* 68**,** 593-601.
KATIYAR, S. K., AFAQ, F., AZIZUDDIN, K. & MUKHTAR, H. 2001. Inhibition of UVB-induced oxidative stress-mediated phosphorylation of mitogen-activated protein kinase signaling pathways in cultured human epidermal keratinocytes by green tea polyphenol (-)-epigallocatechin-3-gallate. *Toxicol Appl Pharmacol,* 176**,** 110-7.
KATSUYAMA, Y., FUNA, N., MIYAHISA, I. & HORINOUCHI, S. 2007. Synthesis of unnatural flavonoids and stilbenes by exploiting the plant biosynthetic pathway in Escherichia coli. *Chemistry & Biology,* 14**,** 613-621.
KERKELÄ, E., ALA-AHO, R., JESKANEN, L., RECHARDT, O., GRÉNMAN, R., SHAPIRO, S. D., KÄHÄRI, V.-M. & SAARIALHO-KERE, U. 2000. Expression of Human Macrophage Metalloelastase (MMP-12) by Tumor Cells in Skin Cancer. *Journal of Investigative Dermatology,* 114**,** 1113-1119.
KESSENBROCK, K., PLAKS, V. & WERB, Z. 2010. Matrix Metalloproteinases: Regulators of the Tumor Microenvironment. *Cell,* 141**,** 52-67.
KHANNA, S., VENOJARVI, M., ROY, S., SHARMA, N., TRIKHA, P., BAGCHI, D., BAGCHI, M. & SEN, C. K. 2002. Dermal wound healing properties of redox-active grape seed proanthocyanidins. *Free Radic Biol Med,* 33**,** 1089-96.
KNEISSL, M. & DEIKMAN, J. 1996. The Tomato E8 Gene Influences Ethylene Biosynthesis in Fruit but Not in Flowers. *Plant Physiol.***,** 537-547.
KORKINA, L. G., MIKHAL'CHIK, E., SUPRUN, M. V., PASTORE, S. & DAL TOSO, R. 2007. Molecular mechanisms underlying wound healing and anti-inflammatory properties of naturally occurring biotechnologically produced phenylpropanoid glycosides. *Cell Mol Biol (Noisy-le-grand),* 53**,** 84-91.
KOSTIN, S. F., MCDONALD, D. E. & MCFADDEN, D. W. 2012. Inhibitory effects of (-)-epigallocatechin-3-gallate and pterostilbene on pancreatic cancer growth in vitro. *Journal of Surgical Research,* 177**,** 255-262.
KOWALCZYK, A., KLENIEWSKA, P., KOLODZIEJCZYK, M., SKIBSKA, B. & GORACA, A. 2015. The Role of Endothelin-1 and Endothelin Receptor Antagonists in Inflammatory Response and Sepsis. *Archivum Immunologiae et Therapiae Experimentalis,* 63**,** 41-52.
KOWALCZYK, M. C., KOWALCZYK, P., TOLSTYKH, O., HANAUSEK, M., WALASZEK, Z. & SLAGA, T. J. 2010. Synergistic Effects of Combined Phytochemicals and Skin Cancer Prevention in SENCAR Mice. *Cancer Prevention Research*.
KUTTNER, V., MACK, C., GRETZMEIER, C., BRUCKNER-TUDERMAN, L. & DENGJEL, J. 2014. Loss of collagen VII is associated with reduced transglutaminase 2 abundance and activity. *J Invest Dermatol,* 134**,** 2381-2389.
LAGARES, D., GARCIA-FERNANDEZ, R. A., JIMENEZ, C. L., MAGAN-MARCHAL, N., BUSNADIEGO, O., LAMAS, S. & RODRIGUEZ-PASCUAL, F. 2010. Endothelin 1 contributes to the effect of transforming growth factor beta1 on wound repair and skin fibrosis. *Arthritis Rheum,* 62**,** 878-89.
LANGCAKE, P. & PRYCE, R. J. 1976. The production of resveratrol by Vitis vinifera and other members of the Vitaceae as a response to infection or injury. *Physiological Plant Pathology,* 9**,** 77-86.
LECHNER, M., LIRK, P. & RIEDER, J. 2005. Inducible nitric oxide synthase (iNOS) in tumor biology: the two sides of the same coin. *Semin Cancer Biol,* 15**,** 277-89.
LEE, M.-F., PAN, M.-H., CHIOU, Y.-S., CHENG, A.-C. & HUANG, H. 2011. Resveratrol Modulates MED28 (Magicin/EG-1) Expression and Inhibits Epidermal Growth Factor (EGF)-Induced Migration in MDA-MB-231 Human Breast Cancer Cells. *Journal of Agricultural and Food Chemistry,* 59**,** 11853-11861.
LEMBACH, K. J. 1976. Induction of human fibroblast proliferation by epidermal growth factor (EGF): enhancement by an EGF-binding arginine esterase and by ascorbate. *Proceedings of the National Academy of Sciences of the United States of America,* 73**,** 183-187.

LEPHART, E. D., SOMMERFELDT, J. M. & ANDRUS, M. B. 2014. Resveratrol: influences on gene expression in human skin. *Journal of Functional Foods,* 10**,** 377-384.
LEWIS, D. A., HENGELTRAUB, S. F., GAO, F. C., LEIVANT, M. A. & SPANDAU, D. F. 2006. Aberrant NF-κB Activity in HaCaT Cells Alters their Response to UVB Signaling. *Journal of Investigative Dermatology,* 126**,** 1885-1892.
LI, J., CHEN, J. & KIRSNER, R. 2007. Pathophysiology of acute wound healing. *Clinics in Dermatology,* 25**,** 9-18.
LI, J., RUZHI, D., HUA, X., ZHANG, L., LU, F., COURSEY, T. G., PFLUGFELDER, S. C. & LI, D.-Q. 2016a. Blueberry Component Pterostilbene Protects Corneal Epithelial Cells from Inflammation via Anti-oxidative Pathway. *Scientific Reports,* 6**,** 19408.
LI, M., SCHNEIDER, K., KRISTENSEN, M., BORODINA, I. & NIELSEN, J. 2016b. Engineering yeast for high-level production of stilbenoid antioxidants. *Scientific Reports,* 6**,** 36827.
LI, S. 2014. Transcriptional control of flavonoid biosynthesis. *Plant Signaling & Behavior,* 9**,** e27522.
LI, Y., WANG, H., ZHANG, Y. & MARTIN, C. 2018. Can the world's favorite fruit, tomato, provide an effective biosynthetic chassis for high-value metabolites? *Plant Cell Rep*.
LI, Y. T., SHEN, F., LIU, B. H. & CHENG, G. F. 2003. Resveratrol inhibits matrix metalloproteinase-9 transcription in U937 cells. *Acta Pharmacol Sin,* 24**,** 1167-71.
LICHTINGHAGEN, R., MUSHOLT, P. B., LEIN, M., RÖMER, A., RUDOLPH, B., KRISTIANSEN, G., HAUPTMANN, S., SCHNORR, D., LOENING, S. A. & JUNG, K. 2002. Different mRNA and Protein Expression of Matrix Metalloproteinases 2 and 9 and Tissue Inhibitor of Metalloproteinases 1 in Benign and Malignant Prostate Tissue. *European Urology,* 42**,** 398-406.
LIM, C. G., FOWLER, Z. L., HUELLER, T., SCHAFFER, S. & KOFFAS, M. A. G. 2011. High-Yield Resveratrol Production in Engineered Escherichia coli. *Applied and Environmental Microbiology,* 77**,** 3451-3460.
LIN, H. S., YUE, B. D. & HO, P. C. 2009. Determination of pterostilbene in rat plasma by a simple HPLC-UV method and its application in pre-clinical pharmacokinetic study. *Biomed Chromatogr,* 23**,** 1308-15.
LIU, H., TUCHINDA, P., FISHELEVICH, R., HARBERTS, E. & GASPARI, A. A. 2014. Human in vitro skin organ culture as a model system for evaluating DNA repair. *J Dermatol Sci,* 74**,** 236-41.
LIU, J., OSBOURN, A. & MA, P. MYB transcription factors as regulators of phenylpropanoid metabolism in plants. *Molecular Plant*.
LIU, L., XIE, H., CHEN, X., SHI, W., XIAO, X., LEI, D. & LI, J. 2012. Differential response of normal human epidermal keratinocytes and HaCaT cells to hydrogen peroxide-induced oxidative stress. *Clin Exp Dermatol,* 37**,** 772-80.
LIU, Z. & KLOMINEK, J. 2003. Regulation of matrix metalloprotease activity in malignant mesothelioma cell lines by growth factors. *Thorax,* 58**,** 198-203.
LIU, Z., SONG, Y., ZHANG, X., LIU, Z., ZHANG, W., MAO, W., WANG, W., CUI, W., ZHANG, X., JIA, X., LI, N., HAN, C. & LIU, C. 2005. Effects of trans-resveratrol on hypertension-induced cardiac hypertrophy using the partially nephrectomized rat model. *Clin Exp Pharmacol Physiol,* 32**,** 1049-54.
LÖFFEK, S., HURSKAINEN, T., JACKOW, J., SIGLOCH, F. C., SCHILLING, O., TASANEN, K., BRUCKNER-TUDERMAN, L. & FRANZKE, C.-W. 2014. Transmembrane Collagen XVII Modulates Integrin Dependent Keratinocyte Migration via PI3K/Rac1 Signaling. *PLOS ONE,* 9**,** e87263.
LONG, X., LI, S., XIE, J., LI, W., ZANG, N., REN, L., DENG, Y., XIE, X., WANG, L., FU, Z. & LIU, E. 2015. MMP-12-mediated by SARM-TRIF signaling pathway contributes to IFN-γ-independent airway inflammation and AHR post RSV infection in nude mice. *Respiratory Research,* 16**,** 11.
LOO, A. E., HO, R. & HALLIWELL, B. 2011. Mechanism of hydrogen peroxide-induced keratinocyte migration in a scratch-wound model. *Free Radic Biol Med,* 51**,** 884-92.
LOPEZ-SEPULVEDA, R., GOMEZ-GUZMAN, M., ZARZUELO, M. J., ROMERO, M., SANCHEZ, M., QUINTELA, A. M., GALINDO, P., O'VALLE, F., TAMARGO, J., PEREZ-VIZCAINO, F., DUARTE, J. & JIMENEZ, R. 2011. Red wine polyphenols

prevent endothelial dysfunction induced by endothelin-1 in rat aorta: role of NADPH oxidase. *Clin Sci (Lond),* 120**,** 321-33.
LOWES, M. A., BOWCOCK, A. M. & KRUEGER, J. G. 2007. Pathogenesis and therapy of psoriasis. *Nature,* 445**,** 866.
LUO, J., BUTELLI, E., HILL, L., PARR, A., NIGGEWEG, R., BAILEY, P., WEISSHAAR, B. & MARTIN, C. 2008. AtMYB12 regulates caffeoyl quinic acid and flavonol synthesis in tomato: expression in fruit results in very high levels of both types of polyphenol. *Plant J,* 56**,** 316-26.
MAGCWEBEBA, T., RIEDEL, S., SWANEVELDER, S., BOUIC, P., SWART, P. & GELDERBLOM, W. 2012. Interleukin-1 Induction in Human Keratinocytes (HaCaT): An In Vitro Model for Chemoprevention in Skin. *Journal of Skin Cancer,* 2012**,** 10.
MAITI, T. K., CHATTERJEE, J. & DASGUPTA, S. 2003. Effect of green tea polyphenols on angiogenesis induced by an angiogenin-like protein. *Biochemical and Biophysical Research Communications,* 308**,** 64-67.
MAKRANTONAKI, E. & ZOUBOULIS, C. C. 2007. Molecular Mechanisms of Skin Aging. *Annals of the New York Academy of Sciences,* 1119**,** 40-50.
MANICKAM, M., RAMANATHAN, M., FARBOODNIAY JAHROMI, M. A., CHANSOURIA, J. P. N. & RAY, A. B. 1997. Antihyperglycemic Activity of Phenolics from Pterocarpus marsupium. *Journal of Natural Products,* 60**,** 609-610.
MANICONE, A. M. & MCGUIRE, J. K. 2008. Matrix Metalloproteinases as Modulators of Inflammation. *Seminars in cell & developmental biology,* 19**,** 34-41.
MANTEGNA, S., BINELLO, A., BOFFA, L., GIORGIS, M., CENA, C. & CRAVOTTO, G. 2012. A one-pot ultrasound-assisted water extraction/cyclodextrin encapsulation of resveratrol from Polygonum cuspidatum. *Food Chemistry,* 130**,** 746-750.
MCCAWLEY, L. J. & MATRISIAN, L. M. 2001. Matrix metalloproteinases: they're not just for matrix anymore! *Current Opinion in Cell Biology,* 13**,** 534-540.
MCCORMACK, D. & MCFADDEN, D. 2013. A review of pterostilbene antioxidant activity and disease modification. *Oxid Med Cell Longev,* 2013.
MEDZHITOV, R. & HORNG, T. 2009. Transcriptional control of the inflammatory response. *Nature Reviews Immunology,* 9**,** 692.
MEHRTENS, F., KRANZ, H., BEDNAREK, P. & WEISSHAAR, B. 2005. The Arabidopsis transcription factor MYB12 is a flavonol-specific regulator of phenylpropanoid biosynthesis. *Plant Physiol,* 138**,** 1083-96.
MEI, Y. Z., LIU, R. X., WANG, D. P., WANG, X. & DAI, C. C. 2015. Biocatalysis and biotransformation of resveratrol in microorganisms. *Biotechnology Letters,* 37**,** 9-18.
MENON, G. K. 2002. New insights into skin structure: scratching the surface. *Advanced Drug Delivery Reviews,* 54**,** S3-S17.
MERTENS-TALCOTT, S. U. & PERCIVAL, S. S. 2005. Ellagic acid and quercetin interact synergistically with resveratrol in the induction of apoptosis and cause transient cell cycle arrest in human leukemia cells. *Cancer Letters,* 218**,** 141-151.
MIHAI, S. & SITARU, C. 2007. Immunopathology and molecular diagnosis of autoimmune bullous diseases. *Journal of Cellular and Molecular Medicine,* 11**,** 462-481.
MILEWICZ, D. M., URBÁN, Z. & BOYD, C. 2000. Genetic disorders of the elastic fiber system. *Matrix Biology,* 19**,** 471-480.
MOILANEN, J. M., LOFFEK, S., KOKKONEN, N., SALO, S., VAYRYNEN, J. P., HURSKAINEN, T., MANNINEN, A., RIIHILA, P., HELJASVAARA, R., FRANZKE, C. W., KAHARI, V. M., SALO, T., MAKINEN, M. J. & TASANEN, K. 2017. Significant Role of Collagen XVII And Integrin beta4 in Migration and Invasion of The Less Aggressive Squamous Cell Carcinoma Cells. *Sci Rep,* 7**,** 45057.
MUKHERJEE, S., DUDLEY, J. I. & DAS, D. K. 2010. Dose-Dependency of Resveratrol in Providing Health Benefits. *Dose-Response,* 8**,** dose-response.09-015.Mukherjee.
MURAKAMI, I., CHALECKIS, R., PLUSKAL, T., ITO, K., HORI, K., EBE, M., YANAGIDA, M. & KONDOH, H. 2014. Metabolism of Skin-Absorbed Resveratrol into Its Glucuronized Form in Mouse Skin. *PLoS ONE,* 9**,** e115359.
MURPHY, G. & NAGASE, H. 2008. Progress in matrix metalloproteinase research. *Molecular Aspects of Medicine,* 29**,** 290-308.
NAGASE, H., VISSE, R. & MURPHY, G. 2006. Structure and function of matrix metalloproteinases and TIMPs. *Cardiovascular Research,* 69**,** 562-573.

NAKASAKI, M., HWANG, Y., XIE, Y., KATARIA, S., GUND, R., HAJAM, E. Y., SAMUEL, R., GEORGE, R., DANDA, D., M.J, P., NAKAMURA, T., SHEN, Z., BRIGGS, S., VARGHESE, S. & JAMORA, C. 2015. The matrix protein Fibulin-5 is at the interface of tissue stiffness and inflammation in fibrosis. *Nature Communications,* 6**,** 8574.

NANNEY, L. B. 1990. Epidermal and Dermal Effects of Epidermal Growth Factor During Wound Repair. *Journal of Investigative Dermatology,* 94**,** 624-629.

NEWBY, A. C. 2006. Matrix metalloproteinases regulate migration, proliferation, and death of vascular smooth muscle cells by degrading matrix and non-matrix substrates. *Cardiovascular Research,* 69**,** 614-624.

NICHOLS, J. A. & KATIYAR, S. K. 2010. Skin photoprotection by natural polyphenols: anti-inflammatory, antioxidant and DNA repair mechanisms. *Archives of Dermatological Research,* 302**,** 71-83.

NICHOLSON, S. K., TUCKER, G. A. & BRAMELD, J. M. 2008. Effects of dietary polyphenols on gene expression in human vascular endothelial cells. *Proc Nutr Soc,* 67**,** 42-7.

NISHIE, W. 2014. Update on the pathogenesis of bullous pemphigoid: An autoantibody-mediated blistering disease targeting collagen XVII. *Journal of Dermatological Science,* 73**,** 179-186.

NORATA, G. D., MARCHESI, P., PASSAMONTI, S., PIRILLO, A., VIOLI, F. & CATAPANO, A. L. 2007. Anti-inflammatory and anti-atherogenic effects of cathechin, caffeic acid and trans-resveratrol in apolipoprotein E deficient mice. *Atherosclerosis,* 191**,** 265-271.

NUNAN, R., HARDING, K. G. & MARTIN, P. 2014. Clinical challenges of chronic wounds: searching for an optimal animal model to recapitulate their complexity. *Disease Models & Mechanisms,* 7**,** 1205-1213.

NUTT, J. E., DURKAN, G. C., MELLON, J. K. & LUNEC, J. 2003. Matrix metalloproteinases (MMPs) in bladder cancer: the induction of MMP9 by epidermal growth factor and its detection in urine. *BJU Int,* 91**,** 99-104.

NYSTROM, A., VELATI, D., MITTAPALLI, V. R., FRITSCH, A., KERN, J. S. & BRUCKNER-TUDERMAN, L. 2013. Collagen VII plays a dual role in wound healing. *J Clin Invest,* 123**,** 3498-509.

OBERRINGER, M., MEINS, C., BUBEL, M. & POHLEMANN, T. 2007. A new in vitro wound model based on the co-culture of human dermal microvascular endothelial cells and human dermal fibroblasts. *Biology of the Cell,* 99**,** 197-207.

OH, J. W., HSI, T. C., GUERRERO-JUAREZ, C. F., RAMOS, R. & PLIKUS, M. V. 2013. Organotypic skin culture. *J Invest Dermatol,* 133**,** e14.

OLIVERA, S. & TOMIC-CANIC, M. 2013. Human Ex Vivo Wound Healing Model. *In:* GOURDIE, R. G. & MYERS, T. A. (eds.) *Wound Regeneration and Repair: Methods and Protocols.* Totowa, NJ: Humana Press.

PAN, M.-H., CHANG, Y.-H., TSAI, M.-L., LAI, C.-S., HO, S.-Y., BADMAEV, V. & HO, C.-T. 2008. Pterostilbene Suppressed Lipopolysaccharide-Induced Up-Expression of iNOS and COX-2 in Murine Macrophages. *Journal of Agricultural and Food Chemistry,* 56**,** 7502-7509.

PAN, M.-H., CHIOU, Y.-S., CHEN, W.-J., WANG, J.-M., BADMAEV, V. & HO, C.-T. 2009. Pterostilbene inhibited tumor invasion via suppressing multiple signal transduction pathways in human hepatocellular carcinoma cells. *Carcinogenesis,* 30**,** 1234-1242.

PAN, M.-H., LIN, Y.-T., LIN, C.-L., WEI, C.-S., HO, C.-T. & CHEN, W.-J. 2011. Suppression of Heregulin-β1/HER2-Modulated Invasive and Aggressive Phenotype of Breast Carcinoma by Pterostilbene via Inhibition of Matrix Metalloproteinase-9, p38 Kinase Cascade and Akt Activation. *Evidence-based Complementary and Alternative Medicine : eCAM,* 2011**,** 562187.

PARIKKA, M., NISSINEN, L., KAINULAINEN, T., BRUCKNER-TUDERMAN, L., SALO, T., HEINO, J. & TASANEN, K. 2006. Collagen XVII promotes integrin-mediated squamous cell carcinoma transmigration—A novel role for αIIb integrin and tirofiban. *Experimental Cell Research,* 312**,** 1431-1438.

PARK, K. & LEE, J. H. 2008. Protective effects of resveratrol on UVB-irradiated HaCaT cells through attenuation of the caspase pathway. *Oncol Rep,* 19**,** 413-7.

PASTORE, S., LULLI, D., FIDANZA, P., POTAPOVICH, A. I., KOSTYUK, V. A., DE LUCA, C., MIKHAL'CHIK, E. & KORKINA, L. G. 2012a. Plant Polyphenols Regulate Chemokine Expression and Tissue Repair in Human Keratinocytes Through Interaction with Cytoplasmic and Nuclear Components of Epidermal Growth Factor Receptor System. *Antioxidants & Redox Signaling,* 16**,** 314-328.

PASTORE, S., LULLI, D., FIDANZA, P., POTAPOVICH, A. I., KOSTYUK, V. A., LUCA, C. D., MIKHAL'CHIK, E. & KORKINA, L. G. 2012b. Plant Polyphenols Regulate Chemokine Expression and Tissue Repair in Human Keratinocytes Through Interaction with Cytoplasmic and Nuclear Components of Epidermal Growth Factor Receptor System. *Antioxidants & Redox Signaling,* 16**,** 314-328.

PASTORE, S., LULLI, D., POTAPOVICH, A. I., FIDANZA, P., KOSTYUK, V. A., DELLAMBRA, E., DE LUCA, C., MAURELLI, R. & KORKINA, L. G. 2011a. Differential modulation of stress-inflammation responses by plant polyphenols in cultured normal human keratinocytes and immortalized HaCaT cells. *Journal of Dermatological Science,* 63**,** 104-114.

PASTORE, S., LULLI, D., POTAPOVICH, A. I., FIDANZA, P., KOSTYUK, V. A., DELLAMBRA, E., DE LUCA, C., MAURELLI, R. & KORKINA, L. G. 2011b. Differential modulation of stress-inflammation responses by plant polyphenols in cultured normal human keratinocytes and immortalized HaCaT cells. *J Dermatol Sci,* 63**,** 104-14.

PERVAIZ, S. 2003. Resveratrol: from grapevines to mammalian biology. *The FASEB Journal,* 17**,** 1975-1985.

PESAKHOV, S., KHANIN, M., STUDZINSKI, G. P. & DANILENKO, M. 2010. Distinct Combinatorial Effects of the Plant Polyphenols Curcumin, Carnosic Acid, and Silibinin on Proliferation and Apoptosis in Acute Myeloid Leukemia Cells. *Nutrition and Cancer,* 62**,** 811-824.

PILLAI, S., ORESAJO, C. & HAYWARD, J. 2005. Ultraviolet radiation and skin aging: roles of reactive oxygen species, inflammation and protease activation, and strategies for prevention of inflammation-induced matrix degradation – a review. *International Journal of Cosmetic Science,* 27**,** 17-34.

PINNELL, S. R. 2003. Cutaneous photodamage, oxidative stress, and topical antioxidant protection. *Journal of the American Academy of Dermatology,* 48**,** 1-22.

PORTUGAL-COHEN, M., SOROKA, Y., FRUSIC-ZLOTKIN, M., VERKHOVSKY, L., BREGEGERE, F. M., NEUMAN, R., KOHEN, R. & MILNER, Y. 2011. Skin organ culture as a model to study oxidative stress, inflammation and structural alterations associated with UVB-induced photodamage. *Exp Dermatol,* 20**,** 749-55.

POTAPOVICH, A. I., LULLI, D., FIDANZA, P., KOSTYUK, V. A., DE LUCA, C., PASTORE, S. & KORKINA, L. G. 2011. Plant polyphenols differentially modulate inflammatory responses of human keratinocytes by interfering with activation of transcription factors NFκB and AhR and EGFR–ERK pathway. *Toxicology and Applied Pharmacology,* 255**,** 138-149.

QUAN, T., QIN, Z., XIA, W., SHAO, Y., VOORHEES, J. J. & FISHER, G. J. 2009. Matrix-degrading Metalloproteinases in Photoaging. *The journal of investigative dermatology. Symposium proceedings / the Society for Investigative Dermatology, Inc. [and] European Society for Dermatological Research,* 14**,** 20-24.

REMSBERG, C. M., YANEZ, J. A., OHGAMI, Y., VEGA-VILLA, K. R., RIMANDO, A. M. & DAVIES, N. M. 2008. Pharmacometrics of pterostilbene: preclinical pharmacokinetics and metabolism, anticancer, antiinflammatory, antioxidant and analgesic activity. *Phytother Res,* 22**,** 169-79.

RENO, C., MARCHUK, L., SCIORE, P., FRANK, C. & HART, D. A. 1997. Rapid isolation of total RNA from small samples of hypocellular, dense connective tissues. *Biotechniques,* 22**,** 1082-1086.

RIMANDO, A. M., CUENDET, M., DESMARCHELIER, C., MEHTA, R. G., PEZZUTO, J. M. & DUKE, S. O. 2002. Cancer chemopreventive and antioxidant activities of pterostilbene, a naturally occurring analogue of resveratrol. *J Agric Food Chem,* 50**,** 3453-7.

RIMANDO, A. M., KALT, W., MAGEE, J. B., DEWEY, J. & BALLINGTON, J. R. 2004. Resveratrol, pterostilbene, and piceatannol in vaccinium berries. *J Agric Food Chem,* 52**,** 4713-9.

RITTIÉ, L. 2016. Cellular mechanisms of skin repair in humans and other mammals. *Journal of Cell Communication and Signaling,* 10**,** 103-120.

ROBB, E. L., WINKELMOLEN, L., VISANJI, N., BROTCHIE, J. & STUART, J. A. 2008. Dietary resveratrol administration increases MnSOD expression and activity in mouse brain. *Biochemical and Biophysical Research Communications,* 372**,** 254-259.

RODRÍGUEZ-BONILLA, P., LÓPEZ-NICOLÁS, J. M., MÉNDEZ-CAZORLA, L. & GARCÍA-CARMONA, F. 2011. Development of a reversed phase high performance liquid chromatography method based on the use of cyclodextrins as mobile phase additives to determine pterostilbene in blueberries. *Journal of Chromatography B,* 879**,** 1091-1097.

ROHANI, M. G. & PARKS, W. C. 2015. Matrix remodeling by MMPs during wound repair. *Matrix Biology,* 44-46**,** 113-121.

ROSANÒ, L., SPINELLA, F. & BAGNATO, A. 2013. Endothelin 1 in cancer: biological implications and therapeutic opportunities. *Nature Reviews Cancer,* 13**,** 637.

RUEF, J., MOSER, M., KÜBLER, W. & BODE, C. 2001. Induction of endothelin-1 expression by oxidative stress in vascular smooth muscle cells. *Cardiovascular Pathology,* 10**,** 311-315.

SAARIALHO-KERE, U., KERKELÄ, E., JESKANEN, L., RANKI, A., VAALAMO, M., HASAN, T., PIERCE, R., STARCHER, B., RAUDASOJA, R. & OIKARINEN, A. 1999. Accumulation of Matrilysin (MMP-7) and Macrophage Metalloelastase (MMP-12) in Actinic Damage. *Journal of Investigative Dermatology,* 113**,** 664-672.

SAINSBURY, F., THUENEMANN, E. C. & LOMONOSSOFF, G. P. 2009. pEAQ: versatile expression vectors for easy and quick transient expression of heterologous proteins in plants. *Plant Biotechnol J,* 7**,** 682-93.

SÁNCHEZ-FIDALGO, S., CÁRDENO, A., VILLEGAS, I., TALERO, E. & DE LA LASTRA, C. A. 2010. Dietary supplementation of resveratrol attenuates chronic colonic inflammation in mice. *European Journal of Pharmacology,* 633**,** 78-84.

SATO, M., MAULIK, N. & DAS, D. K. 2002. Cardioprotection with alcohol: role of both alcohol and polyphenolic antioxidants. *Ann N Y Acad Sci,* 957**,** 122-35.

SCARANO, A., BUTELLI, E., DE SANTIS, S., CAVALCANTI, E., HILL, L., DE ANGELIS, M., GIOVINAZZO, G., CHIEPPA, M., MARTIN, C. & SANTINO, A. 2018. Combined Dietary Anthocyanins, Flavonols, and Stilbenoids Alleviate Inflammatory Bowel Disease Symptoms in Mice. *Frontiers in Nutrition,* 4.

SCHARFFETTER-KOCHANEK, K., BRENNEISEN, P., WENK, J., HERRMANN, G., MA, W., KUHR, L., MEEWES, C. & WLASCHEK, M. 2000. Photoaging of the skin from phenotype to mechanisms. *Exp Gerontol,* 35**,** 307-16.

SCHLACHTERMAN, A., VALLE, F., WALL, K. M., AZIOS, N. G., CASTILLO, L., MORELL, L., WASHINGTON, A. V., CUBANO, L. A. & DHARMAWARDHANE, S. F. 2008. Combined Resveratrol, Quercetin, and Catechin Treatment Reduces Breast Tumor Growth in a Nude Mouse Model. *Translational Oncology,* 1**,** 19-27.

SCHMITT, C. A., HEISS, E. H. & DIRSCH, V. M. 2010. Effect of resveratrol on endothelial cell function: Molecular mechanisms. *BioFactors,* 36**,** 342-349.

SCHOOP, V. M., MIRANCEA, N. & FUSENIG, N. E. 1999. Epidermal Organization and Differentiation of HaCaT Keratinocytes in Organotypic Coculture with Human Dermal Fibroblasts. 112**,** 343-353.

SEBASTIAN, A., IQBAL, S. A., COLTHURST, J., VOLK, S. W. & BAYAT, A. 2015. Electrical Stimulation Enhances Epidermal Proliferation in Human Cutaneous Wounds by Modulating p53–SIVA1 Interaction. *Journal of Investigative Dermatology,* 135**,** 1166-1174.

SEMLIN, L., SCHAFER-KORTING, M., BORELLI, C. & KORTING, H. C. 2011. In vitro models for human skin disease. *Drug Discov Today,* 16**,** 132-9.

SHAPIRO, S. D., GOLDSTEIN, N. M., HOUGHTON, A. M., KOBAYASHI, D. K., KELLEY, D. & BELAAOUAJ, A. 2003. Neutrophil Elastase Contributes to Cigarette Smoke-Induced Emphysema in Mice. *The American Journal of Pathology,* 163**,** 2329-2335.

SHIPLEY, J. M., WESSELSCHMIDT, R. L., KOBAYASHI, D. K., LEY, T. J. & SHAPIRO, S. D. 1996. Metalloelastase is required for macrophage-mediated proteolysis and matrix invasion in mice. *Proceedings of the National Academy of Sciences,* 93**,** 3942.

SINGER, A. J. & CLARK, R. A. F. 1999. Cutaneous Wound Healing. *New England Journal of Medicine,* 341**,** 738-746.

SINHA, A., NOSOUDI, N. & VYAVAHARE, N. 2014. Elasto-regenerative properties of polyphenols. *Biochemical and Biophysical Research Communications,* 444**,** 205-211.

SIREROL, J. A., FEDDI, F., MENA, S., RODRIGUEZ, M. L., SIRERA, P., AUPI, M., PEREZ, S., ASENSI, M., ORTEGA, A. & ESTRELA, J. M. 2015. Topical treatment with pterostilbene, a natural phytoalexin, effectively protects hairless mice against UVB radiation-induced skin damage and carcinogenesis. *Free Radic Biol Med,* 85**,** 1-11.

SOEUR, J., EILSTEIN, J., LÉREAUX, G., JONES, C. & MARROT, L. 2015. Skin resistance to oxidative stress induced by resveratrol: From Nrf2 activation to GSH biosynthesis. *Free Radical Biology and Medicine,* 78**,** 213-223.

SORRELL, J. M., BABER, M. A. & CAPLAN, A. I. 2004. Site-matched papillary and reticular human dermal fibroblasts differ in their release of specific growth factors/cytokines and in their interaction with keratinocytes. *J Cell Physiol,* 200**,** 134-45.

STEINSTRAESSER, L., SORKIN, M., NIEDERBICHLER, A. D., BECERIKLI, M., STUPKA, J., DAIGELER, A., KESTING, M. R., STRICKER, I., JACOBSEN, F. & SCHULTE, M. 2010. A novel human skin chamber model to study wound infection ex vivo. *Archives of Dermatological Research,* 302**,** 357-365.

STOCLET, J. C., CHATAIGNEAU, T., NDIAYE, M., OAK, M. H., EL BEDOUI, J., CHATAIGNEAU, M. & SCHINI-KERTH, V. B. 2004. Vascular protection by dietary polyphenols. *Eur J Pharmacol,* 500**,** 299-313.

TADDESE, S., WEISS, A. S., NEUBERT, R. H. H. & SCHMELZER, C. E. H. 2008. Mapping of macrophage elastase cleavage sites in insoluble human skin elastin. *Matrix Biology,* 27**,** 420-428.

TAMMI, R., JANSÉN, C. T. & SANTTI, R. 1979. Histometric Analysis of Human Skin in Organ Culture.

TAN, W.-F., LIN, L.-P., LI, M.-H., ZHANG, Y.-X., TONG, Y.-G., XIAO, D. & DING, J. 2003. Quercetin, a dietary-derived flavonoid, possesses antiangiogenic potential. *European Journal of Pharmacology,* 459**,** 255-262.

TANG, F. Y., SU, Y. C., CHEN, N. C., HSIEH, H. S. & CHEN, K. S. 2008. Resveratrol inhibits migration and invasion of human breast-cancer cells. *Mol Nutr Food Res,* 52**,** 683-91.

TEWARI, A., GRYS, K., KOLLET, J., SARKANY, R. & YOUNG, A. R. 2014. Upregulation of MMP12 and Its Activity by UVA1 in Human Skin: Potential Implications for Photoaging. *Journal of Investigative Dermatology,* 134**,** 2598-2609.

TOMLINSON, M. L., BUTELLI, E., MARTIN, C. & CARDING, S. R. 2017. Flavonoids from Engineered Tomatoes Inhibit Gut Barrier Pro-inflammatory Cytokines and Chemokines, via SAPK/JNK and p38 MAPK Pathways. *Frontiers in Nutrition,* 4.

UD-DIN, S. & BAYAT, A. 2017. Non-animal models of wound healing in cutaneous repair: In silico, in vitro, ex vivo, and in vivo models of wounds and scars in human skin. *Wound Repair and Regeneration,* 25**,** 164-176.

UITTO, J. 2001. Elastic fibre abnormalities in skin disorders: what's new? *J Eur Acad Dermatol Venereol,* 15**,** 303-4.

VAALAMO, M., KARINIEMI, A.-L., SAARIALHO-KERE, U. & SHAPIRO, S. D. 1999. Enhanced Expression of Human Metalloelastase (MMP-12) in Cutaneous Granulomas and Macrophage Migration. *Journal of Investigative Dermatology,* 112**,** 499-505.

VAN RAVENZWAAY, B. & LEIBOLD, E. 2004. A comparison between in vitro rat and human and in vivo rat skin absorption studies. *Hum Exp Toxicol,* 23**,** 421-30.

VARANI, J., HATTORI, Y., CHI, Y., SCHMIDT, T., PERONE, P., ZEIGLER, M. E., FADER, D. J. & JOHNSON, T. M. 2000. Collagenolytic and gelatinolytic matrix metalloproteinases and their inhibitors in basal cell carcinoma of skin: comparison with normal skin. *Br J Cancer,* 82**,** 657-65.

VERGARA, D., VALENTE, C. M., TINELLI, A., SICILIANO, C., LORUSSO, V., ACIERNO, R., GIOVINAZZO, G., SANTINO, A., STORELLI, C. & MAFFIA, M. 2011. Resveratrol inhibits the epidermal growth factor-induced epithelial mesenchymal transition in MCF-7 cells. *Cancer Letters,* 310**,** 1-8.

WALL, S. J., BEVAN, D., THOMAS, D. W., HARDING, K. G., EDWARDS, D. R. & MURPHY, G. 2002. Differential Expression of Matrix Metalloproteinases During Impaired Wound Healing of the Diabetes Mouse. *Journal of Investigative Dermatology,* 119**,** 91-98.

WALLE, T. 2011. Bioavailability of resveratrol. *Ann N Y Acad Sci,* 1215**,** 9-15.

WALLE, T., HSIEH, F., DELEGGE, M. H., OATIS, J. E., JR. & WALLE, U. K. 2004. High absorption but very low bioavailability of oral resveratrol in humans. *Drug Metab Dispos,* 32**,** 1377-82.

WANG, Q., REDDY, V. A., PANICKER, D., MAO, H. Z., KUMAR, N., RAJAN, C., VENKATESH, P. N., CHUA, N. H. & SAROJAM, R. 2016. Metabolic engineering of terpene biosynthesis in plants using a trichome-specific transcription factor MsYABBY5 from spearmint (Mentha spicata). *Plant Biotechnology Journal,* 14**,** 1619-1632.

WANG, X., ZHAI, W., WU, C., MA, B., ZHANG, J., ZHANG, H., ZHU, Z. & CHANG, J. 2015. Procyanidins-crosslinked aortic elastin scaffolds with distinctive anti-calcification and biological properties. *Acta Biomater,* 16**,** 81-93.

WEIHERMANN, A. C., LORENCINI, M., BROHEM, C. A. & DE CARVALHO, C. M. 2017. Elastin structure and its involvement in skin photoageing. *International Journal Of Cosmetic Science,* 39**,** 241-247.

WERNER, S., KRIEG, T. & SMOLA, H. 2007. Keratinocyte-fibroblast interactions in wound healing. *J Invest Dermatol,* 127**,** 998-1008.

WITTENAUER, J., MÄCKLE, S., SUßMANN, D., SCHWEIGGERT-WEISZ, U. & CARLE, R. 2015. Inhibitory effects of polyphenols from grape pomace extract on collagenase and elastase activity. *Fitoterapia,* 101**,** 179-187.

WOO, J.-H., LIM, J. H., KIM, Y.-H., SUH, S.-I., MIN, D. S., CHANG, J.-S., LEE, Y. H., PARK, J.-W. & KWON, T. K. 2003. Resveratrol inhibits phorbol myristate acetate-induced matrix metalloproteinase-9 expression by inhibiting JNK and PKC δ signal transduction. *Oncogene,* 23**,** 1845.

WU, X.-B., LUO, X.-Q., GU, S.-Y. & XU, J.-H. 2012. The effects of Polygonum cuspidatum extract on wound healing in rats. *Journal of Ethnopharmacology,* 141**,** 934-937.

XU, W., DUBOS, C. & LEPINIEC, L. 2015. Transcriptional control of flavonoid biosynthesis by MYB–bHLH–WDR complexes. *Trends in Plant Science,* 20**,** 176-185.

XU, W., JONG HONG, S., JIA, S., ZHAO, Y., GALIANO, R. D. & MUSTOE, T. A. 2012. Application of a partial-thickness human ex vivo skin culture model in cutaneous wound healing study. *Lab Invest,* 92**,** 584-99.

YAMAGATA, K., TAGAMI, M. & YAMORI, Y. 2015. Dietary polyphenols regulate endothelial function and prevent cardiovascular disease. *Nutrition,* 31**,** 28-37.

YAMAN, I., DERICI, H., KARA, C., KAMER, E., DINIZ, G., ORTAC, R. & SAYIN, O. 2013. Effects of resveratrol on incisional wound healing in rats. *Surgery Today,* 43**,** 1433-1438.

ZAID, M. A., AFAQ, F., SYED, D. N., DREHER, M. & MUKHTAR, H. 2007. Inhibition of UVB-mediated Oxidative Stress and Markers of Photoaging in Immortalized HaCaT Keratinocytes by Pomegranate Polyphenol Extract POMx. *Photochemistry and Photobiology,* 83**,** 882-888.

ZHANG, Y., BUTELLI, E., ALSEEKH, S., TOHGE, T., RALLAPALLI, G., LUO, J., KAWAR, P. G., HILL, L., SANTINO, A., FERNIE, A. R. & MARTIN, C. 2015. Multi-level engineering facilitates the production of phenylpropanoid compounds in tomato. *Nature Communications,* 6**,** 8635.

ZHANG, Y., BUTELLI, E. & MARTIN, C. 2014. Engineering anthocyanin biosynthesis in plants. *Current Opinion in Plant Biology,* 19**,** 81-90.

ZHAO, R., BRUNING, E., ROSSETTI, D., STARCHER, B., SEIBERG, M. & IOTSOVA-STONE, V. 2009. Extracts from Glycine max (soybean) induce elastin synthesis and inhibit elastase activity. *Exp Dermatol,* 18**,** 883-6.

ZOMER, H. D. & TRENTIN, A. G. 2018. Skin wound healing in humans and mice: Challenges in translational research. *Journal of Dermatological Science,* 90**,** 3-12.
ZOU, J. G., WANG, Z. R., HUANG, Y. Z., CAO, K. J. & WU, J. M. 2003. Effect of red wine and wine polyphenol resveratrol on endothelial function in hypercholesterolemic rabbits. *Int J Mol Med,* 11**,** 317-20.